UNIVERSITY of TASMANIA

Developmental dynamics of primordial germ cells, their genetic determinants and role in sex differentiation in *Gambusia holbrooki*

Komeil Razmi

MSc, Bioscience and aquaculture

Institute for Marine and Antarctic Studies (IMAS) | Fisheries and Aquaculture Centre

Submitted in partial fulfilment of the requirements for the Doctor of Philosophy in Biological Sciences

University of Tasmania, April 2022

To mom and dad for their support,

and my wife, Parisa, for her endless care, sacrifices and encouragement.

Declaration of Originality

This thesis contains no material which has been accepted for a degree or diploma by the University or any other institution, except by way of background information and duly acknowledged in the thesis, and to the best of my knowledge and belief no material previously published or written by another person except where due acknowledgement is made in the text of the thesis, nor does the thesis contain any material that infringes copyright.

15/06/2021

Statement of Authority of Access

This thesis may be made available for loan and limited copying and communication in accordance with the Copyright Act 1968.

15/06/2021

Statement of Ethical Conduct

The research associated with this thesis abides by the international and Australian codes on human and animal experimentation, the guidelines by the Australian Government's Office of the Gene Technology Regulator and the rulings of the Safety, Ethics, and Institutional Biosafety Committees of the University. Specifically, this research was part of "Trojan W" as a genetic solution for controlling and eradicating the Eastern mosquitofish, Gambusia holbrooki," project (A0017759).

15/06/2021

Acknowledgements

My deep gratitude goes first for Dr. Jawahar G. Patil, who expertly guided me through my Ph.D. research and who shared the excitement of four years discovery. I am also grateful to Professor Chris Carter and Professor John Purser for their supervision.

My appreciation also extends to my laboratory colleagues, Lisette Robertson, Kwan Tzu nin, Ngoc Tran and Ehsan Mousavi whose assistance has been especially valuable.

I am finally thankful to Australian Research Council (ARC) Linkage Project and Inland Fisheries Service Tasmania for funding this study, and Institute for Marine and Antarctic studies (IMAS) for the opportunity to study in a prominently academic environment.

Table of Contents

List of figures

List of tables

Glossary of abbreviations, terms and gene nomenclature

Abbreviations

3′UTR	3' untranslated regions
5′UTR	5' untranslated regions
aa	amino acids
amh	Anti-Mullerian Hormone
Ant	Anterior
Bb	Balbiani body
AP	alkaline phosphatase
Cdc 25	Cell division cycle 25 phosphatase
cDNA	Complementary DNA
CeB	cerebellum
CNS	central nervous system
cxcr4	C-X-C chemokine Receptor type 4
cyp19a1a	Cytochrome P450 Family 19 Subfamily A Member 1
Dazl1	Deleted in Azoospermia-Like 1
DDX4	DEAD box protein 4
DND	Deadend
dmrt1	Doublesex- and Mab-3-Related Transcription Factor 1
DNMT	DNA methyltransferase
dpp	days post parturition
DSRM-DND	double-stranded RNA binding motif of dead-end protein homolog 1
EDC	endocrine-disrupting chemical
eIF3f	eukaryotic translational initiation factor 3f
eIF4A	eukaryotic translational initiation factor 4A
eIF4E	eukaryotic translational initiation factor 4E
E. somite	early somitogenesis
foxl2	Forkhead Box Protein L2
gDNA	genomic DNA
gapdh	GlycerAldehyde 3-Phosphate DeHydrogenase
Gp	Germ plasm
GOI	gene of interest
GSC	germline stem cell
GSP	gene specific primers
GW	Genome walking
ICR	Imprinting Control Regions
L. somite	late somitogenesis
macf1a	Microtubule-Actin Crosslinking Factor La
MBT	Mid-Blastula Transition
MCLE	mitochondrial cloud localisation element
miRNA	micro RNA

MIQE	Minimum Information for Publication of Quantitative Real-Time PCR Experiments
MUSCLE	MUltiple Sequence Comparison by Log-Expectation
*mykl**α***	*myosin light-chain kinase**α***
M. somite	mid somitogenesis
MZT	maternal-to-zygotic transition
NCBI	National Centre for Biotechnology Information
ncRNA	Non-coding RNA
NS	not significant
ORF	open reading frame
PABP-1234	polyadenylate binding protein human type 1, 2, 3 and 4
PAZ	Piwi, Argonaut and Zwille
PGC	primordial germ cells
pgk1	Phosphoglycerate Kinase 1
PGR	putative gonadal ridge
PIWI	P-element Induced WImpy testis
piRNA	Piwi-interacting RNA
poly(A)	polyadenylation
Pos	posterior
PRM2	Protamine 2
qPCR	quantitative polymerase chain reaction
RA	retinoic acid
RACE	rapid amplification of cDNA ends
RBP	RNA-binding protein
rbpms2	RNA Binding Protein isoform 2
RNAi	RNA interference
rps18	Ribosomal Protein S18
RRM	RNA recognition motif
RT	reverse transcription
SF2_C_DEAD	C-terminal helicase domain of the DEAD box helicases
TAP	tobacco acid pyrophosphatase
TD-PCR	Touch Down PCR
tdrd	Tudor Domain-Containing Protein
WM-ISH	whole-mount *in situ* hybridisation
ZGA	Zygotic Genome Activation

Terms

Nuage: Also known as germ plasm, is an electron-dense material found in oocytes and typically tucked between mitochondria and nuclear envelope.

Trojan sex chromosome: It is a theory which relies on the release of sex reversed individuals (*i.e.*, opposing phenotype and genotype) released into the target population at regular intervals aim to skew the sex ratio in the population.

Gene and protein nomenclature

Gene names are italicised and lower case for fish, italicised with only first letter capital for invertebrates and other higher vertebrates, and all capital and italicised for humans.
Protein names are given with only first letter capital for fish, and all capital for invertebrates and other vertebrates including human.

Thesis structure

There are altogether six chapters including a literature review, a methodological and three experimental chapters. They have been written in the format of a thesis by publication, where each one is a stand-alone article so that it can be published independently. As a consequence of this approach, there may be unavoidable repetitions between chapters. However, all the references are presented only once at the end of the thesis. The structure of the thesis is given below.

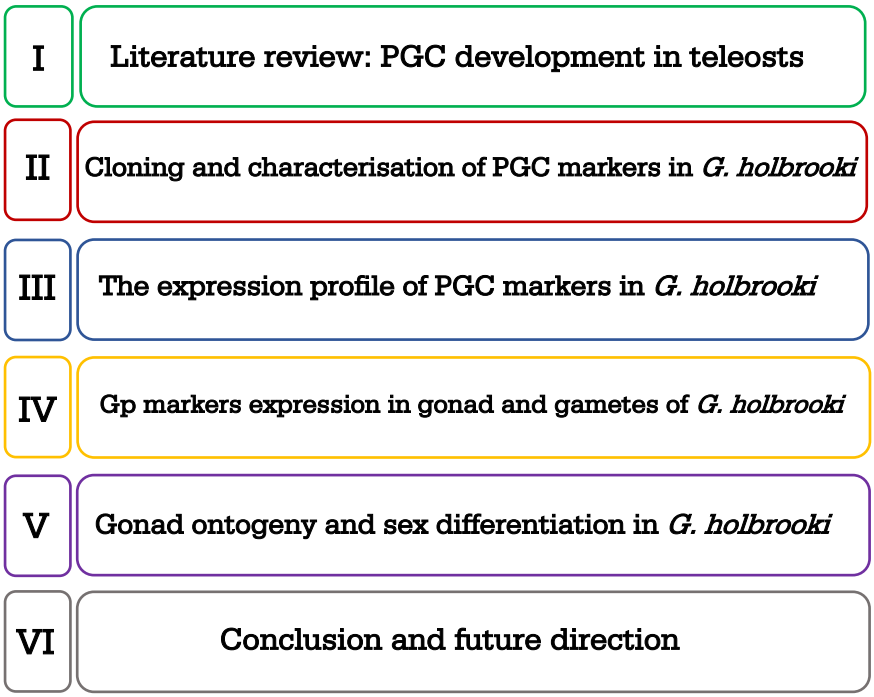

Executive Summary

Primordial germ cells (PGC) are the progenitors of life; they develop into gametes and safeguard gonad function in sexually reproducing animals. By virtue of diverse reproductive strategies, fishes provide an invaluable field to study germ cell emergence and fate. The current knowledge of PGC development in live-bearing fish (poeciliids) is limited and instead it is predominantly restricted to well-studied oviparous teleost models such as zebrafish, *Danio rerio* and medaka, *Oryzias latipes*. To address this basic knowledge gap and to assist future development of species-specific reproductive biotechnologies to control invasive populations, this thesis focused on *Gambusia holbrooki*, a notorious pest fish. Beginning with a review of current knowledge, the developmental dynamics of germ cells in this species was evaluated employing the spatio-temporal expression of key germline markers and screening the morphological changes of gonads during the early stages of development. Also, this study discussed the potency of *G. holbrooki* as a model organism for fertility research, based on its developmental similarities with mammalian models.

First, the study systematically reviewed the available literatures on PGC development, with a particular emphasis on teleosts, to synthesise evolutionary origin and mechanism of germ plasm (Gp) acquisition in fish taxa (Chapter 1). Specifically, the review identified two modes of germ cell development as distinguished by PGC specification of being either maternal (*e.g.*, in teleost) or zygotic (*e.g.*, in mammals) origin based on the role of epigenetic machinery in teleostean PGC emergence and fate. Further, prior knowledge of the interplay between molecular pathways and effector genes involved in germ cell signalling, mobilization and homing, and the regulatory RNA interference (RNAi) mechanisms leading to PGC specificity, their *en route* migration and homing were distilled. These along with the role of non-coding RNAs (ncRNA), *e.g.*, mi-RNA and pi-RNA, in germ line development was graphically illustrated to identify crucial roles and pathways that occur in fish PGC development. The contextual role of the nested germ cells in determining sexual fate of gonad and gonado-soma sexual identity via cell-cycle decisions and the timing of sex-biased germline stem cell (GSC) differentiation was also reviewed. This review formed the basis to address critical questions, including PGC specification mode, the pattern of germline migration, the temporal and spatial expression of key PGC markers during germline formation, and early gonadogenesis in *G holbrooki*.

Spatio-temporal expression of germline markers is a powerful tool to investigate the processes of gonad formation and gametogenesis. Correspondingly, cloning, and characterisation of the target genes is a fundamental need when investigating non-model organisms whose genetic information is scarce and patchy. To address this, the full-length cDNA of the key germline markers including *cxcr4*, *dazl*, *dnd*, *nanos1*, *piwi II* and *vasa* in *G. holbrooki* were cloned and their identity established (Chapter 2). Standard rapid amplification of cDNA ends (RACE) techniques were used to establish testis and ovary specific libraries, followed by amplification of *G holbrooki* homologues using degenerate primers. Subsequently, the full-length cDNAs were cloned, characterised, the functional domains annotated and their

evolutionary relationship to other poeciliid homologues established. The Dazl exhibited RNA recognition motif (RRM) and poly(A) binding protein (PABP) domains, while Deadend (Dnd) was encoded by two alternatively spliced variants, with conserved RRM and DSRM-DND domains in the predicted polypeptide. As expected, Piwi II had PAZ domain contained nucleic acid-binding interface in N-terminus and 5′ RNA guide anchoring site at C-terminus. DEAD-box helicase motif was also conserved in predicted Vasa containing RNA- and ATP-binding sites. Similarly, chemokine binding site and zinc-finger motif in predicted Cxcr4 and Nanos1, respectively were present. Overall, the predicted amino acids of the studied genes showed a strong similarity with respective homologues of other poeciliids.

In teleosts with preformation mode of PGC specification, maternal inheritance of Gp provides sufficient factors to form the germline fate of nascent PGCs protecting their identity, in contrast to the surrounding soma, right from post zygotic activation. Later, during embryonic patterning and cell determination, the Gp components are involved in proliferation, migration, and colonisation of germ cell precursors. To understand how and when PGC are formed, migrate, and colonise putative gonad in *G holbrooki* and how well these events are conserved across teleosts, *in situ* hybridisation and quantitative expression profiles of five Gp markers, namely *dazl*, *dnd1*, *nanos*, *piwi II* and *vasa* were studied (Chapter 3). Based on expression of PGC markers, a group of Gp components was detected in the ovum suggesting maternal inheritance mode of PGC specification in *G. holbrooki.* Subsequent to fertilisation, the results showed that *vasa* positive cells were detectable from late cleavage, later forming as two PGC clusters at the early gastrula stage, migrating anteriorly during somitogenesis and eventually colonised at the genital ridge before the pharyngula stage. Of all the markers only *vasa* and a *dnd* variant signals were restricted to PGCs. The embryonic expression of *piwi II*, *dazl dnd-β* were detected in PGC clusters as well as the central nervous system. Interestingly, the embryonic expression of *nanos1*an indispensable PGC marker in zebrafish, was only found in neural tube. The quantitative gene expression profiles showed a transient female-biased surge of the PGC markers at the gastrula stage, suggesting an early onset of PGC proliferation in females. Strictly zygotic expression pattern of *dnd-β* and *nanos1* also showed maternal to zygotic transition (MZT) occurs before the mid-cleavage stage, in *G. holbrooki*. Collectively, the results suggest that despite sharing preformation mode of PGC specification, their migration pattern in *G. holbrooki* is unlike any other fish species studied so far. Instead, somatic expression of teleostean PGC markers (e.g., *piwi II*, *nanos1* and *dazl*), splicing variation (e.g., *dnd*) and early MZT appear more similar to those of mammalian models.

Gp is an electron dense body in ooplasm involved in germline determination of organisms with preformation mode of PGC specification including teleost. However, the expression patterns of Gp factors during gonadogenesis and their storage in gametes of poeciliids are unknown. To address this, quantitative gene expression of six markers of Gp components namely c*xcr4, dazl, dnd-α, piwi II, tdrd6* and *vasa,* with essential roles in gonad function among vertebrate models were evaluated for their expression profile in pre- (*i.e.,* the pharyngula stage and right before parturition) and post-natal *(i.e.,*

juvenile, and adult phase) stages of genetic male and female *G. holbrooki* (chapter 4). The overall results showed the relative accumulation of Gp components were comparable in prenatal stages of gonadogenesis between genetic males and females. However, their post-natal expression in gonads was female-biased ($p<0.05$), particularly as the animal reached puberty. Interestingly, the existing Gp transcripts and their abundance showed dissimilar patterns between ovum and spermatozoa of *G. holbrooki*. Collectively, this study, for the first time, revealed the Gp components involved in early germline determination are detectable not only in ovum, but also in mature spermatozoa indicating a potency for the contribution of paternal factors in PGC specification and function.

Gonadogenesis is triggered with successful germ cell colonisation and gonadosoma emergence at the genital ridge followed by sexual identity acquisition through sex determination mechanisms or environmental cues. Among vertebrates, teleosts are known to exhibit diversified plans of gonadogenesis and sex differentiation, however, little is known in poeciliids. To ascertain when and what cellular and molecular determinants trigger sex differentiation in *G. holbrooki*, this study (Chapter 5) also documented critical events during early gonadogenesis using gonad histology, *in situ* hybridisation of germ cell markers and quantitative expression of gonadosoma markers. The histological observations showed that germ cells were first colonised at the genital ridge prior to complete somitogenesis to form presumptive gonads. Thereafter, germ cells underwent mitotic proliferation before acquisition of their sexual identity and this pattern was sex-dimorphic in *G. holbrooki*. Moreover, it was shown that sex differentiation of early gonads in *G. holbrooki* occurs right before parturition evinced from emerging meiotic primary oocytes stage I in ovary and formation of spermatogonial stem cell cysts in testis. Gonad histology and germ cell labelling showed that presumptive gonad in *G. holbrooki* undergoes major morphological transformation during its early development. Specifically, presumptive gonads first developed as two distinctive lobes, however, the lobes grew convergently and fused around the parturition stage to form single lobed testis or ovary, as occurs in adults. The quantitative expression pattern of a group of gonadosoma markers, *foxl2*, *cyp19α*, *amh*, *dmrt1*, in pre- and post-natal developmental stages was consistent with morphological changes in early gonad; they were activated at the onset of gonad formation followed by sex-dimorphic expression pattern concurrent with sex differentiation of gonads.

In conclusion, this study enlightened aspects of PGC development, their developmental dynamics and events involved in gonadogenesis of an invasive poeciliid fish, *G. holbrooki*. In concurrence with its ovo-viviparity, it also revealed resemblance between some aspects of its PGC development and those of mammalian models. Interestingly, the study for the first time provided evidence for "paternal origin" of Gp markers, suggesting that both parents contribute to germ line specification in this species, an aspect that might be shared by all teleosts. Moreover, the critical timepoints in gonadogenesis *i.e.*, germ cell colonisation and sex differentiation were ascertained, with further evaluation of the sex-specificity of gonadosoma markers. In doing so, the study generated resources, reagents, and established germline specificity of PGC markers that can assist targeted ablation of germ cell function to produce sterile or

sex reversed animals as may be desired to engineer genetic control options to manage this pest species. The shared features of PGC development with both of oviparous and viviparous vertebrates, suggest the species could serve as a key model to study vertebrate reproduction and reproductive conditions such as sterility.

Chapter I

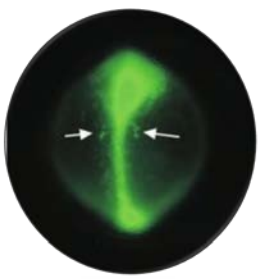

Literature review

Chapter 1 | Primordial germ cell development in teleosts: their origin, fate and role in sex differentiation

Abstract

Primordial germ cells (PGC) are the progenitors of life; they develop to gametes and safeguard reproduction, in sexually reproducing animals. In virtue of diverse reproductive strategies, fishes provide appealing models to study germ cell emergence and fate that are of biomedical applications. This review was undertaken to distil current understanding of the evolutionary cause and effect of Gp acquisition in fish taxa, to serve as a basis to investigate PGC development in poeciliids. In the process, redefined are the two modes of germ cell development distinguished by PGC specification approaches (*i.e.*, maternal messaging and zygotic regulation) through investigating the role of epigenetic machinery in teleostean PGC emergence and fate. This review also elucidates the network of molecular pathways and effector genes involved in germ cell signalling, mobilization and homing as well as the regulatory RNA interference that define the specificity of PGCs and their route of migration. Compiled also are current understanding of germline developmental events underpinned by ncRNAs including the crucial role of mi-RNA and pi-RNA pathways in fish PGC development. Finally, the critical decisions made by nested germ cells to determine sexual fate of gonad, gonado-soma sexual identity, cell cycle decision and the sex-biased timing of GSC differentiation were elucidated. The outcomes served as foundation to comparatively investigate PGC development in a poeciliid model—*Gambusia holbrooki*—to answer critical questions of PGC specification, pattern of germline migration, and their role in sex differentiation, that may be relevant to develop control options for this invasive species.

1.1. Introduction

In 1892, August Friedrich Weismann coined the term '*Keimplasma' or* "germ plasm" in his theory of hereditary refuting Darwin's concept of pangenesis. He proposed traits which pass to the next generation are independent of somatic cells and unaffected by experience. Gp was claimed as a unique immortal substance, inherited from parents (primarily maternal) and transmitted to the next generation (Weismann, 1872, Weismann, 1892). It was later accepted that the Gp is a maternally supplied substance consisting of proteins, RNA and organelle(s) accumulated in ooplasm, later allocated into a group of cells in initial embryonic cleavages and eventually granting primordial germ cell (PGC) identity (Lehmann and Ephrussi, 1994, Ikenishi, 1998), with potential paternal messages largely ignored. PGCs, as the progenitors of gametes, acquire their sexual identity and transfer the genetic and epigenetic information to ensuing generations; allowing evolution to improve individual and population adaptability. Fish have evolved regenerative gametogenesis, notably with diverse plans of gonad ontogenesis and sex determination mechanisms, which ensure their ability to survive, adapt and thrive as the most diverse group of vertebrates providing rich material for both basic (*e.g.*, evolutionary) and applied (*e.g.*, fisheries, aquaculture and medicinal) research (Devlin and Nagahama, 2002, Nikolic et al., 2016).

Based on the function of genes involved in germ cell formation and gonadogenesis (Table. 1.1), four main events of PGC development can be discerned; 1) Gp assembly and localisation (Bontems et al., 2009); i.e., dynamics of maternal determinants during oogenesis and onset of fertilization, 2) PGC sequestration and proliferation (Raz, 2002, Reichman-Fried et al., 2004); how the maternal molecules are first accumulated in four distinctive regions and then partitioned to dividing cells to accurately regulate the PGC proliferation, 3) PGC migration and homing (Raz and Reichman-Fried, 2006, Paksa and Raz, 2015); how the PGCs acquire specific chemical and morphological competence for directed motility, interaction with somatic environment and recruit several molecular pathways including chemotactic and RNAi regulation to home, and 4) germ cell nesting and differentiation (Saito et al., 2007, Nishimura et al., 2015); how germ cells achieve the sexual identity with a commitment to gonado-soma differentiation (Table 1.1).

Reproductive competence of commercial fish species is highly desired for sustainability of fisheries and aquaculture industries although certain circumstances may impose constraints and detrimental consequences. For example, in aquaculture practices, regenerative gametogenesis, abundant gamete production and ready manipulation of spawning cycles allow large scale seed production on demand. However, the fertile escapees can pollute the gene pool of wild conspecifics and compromise survival of native and endangered species (Fiske et al., 2006). Therefore, in-depth insight into the dynamics of fish germ cell development and gonadogenesis may offer solutions to fisheries and aquaculture, whilst mitigating their impacts on other fauna.

Studies on PGC development in fish models such as medaka (Herpin et al., 2007) and zebrafish (Raz, 2003) have already yielded new knowledge on basic cellular mechanisms including cell mobilization (Paksa and Raz, 2015), signalling (Swaney et al., 2010, Boldajipour et al., 2008), pluripotency (Johnson and Alberio, 2015), RNA interference pathways (Bizuayehu and Babiak, 2014) and regenerative reproduction that are of direct medical relevance (Sasaki and Shimizu, 2008, Howe et al., 2013). However, little is known about poeciliids and in particular *Gambusia holbrooki*, which is considered as one of the top 100 invasive species in the world (McLeod, 2004). The eastern mosquitofish, *G. holbrooki*, is a fresh water poeciliid native to Central and North America and known for its notorious invasiveness (Davies, 2012, Nico et al., 2019). Owing to competitive advantages of high tolerance to extreme environments (Otto, 1973, Chervinsky, 1983), relatively higher offspring viability via matrotrophy (Pyke, 2005) and superfetation (Olivera-Tlahuel et al., 2018), and improved mate-selection strategies (Gasparini et al., 2011, Lynch et al., 2012), *G. holbrooki* thrives in fresh and estuarine wetlands. This jeopardises the natural habitat assemblages, eventuating in loss of endemic and endangered aquatic species (Harrington and Harrington, 1982). It is therefore necessary to understand the underpinning reproductive processes including early events of germline determination and gonadogenesis that may provide greater insights into its invasiveness.

This review forms an assembly and analyses of existing information to facilitate investigations on PGC development and their dynamics in *G. holbrooki*. This fundamentally includes salient features of germ cell formation in fish comparatively with those of other well-studied animal models.

1.2. PGC development in teleosts—key events and regulators

The critical events of germ cell formation are highly dependent on PGC specification modes they adopt. In vertebrates, this is typically known to occur through either induction/epigenesis (Ying et al., 2002) or inheritance/preformation mode (Raz, 2003). In induction mode (*e.g.*, mice and urodeles), germ cell formation is entirely controlled by the zygotic mechanisms through a few key events; suppression of somatic differentiation and re-acquisition of pluripotency followed by genome-wide epigenetic reprogramming (Saitou et al., 2002, Seki et al., 2005, Yamaji et al., 2008). In inheritance mode (*e.g.*, *Drosophila melanogaster* and *Xenopus laevis*), fate of the germ cells is predetermined by parentally (primarily maternal) inherited messages, which maintain somatic suppression and specificity of PGCs until maternal-to-zygotic transition occurs, when the first wave of zygotic mechanisms takeover the subsequent developmental events. In the most studied models, irrespective of germline specification mode, PGCs are thought to be the earliest group of cells to undergo lineage restriction (Chatfield et al., 2014, Johnson and Alberio, 2015). Right from specification, a variety of regulatory pathways intensively surveil and safeguard all stages of stromal specificity of PGCs, *en route* their migration and compact colonisation to the presumptive gonad (Raz, 2002, Kurimoto et al., 2008, Nikolic et al., 2016).

1.2.1. The evolution of maternal inheritance mode; cause and effects

Owing to pre-packaged maternal molecules, germ cell formation is an early event in maternal inheritance mode (Raz, 2002, Santos and Lehmann, 2004),whereas, in induction mode, *de novo* PGC specification is a delayed process until embryonic zygotic genome activation (ZGA) (Nikolic et al., 2016, Wang and Cao, 2016).

It was previously thought that utilizing maternal messages in evolutionarily primitive animals is a strategy for expeditious germline development. However, phylogenetic studies, suggest that inheritance mode is not confined to primitive animals but unevenly scattered within clades (Extavour and Akam, 2003, Ewen-Campen et al., 2010). For example, in fish taxa (Fig. 1.1), both germ cell development modes occur within both Chondrichthyes (Teshima and Tomonaga, 1986, Extavour and Akam, 2003) and Osteichthyes (Johnson et al., 2001, Saito et al., 2011, Nagasawa et al., 2013, Saito et al., 2014).

Hypothetically, the consequence of maternal inheritance resulting in early germline specification liberates somatic gene regulatory networks allowing more protein sequence evolution and morphological diversity leading to increased species richness compared to those under induction mode (Evans et al., 2014, Crother et al., 2016). This may in part explain the rich species diversity of teleosts that predominantly display maternal inheritance mode among chordates (Froese and Pauly, 2000). Conversely, Agnatha in which there is evidence for epigenetic origin of germ cells (Beard, 1902, Walvig, 1963, Extavour and Akam, 2003) is one of the least diverse classes among vertebrates (Sayers et al., 2009). As the maternal molecules comprise other essential messages for axial patterning and body formation, the Gp acquisition is thought to be part of a broader strategy to evolve early and sleek embryonic development (Marlow and Mullins, 2008, Chang et al., 2011, Whittle and Extavour, 2017). In animals with elongated embryonic body (*e.g.*, majority of nematodes and fish species) in which stem cells such as PGC first emerge out of tissue anlage, away from their presumptive home, a pre-laid maternal axial pattern likely provides a ready scaffold for the mobilization of specified cells (*i.e.*, PGCs).

Evolution of the two germ cell specification modes among fish species may also have ecological origins. The biologically and environmentally competitive aquatic habitats confer a narrow reproductive window which compel aquatic species to evolve the most efficient strategy for embryonic development including germ cell specification. This is probably mirrored in the different pattern of germ cell specification in evolutionarily (but not ecologically) close species like *Bathyraja aleutica* and *Torpedo marmorata* (Fig. 1.1). However, most studies on Gp acquisition in fish taxa have been confined to cytological observation, with limited and sporadic use of molecular markers to characterize Gp existence and timing of PGC specification.

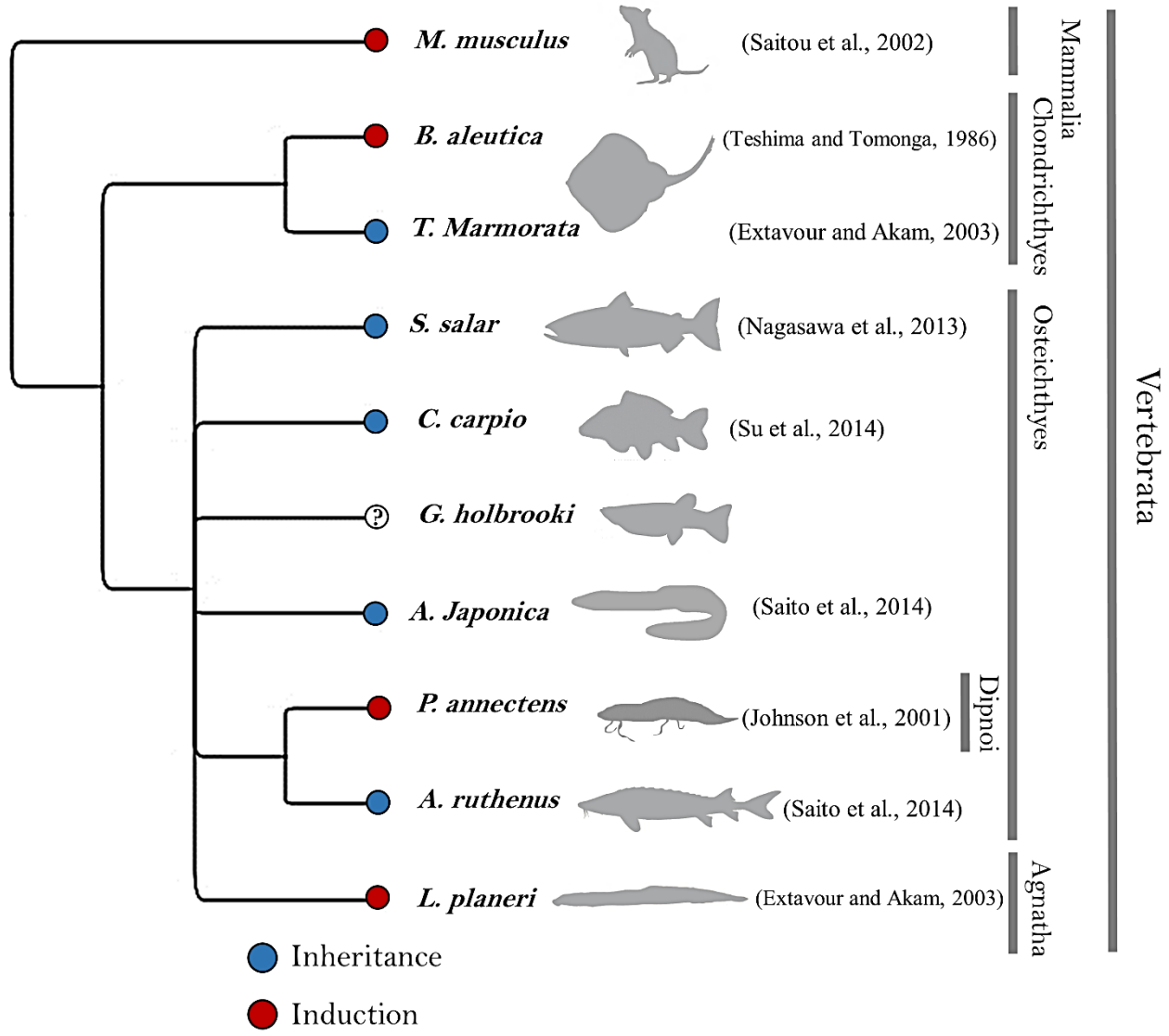

Figure 1.1. CO-1 cladogram showing the evolutionary relationship of fish with known modes of their PGC specification. Both PGC specification modes are interspersed across Chondrichthyes and Osteichthyes suggesting these may have evolved or were acquired independently in different taxa.

As poeciliids share reproductive traits with mammals, *e.g.*, viviparity, placentation and superfetation, it is worth investigating whether ovum, in *G. holbrooki*, are loaded with Gp components playing a role for PGC sequestration in teleosts. This evidence could provide a clue to germline determination mode in poeciliids at large. Overall, Gp acquisition among vertebrates corresponds to increased speciation (Crother et al., 2007, Crother et al., 2016), embryonic innovations (Johnson et al., 2003) and adult morphological changes (Johnson et al., 2011a). However, models with induction mode, in return, may have a higher chance of vertical macroevolution, as totipotency may provide options for fundamental types of novel morphogenesis (Johnson et al., 2003, Johnson et al., 2011a). Irrespective of evolutionary consequences and causes, transition from induction to inheritance mode has been typically observed

throughout the evolutionary path of animals, suggesting Gp induction follows “Dollo’s Law” of irreversibility (Whittle and Extavour, 2017).

1.2.2. Germ plasm assembly; packed up just by mother?

Maternal messaging and its ooplasm architecture are widely conserved in animals within both induction (Pepling et al., 2007, Li et al., 2010) and inheritance (Raz, 2002) modes. However, Gp, the maternally inherited molecules which play a role in PGC emergence, has not been characterised in induction models (Zernicka-Goetz, 1998). In zebrafish, the symmetrically mitotic distribution of Gp changes in early meiotic stages by the transient formation of a Balbiani body (Bb), a distinct cellular and molecular structure which appears adjacent to the germinal vesicle, accommodating organelles and maternal molecules (Nojima et al., 2010, Wylie et al., 2014, Kaufman and Marlow, 2016a). In zebrafish, *bucky ball* (*buc*) is one of the earliest Gp markers and is involved in Bb assembly remarkably similar to those of *oskar* in *Drosophila* (Bontems et al., 2009). Buc regulates Bb formation and the polarity of oocytes through interactions with two Bb-localised RNA binding proteins (RBPs); Deleted in azoospermia-like (Dazl) and RNA binding protein isoform 2 (Rbpms2) (Kaufman and Marlow, 2016a, Kaufman et al., 2018). Indeed, tight regulation of *buc* during oogenesis maintains asymmetric polarity of the ooplasm and inhibits Bb supernumerary (Heim et al., 2014).

Apart from the importance of Bb dynamics and components during oogenesis (Marlow and Mullins, 2008, Bontems et al., 2009), the orchestrated mobility and aggregation of Bb in the ooplasm is essential for proper germ cell development. It has been shown that a group of proteins including Tdrd6 and Rbpms2 are involved in the dynamics of Bb. Tdrd6, a member of the Tudor domain-containing proteins, regulates optimum size of the Bb, overall organisation of its components and eventually ensures proper germ cell development (Roovers et al., 2018). Also, loss of Rbpms2, which affects Buc accumulation and asymmetric polarity in ooplasm, has some adverse effects on gonad formation (Kaufman et al., 2018). Together, the disrupted germ cell formation in *tdrd6* and *rbpms2* mutant lines spotlight the effects of Bb mobility and its aggregation on PGC development.

Regulation of cell polarity and asymmetric localisation of molecules and organelles are crucial to establish developmental programmes including cell motility and specification of cell fates. Cells usually prefer to transport messenger RNAs rather than proteins; transporting RNAs prevent proteins from ectopic function before they are spatiotemporally localised to the desired site (Medioni et al., 2012). This strategy is critical during early stages of development when the improper function of maternal proteins interrupts embryonic patterning and cell specification. Transport-competent RBPs, one of the intracellular transport machinery components, can recognise *cis*-regulatory elements (also termed as localisation element) and bind to them; these regulatory elements are usually found on 3′UTR (Gavis and Lehmann, 1994, Betley et al., 2002, Zearfoss et al., 2004). As summarised in Figure 1.2, the dynamics of *mdazl1* in ooplasm and zygotes is a good example where multiple *cis*-acting elements on

3′UTR of *dazl1* govern the sequential pattern of RNA localisation (Knaut et al., 2000, Kosaka et al., 2007).

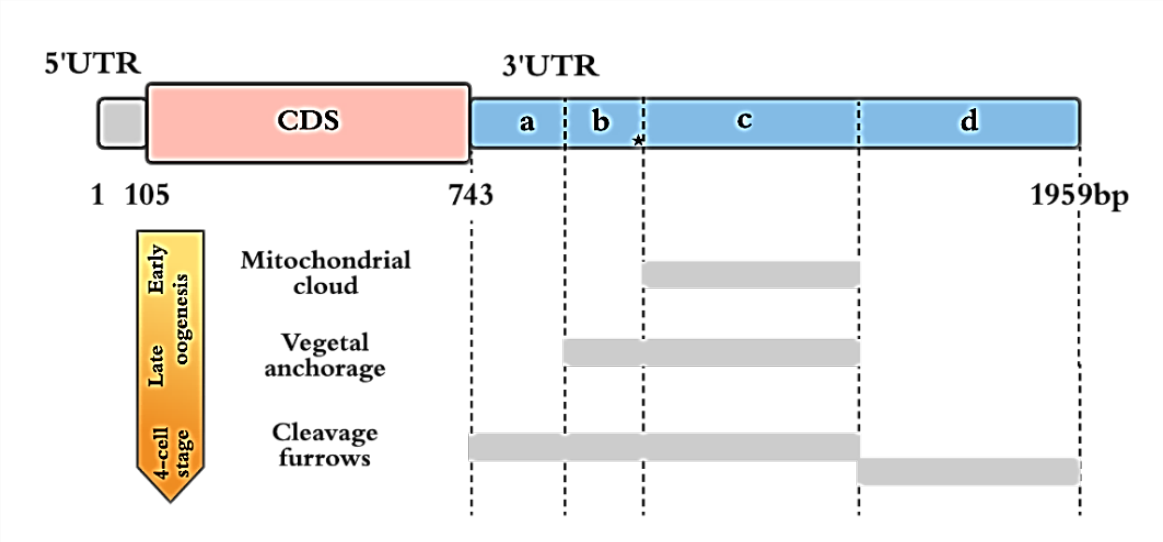

Figure 1.2. Directed localisation of maternal *dazl* by 3′UTR regions. Oogenesis localisation of maternal *dazl* is mediated by region c and into the mitochondrial cloud and b-c to the vegetal anchorage, respectively. At the onset of fertilisation, region a-b-c or individually d governs the zygotic translocation of *dazl* to the cleavage furrows. UGCAC cis-acting motif (*), the mitochondrial cloud localisation element, is found at the border of regions b and c. Several CACA containing *cis*-acting motifs are also found in region d which may suffice to solely direct the maternal *dazl* suggesting multiple elements safeguard its localisation (Adapted from Kosaka et al., 2007).

Noticeably, however, the pattern of these maternal RNA localisations is not conserved among teleosts. For example, unlike zebrafish in which *nanos1* and *vasa* are localised at cleavage furrows (Koprunner et al., 2001), the transcripts of these genes in medaka (*Oryzias latipes*) are uniformly scattered throughout the embryo (Herpin et al., 2007). These differing patterns of mRNA localisation between fish species may suggest that the spatial origin of the nascent PGCs and their migration path are species-specific. Within this context, as the concept of paternal contribution to early embryonic development and offspring fitness has been attentively considered (Chen et al., 2016, Champroux et al., 2018). As a result, identification of key Gp markers in mature spermatozoa transcriptome could be a fundamental step towards understanding their role on early germline determination.

1.2.3. PGC sequestration and proliferation: the fate of four immortal knights

The specification of PGCs through both inheritance and induction, occurs via complex regulatory networks governed by genetic (Herpin et al., 2007, Presslauer et al., 2016), epigenetic (Feng and Chen, 2015) and environmental (Lo et al., 2011) events. The primary difference between the two modes is evident from the first step of germ cell formation where the cells acquire the PGC identity. Germ cell specification in mice occurs through induction; somatic mesodermal program suppression (Saitou et al.,

2002) followed by re-acquisition of potential pluripotency (Yabuta et al., 2006) and two surges of epigenetic reprogramming (Saitou et al., 2012, Seisenberger et al., 2012). In contrast, in a preformation model, such as zebrafish, furrow-associated Gp first becomes sequestered into four distinctive granules after second cleavage and the four *vasa*-positive cells are distinctively observed until the 16 to 32-cell stage (Kaufman and Marlow, 2016a). From the 4-cell to the late blastula stage (3-4 hpf), the four *vasa*-positive cells divide asymmetrically, with only one of the blastomeres from each division inheriting sufficient maternal deposits to maintain PGC identity; these cells will later become PGCs (Raz, 2000). At this early stage of PGC specification in inheritance mode, somatic repression and pluripotency re-acquisition is not required; all cells initially have the potential to become PGCs, but the limited number of maternal molecules restricts their number. Therefore, maternally designated cells (nascent PGCs) are sequestered rather than specified, *i.e.*, determined through deprivation not acquisition. Indeed, the segregation of maternal molecules in the initial stages of development dictates what group of cells will have germ cell fate, serving as an instruction for PGC identity and proliferation in inheritance mode. Mechanistically, maternal *tdrd6α*, in zebrafish, is thought to have a role in loading a relatively fixed ratio of maternal transcripts to PGCs (Roovers et al., 2018). Correspondingly, in *Drosophila* where preformation mode determines PGC sequestration, germ cell survival is a PGC-intrinsic process by which higher Gp inheritance correlates with a higher chance of PGC survival (Slaidina and Lehmann, 2017). Despite sharing the preformation mode for PGC sequestration, the first emergence of PGCs in early embryonic development is not similar among fish species. In zebrafish (Raz, 2002) and Atlantic salmon (Nagasawa et al., 2013), Gp signals are concentrated in nascent PGCs from late cleavage, while in medaka, those signals are scattered until early gastrula where they converge into two PGC clusters (Herpin et al., 2007). Therefore, comparative evaluation of these patterns in diverse representative taxa such as the poeciliids could reveal insights into their adaptations and reproductive strategies.

Studies on the function of maternal gene products, including *vasa*, *nanos1* and *dnd* deposited to the nascent PGCs from early cleavage provide evidence of the initial events of PGC formation and shed light on how nascent PGCs suppress the inner somatic cues, proliferate in distinctive groups (*e.g.*, in zebrafish) and communicate for their proper migration.

Even though the germ cell-specific pattern of *vasa* expression during teleosts gametogenesis and PGC development (Yoon et al., 1997, Knaut et al., 2000) supports the dogma of *vasa* necessity for germ cell function, *vasa* does not seem to have an indispensable role in every stage of teleostean PGC development (Table 1.1). *vasa* expression in invertebrate totipotent cells suggests an inhibitory function hindering nascent PGCs from somatic differentiation (Seydoux and Strome, 1999). A deficiency of *vasa* expression during gonadogenesis and differentiation generally reduces fertility; however, its impact is sex-dimorphic among models, causing female- and male-specific sterility in *Drosophila* (Tanaka et al., 2000) and mice (Gustafson and Wessel, 2010), respectively. In zebrafish, maternal *vasa* is adequate for PGC survival and maintenance as well as juvenile gonad assembly, while the zygotic *vasa* supports

gonad differentiation and maturation (Braat et al., 2001). In zebrafish, development of the zygotic *vasa* null gonad is arrested in pachytene which ceases meiosis, resulting in dysfunctional testis, irrespective of the genetic sex (Hartung et al., 2014). The *vasa* loss-of-function mutation has also shown that *vasa* may support the proliferation and mitosis of GSCs (Hartung et al., 2014). In medaka, *vasa* knockdown did not affect PGC survival and proliferation, but disrupted its proper migration (Li et al., 2009), while Dnd acts as PGC specifier through stabilizing germ plasm RNA (Hong et al., 2016), similar to Dnd function in *Oryzias celebensis* (Zhu et al., 2018). The role of VASA protein in germinal stem cell maintenance was indirectly observed in *Drosophila* where VASA activates translation of *Mei-P26,* a micro RNA (miRNA) repressor, which compromises the miRNA activity and promotes germ cell differentiation (Liu et al., 2009). This suggests Dead-box4 protein may be the mastermind of short interfering RNA machineries in germ cells in other taxa, while it appears unlikely to function as a *bona fide* PGC specifier in teleosts.

Suppression of somatic differentiation is one of the inceptive events that facilitates metazoan PGC formation (Curtis et al., 1997, Lai et al., 2011, Beer and Draper, 2013, Su et al., 2014). Typically, this suppression is orchestrated by *Nanos*-related genes that encode a class of RNA-binding zinc finger proteins. *Nanos,* a Gp component, acts as a highly conserved post-transcriptional repressor (De Keuckelaere et al., 2018, Asaoka et al., 2019) that suppresses endoderm specification (Lai et al., 2012), sex determination (Deshpande et al., 1999) and pro-apoptotic (Sato et al., 2007) genes in PGCs. In addition, *Nanos* controls the precocious differentiation of migrating germ cells by arresting the cell cycle (mitosis) through the accumulation of *cycline B* in PGCs (Deshpande et al., 1999, Deshpande et al., 2010). The suppressing function of *Nanos* is mediated through germline-specific modification of the histone architecture (Schaner et al., 2003).

Germ cells undergo two different rounds of incremental (mitotic) proliferation during their lifespan; 1) PGC proliferation, which occurs immediately after specification and coincides with ZGA (Raz, 2002) and 2) GSC proliferation subsequent to PGC homing and biochemical differentiation in newly formed gonads (Kimble, 2011). The maternally inherited *Nanos* transcript is assumed to accurately control mitosis in developing germ cells and regulate the number of PGCs until ZGA, when zygotic regulators take over and strictly control the number of PGCs, protecting them from soma differentiation, due to diluted Gp factors (Subramaniam and Seydoux, 1999, Hyslop et al., 2005). Early repression of *nanos1* expression in zebrafish significantly reduces the number of *vasa*-positive cells confirming the role of *nanos1* at first round of PGC proliferation (Koprunner et al., 2001). Nevertheless, the role of *Nanos1* in mice is not incorporated into germ cell function but is predominantly expressed in the central nervous system (Haraguchi et al., 2003).

The pluripotency signals are essential for cellular reprogramming (Mitsui et al., 2003), embryonic formation and patterning (Gagnon et al., 2018), as well as germ cell specification (Chambers et al.,

2003, Chambers et al., 2007). The somatic suppression and pluripotency re-acquisition events observed in murine PGC development do not occur in animals with the inheritance mode, however, the pluripotency network components (*e.g.,* Nanog, Oct4 and Soxb1) are maternally provided in zebrafish (Lee et al., 2013). Notwithstanding this, the universal pluripotency markers (Table 1) with critical roles in survival and maturation of PGCs (Kehler et al., 2004, Anderson et al., 2007), are sporadically found in fish species (Sanchez-Sanchez et al., 2010, Onichtchouk, 2012).

Another component of pluripotency machinery—*nanog*—regulates cell proliferation (Camp et al., 2009), first wave of ZGA (Lee et al., 2013) and proper embryonic patterning (Perez-Camps et al., 2016) in teleosts. Despite the lack of pluripotency in nascent PGCs, their overall development is affected in *znanog* (zebrafish *nanog*) knockdown morphants (Gagnon et al., 2018). The peak expression of z*nanog* occurs post mid-blastula transition (MBT) *i.e.,* during gastrulation in concurrence with PGC proliferation (Braat et al., 1999, Schuff et al., 2012). It is also shown that Nanog is involved in maternal transcript clearance at the onset of ZGA (Lee et al., 2013). Moreover, excessive *vasa*-positive cells and ectopic localisation of PGCs is observed in *znanog* mutants (Wang et al., 2016). Collectively, the maternal determinants including *vasa*, *tdrd6*, *nanos1* are thought to tightly control the mitotic segregation of Gp-containing cells to avoid dilution of maternal components and maintain the specificity of PGCs, until ZGA. Subsequently, overexpression of *nanog* regulates PGC proliferation and recruits RNA interference (RNAi) pathways (summarised in Fig. 1.3) to trigger maternal RNA clearance in both PGCs and somatic cells. Nevertheless, the clearance of germ cell markers is protected in PGCs (Fig. 1.3) by a group of germ cell-specific RBPs including Dnd (Ketting, 2007) and Dazl1 (Takeda et al., 2009). Specifically, these counteract RNAi and protect maternal and zygotic transcripts maintaining the specific identity of PGCs against soma and facilitate their programmed motility by chemotaxin titration (Mishima, 2012).

Cytoskeletal dynamics during embryogenesis (Table 1.1) also shapes germ cell formation by spatio-temporally sustaining correct Gp compartmentalisation, mRNA localisation and PGC motility (Theusch et al., 2006). In zebrafish, the cytoskeletal linker *macf1* is involved in Gp localisation through proper translocation of Bb to the vegetal cortex of oocytes (Gupta et al., 2010, Dosch et al., 2004). Subsequently, after fertilization, maternal *kif5βa*, a microtubule motor protein enhances *buc* signals at cleavage furrows indicative of its role in initial PGC specification (Messitt et al., 2008, Yabe et al., 2009, Eno and Pelegri, 2013, Campbell et al., 2015). In the shield stage, a cage of microtubules is formed to keep the granules in the vicinity of the nucleus and retain the structural integrity of nuage (Strasser et al., 2008). This strategy seems to control and confine PGC proliferation by enclosing the maternal germ cell determinants in a limited number of cells. Cellular motor proteins, *e.g., myosin light-chain kinase α* (*myklα),* are also involved in PGC mobilization via regulating cell contractility in readiness for PGC motility and migration (Goudarzi et al., 2012, Paksa and Raz, 2015).

1.2.4. Epigenetic programming; The convergence of PGC specification modes

The global pattern of DNA and histone methylation along with the effectors involved in the epigenetic apparatus are conserved between teleosts and mammals (Varriale and Bernardi, 2006, Zemach et al., 2010, Fang et al., 2013). Among the inherited maternal RNAs, a cluster of transcripts encoding non-methylated and methylated CpG-binding proteins, DNA methyltransferases and histone lysine methyltransferases are detected prior to ZGA. This is consistent with resetting genome methylation and chromatin remodelling during maternal to zygotic transition in zebrafish (Andersen et al., 2013, Dorts et al., 2016). Congruously, thousands of methylated promoters have been characterized during MBT indicating the post-ZGA pattern of gene expression is tightly regulated by epigenetic programs in developing zebrafish (Andersen et al., 2012).

The murine germ cells experience three patterns of epigenetic imprinting throughout their life cycle: 1) the sex-biased methylation of gametes, 2) global demethylation of migrating PGCs which activates the pluripotency network, and 3) locus-specific surge of demethylation upon PGC gonadal anlagen colonisation (Seisenberger et al., 2012, Hill et al., 2018).

Corresponding to the first epigenetic pattern of murine germ cells, zebrafish zygotes receive both sperm and oocyte DNA methylome (Andersen et al., 2012), however, the oocyte pattern of methylation is gradually erased from the 16-cell stage and the methylation mapping of embryo's genome entirely mimics sperm pattern by the sphere stage (Iqbal et al., 2011, Jiang et al., 2013). The germ cell specific markers (e.g. *vasa*, *dazl*, *piwi*) are part of the group of genes that are first methylated (partially or hyper) on the maternal allele but a transition to hypomethylated state by the sphere stage, imitating the paternal methylation pattern (Potok et al., 2013). Therefore, the zygotic transcription of PGC markers in zebrafish, that induces PGC specification, is under regulation of epigenetic machinery, comparable with the second wave of germ cell demethylation in mice (Seisenberger et al., 2012, Jessop et al., 2018). Moreover, high methylation of the *vasa* promoter at the onset of somitogenesis leads to significant down-regulation of its expression (Lindeman et al., 2010, Fang et al., 2013) suggesting epigenetic machinery suppresses the germ cell marker at post-ZGA, ensuring proper PGC development and function. As zygotic *vasa* is dispensable for PGC survival and juvenile gonad differentiation but required for meiosis and gametogenesis (Hartung et al., 2014), *vasa* promoter is likely regulated via epigenetic mechanisms *i.e.,* its methylation from post-ZGA to juvenile gonad differentiation and later demethylated in adult gonads, facilitating gametogenesis.

Collectively, the epigenetic events during zebrafish embryonic development reprogram the expression of Gp markers to maintain zygotic germ cell development. Indeed, in preformation mode the maternal

messaging is crucial for primary (pre-ZGA) PGC specification (sequestration), but post-ZGA PGC survival relies on epigenetic regulation.

1.2.5. PGC migration in teleosts: The Odyssey of germ cells

Compared to other animals, teleost PGC migration encounters more challenges. First, the appearance of four distinctive PGC clusters generates different starting points for migration, all requiring orchestrated coalescence (Kaufman and Marlow, 2016a). Second, the position of the clusters is random with respect to the embryonic axis, resulting in asymmetrical distances from the gonad anlage (Reichman-Fried et al., 2004).

In zebrafish, PGC motility initiates at ~5 hpf and takes place in six morphologically distinctive steps (for details see Raz, 2002). Acquisition of cell motility is key for PGC migration mediated through a subtle tuning of cell adhesion, myosin contractility, cortex-membrane interaction (Goudarzi et al., 2012), proper ion channel function (Liao et al., 2018) as well as cooperation of Dnd (Weidinger et al., 2003) and interfering RNAs (Ketting, 2007, Mickoleit et al., 2011). A molecular pathway (*i.e., rgs14* mediated upregulation, prior to onset of PGC migration) also inhibits premature migration through regulation of E-cadherin expression on PGC surface and cell-cell adhesion (Hartwig et al., 2014, Paksa and Raz, 2015).

Dead-end1 (Dnd1) is another highly conserved germ plasm RBP, required to maintain PGC localisation and migration in zebrafish, but without any vital role in their survival or proliferation (Yoon et al., 1997, Koprunner et al., 2001, Starz-Gaiano and Lehmann, 2001, Weidinger et al., 2003). In contrast, *Dnd1* is not crucial for PGC migration in mammals (Asada et al., 1994, Cook et al., 2011, Northrup et al., 2012). In zebrafish, *dnd1* has a conserved role in preserving the transcriptome of germline markers, *e.g., nanos, tdrd7,* (Youngren et al., 2005, Ketting, 2007) and tumour suppressors, *e.g., hub,* (Mickoleit et al., 2011) during germ cell development (Table 1.1 and Fig. 1.3). Also, maternal *Dnd1* in *Xenopus* exhibits a translational regulatory role for germ cell markers (Fig. 1.3) in which *Dnd1* is dramatically upregulated after fertilization and counteracts the inhibitory function of eukaryotic initiation factor "3f" facilitating *Nanos1* translation (Aguero et al., 2017).

Directed cell migration (also termed cellular chemotaxis) is essential for cell movement and organ formation (Filippi and Geiger, 2011, Iwasa et al., 2017). Chemotaxis signalling pathways help stem cells to colonise and persist in their niches (Swaney et al., 2010, Ciria et al., 2017). Across vertebrates in general, *Cxcl12* and its G-protein-coupled chemokine receptor, *Cxcr4* play a significant role in stem cell motility and development (Nagasawa et al., 1999, Ara et al., 2003a). During embryonic development, *Cxcl12* and *Cxcr4* are expressed by somatic and germ cells, respectively (Table 1.1), providing a highly conserved compass system in vertebrates to navigate PGCs towards the presumptive gonad region (Doitsidou et al., 2002, Reichman-Fried et al., 2004, Nagasawa et al., 1999). Therefore,

embryonic inactivation of *Cxcl12* or *Cxcr-4* results in altered chemotactic signals leading to abnormal PGC localisation (Knaut et al., 2003). As the universal CXCL12/CXCR4 system is involved in different embryonic cell migration (Ivins et al., 2015), a precise consonance among soma and PGC chemotaxins is required to prevent PGCs from moving to other somatic migratory domains to safeguard correct migration to gonad anlage (David et al., 2002, Hollway et al., 2007, Mishima, 2012). Indeed, the spatial expansion of CXCL12 leads to cessation of PGC motility or recruits the PGCs to off-target migratory domain (Ara et al., 2003b, Minina et al., 2007). In teleosts, the Cxcl12/Cxcr4 system has shown a conserved chemotactic function for PGC motility and directed migration. To conserve the specificity of the PGC migratory domain, the precise and restricted expression of Cxcl12a in zebrafish is maintained through internalisation of Cxcl12a by Cxcr7 (Fig. 1.3), a decay somatic CXC chemokine receptor, in the somatic environment (Boldajipour et al., 2008). Similarly, downregulation of Cxcl12a reduces its decay by Cxcr7 endocytosis indicating a robust PGC migrating pathway against the effects of gene dosage gradients (Boldajipour et al., 2008). Consistent with the robustness of the teleost PGC migration process, donor PGCs deliver to the peritoneal cavity of recipient embryos, comfortably migrate to the genital ridge and give rise to functional gametes (Okutsu et al., 2006). In medaka, the chemotaxis pathway delineates PGC migration to two sequential events; where PGCs are initially navigated by the Cxcl12α/Cxcr-4 system, from the onset of gastrulation to late neurula, while late PGC migration and homing is dominated by Cxcl12β from late neurula to mid somitogenesis (Herpin et al., 2008) suggesting gene duplication allows refined migratory processes by evolving more specialised effectors.

As is evident, PGC migration is not fully autonomous in teleosts. Regardless of the chemotaxin signals sent from home (genital ridge), the somatic environment attracts PGCs to intermediate targets. Indeed, PGCs actively migrate in association with somatic neighbours, so functional PGC clustering and transitional positioning highly depends on normal mesoderm development and proper embryonic patterning (Weidinger et al., 1999, Weidinger et al., 2002). Aligning three developmental time points, in zebrafish embryogenesis; PGC sequestration at ~32-cell stage, the onset of global motility at ~1k-cell stage and onset of PGC migration at 50%-epiboly, may indicate the PGC migration process is delayed until the somatic scaffold is ready to establish repulsive and attractive signals.

The mechanism by which the PGCs cease migration and colonise the genital ridge is an important question. Transgenic studies suggest a simple conserved model in which the PGC colonisation is dictated by the high expression of homing signals from the somatic cells of destination e.g. *Hmgcr* in fly (Santos and Lehmann, 2004) and *cxcl12a* in zebrafish (Reichman-Fried et al., 2004). Proper gonad compaction and architecture also depends on the intimate contact of PGC-soma at the destination (Van Doren, 2003, Mathews et al., 2006, Richardson and Lehmann, 2010).

Comparative studies on the pattern of PGC migration in different fish models reveal that PGC clustering, and their migratory routes are not fully conserved among teleosts (Saito et al., 2006, Nagasawa et al., 2013, Saito et al., 2014). Indeed, the diverse reproductive strategies are assumed to dictate the final location and morphology of the gonads and this is likely programmed during embryonic body patterning via adopting specific PGC migration and homing plans. In this context, poeciliids with peculiar reproductive traits (*e.g.*, viviparity and placentation) and gonad structure (unilobed) may exhibit new aspects of embryonic germ cell migration patterns and gonad ontogeny.

1.2.6. RNA interference: The mega role of micro regulators

Over the past decades, the rapidly growing ncRNA repertoire has expanded the blueprint of RNA function in translation. More recently, several classes of small regulatory nonprotein-coding RNAs, such as endogenous short-interfering RNAs, piwi-associated RNAs (Iwasaki et al., 2015) and miRNAs (Gomes et al., 2013) act as negative transcriptional and post-transcriptional gene regulators in cell differentiation and function, including complex germline development in teleosts (Leu and Draper, 2010, Mishima, 2012, Bizuayehu and Babiak, 2014).

micro RNAs

Micro RNAs (miRNAs) generally inhibit functional translation of mRNA through imperfect base-pairing of their seed region with 3′UTR mediated by RNA-induced silencing complex (RISC); hinders amino acid elongation and facilitates transcriptome degradation (Jaskiewicz and Filipowicz, 2008, Filipowicz et al., 2008, Bhin et al., 2015). miRNAs regulate specific pathways including stem cell fate, survival and function.

In zebrafish, miR-430 regulates several hundred targets during embryogenesis including a key role in germ cell development. During development, miR-430 is detectable from MBT (Table. 1.1) when the zygotic expressions begin and targets mostly maternal and sparingly zygotic transcripts to accelerate the clearance of maternal messaging and regulate zygotic programming respectively (Giraldez et al., 2006). The miR-430 correspondingly regulates the Cxcl12a/Cxcr4 signalling pathway (Fig. 1.3) by tuning the expression of *cxcl12a* from somatic cells in order to restrict the expression domain of Cxcl12 and eventually shape the PGC migration path (Proost et al., 2007, Dambly-Chaudiere et al., 2007, Staton et al., 2011).

The broad effects of RNAi on cellular chemotaxis have been demonstrated, in various developmental stages of metazoans. The excessive expression of *cxcl12a* which results in saturation of its receptors and PGC mis-migration (Herpin et al., 2008) is removed by RNAi (Mishima, 2012). The expression pattern of CXCR4 in murine ischemic tissues is also shown to be markedly regulated by RNAi (Tano et al., 2011). The role of miRNAs on PGC-specific chemotaxins and their receptors in fish models is

not explored yet, however, based on relevant studies it is inferred the embryonic Cxcr-4 expression is probably under regulation of RNAi to sustain the robustness of PGC migration in fish (Fig. 1.3).

The miRNAs recruit different strategies to promote mRNA decay. miR-430 triggers the RNA degradation process via binding to a specific region on 3′UTR and inducing poly(A) tail deadenylation (Giraldez, 2010). This machinery is also recruited to remove the maternal messages during in zebrafish. Typically, RBPs in PGC impede downregulating functions of miRNA machinery through two different mechanisms (Fig. 1.3): 1) Transcriptional stabilization; Dazl protects *tdrd7* transcripts in PGCs by preventing miR-430 deadenylation via recruiting poly(A) binding protein (Takeda et al., 2009) and 2) Translational regulation; Dnd facilitates *nanos1* and *hub* translation by overlapping the miR-430 binding site on 3′UTR and abolishing the silencing pathways (Ketting, 2007, Mickoleit et al., 2011). The upstream or early maternal transcript clearance is mediated by transcription initiation; where Nanog binds to the genomic locus of miR-430 and temporally stimulates its expression in both soma and PGC (Lee et al., 2013). This probably explains the reported exclusive localisation of zebrafish Nanog protein in the nucleus, at the onset of ZGA.

Collectively, the role of miR-430 in PGC development is twofold 1) it maintains the necessary number of PGCs through elimination of germ cell determinants in somatic cells and simultaneously 2) protects proper PGC migration through titration of somatic chemotaxin(s) involved in PGC migratory domain (Fig 1.3).

Piwi and Piwi-interacting RNAs

PIWI proteins and their interacting RNAs (piRNAs) are the main components of a highly conserved machinery which shelter cells from the constant threat of motile genetic elements called transposons. The dogma in which PIWI machinery was exclusively found in germ cells has now failed as the ubiquitous somatic expression (Nandi et al., 2016, Lewis et al., 2018) and diverse functions (Jehn et al., 2018) are reported in multicellular organisms. It is already shown PIWI and piRNAs expression are indispensable for stem cell maintenance and their regeneration (Palakodeti et al., 2008), involved in adaptive immunity (Miesen et al., 2015) and sex determination pathways (Kiuchi et al., 2014) and play a role in synaptic plasticity of memory (Rajasethupathy et al., 2012). The PIWI/piRNA apparatus in teleosts is also essential in germ cell development and gametogenesis (Ishizu et al., 2012, Ku and Lin, 2014). As piRNAs originate from protein-coding genes, transposons and intergenic regions (Fig. 1.4), they function as sequence-specific guide of Piwi proteins to protect the integrity of the genome at both transcriptional and post-transcriptional regions (Iwasaki et al., 2015). Piwi and piRNAs are localised in the nuage/cloud and expressed specifically in germ cells (Gruidl et al., 1996, Rongo et al., 1997). Earlier findings from *Drosophila* and mice have revealed that piRNAs and the associated proteins are also involved in epigenetic regulation of genome (Fig. 1.4), through telomere protection, heterochromatin modification and DNA methylation (Han and Zamore, 2014, Iwasaki et al., 2015). In zebrafish, the

genome encodes two Piwi homologues expressed in mitotic and early meiotic differentiating germ cells (Tan et al., 2002, Houwing et al., 2007).

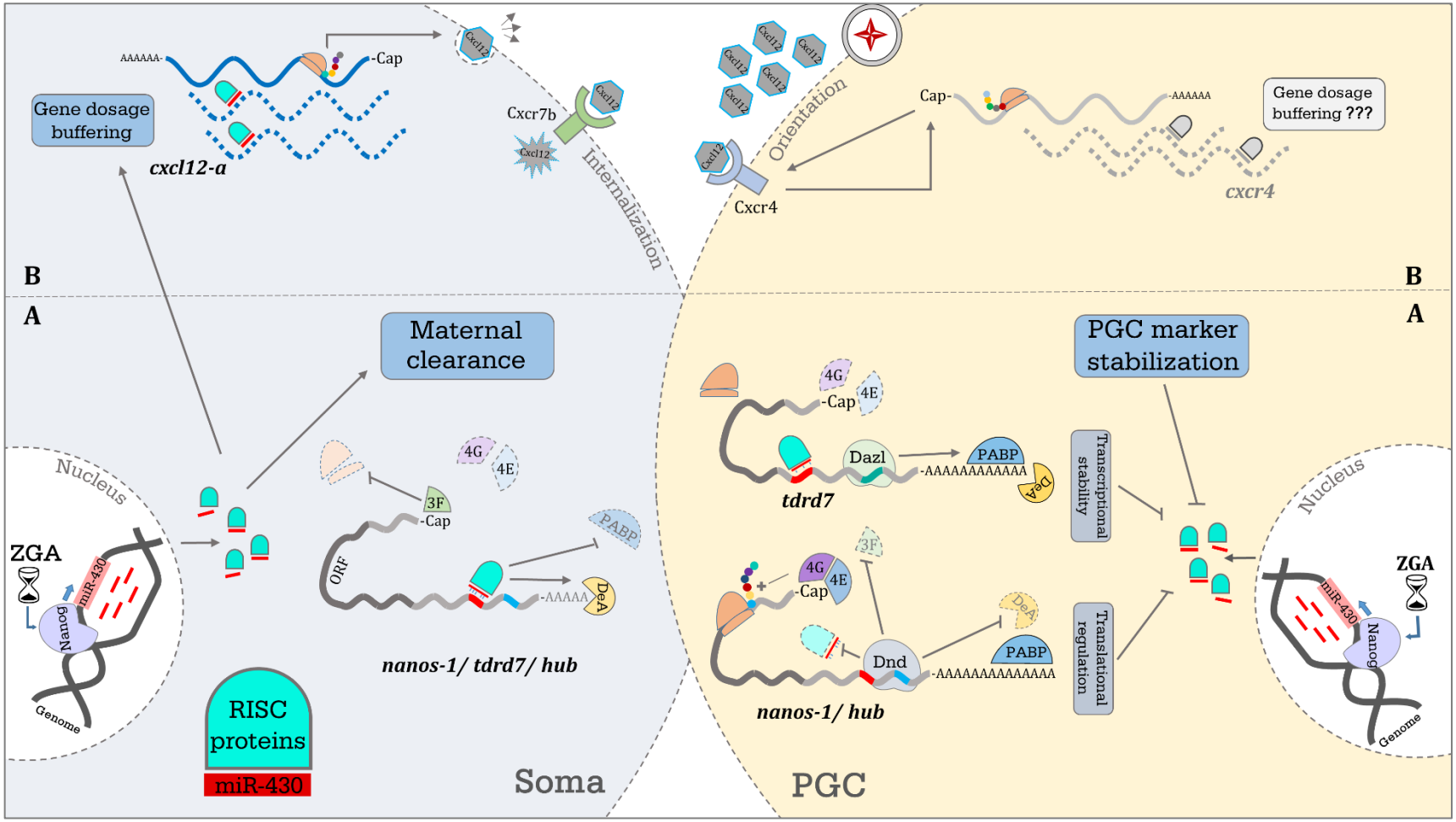

Figure 1.3. The schematic role of miR-430 machinery in conditional regulation of teleost germ cell specification and their migration as inferred from zebrafish model. As in subpanel A (below horizontal dotted line), at ZGA, miR-430 triggers the maternal message clearance when Nanog binds to miR-430 locus, stimulating miRNA transcription, in both soma (left) and PGC (right). However, the universal repressing activity of miR-430 against Gp transcripts is abrogated in PGCs where RBPs including Dazl ensures RNA stability of PGC markers (*tdrd7)* and Dnd facilitates their (*hub* and *nanos1)* translation. Dnd-1 also known to facilitate the translation of *Xenopus Nanos1* through clearing the inhibitory function of eukaryotic initiation factor 3F. As in subpanel B (above the horizontal dotted line), during PGC migration, PGCs are mobilised towards their destination through binding of the somatic chemoattractant, Cxcl12a to the PGC-specific receptor, Cxcr4b. The cooperation of miR-430 and chemokine receptor Cxcr7 spatially tunes the precise expression of *cxcl12a*. To maintain the specificity of PGC migratory domain and tune the Cxcl12a/Cxcr4 components, the excessive Cxc12a ligands are internalized in somatic cells by decay chemokine receptor, Cxcr7. Since the *cxcr-4* expression is also regulated by RNAi, in other cellular mobilization and migratory domains, it is therefore speculated that similar regulative approach is recruited in PGCs to titrate *cxcr-4b* expression to robust PGC migration. Abbreviations: deadenylase (DeA), poly(A) binding protein (PABP), eukaryotic initiation factor 3F (3F), eukaryotic initiation factor 4G (4G), eukaryotic initiation factor 4E (4E), RNA binding proteins (RBPs), RNA-induced silencing complex (RISC), micro RNA 430 (miR-430),

The z*iwi* $^{-/-}$ mutants develop an agametic testis with pro-apoptotic signals throughout the gonad (Houwing et al., 2007). Unlike Ziwi which is maternally expressed and detected from 24 hpf (Table 1.1), Zili is not detectable before 3 days post-fertilization, so Zili may not have a maternal contribution on germ cell development (Houwing et al., 2008). The spatial localisation of Piwi proteins in zebrafish explicates the scope of their function; whether their role is confined to cytoplasmic piRNA maturation and/or they are involved in epigenetic machinery (Fig. 1.4). Specifically, Zili first appears in the cytoplasm as well as nucleus and subsequently translocates to the cytoplasm, while Ziwi is exclusively located in the cytoplasm throughout germ cell development (Houwing et al., 2008). The universal cytoplasmic piRNA amplification known as the ping-pong pathway is performed by Zili and Ziwi proteins in zebrafish (Fig. 1.4). Moreover, a group of proteins act as piRNA biogenesis intermediates; Hen1 is involved in piRNA maturation by adding the 2′-O-methyl group (Kamminga et al., 2010) and Tdrd1 functions as a scaffold for piRNA modification (Huang et al., 2011). Hen1 also stabilizes miRNA and piRNA activity through the inhibition of uridylation and adenylation (Kamminga et al., 2010).

The number of germ cells in wildtype and *ziwi*$^{-/-}$ mutants remain unchanged at 2 weeks post-fertilization (wpf), however, at 6 wpf, no germ cells could be detected in *ziwi* $^{-/-}$ mutants suggesting the maternal *ziwi* is essential for PGC development and gametogenesis (Houwing et al., 2007, Ishizu et al., 2012).

Beyond the transposon defence function, Piwi proteins demonstrate sex-dimorphic characteristics, in zebrafish. Zili regulates female meiosis and ensures proper germ cell development. Contrary to the *ziwi* $^{-/-}$ line, the pro-apoptotic process is not detectable in *zili* $^{-/-}$ mutants and it is assumed that germline decay is due to aborted meiosis (Houwing, 2009). Indeed, deletion of *ziwi* from the Gp complex results in PGC depletion and generation of infertile males, while *zili* mutants retain the PGCs, however, the deprived meiosis prevents PGCs to give rise to meiotic germ cells (Houwing et al., 2008). Although Zili has been temporally detected in the nucleus of PGCs, the epigenetic role of Piwi/piRNA machinery in fish is still elusive. In medaka, Ziwi/Zili orthologs are distilled in a single gene, *opiwi* and expressed in PGCs and the central nervous system. Opiwi is not essential for PGC formation but regulates its proliferation and mobility (Li et al., 2012a).

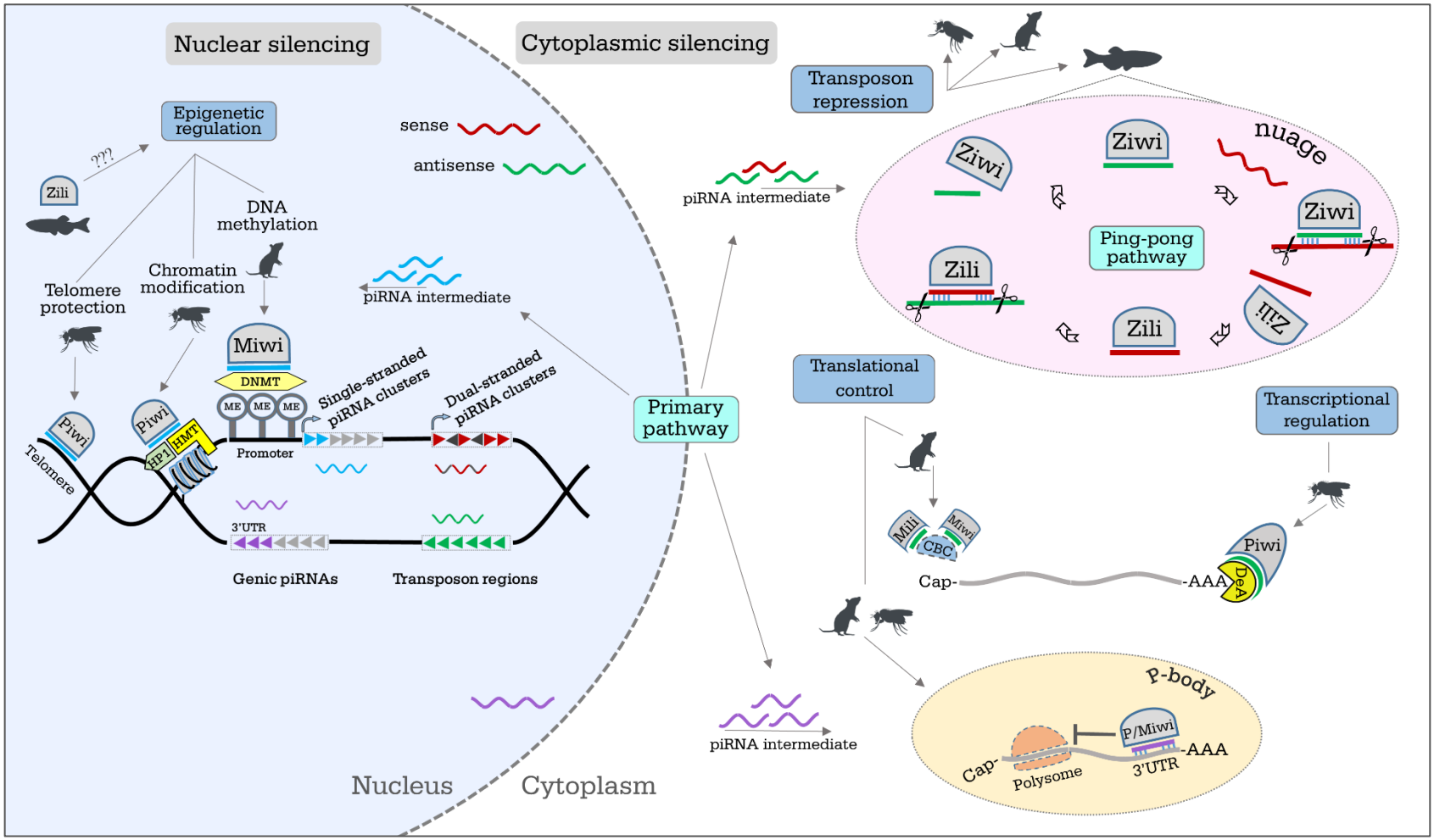

Figure 1.4. A schematic representation of piRNA/Piwi biogenesis pathway. The piRNA/Piwi machinery spatiotemporally regulates genes and transposons, in germ cells. piRNAs are processed and modified in two pathways; primarily, piRNA intermediates are transcribed from specific genomic regions (*e.g.*, single and double-stranded piRNA clusters, transposon and genic regions) and coupled with associated proteins including Aubergine and Argonaute (*e.g.*, Ziwi and Zili in zebrafish) proteins. piRNAs and the associated proteins undergo a secondary pathway called ping-pong cycle, in nuage, engaged to transposon repression. Cytoplasmic piRNA/Piwi machinery also mediates mRNA decay through mRNA deadenylase (*i.e.*, *Drosophila*) and translational silencing via interacting with mRNA cap-binding complex (observed in mice) and recruiting/forming the P-body (Thomson et al., 2008, Aravin et al., 2009) where the Piwi is mapped to 3'UTR and inactivate Polysome function. Nuclear piRNA/Piwi pathway also regulates epigenetic manipulation including heterochromatin remodelling (observed in mice), DNA methylation of regulatory regions and telomere protection (observed in *Drosophila*) (Ku and Lin, 2014) however, the role of nucleus Zili in epigenetic regulation is not yet characterised. Abbreviations: CBC, cap-binding complex; DeA, deadenylase; DNMT, DNA methyltransferase; HP1, heterochromatin protein; HMT, histone methyltransferase (Adapted and modified from Ku and Lin, 2014, Iwasaki et al., 2015).

1.3. Gonadogenesis; How germ cells contribute.

The successfully sequestered and migrated PGCs as the ancestors of gametes are homed at the genital ridge to acquire sexual identity in collaboration with soma (DeFalco and Capel, 2009, Murray et al., 2010). Subsequent to final colonisation, PGCs are sheltered and nurtured in the somatic environment of early gonad and eventually differentiate to spermato- or oo-gonial stem cells. This is decided according to the genetic architecture of the individual or environmental/social conclusion (Devlin and Nagahama, 2002, DeFalco and Capel, 2009, Bobe and Labbe, 2010). However, creating a synergy between teleostean germline and soma with distinctive totipotency background, genetic contents and cell cycle can be a challenging task.

1.3.1. Soma-gonad differentiation

Typically, in higher vertebrates, germ cells have null effects on soma-gonadogenesis, *i.e.*, in mammals, germ cells are not required to maintain the sexual identity of soma-gonad (Uhlenhaut et al., 2009, Sinclair and Smith, 2009, Matson et al., 2011), the Sertoli cells of PGC deficient XY gonads are still observed in testis cords (Youngren et al., 2005) and similarly, foetal ovarian development is not disrupted in the absence of germ cells (Maatouk et al., 2012).

In a specific group of teleosts, *e.g.*, fresh water loach (Fujimoto et al., 2010) and goldfish (Goto et al., 2012), development of gonadosoma in germ cell-deficient gonad displays a dimorphic pattern (*i.e.*, null effect) with a distinctive testicular and ovarian structure. It is therefore hypothesised gonadosoma differentiation in this group of fish follows a robust sex determination mechanism such as a sex chromosomal pathway which dictates the sexual identity of gonadosoma in early embryogenesis but also sustains its sexual integrity throughout the lifespan, similar to those of mammals. In contrast, in another group of fish species including medaka and zebrafish, PGC stimulates feminization of gonad-supporting and -steroidogenic cells. For instance, PGC deficient XX gonads in medaka, initially fail to support estrogen-producing cells (*e.g.*, granulosa) and subsequently, unaffected androgenic regulation overrides endocrinal pathways and results in testicular development (Kurokawa et al., 2007). Similarly, the germ-cell depleted zebrafish develop as sterile males with suppressed ovary-specific gene expression, *e.g.*, *cyp19α1α* and *foxl2* (Siegfried and Nusslein-Volhard, 2008, Zhou et al., 2018). Also, following estrogen treatment, the PGC-null gonads exhibit ovary-like characteristics in zebrafish (Slanchev et al., 2005) implying germ cells stimulate ovary differentiation via steroidogenic pathways.

1.3.2. Genetic identity of germ cells and soma; to sync or not to sync?

The sexual identity of gonad is contested by germ cells and soma. In some animals like housefly (Hilfiker-Kleiner et al., 1994), *C. elegans* (Ellis, 2008) and *Xenopus* (Blackle, 1965), somatic cells are sufficient to direct the sexual fate of gonad and no autonomous determination mechanism in the germ

cells governs the gonad differentiation (Murray et al., 2010). For example, when the germ cells with opposite sex are transplanted to a host soma or when the sex of the soma is reversed, the fertile gonad is differentiated based on the sex of somatic cells but not the sex chromosomes constitution of germ cells (Murray et al., 2010). In *C. elegans*, the complex sex determination (XX/XO) mechanism is underpinned by a group of soma genes, *e.g.*, *her-1*, *tra-1*, whose orchestrating is adequate for the masculinization of both XO or XX germ cells (Wolff and Zarkower, 2008, Ellis, 2008).

Contrastingly, in another group of animals including *Drosophila* (Hempel et al., 2008, Dansereau and Lasko, 2008, Casper and Van Doren, 2009) and mice (Taketo-Hosotani et al., 1989), sexual identity of the organism is determined by the sex chromosomes of germ cells, however, sexual harmony between germ cells and soma is a prerequisite for functional gametogenesis. In the female soma, XY germ cells undergo precocious meiosis (Uhlenhaut et al., 2009), whereas in the testis environment, XX germ cells encounter cell cycle arrest (McLauren, 1981); in both cases, germ cells do not survive to normal gametogenesis (Murray et al., 2010). In other words, although germ cell sex chromosomes override the environmental signals and determine the sex, their sex-determining effectors cannot repeal the somatic effect or solely supervise normal gonad differentiation (Swain and Lovell-Badge, 1999, Koopman et al., 1991). Similarly, in *Drosophila* both XY and XX germ cells in sex reversed soma cannot manage to complete functional gonadogenesis indicating soma individually is not able to maintain the gonad development either (Hempel et al., 2008, Waterbury et al., 2000).

The sexual identity of fish have shown to be determined by genetic (Matsuda et al., 2002, Volff and Schart, 2001), environmental (Baroiller et al., 2009a) and social signals (Hobbs et al., 2004). Therefore, the sexual plasticity in teleosts potentially gives the somatic and germ cells more capacity to influence the sex differentiation pathway. In rainbow trout, spermatogonial stem cells transplanted in the ovary give rise to fully matured oocytes, with the ability to produce viable offspring of both sexes (Okutsu et al., 2006). Correspondingly, the transplantation of oogonial cells is sexually synched with the recipient male soma (Yoshizaki et al., 2010). In zebrafish, ovary proliferates the donor spermatogonial cells and nurtures them to advanced oocytes (Nobrega et al., 2010, Wong et al., 2011). It may be concluded that the steroidogenic and somatic supporting cells in fish establish the sexual fate of gonad, independent from the genotype of germ cells, however, the function of *foxl3*, a germ cell marker, has shown a discrepancy in this conclusion as it affects egg-sperm decision in medaka (Nishimura et al., 2015). In *foxl3*$^{-/-}$ medaka, testis development in XY individuals is intact, while XX gonads lack type I mitotic cells and show periphery spermatogonial stem cells with a male-specific expression pattern (Nishimura et al., 2015). This concludes that *foxl3* is one of the effectors which designate feminizing effects to medaka germ cells (Nishimura et al., 2018), however, it cannot dictate its feminising inherent to XY gonadosoma. Therefore, teleosts may suggest a third method of gonad sex differentiation in which a lack of germline-soma synchronisation leads to chimeric intersex gonadogenesis.

1.3.3. Germ cell nesting and sexual differentiation

Immediately after genital ridge colonisation, the germ cells encounter crucial decisions such as 1) proliferation to stem cell self-renewal or differentiation, 2) acquisition of sexual identity *i.e.*, oogonia or spermatogonia, and 3) cell cycle status; mitosis or meiosis (Kimble, 2011). The molecular regulators involved in the decisions have been studied in different models (Harigaya and Yamamoto, 2007, Angelo and Van Gilst, 2009). However, lack of a distinctive sex determination and (early) differentiation mechanism in zebrafish, the most popular fish model, constrain insights into post-colonisation dynamics of germ cells in fish.

In medaka, two types of germ cells — cyst forming and individually generating are evident post PGC colonisation (Marlow, 2010b). The cyst-forming germ cells (type II) proliferate by two to four incrementally accelerated mitotic divisions in preparation for meiotic proliferation and initiation of gametogenesis (Saito et al., 2007). The cysts are characterised by skirting a thin layer of somatic cells and incomplete cytokinesis that interconnects the differentiated germ cells (Saito et al., 2007). The type I germ cells (individual stem-like cells) are surrounded by somatic cells (Saito et al., 2007) and are divided into two subtypes — quiescent and active cells (Nishimura et al., 2015). Indeed, type I germ cells, proliferate through a stochastic self-renewal process and function as an inexhaustible source of germ cells for gametogenesis (Saito and Tanaka, 2009). The study of medaka *zenzai* mutants (Morinaga et al., 2004), in which the type I germ cells are depleted, demonstrates that type I germ cells are critical for both gonad formation and functional gametogenesis (Saito et al., 2007). The transition from Type I to type II in the testis is usually postponed to the pubertal gonad when the molecular regulators of meiosis are observed in spermatogonia (Nishimura et al., 2015).

Meiosis is a germ cell-specific cycle specialised to reduce ploidy in gonial cells that transition from mitosis in a sex- and species-dependent manner (Kimble, 2011). For example, this mitosis-meiosis transition appears triggered by nutritional cues in *S. cerevisiae* (Jin and Neiman, 2016), BMP signalling in *Drosophila* (Kawase et al., 2004) and the retinoic acid (RA) pathway in mice (Griswold, 2016). The murine mitosis/meiosis decision is modulated by both sex-dependent and -independent pathways but its timing in the respective sex is regulated by the presence or absence of the sex determining gene (Feng et al., 2014). *Stra8*, one of the target genes of the RA signalling pathway and the miosis gatekeeper, is sex-specifically expressed in the fetal ovary and mediates meiosis onset (Anderson et al., 2008); whereas, the simultaneous *Stra8* signalling is blocked in male fetal germ cells through expression of cytochrome P-450 enzymes. Moreover, the translational repressors, NOS2 and DAZ, suppress the constituents of meiosis machinery (e.g. *Stra8* and *Cycp3*) in germ cells of either sex (Kimble, 2011).

In teleosts, the RA signalling network is thought to be involved in the mitosis/meiosis decision (Pradhan and Olsson, 2015), however, *stra8* has been characterised in only a few fish species (Dong et al., 2013, Pasquier et al., 2016). Correspondingly, in medaka, a species lacking *stra8*, retinoic signalling has been

detected in meiotic germ cells of both testis (*i.e.,* somatic and premeiotic spermatogonial cells) and ovary (*i.e.,* meiotic oocytes) prior to sex determination (Adolfi et al., 2016). This indicates the RA pathway may play a role in meiotic proliferation in teleosts, but unlike in mice, it does not trigger meiosis in either sex or is not synchronised with the sex determination decision. Indeed, the teleostean mitosis-meiosis transition may evolve to liberate gametogenesis from genetic sex determination mechanisms and give more plasticity to their reproductive strategies.

In some fish species including medaka (Hamaguchi, 1982) and three-spined stickleback, *Gasterosteus aculeatus*, (Lewis et al., 2008) the germ cell proliferation pattern has shown a sex-dimorphic discrepancy, where the developing embryos with a significantly higher number of GSCs differentiate to females. However, the start point of deviation in germ cell quantity is not chronologically correlated, among different species (Swarup, 1958, Iwamatsu, 2004). In medaka, the migrating PGCs undergo a few rounds of mitotic cycles, prior to gonad anlagen colonisation (Saito and Tanaka, 2009); however, the significant sex-dimorphic pattern of GSC proliferation in medaka occurs post-genital ridge homing (Hamaguchi, 1982). Unlike medaka, the migrating PGCs are assumed to be mitotically inactive in some fish species including three-spined stickleback (Lewis et al., 2008) and zebrafish (Ye et al., 2019). In zebrafish, live screening of labelled PGCs demonstrates the sex-dimorphic number of PGCs diverge one day post-fertilization, right after germ cell colonisation (Ye et al., 2019). Conclusively, the sex-dimorphic pattern of germ cell proliferation in some teleosts may correspond with the proliferating status of male and female germ cells; quiescent division of spermatogonial stem cells type I versus the rapid mitosis of oogonial cells type II.

The reproductive biology of teleosts is known to be diverse and is likely reflected/underpinned by similarly diverse cellular and molecular pathways. Further, there is limited understanding of these events in poeciliids, a key taxon, which shares aspects of both oviparity and viviparity. As a lead up to understanding the critical events involved in early gonadogenesis and sex differentiation in an invasive poeciliid, *G. holbrooki*, this chapter has rigorously reviewed the existing literature to identify knowledge gaps such as sex-dimorphic patterns of germ cell numbers, the time-point of sex differentiation and the arrangement of gonial stem cells in the presumptive gonad, and their molecular determinants.

Table 1.1: The functional scope and spatiotemporal expression of genes involved in PGC development and gametogenesis in fish models.

Genes	Functions	Spatiotemporal expression of genes in germ cells during PGC development **Oogenesis** (Gp assembly) / **Cleavage** (emergence) / **MBT** (Specification) / **Gastrulation** (migration) / **Pharyngula** (homing) / **Larvae** (differentiation)	References
buc	- Oocyte polarity - Regulates micropyle numbers - Gp formation - Gp distribution		(Bontems et al., 2009) (Heim et al., 2014)
hub	- The exact function is unknown		(Mickoleit et al., 2011)
rbpms2	- oocyte asymmetric polarity - *buc* dosage and localization		(Heim et al., 2014) (Kaufman and Marlow, 2016a)
zili	- meiosis regulation - piRNA biogenesis		(Houwing et al., 2008)
ziwi	- PGC specification and maintenance - piRNA biogenesis		(Houwing et al., 2007)
vasa	- Translational regulation - PGC migration (maternal transcript) - Regulates female differentiation		(Yoon et al., 1997) (Gustafson and Wessel, 2010) (Hartung et al., 2014)
nanos1	- PGC survival and proliferation - PGC motility and migration		(Koprunner et al., 2001) (Curtis et al., 1997)
dazl1	- Vital for PGC survival and maintenance* - Transcriptional stability of *tdrd7* - Relieves miR-430 repression		(Takeda et al., 2009) (Li et al., 2016)

granulito	- Unknown on germ cell development - Gastrula arrest in morphants	(Strasser et al., 2008)
dnd-1	- PGC motility and migration - Protect mRNAs against miR-430	(Weidinger et al., 2003) (Ketting, 2007) (Aguero et al., 2017)
nanog	- Regulates PGC proliferation - Induces maternal clearance during ZGA	(Lee et al., 2013) (Wang et al., 2016)
oct4 *	- A pluripotency marker - Unknown in fish PGC development	(Sanchez-Sanchez et al., 2010)
dynein	- Germ cell division - PGC size maintenance	(Strasser et al., 2008)
mylkα	- Regulates cell contractility	(Hartwig et al., 2014) (Paksa and Raz, 2015)
macf-1	- Organelle localization - mRNA localization - Oocyte polarity	(Gupta et al., 2010)
kif5βα	- Enrich Gp at cleavage furrows - Dorsoventral patterning	(Campbell et al., 2015)
tdrd7	- Regulates PGC size homogeneity - Regulates normal PGC proliferation	(Strasser et al., 2008)
tdrd1	- A scaffold for Piwi proteins - murine testis differentiation	(Chuma et al., 2006) (Strasser et al., 2008)
tdrd6	- Bb mobility - mRNA deposition to nascent PGCs	(Roovers et al., 2018)
tdrd9	- Interaction with Piwi proteins	(Dai et al., 2017)
tdrd4	- Unknown in fish - Involved in murine spermiogenesis	(Pan et al., 2005) (Strasser et al., 2008)
hen1	- miRNA and piRNA stability - piRNA maturation - Sex differentiation timing	(Kamminga et al., 2010)

cxcl12	- Somatic chemoattractant with affinity to Cxcr4		(David et al., 2002) (Paksa and Raz, 2015)
cxcr4	- The PGC-specific receptor for Cxcl12 - Proper PGC shape for motility		(David et al., 2002) (Paksa and Raz, 2015)
rgs14a	- Regulates cell-cell adhesion - Mediates polar protrusion formation - Involved in the onset of PGC motility		(Hartwig et al., 2014) (Paksa and Raz, 2015)
miR-430	- Maternal RNA clearance - Gene dosage buffering in PGC and soma - PGC-specific RNA clearance in soma		(Giraldez et al., 2006) (Giraldez, 2010) (Mishima, 2012)

* Exclusively observed in medaka

The schematics of developmental stages are adopted and modified from Raz, 2002.

RNA binding

Cytoskeletal/motor protein

The expression is not specific to germ cell

Methyltransferase

micro RNA

The expression is germ cell-specific

Tudor domain-containing

Chemotaxin/Chemotaxin receptor

Transcriptional factor

Chapter II

PGC markers cloning and characterisation

Chapter 2 | Structure, content and phylogenetic relationship of key genes involved in PGC development and sex differentiation isolated from *G. holbrooki*

Abstract

Studying spatio-temporal expression of germline markers is a powerful tool to investigate the chronology of gonad formation, differentiation and gametogenesis. Cloning, and characterisation of target genes is therefore essential, particularly in non-model organisms whose genetic information is scarce, and relevant assays/studies are not readily available. For this purpose, the full-length cDNA of the key germline markers including *cxcr4*, *dazl*, *dnd*, *nanos1*, *piwi II* and *vasa* of *G. holbrooki* were cloned. This was conducted by rapid amplification of cDNA ends (RACE) library generation from testis and ovary, cloning the amplified RACE fragments into a plasmid vector and sequencing the fragments. Subsequently, the full-length cDNAs were characterised and the domains involved in regulatory functions of the target genes annotated. Of the recognised regulatory regions, the predicted polypeptides of *dazl* contained the RNA recognition motif (RRM) and poly(A) binding protein (PABP) domains. *dnd* encoded two alternatively spliced variants, however, both variants had retained the conserved RRM and DSRM-DND domains in the predicted polypeptide. Similarly, *piwi II* had the characteristic PAZ domain containing a nucleic acid-binding interface in the N-terminus and a 5′ RNA guide anchoring site at the C-terminus. A DEAD-box helicase motif was conserved in *vasa* and contained RNA- and ATP-binding sites in the predicted protein. A chemokine binding site and zinc-finger motif that are diagnostic of *cxcr4* and *nanos1*, respectively were also identified. Overall, the predicted amino acids of all cloned genes showed high similarity with the respective genes of other poeciliids and higher vertebrates, as was evident from the phylogenetic trees. These results form a significant resource to study PGC development, gonadogenesis and potential manipulation of sex in this species.

2.1. Introduction

In sexually reproducing animals, germ cells are specified from a group of precursor cells formed during early embryogenesis called primordial germ cells (PGC). Typically, the early specification is known to occur via zygotic activation and epigenetic reprogramming, *i.e.*, induction mode or by relying on maternal deposits *i.e.*, preformation mode (Johnson et al., 2001, Johnson et al., 2011a). The specificity of PGCs (Koprunner et al., 2001, Li et al., 2016), their proliferation (Feng et al., 2020) and route of their migration (Li et al., 2012b, Paksa and Raz, 2015) is regulated by a group of specific genes/molecules. Indeed, these genes recruit diverse regulatory plans including ncRNA machinery (Slanchev et al., 2009, Mickoleit et al., 2011), signalling pathways (Goudarzi et al., 2013, Paksa and Raz, 2015), and RNA-binding competence of their protein (Knaut et al., 2000, Gustafson and Wessel, 2010) to safeguard proper PGC formation. Therefore, cloning and characterisation of these key markers is necessary to study germ cell development in any species of interest.

Sharing reproductive traits with both mammals and teleosts, viviparous poeciliids have been of interest to study the evolutionary transition from lecithotrophy to placental matrotrophy (Pollux et al., 2009, Blackburn, 2015, Pollux et al., 2014). However, basic biological information such as germline determination, the molecular pathways involved in PGC formation and their function in poeciliids remain poorly understood. To address this, study of candidate genes with known roles in PGC sequestration, maintenance, and migration in teleost, is necessary in *G. holbrooki*. Importantly, the *G. holbrooki* is emerging as an ideal system to study the effects of environmental endocrine-disrupting chemicals, EDCc, (Kumar et al., 2020) due to its high tolerance to environmental parameters changes (Batty and Lim, 1999, Pyke, 2005). An in-depth understanding of factors regulating *G. holbrooki* reproduction would also aid the development of reproductive biotechnologies used to biologically control the pest species (Taylor et al., 2012).

In this chapter, six genes were cloned and characterised from *G. holbrooki* with their key role in PGC function during embryonic development, germ cell maintenance and its maturation in teleosts (Chapter 1). Specifically, full-length cDNA of six genes, namely *deadend* (*dnd,* regulating miRNA activity in germline), *P-element Induced WImpy testis II* (*piwi II*, protecting germ cells from transposon silencing), *dead box4* (*ddx4* or *vasa* homologous, maintaining the specificity of migrating PGCs in soma environment), *deleted in azoospermia-like* (*dazl*, a germline-specific RNA repressor and activator), *nanos1* (a zinc-finger coding gene with somatic repressing role in germ cells), and *C-X-C chemokine receptor type 4* (*cxcr4*, a component of chemotaxis signalling in PGCs) were targeted. This with a view to understand the basic biology of PGC formation and their dynamics during early development (Chapter 3 and 4), their biogenesis in gonad and accumulation in gametes (Chapter 4) in this species.

2.2. Methods

Broadly the cloning and characterisation strategy involved partial CDS identification, RACE library generation, amplification of full-length cDNA ends using touch down (TD) PCR, its cloning, sequencing and characterisation. The critical domains of the cDNAs of interest were characterised by the conserved polypeptide motifs in the predicted proteins. The homology and evolutionary relatedness were also compared by constructing phylogenetic trees for each of the homologues across multiple vertebrate taxa.

2.2.1. Wild fish collection and housing

Juvenile (females; 150 ±15 mg, males; 95 ± 12 mg) and adult (females; 560 ± 80 mg, males; 210 ± 43 mg) Gambusia from both sexes (n = 22 females, n = 17 males) were collected, from the Tamar Island Wetland Reserve, Tasmania (41°23.1'S; 147°4.4'E). The fish were transported to the Institute for Marine and Antarctic Studies (IMAS), Taroona, University of Tasmania. They were maintained in a recirculating facility for small fish. Rearing conditions are summarized in Table 2.1. The fish were fed with commercial pellets (TetraMin1 tropical granules, Germany) and freshly hatched Artemia nauplii (INVE Aquaculture, USA).

Table 2.1. Housing conditions of *Gambusia*

Parameters		**Range**
Water quality	Temperature (˚C)	25.0 ±1.0
	pH	7.1-7.5
	Dissolved oxygen (%)	85-90
	Salinity (g/l)	0
	NO_2 (mg/l)	<0.008
	NH_4^+ (mg/l)	<0.009
Rearing conditions	Female tank volume (l)	6
	male tank volume (l)	2
	Water flow (l/h)	10-13
	density (fish/10 l tank)	15-25
	Light regime (L:D)	16:9 h

All procedures including biological measurement, anaesthesia, euthanasia, dissection, tissue sampling and injection were undertaken as per established and approved protocols (Inland Fisheries Service Tasmania and University of Tasmania Animal Ethics permit, A0015354).

2.2.2. Tissue sampling, RNA/DNA isolation and cDNA synthesis

Mature female fish (n = 5) were selected and euthanised with 250mg/L of AQUI-S®. The gonads were isolated and harvested for RNA extraction. To obtain the highest quality RNA, the tissues were immediately cut to small slices (~50 mm^3) and stored in RNA*later*® (Thermo Fisher Scientific, VIC, Australia) at 2-8 ˚C, overnight for stabilisation. Then the RNA*later*® was removed and the samples

stored at -80 ˚C until use. For RNA extraction, the 30 mg of frozen tissue was thawed, homogenised carefully in lysis buffer using syringe and needles (19 and 27 G) and RNA was isolated using ISOLATE II® RNA Mini kit, (Bioline, UK) according to the manufacturer's instructions. Any gDNA contamination was subsequently eliminated from RNA samples using Ambion™ DNase I (Thermo Fisher Scientific, USA) and the DNase treated samples were purified by a column-based method using Monarch® RNA Cleanup Kit (NEB, England). The RNA integrity was verified by visualising the integrity of 18S and 28S ribosomal RNA on 1% TAE/agarose gel stained with SYBER™ Safe (Thermo Fisher Scientific, USA). The purified RNA was then quantified using Qubit™ RNA high sensitivity (HS) assay kit (Invitrogen, Australia) and reverse transcribed using Tetro cDNA Synthesis Kit (Bioline) according to manufacturer's protocol. The reverse transcription reaction contained 200 units of MMLV reverse transcriptase, 1X RT buffer, 15 units of RNase inhibitor, 0.75 mM dNTP mix, 300 ng Oligo(dT)18 primer mix (Tetro cDNA synthesis kit, Bioline). The resulting cDNA diluted five times and stored in -20˚C until use.

To identify the introns of the target genes, gDNA from the caudal fin and muscle of adult fish (n = 6) was isolated using ISOLATE II Genomic DNA Kit (Bioline), and the 5′ and 3′UTR primers were used to amplify the gDNA complete sequence including the introns.

2.2.3. Amplification of Partial coding sequences

To obtain partial coding sequences from *G. holbrooki*, full-length cDNA sequences of the genes of interest (GOI) from several other poeciliid species including *Poecilia latipinna*, *P. mexicana*, *P. formosa*, *P. reticulata* and *Xyphophorus maculatus* were retrieved from the NCBI database (Sayers et al., 2009) were selected and aligned using MUSCLE (Edgar, 2004). A primary and a nested pair of degenerate primers were designed using the most conserved region of consensus sequence (Fig. 2.1) and applied in PCR amplification of the respective target genes. The cDNA of ovary, in which all the GOIs are normally expressed was used as template in PCR reactions. The specific PCR products were identified based on expected size on a 0.7%-1% agarose gel. The bands were excised from the agarose gel and purified using ISOLATE II PCR and gel kit (Bioline, NSW, Australia). The purified products were sequenced and used to design gene specific primers (GSP) for RACE amplifications.

2.2.4. RACE library generation and amplification of cDNA ends

Full length amplification from mRNA from GOI was facilitated by GeneRACER™ kit (Invitrogen, Australia). Briefly, A RACE library was made by selection of intact RNA and its protection by capping, followed by reverse transcription and modifying the cDNA ends to facilitate the amplification of target cDNA from both 5′ and 3′ ends (Fig. 2.2).

Full-length mRNA selection

To select for intact mRNAs, calf intestinal phosphatase (CIP), was used to cleave the free 5' phosphate of non-mRNAs and truncated mRNAs, with 5′cap and poly (A) tail protecting intact mRNAs (Fig 2.2A). Isolated total RNA was quantified using Qubit4® fluorometer (Thermo Fisher Scientific, USA). About 2-5 µg of total RNA was used in a 10 µl dephosphorylation reaction (Table A1), mixed well and incubated at 50 ˚C for 1 hour. The dephosphorylated mRNA was column purified as per the manufacturer's instructions and eluted with 8 µl of DEPC water. Integrity of the RNA was verified using TAE/agarose gel electrophoresis.

Decapping full-length mRNA and oligo ligation

The intact mRNA was subsequently treated with tobacco acid pyrophosphatase (TAP) to remove the 5′cap (Fig. 2.2B). Specifically, a 10 µl decapping reaction was prepared (Table A2), mixed well by pipetting and incubated at 36 ˚C for 1 hour. The decapped mRNA was column purified, eluted in 8 µl of DEPC water, and the integrity of RNA verified on agarose gel.

Immediately, a specific RNA oligo was ligated to the 5′ end of the mRNA (Fig. 2.2D). The ligation reaction (Table A3) was as described in the RACE kit. The reaction was incubated at 65 ˚C for 5 min to remove RNA secondary structure and placed on ice for 10 min for ligation. The ligated mRNA was column purified and eluted in 11 µl of DEPC water.

Reverse transcription by a modified oligo dT

To amplify the 3′end of mRNA, reverse transcription (RT) was carried out by a modified dT primer containing 18 d(T) along with a priming site at its 5′end (Fig. 2D), as per instructions. Briefly, dNTP mix and the modified oligo dT were added to the ligated RNA and incubated at 65 ˚C for 5min to relax any RNA secondary structures. The remaining reaction components were then added (Table A4), incubated at 45 ˚C for 90 min and subsequently the RT was inactivated at 85 ˚C for 15 min. The synthesised RACE library was stored at -20 ºC until use for PCR reaction. The resulting RACE library contained modified cDNA ends (Fig. 2.3A) with a set of nested priming sites (Fig. 2.3B) for PCR amplification on each end.

GSP design and PCR conditions for RACE amplifications.

To amplify cDNA ends two GSPs were designed for each gene to use in primary and nested RACE PCR reactions. The primers were designed to meet the following conditions; 1) high GC content (50-70%), 2) 23-27 nucleotide length, 3) low GC content (less than three) at their 3′ ends, 4) no self-complementary sequences within the primer (hairpin) or with the primers of ligated oligos (primer-dimer), and 5) annealing temperature greater than 72˚C.

To amplify target cDNA ends, Touch Down (TD)-PCR was carried out to enhance amplification of specific targets (Don et al., 1991, Roux, 1995). Specifically, the initial annealing temperature was set 4 to 5˚C higher than the optimal annealing temperature, and it was gradually decreased over 10-15 cycles until it reached the optimal annealing temperature (Table A5). For nested TD-PCR, 1µl of primary PCR product was diluted 500 times and 1µl of it was used as the template. The PCR products were visualised in 1% agarose gel and their size verified.

2.2.5. Cloning fragments of interest

Bacterial cloning of full-length cDNAs from all six GOI was carried out using the TOPO TA cloning kit.

Fragment insertion

Briefly, the TOPO reaction was prepared (Table A6) using TOPO® TA Cloning kit (ThermoFisher, USA) and incubated for 5 min at room temperature as per the manufacturer's instructions.

Vector transformation and fragment proliferation

One Shot® chemically competent *E. coli* (Thermo Fisher Scientific, VIC, Australia) was used for chemical transformations. Briefly, 3 µl of insertion mix was added 30 µl of competent cells, swirled gently and incubated for 15 min on ice. The cells were then heat-shocked for 30 sec at 42 ˚C and immediately put on ice. The cells were then allowed to recover by incubated in 25 µl of S.O.C medium at 37 ˚C, for 1 hour. A 50 µl of X-gal solution (Thermo Fisher Scientific, VIC, Australia) was first spread on a pre-warmed selective plate. Then about 40 µl of recovered cells were spread, sealed, and incubated at 37 ˚C for 12-14 hours.

Vector isolation and insert verification

The positive colonies (n = 7-10/ plate) from selective plates were isolated and the vectors were purified using PureLink® Quick Plasmid Miniprep kit (Thermo Fisher Scientific, VIC, Australia). The specificity of the inserts and their orientation were verified using PCR screening as well as sequencing.

2.2.6. Gene mapping, annotations, and phylogenetic tree construction

For gene mapping and multiple alignment, the available genome sequences, and their accession numbers (Table 2.2) were collected from the National Centre for Biotechnology Information, NCBI data base (Table A7). For gene annotation, the predicted proteins from cloned gene sequences were checked for conserved domains using the NCBI conserved domain database (Marchler-Bauer et al., 2015). The number of introns in the target genes were identified via end-point PCR screening and their approximate size were verified using TAE/agarose gel electrophoresis, before reconstructing the schematic for genomic loci of each genes (Table A8). To establish phylogenetic relationships based on

each of the genes, the predicted protein sequences from a cartilaginous fish, 11 teleosts, a reptile, an ave, and a mammal were extracted from the NCBI data base and aligned for each gene, separately. The mammal species as the reference was used as a base taxon for relative comparison.

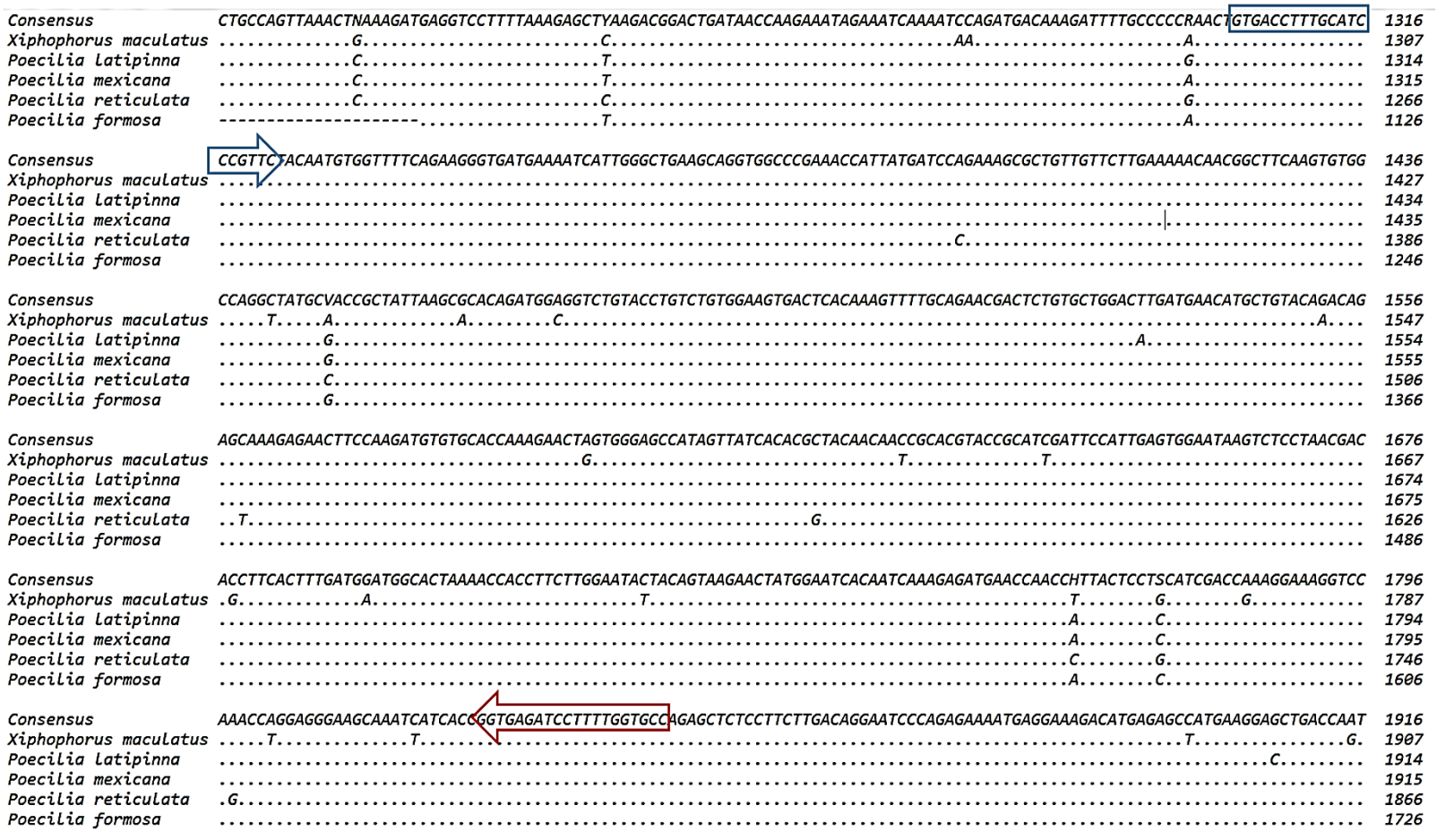

Figure 2.1. A representative (*piwi II*) multiple sequence alignment of homologous genes in live-bearing poeciliids. The degenerate primers were selected based on the most conserved regions. The blue and red arrows show the location of forward and reverse degenerate primers, respectively. Where sequences were non-identical, a degenerate base code (IUPAC) was used to design primers.

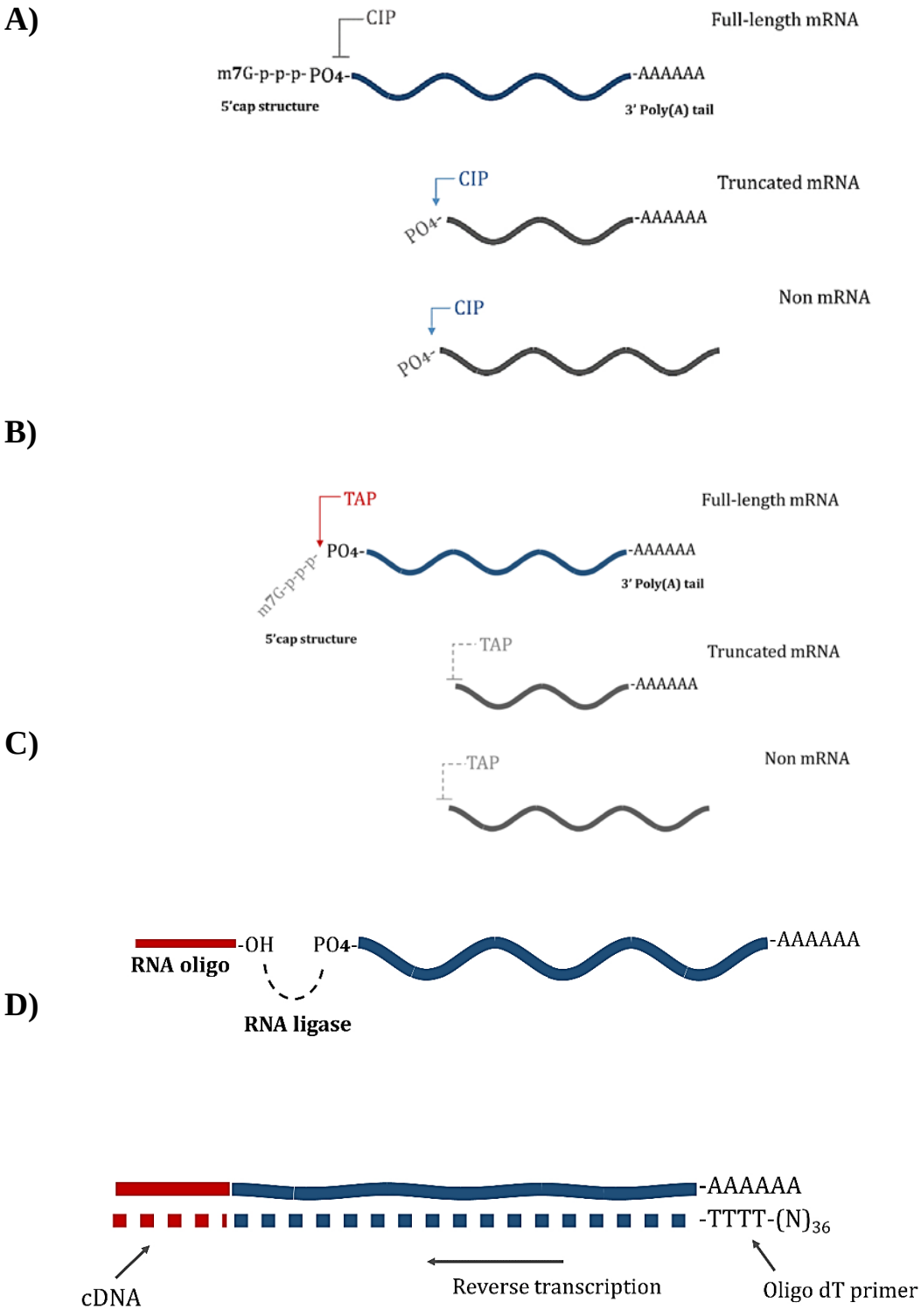

Figure 2.2. Schematic panel showing the stages of mRNA modification in the RACE strategy employed. This included, intact mRNA selection by removing truncated and non-mRNAs (A), 5′cap elimination (B), 5′RNA oligo ligation (C) and reverse transcription to generate modified 3′ RNA ends (D).

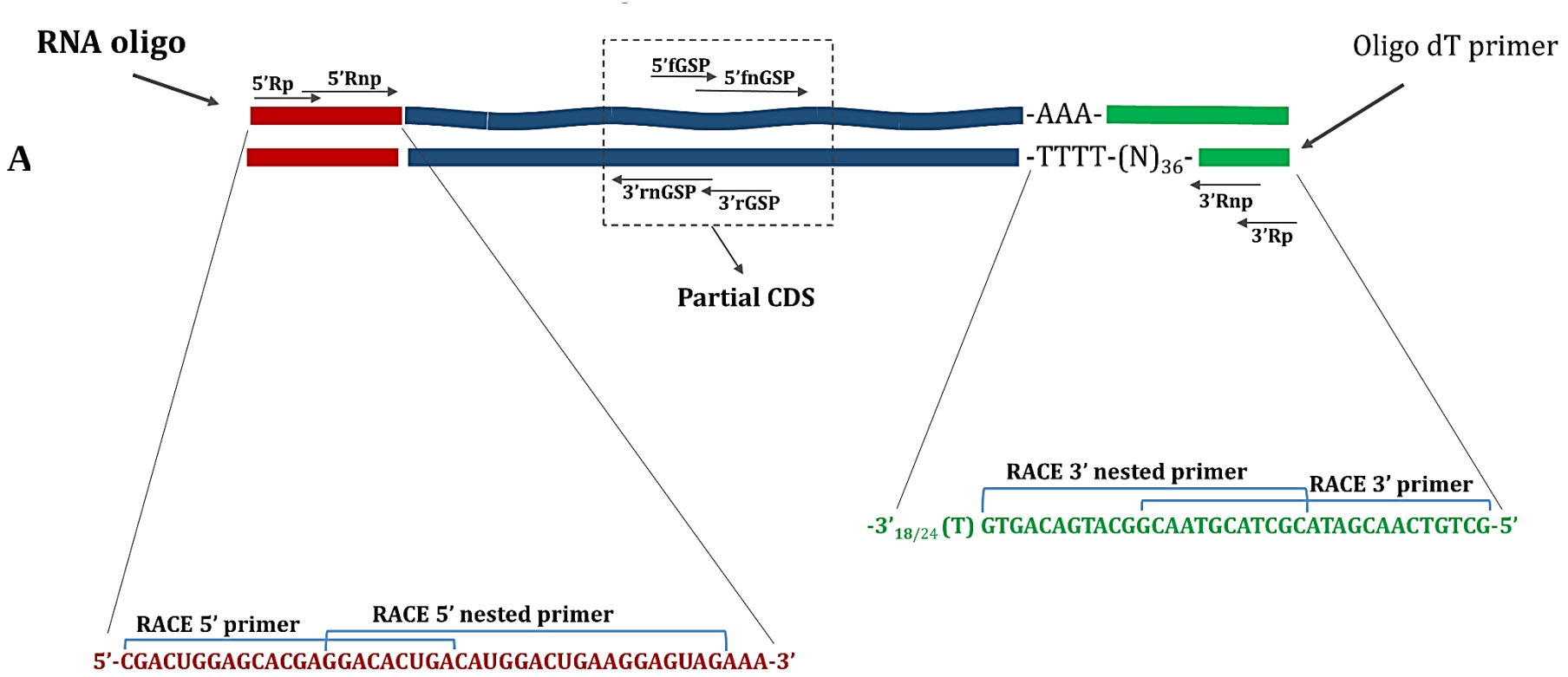

Figure 2.3. Schematic showing modified cDNA ends. The ligated sequences contain primary and nested primer sites facilitating cDNA end amplification (A). Primer pairs used for amplifying the 5′ and 3′ ends of the cDNA are marked as well as presented in B. Abbreviations; Rp, RACE primers; Rnp, RACE nested primers; fGSP, forward gene-specific primers; fnGSP, forward nested gene-specific primers

B

Primer pairs	Primary PCR	Nested PCR
5'end amplification	5'Rp D 3'rGSP	5'Rnp D 3'rnGSP
3'end amplification	5'fGSP D 3'Rp	5'fnGSP D 3'Rnp

The phylogenetic trees were produced using neighbour-joining method with bootstrap resampling (1000 replicates), and the genetic distance was measured by Jukes and Cantor model (Jukes and Cantor, 1969) in Geneious Prime® 2020.2.3.

2.3. Results

The full-length cDNA of six genes that are key to teleostean PGC development and function were successfully cloned and characterised from *G. holbrooki*. The salient features of each of the marker genes are summarised below.

2.3.1. *piwi II* in *G. holbrooki* encoded domains necessary for gene silencing.

The genomic structure of *piwi II* in *G. holbrooki* comprised of 24 exons, while the cDNA contained 97 bp 5′UTR, 294 bp 3′UTR and 3162 bp coding sequence (Fig. 2.4A) which encoded 1054 amino acids (aa) (Fig. 2.4B). The *piwi II* cDNA from *G. holbrooki* showed 94-95% homology with *piwi II* from poeciliid species and the closest homology to *X. helleri*. Multiple sequence alignments demonstrated high homology between Piwi II predicted protein in poeciliids and *G. holbrooki*, ranging from the lowest (84%) with *P. formosa* and to the highest (93%) with *X. maculatus*. Similarly, phylogenetic analysis of the complete proteins clustered *G. holbrooki* Piwi II with those of poeciliids (Fig. 2.5). However, the homology of *G. holbrooki* Piwi II with *Mus. musculus*, *D. rerio* and *Oryzias latipes* was relatively low at 56%, 66% and 67%, respectively. The predicted Piwi II polypeptide in *G. holbrooki* was characterised by the presence of Piwi, Argonaut and Zwille (PAZ) domains, and a non-specific PIWI-like superfamily domain at C-terminus (Table 3.2). The PAZ domain contained a nucleic acid-binding interface (Fig. 2.4B), while the PIWI-like superfamily domain consisted of two subdomains, one of which provides the 5′ anchoring of the guide RNA and the other is the active site for slicing function (Fig. 2.4B).

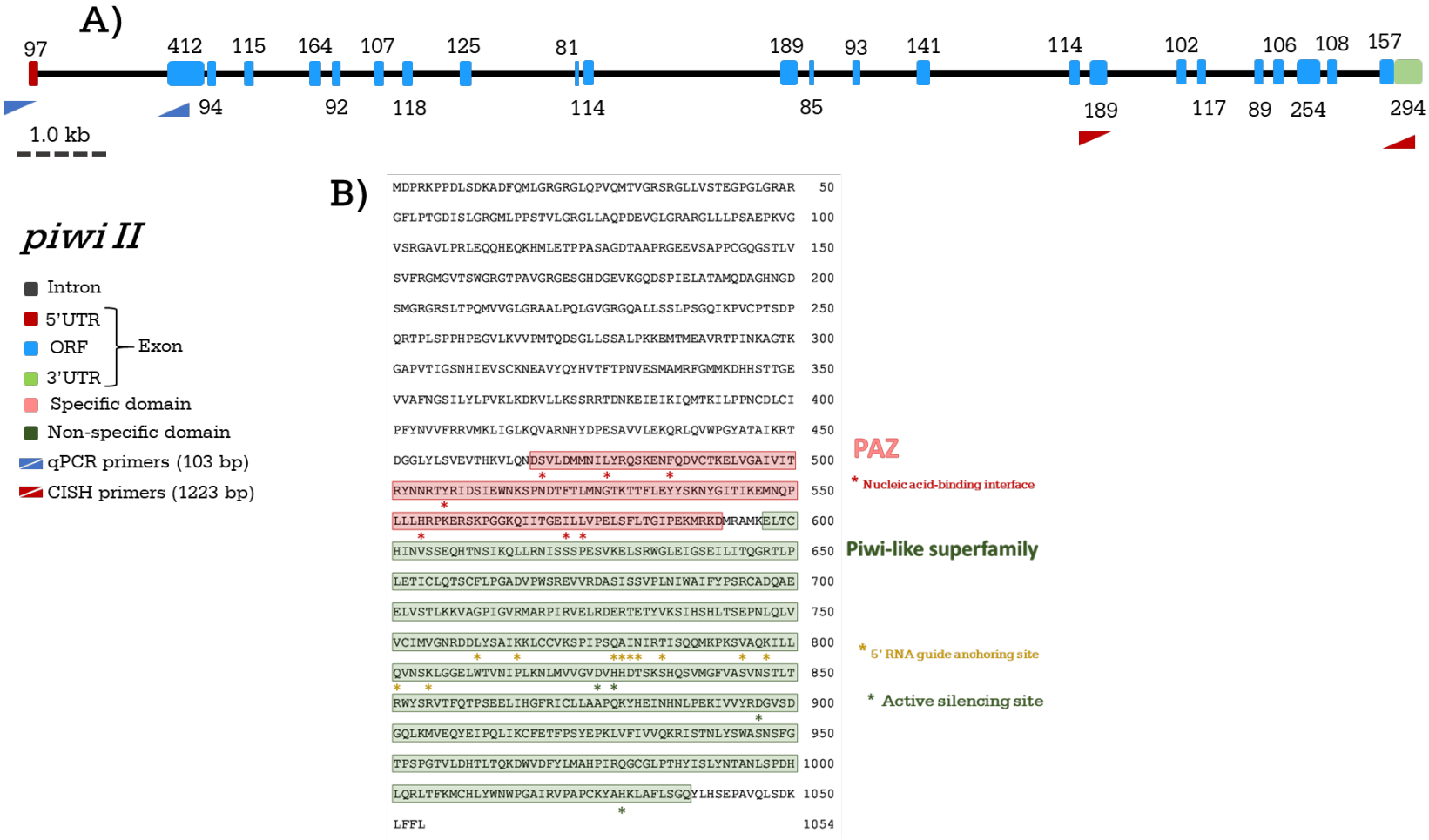

Figure 2.4. Schematics showing genetic structure (A) of *piwi II* and the annotated regions of its predicted polypeptide (B) in *G. holbrooki*. The cDNA contained 24 exons, with a 3162 bp coding region (marked blue in panel A) and 1054 peptides in the predicted protein (B). The PAZ domain (marked red in panel B) with nucleic acid-binding interface (red asterisks in panel B) and PIWI-like superfamily domain (marked green in panel B) with active site (green asterisks in panel B) are marked. In panel A, the approximate location of primers used for quantitative PCR (qPCR, blue triangles), chromogenic *in situ* hybridisation (CISH, red triangles) probe (Chapters 3 and 4) and the exon lengths (numbers on blue blocks) are also marked. The scale bar indicates an approximate size of 1.0 kb.

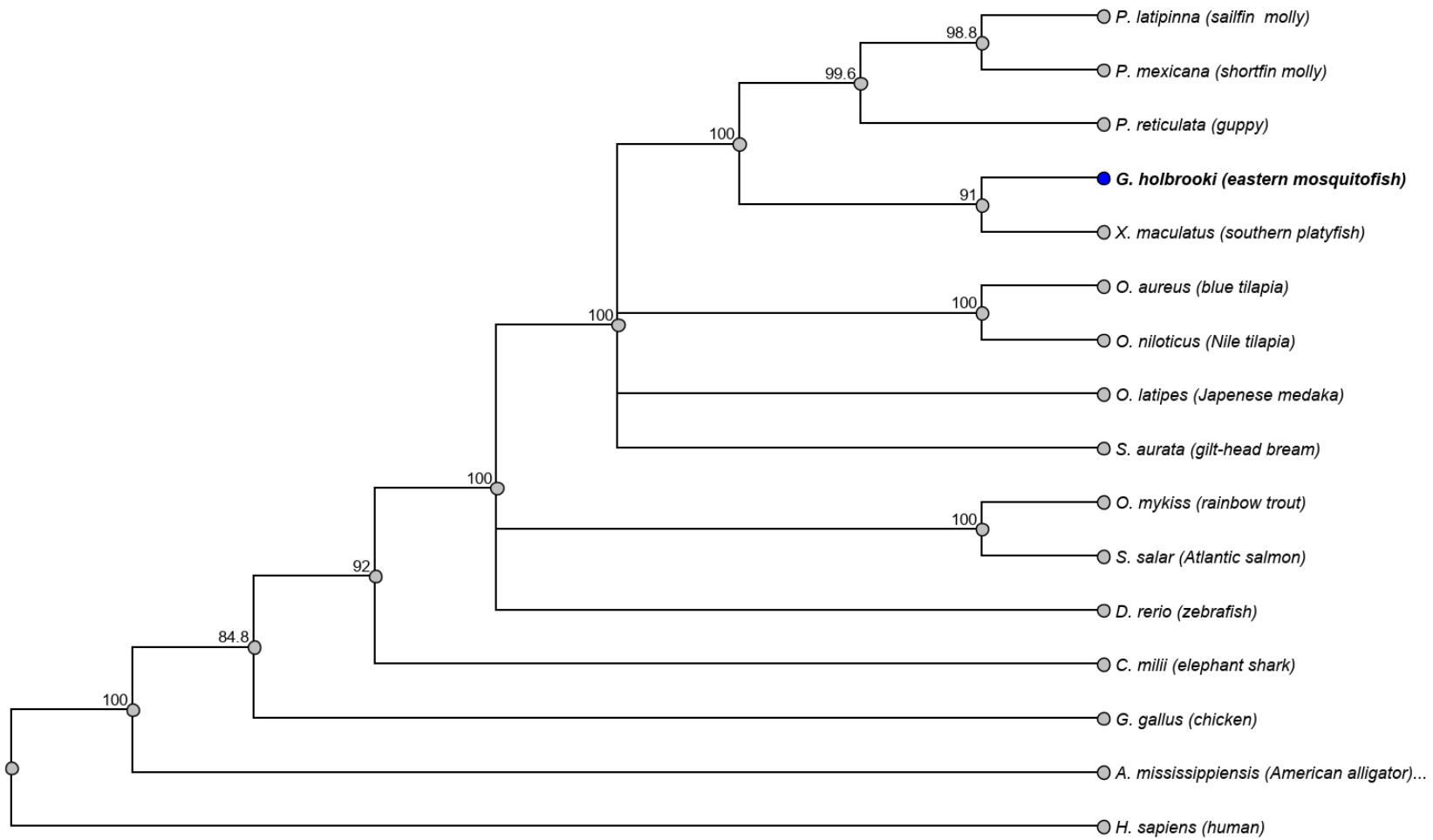

Figure 2.5. Phylogenetic tree showing the relationship of the predicted *G. holbrooki* Piwi II with those of select fish and higher vertebrates. The phylogenetic tree was built using *Homo sapiens* as the reference taxa. The predicted *G. holbrooki* Piwi II was most similar to that in *X. maculatus* and unsurprisingly clustered with other poeciliids.

2.3.2. *dazl* contained a highly conserved RRM and a domain to bind poly(A) tail.

The *dazl* cDNA in *G. holbrooki* consisted of 10 exons containing 97 bp 5′UTR, 654 bp coding sequence and 396 bp 3′UTR (Fig. 2.6A). The full-length cDNA showed 95-97% homology with available poeciliid species. The *dazl* open reading frame (ORF) encoded 217 aa characterised by two domains (Fig. 2.6B); 1) a RNA recognition motif (RRM) located in the middle of the polypeptide chain, and 2) a polyadenylate binding protein human type 1, 2, 3 and 4 family (PABP-1234) domain located at the C-terminus (Table 2.2). The NCBI BLAST showed a relatively high homology between predicted Dazl in *G. holbrooki* and that from poeciliids, ranging from the lowest (98%) with *P. formosa* to the highest (>99%) with *X. maculatus*. Correspondingly, phylogenetic analysis of complete proteins clustered *G. holbrooki* Dazl with those of poeciliid species (Fig. 2.7). However, homology was reduced to less than 35%, 67% and 72 % with its homologous in *D. rerio* and *O. latipes*, and *M. musculus*.

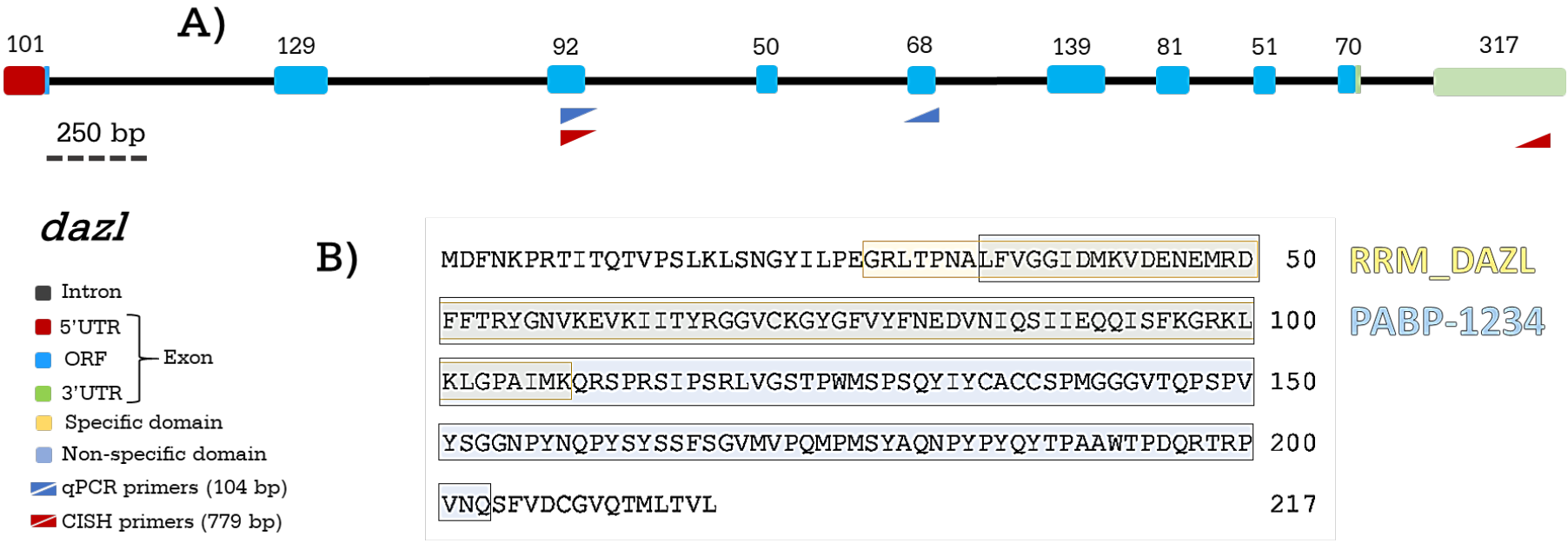

Figure 2.6. Schematic representation of genetic structure (A) of *dazl* and its conserved protein domains (B) in *G. holbrooki*. The cDNA contains 10 exons, with a 651 bp coding region (marked blue in panel A) and 217 polypeptide (B) in the predicted protein. The predicted polypeptide contains an RNA recognition motif domain (RRM, marked yellow), at N-terminus and a polyadenylate binding protein family, (PABP-1234, marked blue in panel B) which overlap each other, with the latter covering most of the polypeptide. In panel A, the approximate location of primers used for quantitative PCR (qPCR, blue triangles), chromogenic *in situ* hybridisation (CISH, red triangles) probe (Chapters 3 and 4) and the exon lengths (numbers on blue blocks) are also marked. The scale bar indicates an approximate size of 250 bp in the schematic DNA.

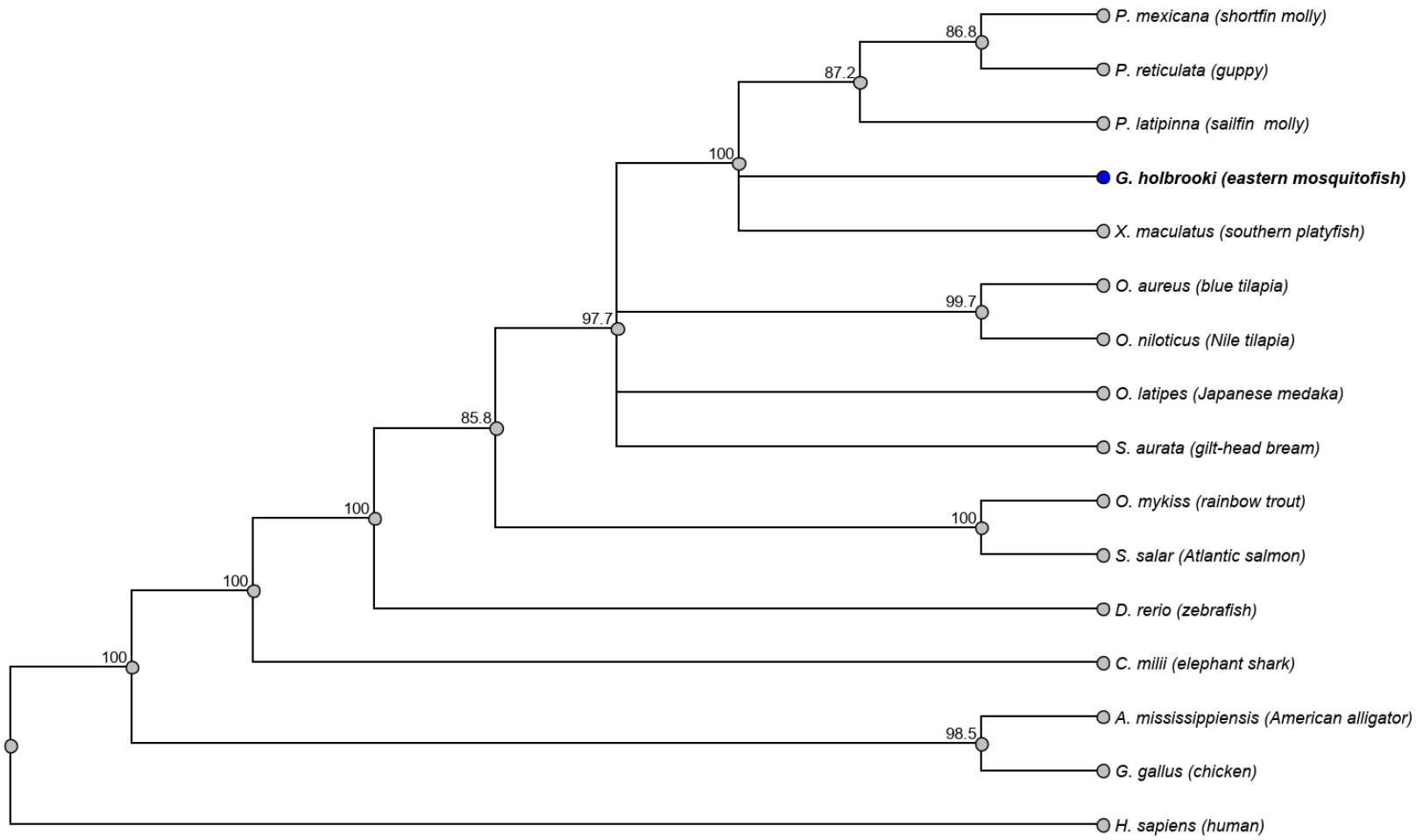

Figure 2.7. Phylogenetic tree showing the relationship of the predicted *G. holbrooki* Dazl with those of select fish and higher vertebrates. The phylogenetic tree was built using *H. sapiens* as the reference taxa. The predicted *G. holbrooki* Dazl was most similar to that in *X. maculatus* and unsurprisingly clustered with other poeciliids.

2.3.3. *G. holbrooki vasa contained the conserved* DEAD box and associated binding sites

The genomic structure of *vasa* in *G. holbrooki* consisted of 22 exons. The cloned cDNA was1914 bp with a short (<50bp) 5′UTR and 201 bp 3′UTR (Fig. 2.8A) encoding 638 aa (Fig. 2.8B). The full-length cDNA showed 94%-95% homology with those of poeciliid species. The predicted Vasa was characterised by the presence of DEAD box protein 4 (DDX4) a diagnostic feature containing ATP and RNA binding sites, and the C-terminal helicase domain of the DEAD box helicases (SF2_C_DEAD) that harboured a non-specific ATP binding site (Fig. 2.8B, Table 2.2). Multiple sequence alignment of predicted Vasa proteins in poeciliids showed *G. holbrooki* shared a strong homology with those of Poeciliids, ranging from 94% (*P. reticulata*) to 96% (*X. maculatus*). The phylogenetic analysis of complete protein also clustered *G. holbrooki* Vasa with poeciliids (Fig. 2.9). However, the homology was as low as 63% and 69% with those of *M. musculus* and *O. latipes*, respectively.

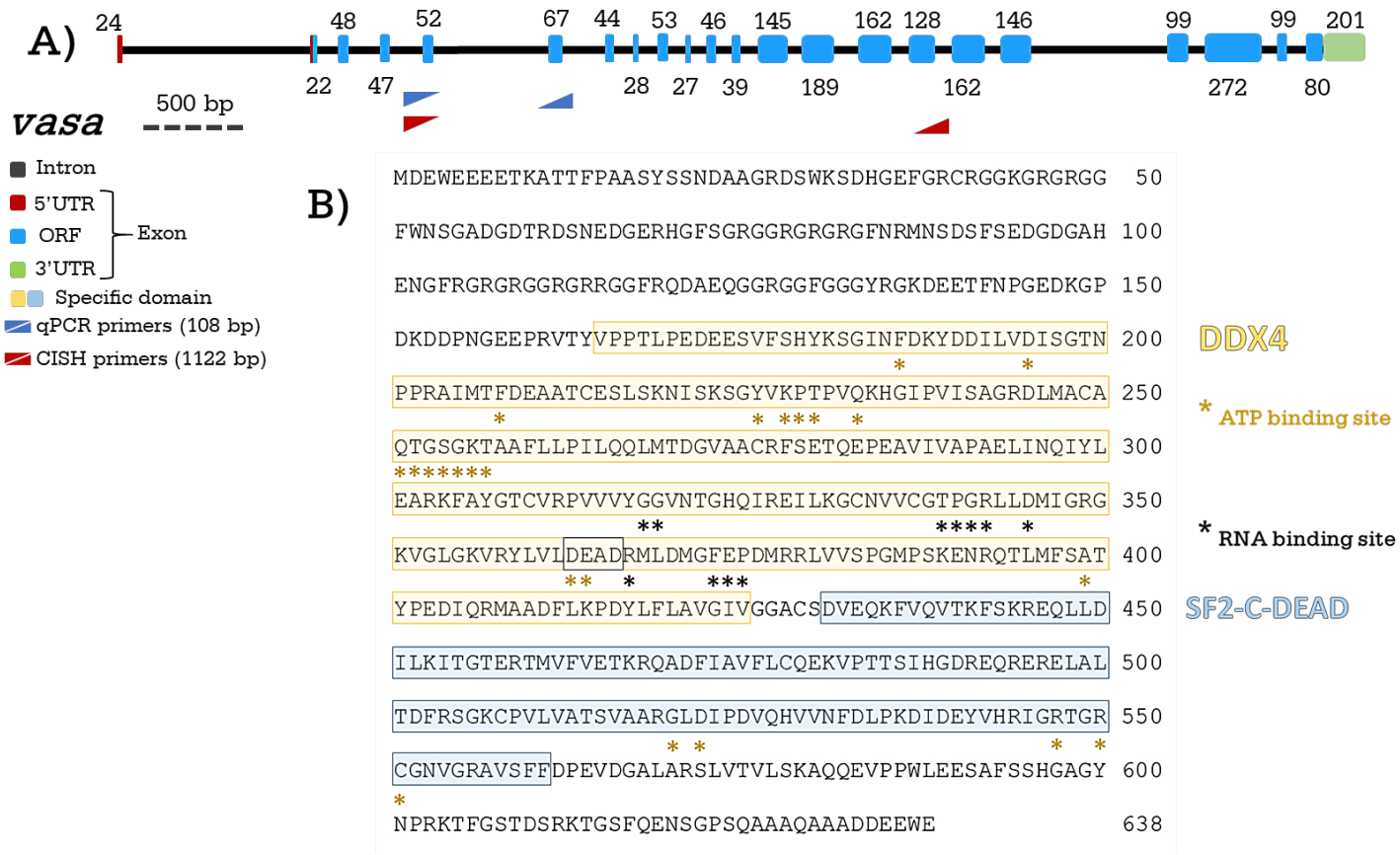

Figure 2.8. Schematic representation of genetic structure (A) and predicted polypeptide (B) of Vasa in *G. holbrooki*. The genetic structure contains 22 exons, with a 1914 bp coding region (marked blue in panel A) which encodes 638 aa (B). The predicted polypeptide was characterised by DEAD box protein 4 (DDX4, marked yellow in panel B) domain in the middle of the polypeptide chain containing DEAD-box helicase (the marked box in panel B) harbouring ATP and RNA binding sites (yellow and black asterisks in panel B, respectively). The C-terminal helicase domain of the DEAD box helicases (SF2_C_DEAD, marked blue in panel B) was also characterised harbouring ATP binding site (yellow asterisks in panel B). In panel A, the approximate location of primers used for quantitative PCR (qPCR, blue triangles), chromogenic *in situ* hybridisation (CISH, red triangles) probe (Chapters 3 and 4) and the exon lengths (numbers on blue blocks) are also marked. The scale bar indicates an approximate size of 500 bp in panel A.

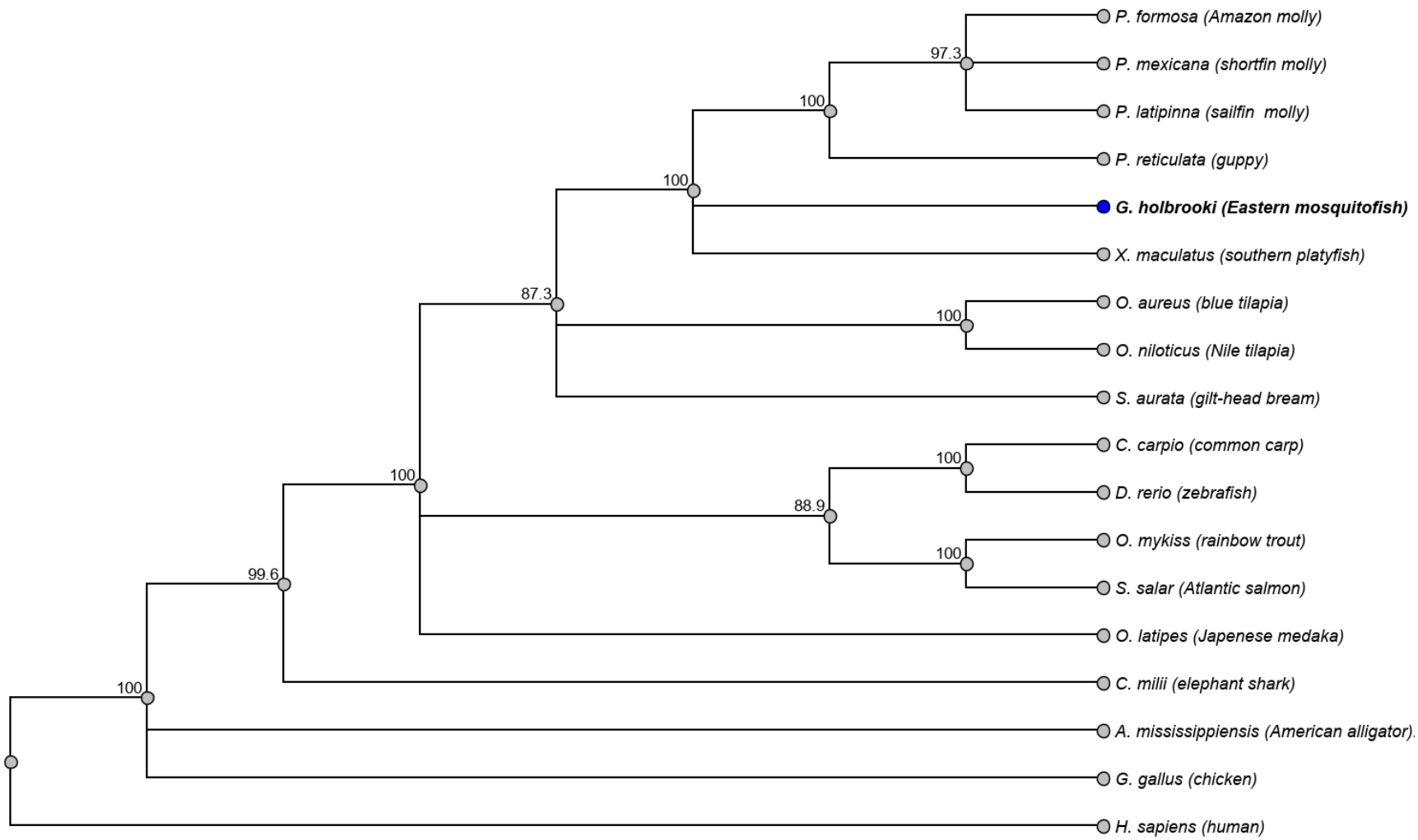

Figure 2.9. Phylogenetic tree showing the relationship of the predicted *G. holbrooki* Vasa with those of select fish and higher vertebrates. The phylogenetic tree was built using *H. sapiens* as the reference taxa. The predicted *G. holbrooki* Vasa was most similar to that in *X. maculatus* and clustered with other poeciliids

2.3.4. *nanos1* contained characteristic zinc-finger motif and the translational repression site.

The *nanos1* gDNA was lacking intron in *G. holbrooki*. The cDNA comprised of 138 bp 5′UTR, 669 bp coding sequence and 420 bp 3′UTR (Fig. 2.10A) that encoded 223 aa containing two CCHC zinc-finger domain (Fig. 2.10B, Table 2.2). The multiple sequence alignment showed the cDNA had 97-98% homology with other poeciliid species. In the predicted Nanos1 of poeciliids, this ranged from the lowest (98%) homology with *P. formosa* to the highest (99%) with *X. helleri*. Similarly, the phylogenetic analysis grouped the predicted *G. holbrooki* Nanos1 with other poeciliid species (Fig. 2.11). Homology of Nanos1 *G. holbrooki* with other vertebrates' models was relatively low ranging from 33% and 53% to 81% with its orthologous in *M. musculus*, *D. rerio* and *O. latipes*, respectively.

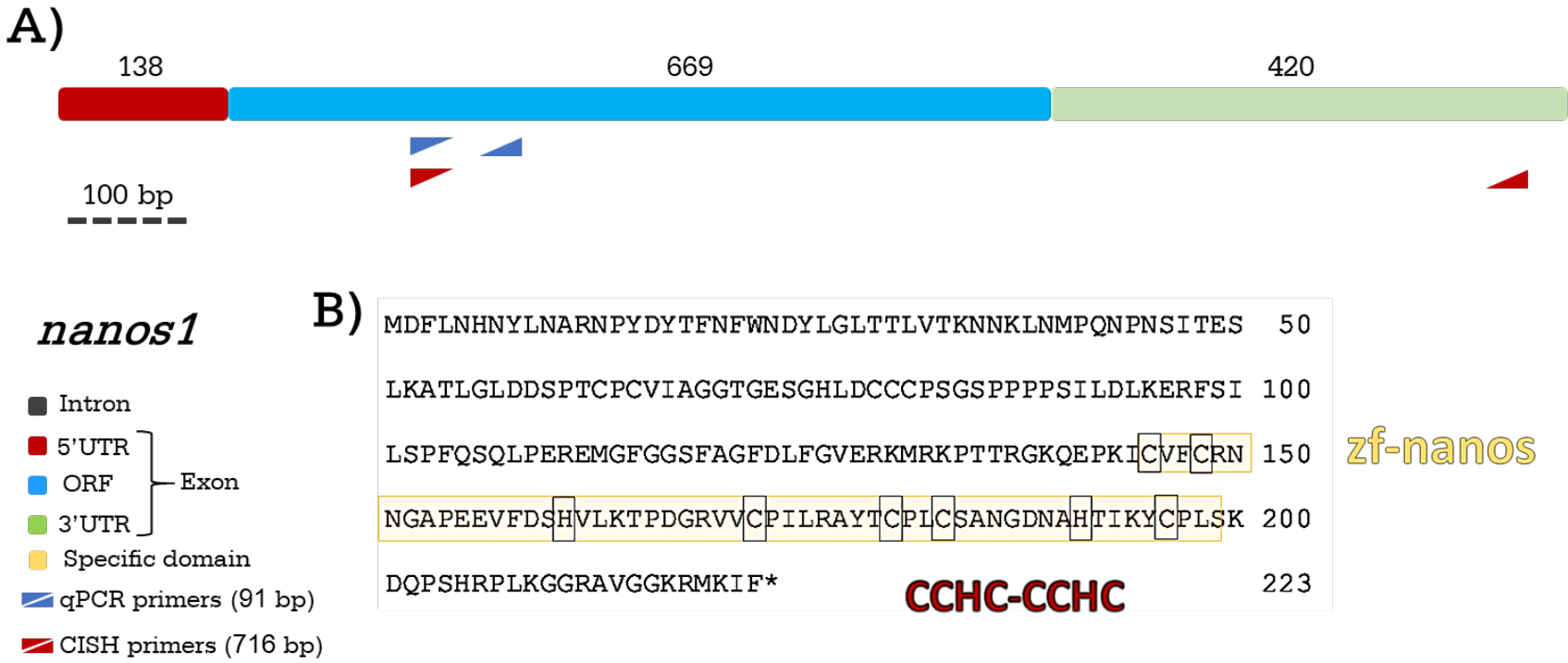

Figure 2.10. Schematic representation of genetic structure (A) of *nanos1* and the annotated regions of its polypeptide (B) in *G. holbrooki*. With no introns in the gene, the cDNA consisted of a single exon, with a 669 bp coding region (marked blue in panel A) encoding 223 aa (B). The predicted polypeptide contained two CCHC (boxed in panel B) in the zinc-finger domain (marked yellow in panel B) at C-terminus. In panel A, the approximate location of primers used for quantitative PCR (qPCR, blue triangles), chromogenic *in situ* hybridisation (CISH, red triangles) probe (Chapters 3 and 4) and the exon lengths (numbers on blue blocks) are also marked. The scale bar indicates an approximate size of 100 bp in panel A.

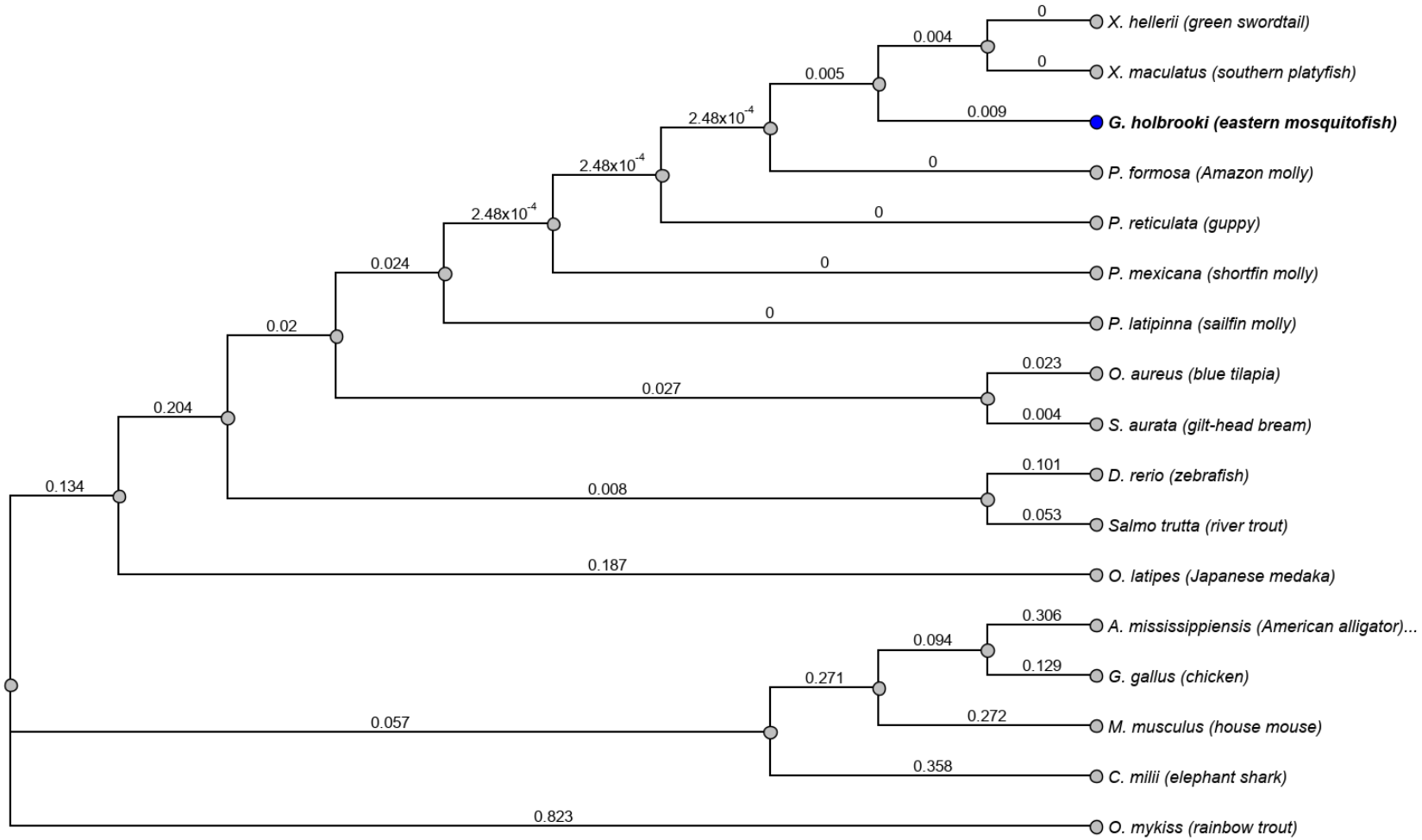

Figure 2.11. Phylogenetic tree showing the relationship of the predicted *G. holbrooki* Nanos1 with those of select fish and higher vertebrates. The phylogenetic tree was built using *Mus musculus* as the reference taxa. The predicted *G. holbrooki* Nanos1 was most similar to that in *X. maculatus* and unsurprisingly clustered with other poeciliids.

2.3.5. *dnd* was alternatively spliced but retained conserved domains in both variants.

Two alternatively spliced variants were found for *dnd* in *G. holbrooki*. The longer variant, *dnd-α*, contained five exons with 1122 bp cDNA encoding 374 predicted peptides (Fig. 2.12A). The last exon of *dnd-α* was spliced in two resulting in a shorter (1056 bp) *dnd-β* variant that contained six exons coding for 352 aa (Fig. 2.12B). The variant *dnd-β* was a result of truncation and loss of 66 bp from the last exon of *dnd-α* (Fig. 2.12B) and corresponding 22 aa truncation upstream of double-stranded RNA binding motif of dead-end protein homolog 1 (DSRM-DND) region (Fig. 2.12C). The *dnd-α* cDNA showed 90-95% homology with *dnd1* of poeciliid species; the lowest homology with *P. formosa* and the highest with *P. reticulata.* Both variants of predicted Dnd protein in *G. holbrooki* were characterised by the presence of RRM at the N-terminus and DSRM_DND1 at the C-terminus, the latter harboured an RNA-binding site (Table 2.2, Fig. 2.12C). Phylogenetic analysis clustered *G. holbrooki* Dnd-α with other poeciliid species (Fig. 2.13). The NCBI BLAST results revealed predicted Dnd-α of *G. holbrooki* had 77% (*P. reticulata*) to 86% (*X. maculatus*) homology with those of poeciliid species.

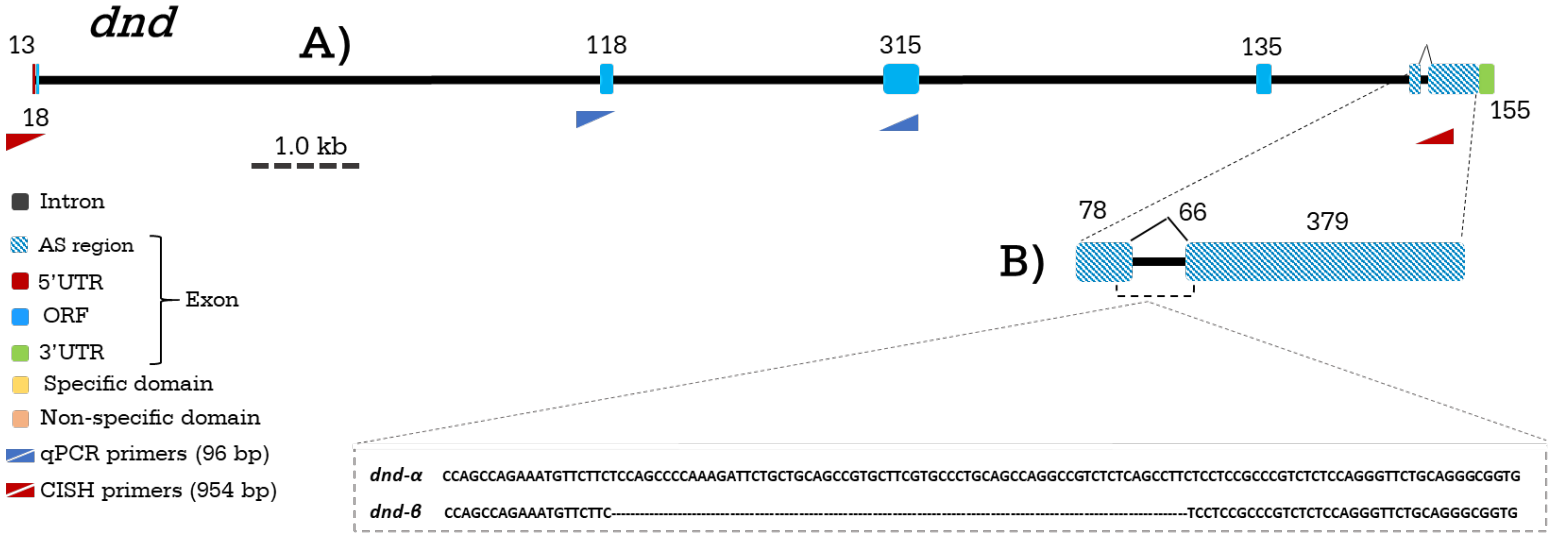

C)

```
MENKCSQVQNIERVQALEAWLEMTNTKLTQVNGQRKYGGPPEGWDGPTPG  50
ERCEVFISHIPRDAYEDLLIPLFSSVGPLWEFRLMMNFSGQNRGFAYAKY 100  RRM
GTPALATEAVLKLNGYMLEPKSYLCVRRSTEKRHLCIGNLPAATKQEDLK 150
QVLRRLVEGVVRVSLKTGPGIEGVSAVVAFSSHHTASMAKKDLVAEFKKR 200
FLLEISINWEPGENPNPSQKCSSPAPKILLQPCFVPCSQAVSQPSPPPVS 250  AS region
PGFCRAVGEPVSSPHPHVCYPVPASHHPQQHLVCTPSPTMLLRKVCEANG 300  DSRM-DND
                                    * **  **  **
FGQPLYDLHYSLARPDGFVKFTYKVLIPGISSAFRGKVMVLPGPSVRVMM 350  * RNA binding site
  **              * **                          **
EGGPGGPPPSSCCKKLFHNPAGCP                          374
*
```

Figure 2.12. Schematic representation of genetic structure (A and B) of *dnd* and the annotated regions of Dnd polypeptide (C) in *G. holbrooki*. Two alternatively spliced variants were found in *G. holbrooki dnd* (B). *dnd-α*, the longer variant, contained five exons, with a 1122 bp coding region and 374 peptides, while *dnd-β* contained 1059 bp and 353 peptides in the predicted protein. Panel B indicates the location of splicing activity (dashed blue box in panel B) and the genetic sequence dimorphism (dotted box in panel B) between dnd variants. The predicted polypeptide contained RNA recognition motif (RRM, marked yellow in panel C) at the N-terminus domain as a specific domain, and double-stranded RNA binding motif of dead end protein homolog 1 (DSRM_DND, marked orange in panel C) as non-specific domain at the C-terminus harbouring putative RNA-binding sites (black asterisks in panel C). The alternatively spliced region (AS region, marked blue in panel C) was located between two domains. In panel A, the approximate location of primers used for quantitative PCR (qPCR, blue triangles), chromogenic *in situ* hybridisation (CISH, red triangles) probe (Chapters 3 and 4) and the exon lengths (numbers on blue blocks) are also marked. The scale bar indicates an approximate size of 1.0 kb in panel A.

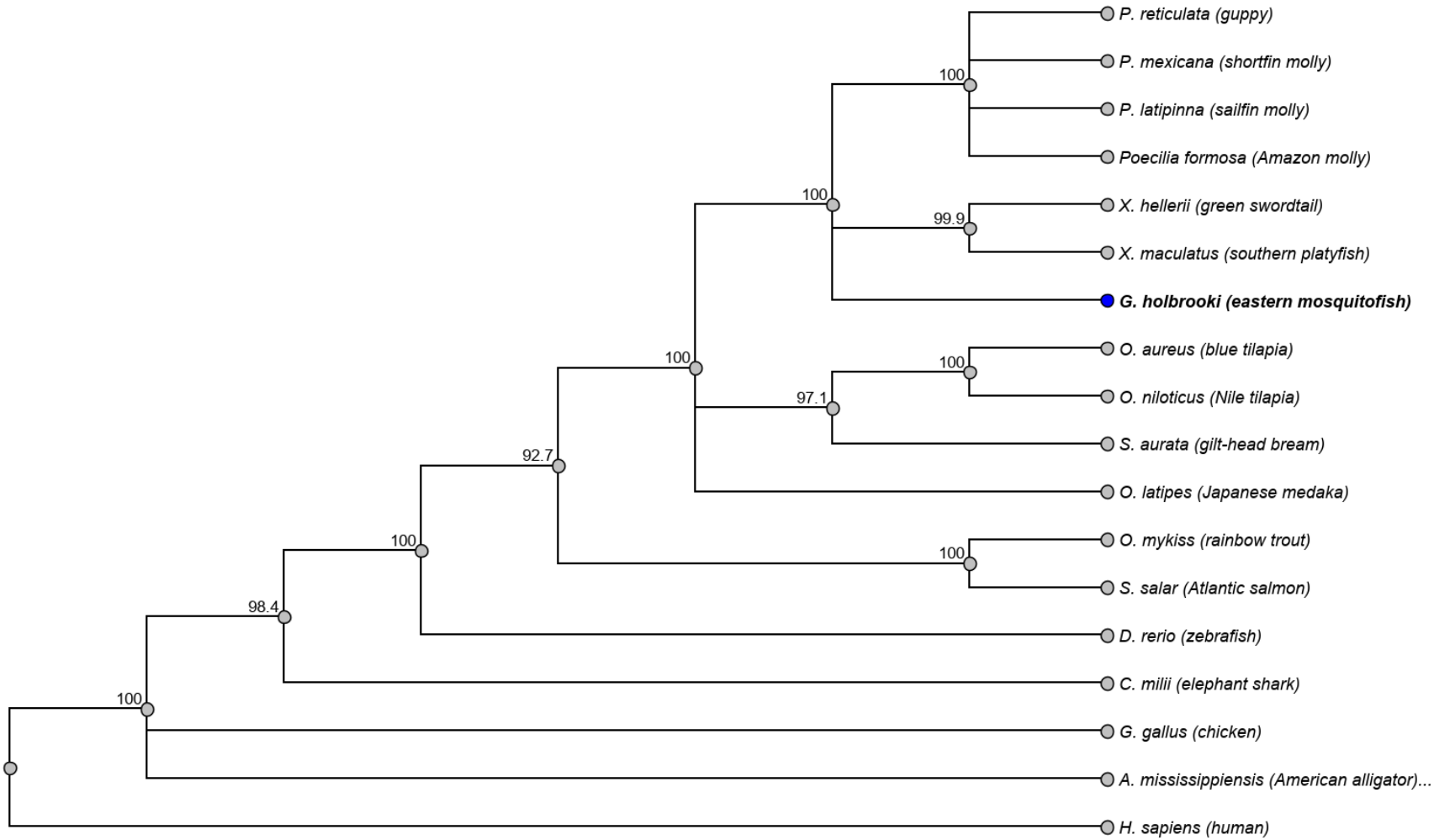

Figure 2.13. Phylogenetic tree showing the relationship of the predicted Dnd-α in *G. holbrooki* with those of select fish and higher vertebrates. The phylogenetic tree was built using *H. sapiens* as the reference taxa. The predicted *G. holbrooki* Dnd-α was most similar to that in *X. maculatus* and unsurprisingly clustered with other poeciliids.

2.3.6. *cxcr4* in *G. holbrooki* conserved seven transmembrane G-protein receptors.

The gDNA of *cxcr4* in *G. holbrooki* had two exons. cDNA consisted of 108 bp 5′UTR, 996 bp coding sequence and 540 bp 3′UTR (Fig. 2.14A) encoding 332 aa (Fig. 2.14B). The cDNA showed 91-96% homology with *cxcr4* orthologues in other poeciliids. The predicted polypeptide was characterised by the presence of CXC chemokine receptor type 4, a member of the class A family of seven-transmembrane G protein-coupled receptors (7tmA-CXCR4) marked as TM 1 to TM 7 (Fig. 2.14B). Also, phylogenetic analysis clustered *G. holbrooki* Cxcr4 with poeciliid species (Fig. 2.15). This was similar to NCBI BLAST results, showing a relatively high homology between *G. holbrooki* Cxcr4 and those of poeciliids ranging from 90% (*P. mexicana*) to 94% with (*X. maculatus*). Compared to other vertebrates, *G. holbrooki* Cxcr4 showed 62%, 69% and 75% homology with M. musculus and *D. rerio* Cxcr4a and *O. latipes* Cxcrb, respectively.

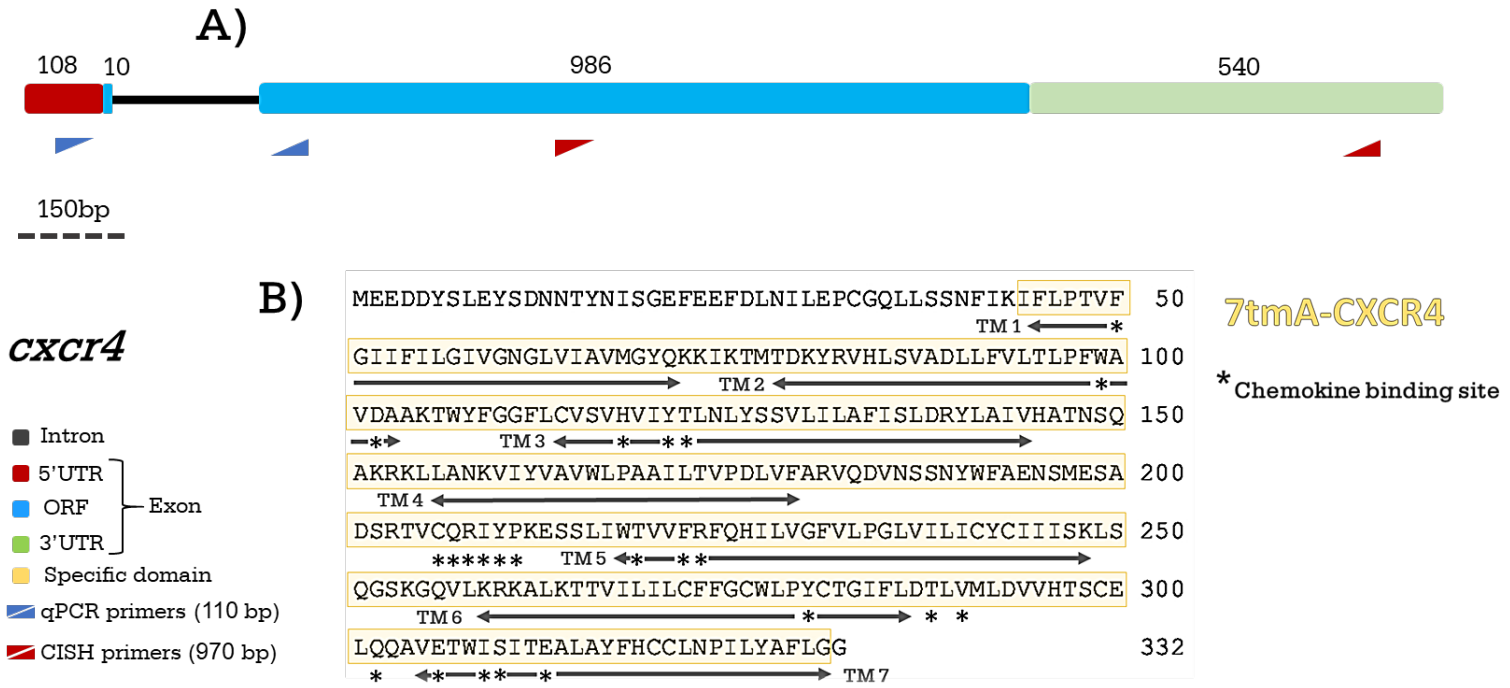

Figure 2.14. Schematics showing genetic structure (A) of *cxcr4* and the annotated regions of its polypeptide (B) in *G. holbrooki*. The genetic structure consisted of two exons, with a 996 bp coding region (marked blue in panel A) which encodes 332 peptides (B). The main region of predicted polypeptide is annotated as CXC chemokine receptor type 4, the member of the class A family of seven transmembrane G protein-coupled receptors (7tmA-CXCR4, marked yellow in panel B). The domain of seven transmembrane helices (TM 1 to TM 7, marked separately as double-ended arrows) are shown containing chemokine binding site (black asterisks). In panel A, the approximate location of primers used for quantitative PCR (qPCR, blue triangles), chromogenic *in situ* hybridisation (CISH, red triangles) probe (Chapters 3 and 4) and the exon lengths (numbers on blue blocks) are also marked. The scale bar indicates an approximate size of 150 bp in panel A.

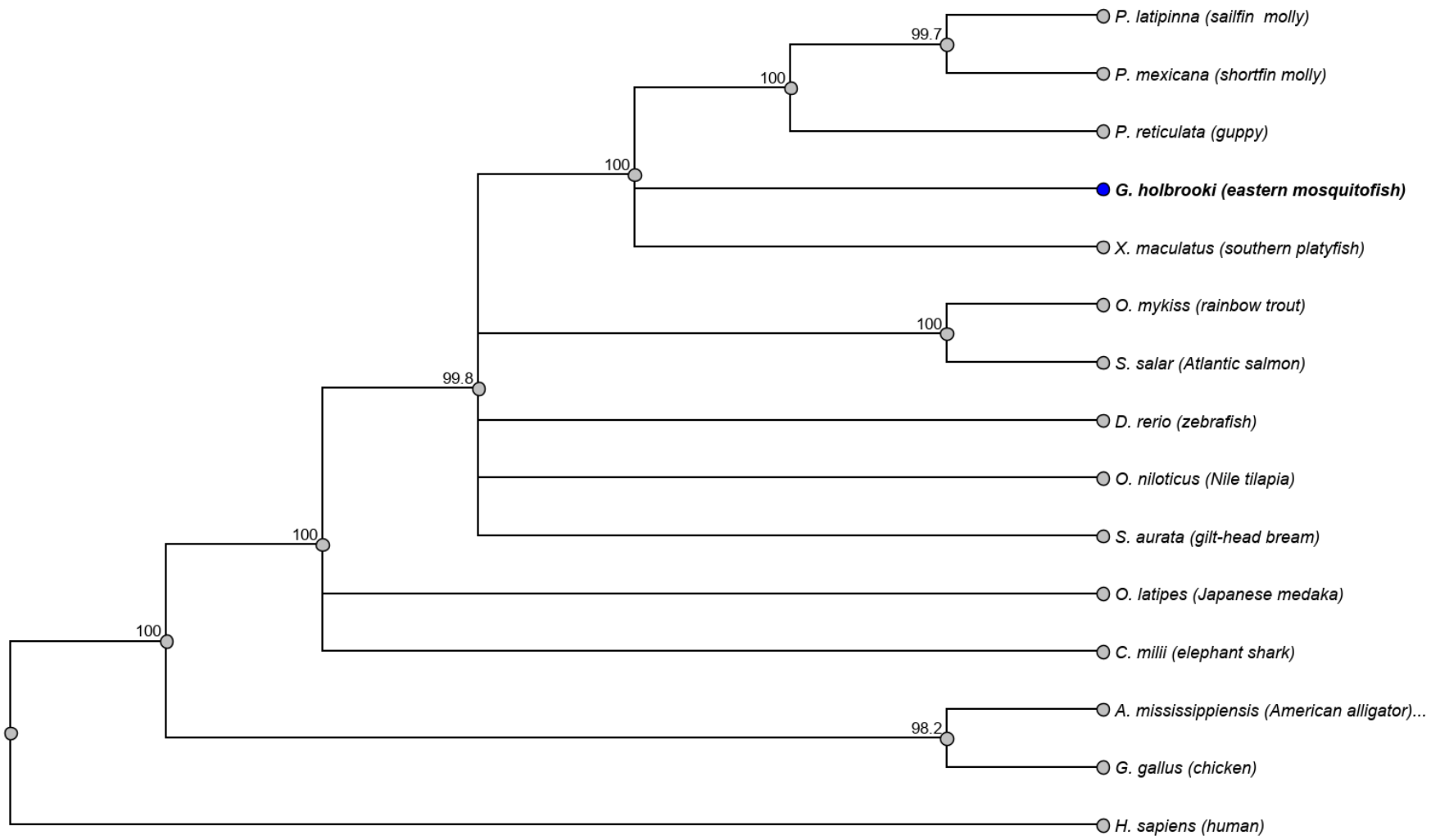

Figure 2.15. Phylogenetic tree showing the relationship of the predicted *G. holbrooki* Cxcr4 with those of select fish and higher vertebrates. The phylogenetic tree was built *H. sapiens* as the reference taxa. The predicted *G. holbrooki* Cxcr4 was most similar to that in *X. maculatus* and unsurprisingly clustered with other poeciliids.

Table 2.2. List of key PGC markers and their conserved domains in vertebrates characterised in respective homologues of *G. holbrooki* in this study.

Gene	Domains and sites	Salient features	Accession	Reference
piwi	PAZ	specific region	cd02845	(Lingel et al., 2003)
	Piwi-like superfamily	Superfamily, non-specific region	cd04658	(Yuan et al., 2005)
	DNA/RNA-binding interface	ssDNA & siRNAs recognition site	cd02825	(Lingel et al., 2004)
	active site	catalytic site for slicing	cd02826	(Lingel et al., 2004)
	5' RNA anchoring site	RNA guide for slicing point	cd02826	(Lingel et al., 2004)
vasa	SrmB superfamily	Superfamily II DNA and RNA helicase	COG0513	(Johnson and McKay, 1999)
	DEADc_DDX4	DEAD-box helicase domain of DEAD box protein 4	cd18052	(Schmid and Linder, 1992) (Tanner and Linder, 2001) (Hilbert et al., 2009)
	SF2_C_DEAD	C-terminal helicase domain of the DEAD box helicases	cd18787	(Linder and Jankowsky, 2011)
dazl	RRM_DAZL	RNA recognition motif	smart00360	(Venables et al., 2001)
	PABP-1234	polyadenylate binding protein	TIGR01628	(Yang et al., 1995)
nanos1	zf-Nanos	Nanos RNA binding domain	pfam05741	(Mosquera et al., 1993) (Curtis et al., 1995) (Curtis et al., 1997)
dnd	RRM	RNA recognition motif	smart00360	(Nietfeld et al., 1990)
	RNA binding site	---	cd00048	(Ketting, 2007)
	DSRM_DND	dsRNA binding motif of Dnd protein homolog 1	cd20313	(Gross-Thebing et al., 2017)
cxcr4	7tmA-CXCR4	member of the class A family of seven transmembrane G protein-coupled receptors	cd00637	(Horuk, 2001)
	chemokine-binding site	harbours seven transmembrane helices	cd14984	(Singh et al., 2013) (Kufareva et al., 2015)

2.4. Discussion

The key RNAs and proteins (Chapter 1) involved in maintaining germ cell identity, *i.e.*, against somatic differentiation (Gross-Thebing et al., 2017), and their proper mobilisation (Boldajipour et al., 2008, Herpin et al., 2008) have specific nucleic acid-binding capabilities that enable a range of regulatory functions. These include repression or activation of transcription/translation (Bhandari et al., 2014, Asaoka et al., 2019) or protecting mRNAs from decay through preserving the poly(A) tail from degradation (Zagore et al., 2018) and/or via counteracting short interfering RNAs-Dicer machineries (Ketting, 2007). Comparative studies of the PGC markers (structure and content) across taxa provide direct clues to their shared functions and evolutionary relatedness (Chapter 1). Amongst the shared features, they often exhibit subtle species-specific differences (Chapter 3 and 4), providing clues of novelties that may hold promise for manipulating reproductive functions (Chapter 4) that are species-specific. Hence, cloning of PGC markers from *G. holbrooki* marks a key first step towards investigating developmental dynamics (Chapter 3) and unique features of PGCs in this species. Regarding this, annotating the domains further assisted us during *in silico* procedures of the whole study with regard to designing highly specific PCR primers and *in situ* hybridisation probes (Chapters 3, 4 and 5).

2.4.1. The structure of *piwi* and its regulatory function

Unlike most eukaryotes, *piwi II* in *G. holbrooki* did not have the conserved canonical (Proudfoot, 2011) polyadenylation (polyA) signal (AUUAAA). Instead, the AU-rich 3′UTR may serve as a polyA signal region (with multiple UGUA sites) presented upstream of the cleavage signal (CA-rich) region (Ustyantsev et al., 2017).

The PAZ/PIWI domains characterised in *G. holbrooki* contain nucleic acid-binding site that are conserved across taxa. These binding sites are known to be essential to recruit and assemble small ncRNAs for inducing transcriptional and post-transcriptional silencing of the target genes (Tolia and Joshua-Tor, 2007, Jinek and Doudna, 2009) which is essential for their regulation. Based on the structural similarities, the characterised PAZ domain encoded by *piwi II* in *G. holbrooki* suggests that the predicted protein has the ability to bind ncRNAs and mRNAs. Moreover, characterisation of the Piwi-superfamily domain with a 5′-guide RNA anchoring site in the *piwi II* ORF indicates the potency of the protein to RNA cleavage and decay.

Mechanistically, the structure of Argonaute is organised into N-, PAZ, MID (middle) and PIWI domains (Wang et al., 2008, Ryazansky et al., 2018). The associated ncRNAs which maintain Watson-Crick base-pairing with the target mRNA are settled between the domains facilitating a stable interaction between proteins and target RNAs (Miyoshi et al., 2016, Ma et al., 2004). Particularly, the 5′-phosphate of guide RNA is anchored in the MID domain binding to the side chains of amino acid residues with its oxygen hydrogen-bonds (Wang et al., 2008). On the other hand, the 3′end of the nucleic acid guide is

anchored within the binding pocket in the PAZ domain (Lingel et al., 2004, Boland et al., 2011, Ryazansky et al., 2018). In another model, typically observed in short interfering RNAs (siRNA), the 3′-end of nucleic acid guide is not anchored in the PAZ domain. Instead, the nucleic acid guide is base-paired to the target mRNA and forms a heteroduplex (Nielsen et al., 2007, Bartel, 2009). The PIWI domain adopting an RNase H-like fold with a catalytic tetrad of amino acid residues is involved in target mRNA decay through clamping the guanidium groups on target base and using that region as a cleavage site (Yuan et al., 2005). Together,

The effector domains of PIWI protein have been shown to be key for germline specification and gonad function (Houwing et al., 2007, Ishizu et al., 2012). The GSC function of PIWI was first characterised in *Drosophila* germ cells localised in the nucleus of developing PGCs (Cox et al., 1998, Lingel et al., 2003). In fish models such as zebrafish and medaka, *piwi* expression is restricted to germ cells and is indispensable to PGC migration (Li et al., 2012b), germline formation (Houwing, 2009) and gonad function (Houwing et al., 2008). Unlike zebrafish, ubiquitous expression of PIWI proteins and the associated RNAs, with a conserved role in the gene silencing process, have been detected in mammalian somatic tissues (Grimson et al., 2008, Ha et al., 2014, Nandi et al., 2016, Jehn et al., 2018). However, the spatial and temporal expression pattern of *piwi II* during *G. holbrooki* embryonic development and its role in germ cell formation is still elusive (Chapter 3). Also, sex-dimorphic expression of *piwi II* in gonads and its storage in *G. holbrooki* gametes as one of the Gp components is unknown (Chapter 4).

2.4.2. *dazl*; a regulatory machinery for germline formation and meiosis

The cDNA length and number of exons (10) in *G. holbrooki dazl* is comparable with those of poeciliids and *O. latipes*. However, *dazl* in *D. rerio* and *M. musculus* contained 11 and 12 exons, respectively, with relatively longer cDNA. Evident from the genetic sequence analysis of *dazl* in *G. holbrooki*, the 3′UTR (*i.e.*, less than 350 bp) is noticeably shorter than those of zebrafish, medaka and house mice (*i.e.*, longer than 1.0 kb). As reviewed (Chapter 1), the dynamic localisation of maternal *dazl* is underpinned by a group of *cis*-acting motifs located in the 3′UTR. In *Xenopus* (Betley et al., 2002) and *D. rerio* (Kosaka et al., 2007), *dazl* contains several UGCA regions in its 3′UTR functioning as a mitochondrial cloud localisation element (MCLE), however, this element was not detected in *G. holbrooki dazl*. Instead, multiple CACA *cis*-acting motifs found in the 3′UTR may confer maternal as well as domain-specific localisation in the developing embryos. The CACA signal is known to be sufficient for localisation of maternal *dazl* in oocytes and early embryonic development (Kosaka et al., 2007). Therefore, despite the short 3′UTR, the *G holbrooki dazl* seems adequate for functional mobilisation of the maternal transcript.

The *dazl* encoded RRM and PABP domains in *G. holbrooki*. Proteins containing RRMs comprise the largest group of single stranded RNA-binding proteins (RBP) family with a variety of binding preferences (Maris et al., 2005). Also, proteins with a PABP domain are categorised as RRM proteins

that regulate RNA stability and translation (Query et al., 1989, Yang et al., 1995, Féral et al., 2001). Mechanistically, PABP couples the poly(A) tail of the target mRNA and interacts with eIF4E, bound the 5′-cap, to initiate translation (Brook et al., 2009). Also, PABP is assumed to recruit eIF4A to ease the secondary structure within the 5′UTR (Gallie et al., 2000) and facilitate the process of mRNA translation (Niepel et al., 1999). The potency of these domains may unravel the *dazl* function during germ cell development and gonadogenesis among taxa (Reijo et al., 2000), as its downregulation or deletion results in abolished PGC formation in medaka (Li et al., 2016) and *Xenopus* (Douglas and King, 2000). Evaluating the spatio-temporal expression of *dazl* during *G. holbrooki* early development may shed some light on its role in the reproductive biology of poeciliids (see Chapter 3).

Dazl is a key regulator of meiosis among metazoans, lack of which in *Drosophila* halts G2-M transition in meiosis-I through compromising spindle formation and H3 histone phosphorylation (Houston. et al., 1998). Similarly, loss of *dazl* expression in the hermaphrodite *Caenorhabditis elegans* blocks oogenesis due to suppressed pachytene stage of meiosis-I (Karashima et al., 2000). In higher vertebrates, Dazl function is more involved in testis development. For example, the RRM domain of murine DAZL binds a large number of testicular transcripts at their 5′ (Venables et al., 2001) and 3′UTRs (Li et al., 2019) to accelerate germ cell maturation. In mice, post-natal ablation of *Dazl* did not affect oogenesis but resulted in deprived spermatogonial stem cell genesis and blocked meiosis eventuating in decreased polysome-associated target transcripts (Li et al., 2019). Screening the expression pattern of *dazl* in gonad and gametes of *G. holbrooki* may reveal its sex-dimorphic role in critical events of germ cell maturation, *e.g.*, sex differentiation, mitosis-meiosis transition, and parental factor packaging, in poeciliids (Chapter 4).

2.4.3. *vasa*; multiple role for RNA metabolism and function

The genetic structure of *vasa* in *G. holbrooki*, *e.g.*, cDNA length and the number of exons, was comparable to those of poeciliids, *O. latipes* (Tanaka et al., 2001) and *M. musculus* (Tanaka et al., 2000), however, *vasa* in *D. rerio* (Howe et al., 2013) contained 27 exons. DEAD (D-E-A-D = Asp-Glu-Ala-Asp) box, a critical element of *vasa* is conserved among vertebrates as was also shown to be the case for *G. holbrooki* in this study. The DEAD protein family includes a group of RNA helicases involved in unwinding RNA secondary structures and proper refolding (Tanner and Linder, 2001), ribosome biogenesis (Pugh et al., 1999), pre-mRNA splicing (Schwer and Meszaros, 2000) and translational regulation (Chuang et al., 1997). As evident in *G. holbrooki*, RNA helicases in *vasa* contain several conserved motifs known to recruit an ATP and incorporate the energy of hydrolysis into RNA metabolism (Staley and Guthrie, 1998). Indeed, ATPase cycle results in alterations in RNA strands affinity and facilitates DEAD-box proteins to bind and rearrange target RNAs (Gustafson and Wessel, 2010). Also, DEAD-box domain contained RNA binding sites in *G. holbrooki*, which underpin RNA modification through restructuring RNA molecules, remodelling RBPs and separating the strands of

short duplex regions of RNA (Hilbert et al., 2009, Jarmoskaite and Russell, 2011). These regulatory functions have been shown to protect germline identity during embryogenesis (Styhler et al., 1998), proper mitosis-meiosis transition (Shibata et al., 2004) and germ cell maturation (Kitamura et al., 2007, Liu et al., 2009). As has been shown in zebrafish (Hartung et al., 2014) and medaka (Li et al., 2009) evaluating spatio-temporal expression of *vasa* during embryonic development can shed light on its pre- (Chapter 3) and post-natal function (Chapter 4) in *G. holbrooki* and may improve knowledge about *vasa* function in poeciliids.

2.4.4. *dnd* encoded spliced variants with conserved regulatory regions.

As evident from the results, in *G. holbrooki*, the shorter variant, *dnd-β,* encoded a truncated protein lacking 22 aa compared to *dnd-α.* Despite the truncation, the RRM and DSRM-DND domains were intact suggesting both *dnd* variants encode a functional protein in *G. holbrooki*. In other teleosts such as *O. celebensis* (Zhu et al., 2018), *Salmo salar* (Wargelius et al., 2016) and *D. rerio* (Weidinger et al., 2003), no alternative spliced variants of *dnd* have been reported, and the expression of *dnd* was exclusively detected in germ cells. On the contrary, two alternatively spliced variants were detected for *Dnd* in mice with dissimilar temporal and spatial expression pattern in foetal stages. The murine shorter variant lacks 12 aa, spread across three regions, located upstream of the RRM domain (Bhattacharya et al., 2007). It is therefore interesting to investigate the expression pattern of *dnd* variants in *G. holbrooki* (see Chapter 3), which may reveal patterns indicative of *dnd* functions in poeciliids and their comparative relevance to the evolution of reproductive strategies in vertebrates.

Both variants of *dnd* in *G. holbrooki* encoded canonical RRM. This motif has been shown to interacts with the UTRs of mRNAs but is also involved in post-transcriptional modification including alternative splicing (Lee et al., 2017), RNA stability (Ripin et al., 2019) and translation (Slanchev et al., 2009). The translational regulatory mechanism of Dnd has been elaborated in *Xenopus* PGC development where zygotic expression of *dnd* is dramatically increased to override the inhibitory activity of translational initiation factor 3f (eIF3f), and tune translation of Nanos1 (Aguero et al., 2017).

The 3′UTR of *nanos1*, known to interact with Dnd (Slanchev et al., 2009, Aguero et al., 2018) , has a U-rich region (*i.e.*, less than 32% GC contents) in *G. holbrooki*. Indeed, Dnd has been shown to rely on U-rich regions of the 3′UTR of target mRNA to neutralise miRNA repressing activities (Anderson et al., 2006, Ketting, 2007). Specifically, the RNA-binding site characterised at the C-terminus of predicted Dnd in *G. holbrooki* will likely enable the protein to bind a UU(A/U) trinucleotide motif predominantly located at the 3'UTR of the target mRNA. The *nanos1* of *G. holbrooki* contained several of the (21 UUU and 9 UUA) trinucleotide motifs on its 3′UTR suggesting its potency to interact with Dnd in order to protect from miRNA-directed degradation (Ketting, 2007, Gross-Thebing et al., 2017) or facilitate its translation (Aguero et al., 2017). Furthermore, both *dnd* variants in *G. holbrooki* encoded DSRM at the C-terminus which is necessary to interact with other target molecules (Baloch et al., 2019)

with varied affinity to RNAs or proteins (Tian et al., 2004). Interestingly, the exact function of DSRM itself is largely unknown in most taxa.

2.4.5. *nanos1* has a conserved motif with multiple function.

The presence of a single exon in the *nanos1* of *G. holbrooki* and poeciliids in general is shared with *D. rerio (Koprunner et al., 2001)* and *M. musculus* (Haraguchi et al., 2003). Whereas *nanos1* in *O. latipes* (Aoki et al., 2009) and *Drosophila* (Forbes and Lehmann, 1998) comprised of two and three exons, respectively. Nevertheless, in all the studied models, *nanos1* encodes two CCHC zinc-finger motif domains at the C-terminus of the protein.

As key regulatory proteins for cell development and tissue function, NANOS family proteins recruit (CCHC)-TYPE zinc-finger motifs (Hashimoto et al., 2010) to bind within the 3′UTR with no sequence specificity eventuating in the translational repression of its target mRNAs (Kuersten and Goodwin, 2003, Lai et al., 2011). Also, transcriptional silencing role of NANOS proteins have been reported through engaging CCR4–NOT deadenylase complex to facilitate target mRNA decay (Bhandari et al., 2014). These regulatory potencies have been shown to protect the identity of germ cells (Koprunner et al., 2001) and program body patterning during embryonic development (Curtis et al., 1995, Lall et al., 2003). Unlike oviparous fish models and *Drosophila*, NANOS1 is not a PGC marker in foetal mice, instead, its expression is detected in the central nervous system (Haraguchi et al., 2003). Taken together, this study showed *nanos1* has conserved zinc-finger domains in *G. holbrooki*, a component to embryo body patterning and translational repression. Evaluating the spatio-temporal expression of *nanos1* during *G. holbrooki* embryogenesis may reveal the spatial domain and evolutionary relatedness of this gene in this species (Chapter 3).

2.5. Conclusion

The six isolated GOIs had conserved structure and content compared to those of other vertebrates, albeit with some taxa specific differences. The phylogenetic evaluations of the studied genes revealed a strong homology between *G. holbrooki* and those of poeciliids, indicating they share the most recent common ancestor. In addition, all six candidate genes have the critical domains, previously shown to be essential for germline determination and maintenance in teleosts. Therefore, it is expected that the isolated genes will be instrumental in PGC formation (Chapter 3) and gonad function (Chapter 4), in *G. holbrooki*.

Chapter III

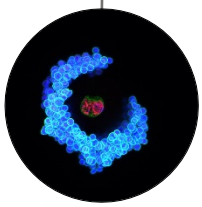

PGC development in *G. holbrooki*

Chapter 3 | The expression profile of PGC markers in the invasive species *Gambusia holbrooki*

Abstract

In teleosts with preformation mode of PGC specification, maternal inheritance of Gp provides sufficient factors to form the germline fate of nascent PGCs, protecting their identity against surrounding soma. Later, during embryonic patterning and cell determination, the Gp components are involved in proliferation, migration, and colonisation of germ cell precursors. To understand how and when PGCs are formed, migrate, and colonise putative gonad in *G. holbrooki* and how well these events are conserved across teleosts, *in situ* hybridisation and quantitative expression profiles of five PGC markers, namely *dazl*, *dnd*, *nanos1*, *piwi II* and *vasa* were studied. Based on their expression profiles, a group of Gp components were detected in the ovum suggesting maternal inheritance mode of PGC specification in *G. holbrooki*. Subsequent to fertilisation, the results showed that *vasa* positive cells were detectable from late cleavage, later forming as two PGC clusters at the early gastrula stage, migrating anteriorly during somitogenesis and eventually colonising at the genital ridge before the pharyngula stage. Of all the markers studied, only *vasa* and a *dnd* variant had signals restricted to PGCs. The embryonic expression of *piwi II*, *dazl* and *dnd-β* were detected in PGC clusters as well as the central nervous system. Interestingly, the embryonic expression of *nanos1*, an indispensable PGC marker in zebrafish, was only found in neural tube. The quantitative gene expression profiles showed a transient female-biased surge of the PGC markers at the gastrula stage, suggesting an early onset of PGC proliferation, in females. Strictly zygotic expression patterns of *dnd-β* and *nanos1* also showed maternal to zygotic transition (MZT) occurs before the mid-cleavage stage, in *G. holbrooki*. Collectively, the results suggest that despite sharing preformation mode of PGC specification, their migration pattern in *G. holbrooki* is unlike any other fish species studied so far. Instead, somatic expression of teleostean PGC markers (*e.g.*, *piwi II*, *nanos1* and *dazl*), splicing variation (*e.g.*, *dnd*) and early MZT appear more similar to those of mammalian models.

3.1. Introduction

Primordial germ cells are the stem cells of life; they give rise to either gamete, safeguarding the reproductive function of an individual and transferring genetic material to ensuing generations. Two patterns of germ cell development are known in sexually reproducing animals; 1) Preformation mode, in which pre-packaged molecules in gametes trigger PGC specification in early zygotes (Raz, 2002, Santos and Lehmann, 2004) and 2) Induction mode, where epigenetic reprogramming in a group of pluripotent cells induces PGC identity (Wang and Cao, 2016). Thriving on a range of reproductive approaches (Devlin and Nagahama, 2002), fish taxa have evolved both modes of PGC specification (Walvig, 1963, Extavour and Akam, 2003), however, the majority of teleosts including research models (Raz, 2002, Herpin et al., 2007) and commercial species (Nagasawa et al., 2013, Su et al., 2014) follow the preformation mode. Indeed, germ cell formation is preceded by several successive stages which their precursors (PGCs) encounter during embryogenesis; 1) PGC specification through parental derivates or epigenetic reprogramming, 2) mobility acquisition and migration path *en route* to the gonad anlage, 3) their colonisation at the genital ridge and eventually 4) attaining sexual identity, influenced by genetic or environmental cues. Based on the insight acquired from well-studied models, every task is governed by a group of genes which recruit epigenetic machinery (Andersen et al., 2012), RNA interference apparatus (Giraldez et al., 2006) and signalling pathways (Paksa and Raz, 2015) to safeguard the development program protecting them from somatic differentiation, ectopic migration and eventual apoptosis. Despite the shared biochemical pathways in PGC development, fundamental differences in the mode of PGC specification (*i.e.*, preformation vs epigenesis) are brought about by differences in the spatio-temporal expression profiles between taxa (Evans et al., 2014, Crother et al., 2016). For instance, maternally supplied *vasa* (Hartung et al., 2014) and *nanos1* (Koprunner et al., 2001) respectively maintain the specificity and quantity of PGCs, during zebrafish (*Danio*) embryogenesis. Moreover, *deadend* as one of the regulators of the RNA interference machinery is indispensable for PGC migration (Ketting, 2007) and sequestration (Hong et al., 2016) in teleost models. In higher vertebrates, instead, maternal deposits are erased very early (*i.e.*, before the two-cell stage) and the epigenetic machinery governs PGC specification (Saitou et al., 2012, Seisenberger et al., 2012). Correspondingly, *Ter* mutation introduces a premature termination codon in the murine ortholog of *Deadend* (*Dnd*) and does not completely ablate germ cells (Youngren et al., 2005). Also, *Nanos1* expression, an embryonic germ cell-specific marker in zebrafish, is not observed in murine PGCs and its mutation does not affect the fertility of mutants mice (Haraguchi et al., 2003). Therefore, PGC specification, their pattern of migration and the underpinning genetic mechanisms maybe more diverse than currently known.

The ovi-viviparity transition observed in poeciliids has incorporated complex alteration in the biology of reproduction; including developing spermatozoa bundles (Grier et al., 1981) and an intromittent

organ *i.e.*, gonopodia for deposition of sperm (Gasparini et al., 2011) in males, and matrotrophy, intrafollicular gestation (Pollux et al., 2014, Roberts et al., 2016) and superfetation (Guzman-Barcenas and Uribe, 2019) in females. The pseudo-placenta which has evolved in poeciliids provides a maternal-fetal interface (Olivera-Tlahuel et al., 2018) displaying similar reproductive traits to mammals. However, the consequences of this evolutionary convergence on germ cell formation and gonadogenesis is yet to be explored.

Live-bearing eastern mosquitofish, *Gambusia holbrooki*, are is native to the Atlantic and Gulf Slope drainages as far west as southern Alabama (Meffe et al., 1990). Taking advantage of its environmental (Otto, 1973) and reproductive (Pyke, 2005, Norazmi-Lokman et al., 2016) resilience, *G. holbrooki* has established globally and spread its population in natural inlets and estuaries, posing a threat to local biodiversity (Ayres et al., 2012). Classified as a predatory invasive species (Lowe et al., 2000), a number of approaches have been suggested to control *G. holbrooki* populations, however, none are effective, particularly at large spatial scales. In this regard, gaining insight into cellular and genetic pathways associated with germ cell development and gonadogenesis in *G. holbrooki* is expected to enhance our understanding of reproductive biology in live-bearing poeciliids in general and may provide promising approaches for their genetic control. Towards this goal, this study investigated the spatio-temporal expression of key genes (*dazl*, *dnd*, *nanos1*, *piwi II* and *vasa*) involved in PGC development during embryogenesis to trace the migration pathway and fate of PGCs in *G. holbrooki.* The outcome compares the spatial domains of PGC markers during embryonic development in *G. holbrooki* with those of teleost, t which may suggest the ingredients of precise germ cell ablation targets in poeciliids. As poeciliids show shared reproductive traits with teleosts and mammals, this study may provide a potency to evaluate the evolution of the candidate gene expression with further inference in their function.

3.2. Methods

3.2.1. Wild fish collection and housing

Rearing and handling of animals was as described in Chapter 2. The experimental ovum and developing embryos were obtained from gravid females as previously described (Norazmi-Lokman et al., 2016) and processed according to laboratory procedures.

3.2.2. RNA isolation and quantification

To evaluate expression profile of the key PGC markers during early development, total RNA from six distinct developmental stages including ova (*i.e.*, vitellogenic oocytes stage V obtained from virgin females), cleavage (*i.e.*, mid-morula stage), blastula (*i.e.*, 1000-cell stage), gastrula (*i.e.*, the onset of embryonic shield elongation), early segmentation and late segmentation were isolated and used in

quantitative PCR assay (n = 4-8 /sex/developmental stage). In addition, to distinguish the spatial domains (*i.e.*, anterior and/or posterior of the developing embryos) of expression, somite stage embryos (n = 5) were used. For this, most of the yolk was removed by puncture using Dumont #5 fine forceps (F.S.T, Canada) and the tissue partitioned as head (anterior to otic vesicle) and trunk halves (Fig. 3.2C) using a dissecting knife with a fine straight tip (10055-12, F.S.T, Canada) and each half processed separately for RNA isolation. The expression of the target genes in adult (n = 4/tissue/sex) liver, kidney, spleen, skeleton muscle, heart, eyes, brain, testis and ovary were also tested.

For RNA isolation, individual embryos and adult tissues were rinsed in cold PBS and stored in RNAlater (Sigma-Aldrich, Missouri, USA) until nucleic acid extraction. The total RNA from individual embryos and 15 - 25 mg of tissues were isolated using AllPrep DNA/RNA Mini Kit (QIAGEN, USA). The residual genomic DNA of late embryos and adult tissue was removed using Ambion™ DNase (Thermo Scientific, USA) treatment and the treated RNA was purified by Monarch® RNA Clean-up Kit (New England Biolabs). The quantity of isolated RNA was measured by Qubit® 4 Fluorometer (ThermoFisher Scientific, Massachusetts, USA) and the RNA integrity was confirmed visually using agarose gel electrophoresis. The purified RNA was then reverse transcribed using MMLV Reverse Transcriptase (Takara, Kusatsu, Japan), with a final concentration of 6 - 230 and 250 ng/µl for embryos and tissues, respectively (Qubit™ RNA high sensitivity (HS) assay kit, Invitrogen, Australia). For non sex-segregated assay, the cDNA concentration of the samples were normalised to the stage with the lowest concentration (*i.e.*, cleavage embryos) before using in qPCR. For sex-segregated assay, the cDNA concentration was normalised between sexes within the same developmental stage. The synthesised cDNA from adult tissues and somite embryos were later used in end-point PCR assays (Fig. 3.2A and B).

3.2.3. cDNA Cloning and full-length sequencing

To obtain full-length cDNA of the genes from *G holbrooki* (see Chapter 2), the predicted cDNA sequences from different poeciliid species were retrieved from the NCBI database and multiple sequence alignments were applied using MUSCLE (Edgar, 2004). Subsequently, degenerate primers were designed based on highly conserved regions of the target cDNA homologues using a modified version of Primer3 3.2.7 (Geneious Prime® 2020.2.3). The primers were recruited to amplify target cDNA fragments through conventional polymerase chain reaction (PCR) and the PCR products were purified and cloned into pCR®2.1-TOPO® vectors using TOPO™ TA Cloning Kit (Life Technologies Corporation, CA, USA) for sequencing. The resulting sequences were used to design *G. holbrooki* specific primers and used in RACE (Rapid Amplification of cDNA Ends) PCR to amplify the full-length cDNA using GeneRacer™ Kit (Life Technologies) according to the manufacturer's protocol.

3.2.4. Primer design, qPCR data normalisation and statistical analysis

The oligomers used for end-point and qPCR assay (Table 3.1) were designed using Primer 3.2.7 (Geneious Prime® 2020.2.3) with slight modification to avoid self-dimer and secondary structures (Untergasser et al., 2012). The efficiency of primers was also tested with different dilutions for each gene, separately. The real time PCR mix (10 µl) comprised of 1X iTaq Universal SYBR Green Supermix (Bio-Rad, NSW, Australia), 5-10 ng cDNA Template, 0.4 µM of each primer, and adjusted to 15 µl using MilliQ water. Duplicate reactions were run for each cDNA sample using CFX96 Touch Real-Time PCR Detection System (Bio-Rad, NSW, Australia) consisted of 95 ˚C for 1 min, followed by 40 cycles of 95 ˚C for 5 s, 66-68 ˚C for 10 s, and 72 ˚C for 7-15 s. For positive and negative control, 5 ng cDNA (from a tissue where the target gene is expressed) and MilliQ water were used as template, respectively. Melting curve analysis, gel visualisation and sequencing of qPCR products were subsequently performed to check unwanted products and gDNA contamination. The Minimum Information for Publication of Quantitative Real-Time PCR Experiments (MIQE) of the qPCR assay was provided in Table A10 (Bustin et al., 2009).

Four housekeeping genes, namely *rps18*, *gapdh*, *pgk1* (Panina et al., 2018) and *β-actin* (Kwan and Patil, 2019) were tested for biological normalisation of qPCR data through geometric averaging of the candidate genes (Vandesompele et al., 2002). Geometric averaging and stability of the selected genes were analysed using geNorm algorithm (Hellemans et al., 2007) provided by qbase+ software, version 3.0 (Biogazelle, Belgium). The *β-actin* with no sex-biased expression was selected to normalise qPCR data as the most stable housekeeping gene (M value 0.41). The relative transcription of target genes was calculated using the comparative threshold cycle (Cq) method with efficiency correction (Ruijter et al., 2009). Relative expression of genes of interest (ΔCq) was calculated against the selected reference gene and presented in plots. The expression fold changes presented were measured using the $2^{(-\Delta\Delta Cq)}$ method (Livak and Schmittgen, 2001).

All qPCR data were presented as mean ±standard deviation (SD). Shapiro–Wilk and Levene's tests were used to test data normality and homogeneity of variances, respectively. A one-way analysis of variance (ANOVA) was used to identify significant differences between experimental groups of the pooled gene expression data using developmental stages as the only independent variable. For the sex-segregated gene expression data, a two-way ANOVA was used to identify significant differences between groups using developmental stages and sexes as two factors. When applicable, Tukey HSD tests were used to compare the significance level of differences across treatments (Tukey, 1949). The difference between two means was considered significant when $p < 0.05$. Statistical analysis and plotting were performed using OriginPro, Version 2021 (OriginLab Corp, MA, USA).

Table 3.1. Oligomers used in qPCR and WM-ISH assays used in Chapters 3 and 4.

Gene	Purpose	Accession number/reference	Annealing/hybridisation temp (C °)	Sequence (5′– 3′)	Length (bp)
vasa	q-PCR	MZ542293	66.1	GCAAAGGGAGAGGCAGAGGAGGA	108
				CTCTACCGCCTCTCCCACTGAAACCA	
	WH-ISH		69.0	CATAAATATGGACGAGTGGGAAGAAG	1122
				ATGTCCAACATCCGGTCGGCCTCGTC	
nanos1	q-PCR	MZ542291	67.5	TCGATCTCTTTGGTGTGGAGCGGAAGAT	91
			67.0	CCGTTATTCCGGCAGAACACGCAGATTT	
	WH-ISH			TCGATCTCTTTGGTGTGGAGCGGAAGAT	716
				ACATAACTTTGGTTTCTCTAAGACATG	
dnd-α	q-PCR	MZ542289	69.0	GTTAACGGGCAGAGGAAGTACGGAGGA	96
				CCGAGGGATGTGGCTGATGAAGACC	
	WH-ISH			GCCTGGCTGGAAATGACCAA	896
				CCATCCGGTCTGGCCAAACTGTAGTG	
dnd-β	q-PCR	MZ542290	68.0	GTTAACGGGCAGAGGAAGTACGGAGGA	96
				CCGAGGGATGTGGCTGATGAAGACC	
	WH-ISH			GCCTGGCTGGAAATGACCAA	830
				CCATCCGGTCTGGCCAAACTGTAGTG	
piwi II	q-PCR	MZ542292		TGAACACCTGGTGAGACGGATCGGAA	103
				TGGAAGTCTGCCTTGTCACTGAGGTCA	
	WH-ISH		69.0	TGAACACCTGGTGAGACGGATCGGAA	1419
				ACAGCCCTCCATCTGTGCGCTTAATA	
dazl	q-PCR	MZ542288	67.8	GGGTTTGCAAAGGGTACGGGTTTGTGT	104
				GCCCAGCTTGAGTTTCCGCCCTTTA	
	WH-ISH		69.0	AGGGCAGACTGACCCCCAA	908
				TGGCTGGTATACCAAATGTGCTCT	
cxcr4	q-PCR	MZ542287	65.3	AACACACGTTCCCTGCTGCCAAAACTT	110
				CCCGGAGATGTTGTAGGTGTTGTTATCG	
tdrd6	q-PCR		64.0	GAAGGAGACGACGGATACAGAATTGGA	108
				TCTCCAGCCTCAGTTTCCTGCTCAC	
β-actin	qPCR	MZ542286	67.2	CGGCAGGACTTCACCTACAGACACCT	99
				CTTGCACAAACCGGAGCCGTTGTCA	
gapdh	q-PCR	(Kwan and Patil, 2019)	64.5	CGTTGCATTTTTCCAGGACAGATGGA	103
				GCAGAACTCAGCAAAACCCTGGGA	
rps18	q-PCR	OL988674	66.5	GGAGAGGCTGAAGAAGATCAGGGCTC	109
				ACCGACAGTGCGACCACGACG	
pgk1	q-PCR	OL988673	66.0	GATGATCATCGGTGGCGGCATGG	96
				ATACCAGCGCCTTCCTCGTCGAACA	

3.2.5. Whole mount *in situ hybridization* (WM-ISH)

The WM-ISH was used to investigate the spatial expression of the target genes in nine embryonic stages (*i.e.,* from late cleavage to early pharyngula) of *G. holbrooki*. To ensure specificity, the sense and antisense RNA probes were generated from a less conserved region of target cDNAs such as untranslated regions (Thisse and Thisse, 2008). The respective cDNAs were first inserted into pCR®2.1-TOPO vector (Chapter 2). Both sense and antisense DIG-labelled RNA probes were produced through *in vitro* transcription using T7 RNA polymerase (NEB) and DIG RNA labelling mix (Roche, Mannheim, Germany). Any traces of cDNA in the probes were eliminated using Ambion™ DNase (Thermo Scientific, USA), purified by ethanol precipitation and stored with RNase inhibitor, RNasein® Plus (Promega, USA) at -20 ºC.

The WM-ISH followed those described for fish embryos (Thisse and Thisse, 2008), with modifications. Briefly, the dissected clutches of developing embryos were individually detached from placenta, rinsed with cold PBS, and fixed using 4% paraformaldehyde (Emgrid) overnight at 4˚C. The fixed embryos were washed in PBS containing 0.1% Tween 20 (PBST), progressively dehydrated with PBST-methanol, and stored in 100% methanol until use. The embryos at the early and mid-pharyngula stages were depigmented before dehydration using 3% H_2O_2 and 1% KOH. On the day of hybridization, the embryos were sequentially rehydrated in four stages with progressively increasing concentrations of methanol-PBST, manually dechorionated, permeabilized with 10-25 µg/ml proteinase K (Bioline) and postfixed with 4% paraformaldehyde for 30 min. The embryos were prehybridized at 68 ˚C for 3 hours in hybridization buffer (50% formamide, 5X SSC, 0.01% Tween 20, Torula Yeast tRNA, 50 µg/ml heparin) and hybridized in the same buffer containing antisense RNA probes (100-250 ng/ml) at 67-69˚C for 16-24 hours, as required for target gene and developmental stage. This was followed by stringency washes in PBST under gentle agitation, with progressively lower salt concentrations, to remove any non-specifically bound probes. For immuno-labelling, the potential non-specific binding was blocked using blocking solution (5% blocking reagent (Roche) in maleic acid buffer containing 0.1% Tween 20). The embryos were then treated with 1:3000–1:5000 anti-DIG alkaline phosphatase (AP) antibody (Roche) at 4 ˚C for 16 hours. The antibody-labelled embryos were washed with PBST 8 times, 30 min each, at room temperature, under gentle agitation. To stain, embryos were first treated with staining buffer (100 mM Tris HCl pH 9.5, 50 mM MgCl2, 100 mM NaCl, 0.1% Tween 20) three times by replacing with fresh buffer every 10 min and then incubated in BM-purple stain (Roche) at room temperature and protected from light. The optimum staining time was adjusted according to developmental stages and target genes ranging from 5 to 45 hours. Following staining, the embryos were washed in PBST until all excess stain was removed and postfixed with 4% paraformaldehyde

overnight at 4˚C. The fixed embryos were washed and stored in PBS for imaging using MZ16FA stereomicroscope (Leica Microsystems, Germany).

3.2.6. Genetic sexing of *G. holbrooki* embryos

The DNA of developing embryos was isolated during RNA extraction procedure using AllPrep DNA/RNA Mini Kit (QIAGEN, USA). The isolated DNA samples were subsequently used in a simplex PCR assay targeting a sex-specific loci described previously for the species (Kwan and Patil, 2019, Patil et al., 2020). Briefly, PCR mix (10 µl) comprised of 1X MyTaq™ HS Red mix (Meridian Life Science, OH, USA), 0.4 mM of each primer and 50 ng of genomic DNA template. Thermal cycling (T100™ Thermal Cycler, Bio-Rad Laboratories, NSW, Australia) consisted of 95 ˚C for 1 min, followed by 30 cycles of 95 ˚C for 5 s, 60 ˚C for 5 s, and 72 ˚C for 20 s. Female and male specific amplicons were visualised using 1% (in TAE buffer) gel electrophoresis.

3.3. Result

The PGC migration pattern, spatio-temporal expression of teleostean PGC markers and their specificity to embryonic germline were successfully documented for *G. holbrooki* and the salient features are detailed below.

3.3.1. The pattern of PGC migration in *G. holbrooki*

As evident from WM-ISH, the *vasa* mRNA signals were first detectable at the cleavage plane emerging as a few tiny spots distributed throughout the blastomere (Fig. 3.1A). At this stage, the blastomere was partially obscured by egg yolk (*i.e.*, meroblastic cleavage) and the buried (deep) cells were masked by oil-droplets, *i.e.*, the signals were detected underneath the oil droplets. At early blastula (1000-cell stage) concurrent with increased blastoderm area (400-450 µm) and asynchronous cell divisions, the *vasa* signal was intense in a few distinctive regions with asynchronous distribution (Fig. 3.1B). At mid-blastula, four distinctive spots were detectable buried underneath a superficial layer of cells (Fig. 3.1C). At late blastula, the *vasa*-positive signals had increased and were arranged peripherally as small clusters (Fig. 3.1D).

At the onset of the gastrula stage (*i.e.*, dome to 30%-epiboly), the blastoderm had begun to expand over the surface of the yolk, the dome boundaries were difficult to recognise, and the anterior-posterior axis was yet to be distinguished (Fig 3.1E). At the early gastrula stage, the *dnd-α* signals had coalesced and appeared as two compact clusters of cells located at the margin of the dome (Fig. 3.1E). At the mid to late gastrula stage, the anterior-posterior axis of the embryo was distinguishable, for the first time, and the optic primordia began to form as the body-axis lengthened and thickened. Here, the *vasa*-positive cells appeared pellucid and were located at the posterior part of the embryo.

At this stage, the PGCs were identified as clustered and individual germ cell precursors being located at the junction of yolk extension, close to the posterior trunk (Fig. 3.1F). At the onset of somitogenesis, concurrent with considerable expansion of the head, rudimentary brain formation and first visible somites, the two clusters of PGCs were still visible, one on either side of the body axis, forming narrow queues of cells (Fig. 3.1G and Fig. 4D). Based on the spatial distribution of PGCs two directions of motility were discernible, with the two clusters beginning to 1) converge inwards, i.e., PGC clusters moved towards each other and 2) migrating anteriorly.

At early to mid-somitogenesis, coinciding with significant body elongation, PGCs exhibited a relatively enhanced mobilisation compared to the late gastrula stage evident from the translocation of signals. At mid-somitogenesis, where 12-14 somites, solid optic capsules and otic vesicles were visible, the two PGC clusters were clearly observed extending from the 6th to 8th somite (Fig. 3.1G). The PGC clusters maintained their integrity (i.e., cells moving in a close vicinity to each other), however, the narrow queue of cells clustered tightly (thickened and shortened cluster of cells), compared to preceding developmental stages. At late segmentation, PGC clusters were observed on either side of the body axis, directly underneath the somites and the spinal cord, in closest proximity to each other (Fig. 3.1H). At early pharyngula, the PGCs had migrated and coalesced at the genital ridge and remained in two distinctive clusters (Fig. 3.3E). At the mid pharyngula stage, the signal from the germ cell marker in the gonad lobes intensified and expanded towards each other (Chapter 5).

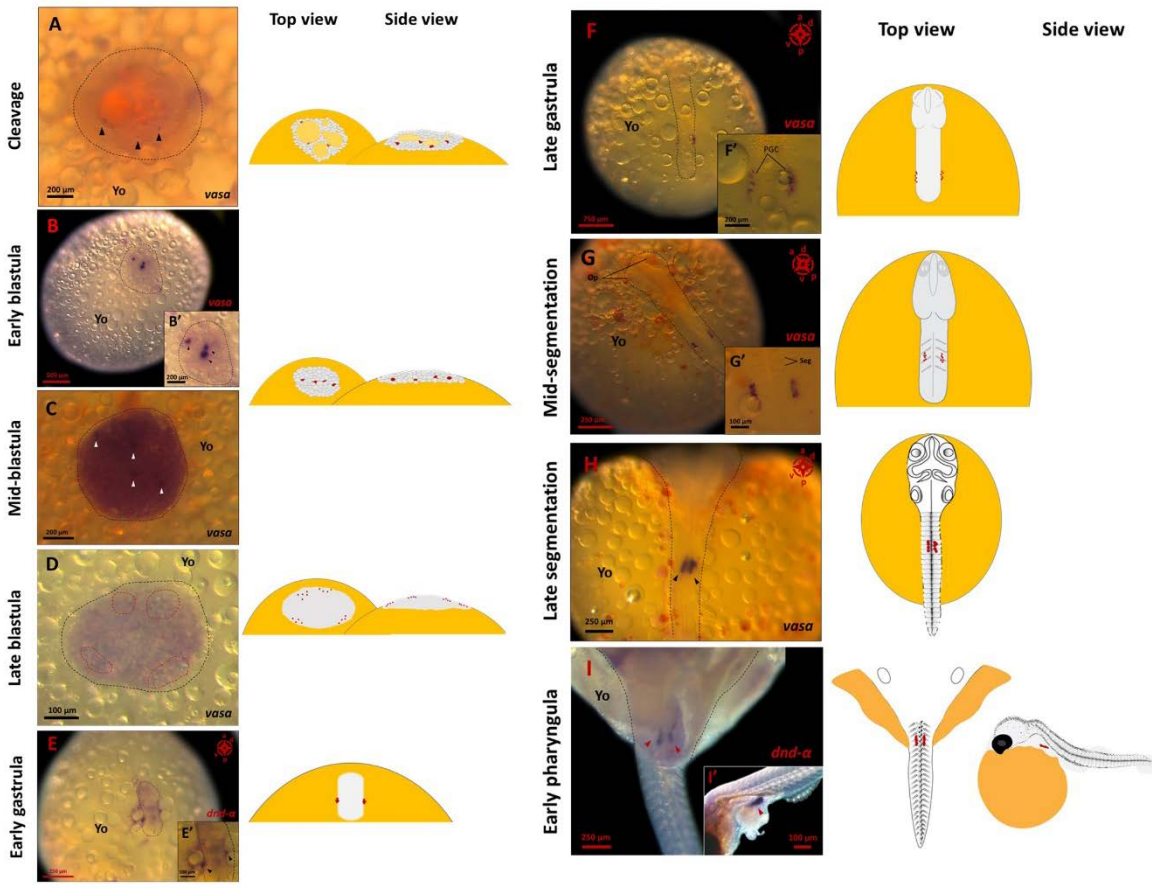

Figure 3.1. WISH panels showing the actual and schematic locations of PGC during *G. holbrooki* embryogenesis. The PGC markers, either *vasa* or *dnd-α* signals at nine developmental stages are presented. The *vasa*-positive cells are first detectable (A, black arrowhead) emerging as a few tiny spots distributed throughout the cell mass (n=3). At early blastula (B), the *vasa* signal was intensified in a few distinctive regions (black arrowhead in close-up B') with asymmetric distribution (n=4). Later, four distinctive spots (C, white arrowhead) are detectable buried underneath the superficial layer of cells (n=3). At late blastula (D), the *vasa*-positive signals increase and appear peripherally as small clusters (n=4). At early gastrula (E), the PGCs coalesce as two compact clusters of cells (black arrowhead in the close-up E') located at the margin of the dome (n=4). At late gastrula (F), the PGCs were located at the posterior half of the embryo (n=3). During segmentation stages (G, n=5 and H, n=4), the PGC clusters migrate convergently and anteriorly, and at early pharyngula (I), they eventually home at genital ridge (red arrowheads) and form a bi-lobular presumptive gonad (n=7). The black dashed lines indicate the area of the cleavage plane and blastodisc (A and B), and embryonic axis (E, F, G, H and I) respectively. The red dashed lines (D) show the signals clustered in four groups. The red dots in schematics represent relative position of the PGC marker signals. Op, optic bud; Yo, yolk; Seg, segments. The compass indicates the orientation of body axis where applicable (a, anterior; p, posterior; d, dorsal and; v, ventral).

At early to mid-somitogenesis coinciding with significant body elongation, PGCs exhibited a relatively enhanced mobilisation compared to late gastrula stage evident from translocation of signals. At mid-somitogenesis, where 12-14 somites, solid optic capsules and otic vesicles were visible, the two PGC clusters were clearly observed extending from the 6th to 8th somite (Fig. 3.1G). The PGC clusters maintained their integrity (*i.e.*, cells moving in a close vicinity to each other), however, the narrow queue of cells clustered tightly (thickened and shortened cluster of cells), compared to preceding developmental stage. At late segmentation, PGC clusters were observed on either side of the body axis, directly underneath the somites and the spinal cord, in closest proximity to each other (Fig. 3.1H). At early pharyngula, the PGCs had migrated and coalesced at the genital ridge and remained in two distinctive clusters (Fig. 3.3E). At the mid pharyngula stage, the signal from the germ cell marker in the gonad lobes intensified and expanded towards each other (chapter 5).

3.3.2. The relative spatio-temporal expression of the teleost PGC markers in *G. holbrooki*

dnd

Two spliced variants were cloned and characterised in *G. holbrooki* (Chapter 2). In adult tissues, those spliced variants were only found in the testis and ovary although *dnd-β* had a very weak signal in gonads (Fig. 3.2A). However, in somitogenesis embryos, *dnd-α* and *dnd-β* was exclusively detected in the posterior and anterior parts, respectively (Fig. 3.2B). Also, the WM-ISH assay revealed that the *dnd-α* signal corresponded to the location *of vasa*-positive cells in all embryonic stages including labelling homed germ cells at the genital ridge (Fig. 3.3A, C and E). In contrast, *dnd-β* was in the head; at the anterior region at early gastrula (Fig. 3.3B), expanded in both sides of the neural tubes at early segmentation (Fig. 3.3D), and mainly restricted to the cerebellum during early pharyngula (Fig. 3.3F).

The qPCR assay showed the expression level of *dnd-α* in ovum was slightly decreased after fertilisation (ANOVA, $F_{5,55} = 55.11$, $p < 001$, Fig. 3.5.C) eventuating in a slight reduction at blastula ($\Delta\Delta Cq = 1.4 \pm 0.37$ $\log_2$, $p<0.1$, Fig. 3.5C). At the gastrula stage, the relative *dnd-α* expression rose to 4 times higher compared to that at the blastula stage ($\Delta\Delta Cq = 2.1 \pm 0.47$ $\log_2$, $p<0.05$, Fig. 3.5C), however, its expression strongly dropped at the onset of somitogenesis ($\Delta\Delta Cq = 4.25 \pm 0.31$ $\log_2$, $p<0.01$) and the relative downregulation was consistent until PGC colonisation (Fig. 3.5C). The expression pattern of *dnd-α* mainly did not exhibit a sex-dimorphic trend in the studied window (ANOVA, $F_{9,44} = 35.12$, $p<001$, Fig. 3.5.D), excluding the gastrula stage where *dnd-α* transcription was more than 18 fold higher in females than that in males ($\Delta\Delta Cq = 4.21 \pm 0.31$ $\log_2$, $p<0.01$, Fig. 3.5D).

The expression of *dnd-β* was barely detectable or absent in unfertilised eggs (ANOVA, $F_{5,41} = 27.45$, $p<001$, Fig. 3.6.A). However, a surged expression at cleavage ($\Delta\Delta Cq = 6.7 \pm 0.72$ $\log_2$, $p<0.001$, Fig. 3.6A) and blastula ($\Delta\Delta Cq = 6.0 \pm 0.50$ $\log_2$, $p<0.001$, Fig. 3.6A) was observed compared to ova.

Nevertheless, the expression of *dnd-β* showed an inclining trend within the PGC development window (Fig. 3.6A).

dazl

The end-point PCR assay showed *dazl* transcription was restricted to ovary and testis among adult tissues (Fig. 3.2A). However, *dazl* expression was detected in both head (anterior) and trunk (posterior) regions of the developing embryos during mid- and late somitogenesis (Fig. 3.2B). The spatial expression of *dazl* was observed in a few distinct regions. At the anterior part, a strong signal was found in the otic vesicles with a weak signal in the eyes (Fig. 3.4A), and at the posterior part of the embryos, a *dazl* signal was observed in *vasa*-positive cells (Fig. 3.4B).

The relative expression level of *dazl* at cleavage and blastula stages did not show a significant change compared to its expression level in unfertilised egg (ANOVA, $F_{5,46} = 70.47$, $p<001$, Fig. 3.5A). However, the highest zygotic expression of *dazl* during PGC development was detected during the gastrula stage; 1.5 ($\Delta\Delta$Cq=0.56±0.31 log2, $p<0.05$) and 22 fold ($\Delta\Delta$Cq=4.48±0.42 log2, $p<0.001$) higher than blastula and early segmentation, respectively (Fig. 3.5A). Also, the sex-dimorphic pattern of *dazl* expression (ANOVA, $F_{5,55} = 55.11$, $p <001$, Fig. 3.5.B), showed a comparable trend during cleavage and blastula stages, while its transcription demonstrated a sex-dimorphic level at the gastrula stage, displaying more than 21 fold higher expression in females ($\Delta\Delta$Cq=4.4±0.61 log2, $p<0.001$, Fig. 3.5B). At early somitogenesis, the sex-dimorphic pattern of *dazl* expression remained unchanged (*i.e.*, females biased) with a converging trend observed in late somitogenesis (Fig. 3.5B).

piwi II

The expression of *piwi II* in adults was only detected in testis and ovary (Fig. 3.2A). The embryonic expression of *piwi II* was detected in both anterior and posterior regions at mid- and late segmentation (Fig. 3.2B). Similarly, the spatial transcription of *piwi II* was found in two distinct regions; 1) a large part of the developing brain restricted to the mesencephalon and diencephalon but excluding the peripheral area (Fig. 3.4C) and 2) corresponding to the *vasa*-positive cells migrating towards the genital ridge (Fig. 3.4D). The qPCR assay showed early embryonic expression of *piwi II* at cleavage ($\Delta\Delta$Cq=3.9±0.41 $\log_2$, $p<0.001$) and blastula ($\Delta\Delta$Cq=4.6±0.43 $\log_2$, $p<0.001$) was much lower compared to its maternal expression in ova (ANOVA, $F_{5,43} = 22.92$, $p <001$, Fig. 3.5E). The zygotic expression of *piwi II* surged and was at its highest at the gastrula stage with a significant change compared to blastula ($\Delta\Delta$Cq=2.1±0.43 $\log_2$, $p<0.05$, Fig. 3.5E) and early somitogenesis ($\Delta\Delta$Cq=3.9±0.66 $\log_2$, $p<0.001$, Fig. 3.5E). Embryonic transcription of *piwi II* did not follow a sex-dimorphic pattern excluding the gastrula stage (ANOVA, $F_{9,33} = 17.15$, $p <001$, Fig. 3.5.F), in which females showed a significantly higher surge of *piwi II* transcription compared to males ($\Delta\Delta$Cq=4.9±0.46 $\log_2$, $p<0.05$, Fig. 3.5F).

nanos1

In adult tissues, *nanos1* was strongly detected in the ovary, although weak expression was also found in the testis and brain (Fig. 3.2A). In late somitogenesis embryos, *nanos1* transcripts were detected in the anterior part (Fig. 3.2B), congruous with its spatial expression throughout the rudimentary brain (Fig. 3.4E). Specifically, the *nanos1* signal was strongly expressed in the diencephalon, metencephalon, and otic vesicles, weakly detected in the optic cup but not detected in the lens (Fig. 3.4E).

The expression level of *nanos1* in ovum was low and barely detectable in some individuals, nevertheless, its expression increased significantly post-fertilisation (ANOVA, $F_{5,47} = 47.92$, p <001, Fig. 3.6B). At cleavage and blastula stages, the *nanos1* expression was about 168 ($\Delta\Delta Cq = 7.4 \pm 1.21 \log_2$, p<0.001, Fig 3.6B), and 512 ($\Delta\Delta Cq = 9.0 \pm 0.94 \log_2$, p<0.001, Fig. 3.6B) fold higher respectively, compared to its levels in ova. The *nanos1* expression was not sex-biased during early embryogenesis to late somitogenesis.

vasa

In relation to adult tissues, the end-point PCR assay only detected *vasa* transcription in gonads (Fig. 3.2A). However, females displayed stronger *vasa* levels in the ovary compared to levels detected in the male testis (see Chapter 4). Consistent with WM-ISH, the *vasa* transcription in the posterior part of the mid- and late somitogenesis embryos was prominent, with none in the anterior part (Fig. 3.2B).

From ova to early somitogenesis, the relative expression of *vasa* gradually decreased (ANOVA, $F_{5,52} = 6.98$, p <001, Fig. 3.5.G), but the expression was significantly reduced at late somitogenesis compared to early somitogenesis ($\Delta\Delta Cq=2.7\pm0.72$ log2, p<0.01, Fig. 3.5G). However, a sex-biased pattern of *vasa* expression was observed at the blastula stage with a higher expression in females ($\Delta\Delta Cq=2.7\pm0.63 \log_2$, p<0.05, Fig. 3.5H) but a more conspicuous difference during the gastrula stage, with a 34 fold higher expression in females ($\Delta\Delta Cq=5.1\pm0.73 \log_2$, p<0.001, Fig. 3.5H). Regardless of these gender differences, during somitogenesis, where PGCs displayed their most mobility, *vasa* expression did not show any noticeable sex-dimorphism (ANOVA, $F_{9,42} = 6.95$, p <001, Fig. 3.5H).

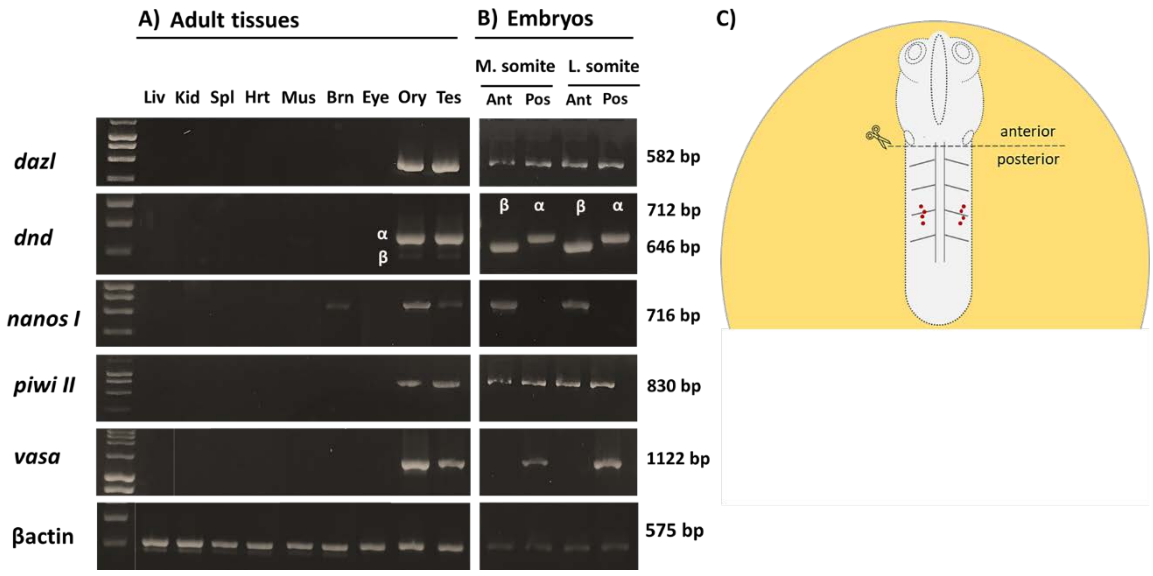

Figure 3.2. Photomicrograph, showing the expression of PGC marker genes in adult tissues (A) and embryos (B). Gene names and the amplicon size, in base pairs (bp) are indicated on the right and left of the panel respectively. βactin was used as an endogenous reference. Schematic (C) showing the anterior and posterior partitioning of the somite stages embryos for RNA extraction and end-point PCR assay. The red dots (C) show the location of migrating PGCs in mid-segmentation embryos. Liv, liver; Kid, kidney, Spl, spleen; Hrt, heart; Mus, skeletal muscle; Brn, brain; Eye, eyes; Ory, ovary; Tes, testis; M. somite, mid-somitogenesis; L. somite, late somitogenesis; Ant, anterior; Pos, posterior.

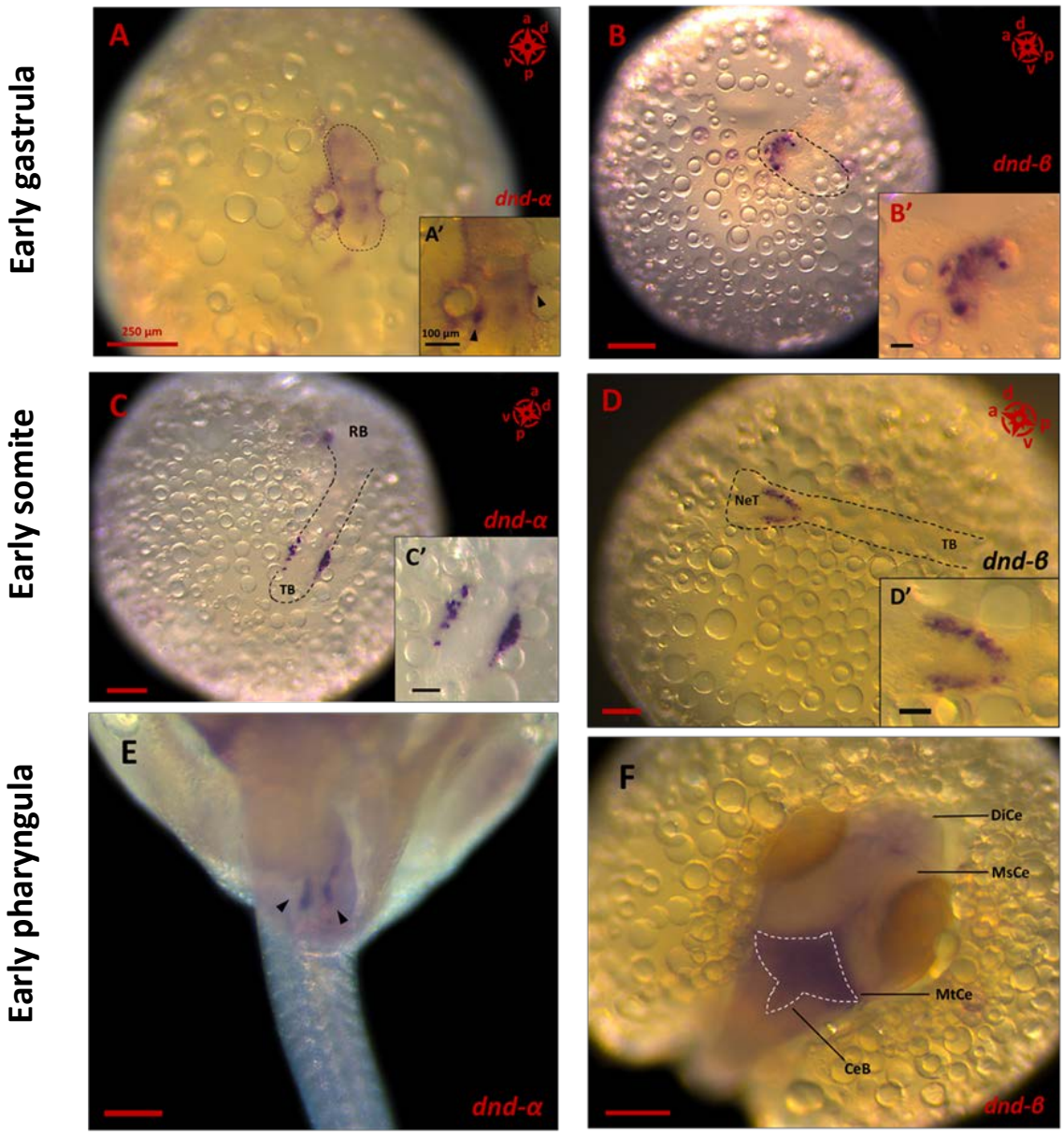

Figure 3.3. WM-ISH panels showing spatial expression of *dnd* spliced variants in three developmental timepoints of *G. holbrooki*. *dnd-α* is expressed in the posterior region of early gastrula (A, and A′), with condensed signals at two spots (black arrowheads in A') in the peripheral embryonic shield. At early segmentation, two clusters of *dnd-α* signals (corresponding to the location of PGCs) later appeared close to the tail bud (TB), (C and C′). At early pharyngula, *dnd-α* transcription marked the homed germ cells (black arrowheads) located as two distinctive lobes at the genital ridge (E). The *dnd-β* was first detected at the anterior region of the elongating body (B and B′). The *dnd-β* signal emerged as a crescent line at the putative head of gastrula but expanded in both sides of the neural tube (NeT) or rudimentary brain (RB) at early segmentation (D and D′) and eventually marked the metencephalon (MtCe) and cerebellum (CeB) of early pharyngula (F) with no expression in Mesencephalon (MsCe) and diencephalon (DiCe). The compass indicates the orientation of body axis where applicable (a, anterior; p, posterior; d, dorsal and; v, ventral). The black dashed lines indicate the location of embryonic shield (A and B) or body (C and D). The white dashed line displays the expression area of *dnd-β* in hindbrain. The scales represent 100 and 250 µm in A′–D′ and A–F, respectively.

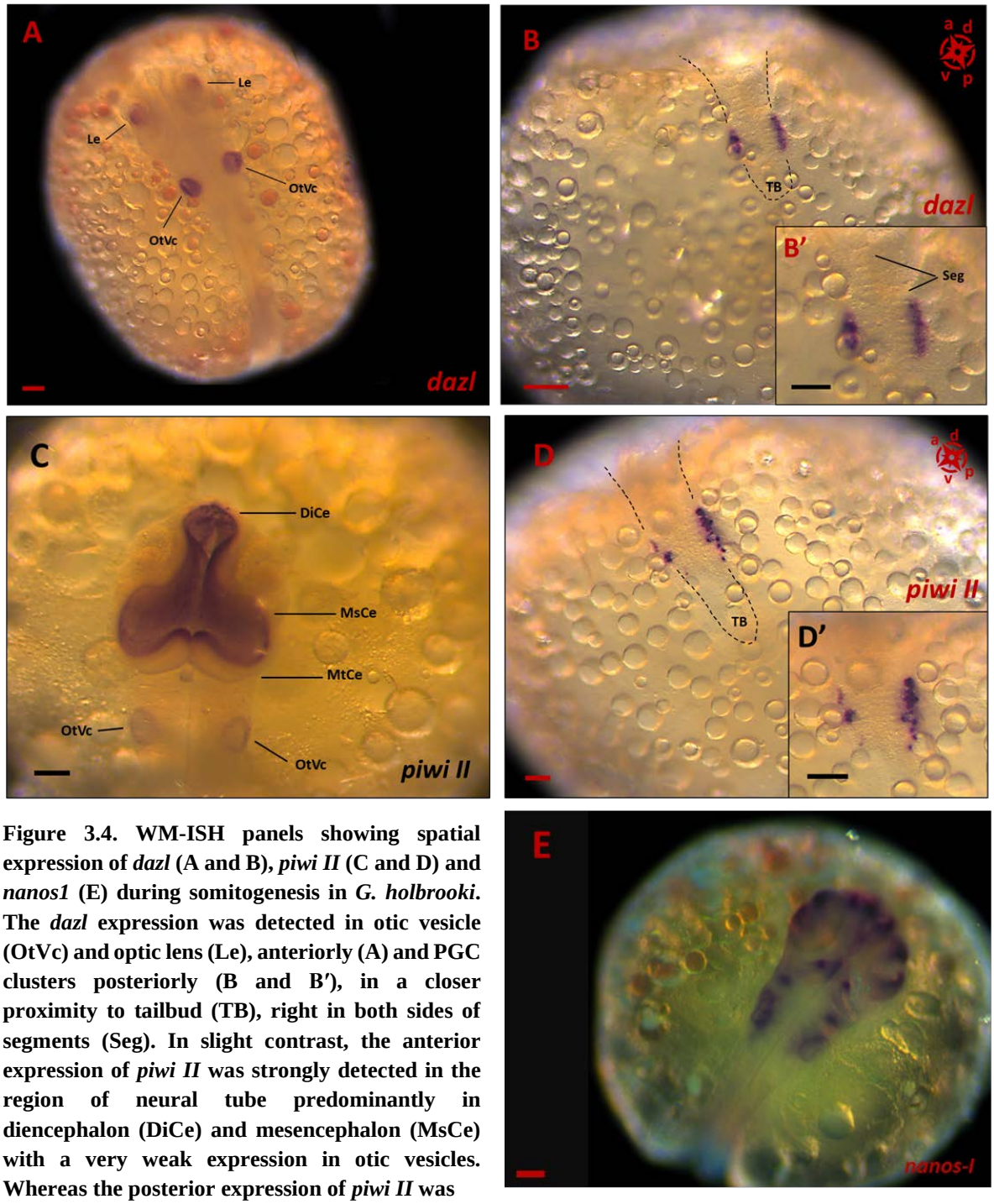

Figure 3.4. WM-ISH panels showing spatial expression of *dazl* (A and B), *piwi II* (C and D) and *nanos1* (E) during somitogenesis in *G. holbrooki*. The *dazl* expression was detected in otic vesicle (OtVc) and optic lens (Le), anteriorly (A) and PGC clusters posteriorly (B and B′), in a closer proximity to tailbud (TB), right in both sides of segments (Seg). In slight contrast, the anterior expression of *piwi II* was strongly detected in the region of neural tube predominantly in diencephalon (DiCe) and mesencephalon (MsCe) with a very weak expression in otic vesicles. Whereas the posterior expression of *piwi II* was restricted to migrating PGCs (D and D′). *nanos1* expression was exclusively detected in neural tube and otic vesicle of mid-somitogenesis embryos. The compass indicate the orientation of developing embryos where applicable. The black dashed lines indicate the location of embryonic body. The scale bars represent 100 µm.

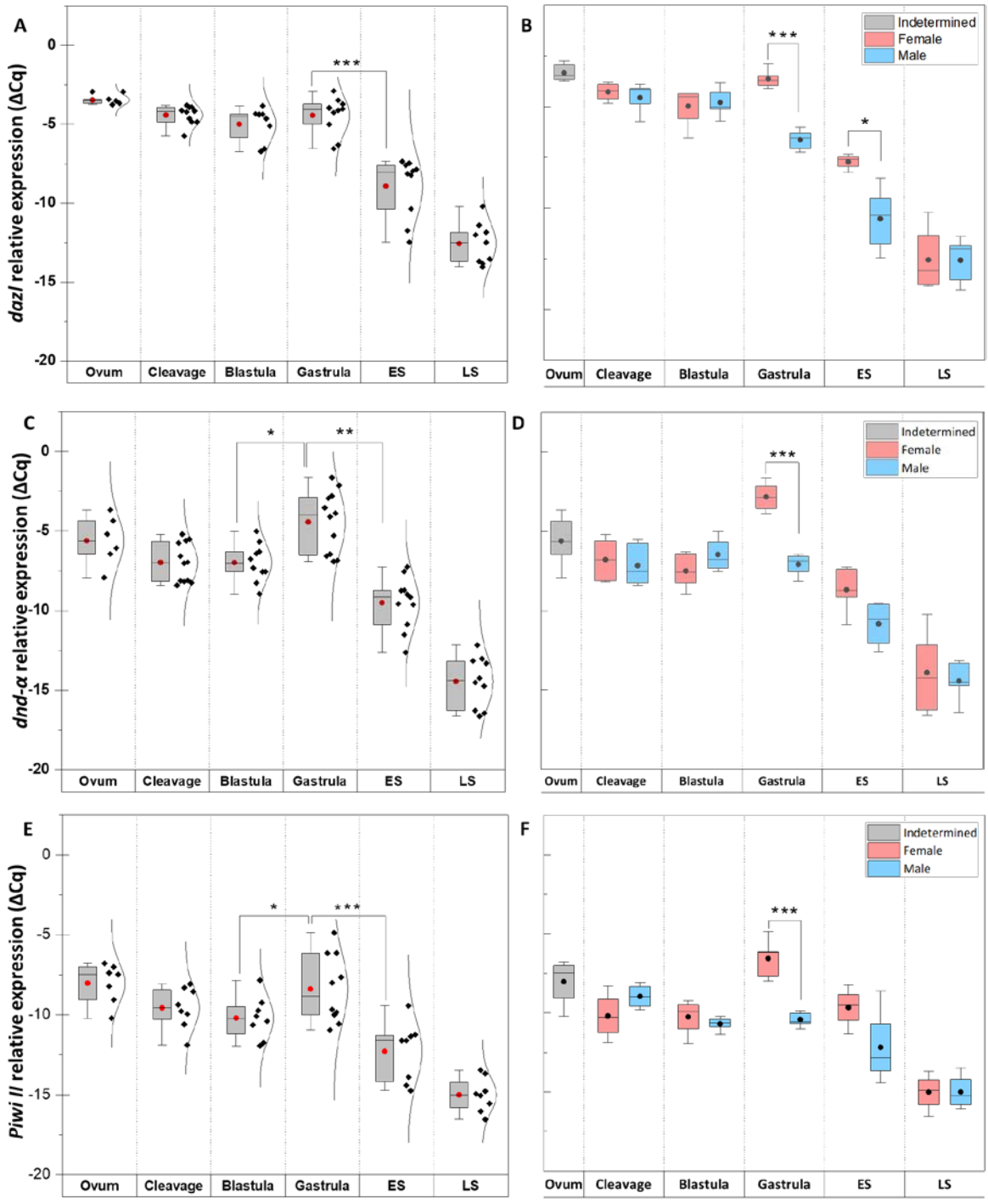
A
B
C
D
E
F
dazl relative expression (ΔCq)
dnd-α relative expression (ΔCq)
Piwi II relative expression (ΔCq)
0
-5
-10
-15
-20
Ovum
Cleavage
Blastula
Gastrula
ES
LS
Indetermined
Female
Male
*
**
***

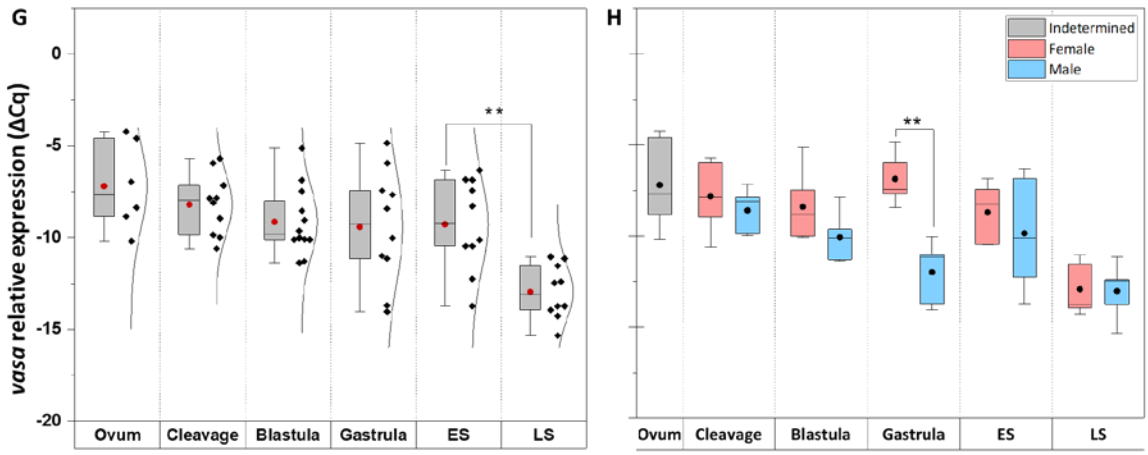

Figure 3.5. The pooled (left panel) and sex-segregated (right panel) quantitative expression of *dazl* (A, n = 9 – 11 and B, n = 7 - 8), *dnd-α* (C, n = 7 - 13 and D, n = 7 - 8), *piwi II* (E, n = 7 – 11, and F, n = 6 - 9) and *vasa* (G, n = 7 -12, and H, n = 7 - 8) in six embryonic developmental stages of *G holbrooki*. The dots and the horizontal line within the bars indicate mean and median of the data presented within the groups. The normal distribution curves are given in the pooled expression plots. The asterisks show the level of significance between groups; *= 0.05, **= 0.01, *= 0.001.**

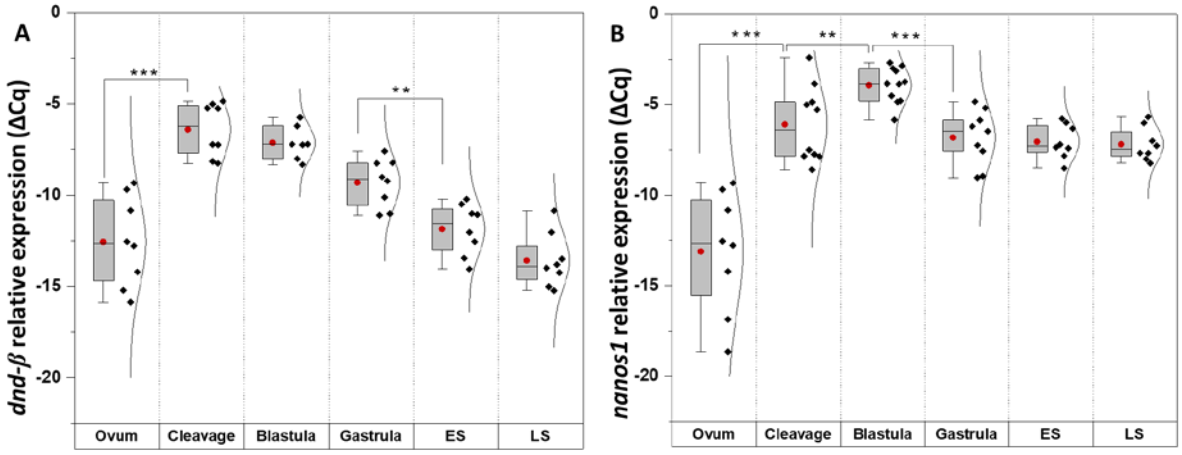

Figure 3.6. The panel representing quantitave expression of *nanos1* (A, n = 9 - 11,) and *dnd-β* (B, n = 8 – 9) in six embryonic developmental stages of *G. holbrooki*. Early (E. somite) and late (L. somite) somitogenesis stages are abbreviated. The dots and the line within the bars indicate mean and median of the data presented within the groups. The normal distribution curves are given in the global expression plots. The asterisks show the level of significance between the marked groups; *= 0.05, **= 0.01, *= 0.001.**

3.4. Discussion

To understand the germline biogenesis and the underpinning cellular processes in viviparous poeciliids, this study, for the first time, evaluated the chronology of PGC formation, their migration and colonisation pattern during the embryonic development of *G. holbrooki*.

3.4.1. Evidence for maternal inheritance of PGC specification in *G. holbrooki*.

The occurrence of the PGC markers tested (*dazl, dnd-α, piwi II* and *vasa*) and their relatively high expression in unfertilised eggs of *G. holbrooki* suggests their maternal inheritance and implies PGC specification in this species is dictated by maternal derivates. This pattern is similar to those observed in oviparous species such as zebrafish (Kaufman and Marlow, 2016b) and medaka (Herpin et al., 2007) as well as those of *Drosophila* (Rongo and Lehmann, 1996), and *Xenopus* (Chan et al., 2007). It was first shown that the maternal PGC determinants in *Drosophila* Gp (*e.g., oskar)* are necessary (Ephrussi and Lehmann, 1992) to maintain the identity and numbers of PGCs. Similarly, lack of maternal *dazl* in *Xenopus* led to their ectopic migration (Houston and King, 2000). In teleosts, these maternal factors, such as *tdrd6*, safeguard proper germplasm segregation (Roovers et al., 2018), *dnd1* (Hong et al., 2016, Zhu et al., 2018) and *dazl* (Li et al., 2016) are necessary for maintaining PGC identity, while *nanos1* (Koprunner et al., 2001) and *vasa* (Braat et al., 2001, Li et al., 2009) provide necessary signals for their proliferation and correct migration. The maternal accumulation of these markers (*e.g., dazl, dnd-α, piwi II* and *vasa*) in ova may support early germline sequestration and PGC migration in *G. holbrooki*, with comparable function as observed in other models. Nevertheless, among the essential PGC markers identified in some vertebrates (Koprunner et al., 2001) and invertebrates (Forbes and Lehmann, 1998), *nanos1* transcripts were barely detectable in *G. holbrooki* ova supported by the lack of *nanos1* expression in embryos' trunk and *vasa*-positive cells. This suggests *nanos1* is not a PGC marker in *G. holbrooki*.

In mice, where PGC specification is governed by an induction mode, mechanical ablation of the vegetal or animal pole of the fertilised egg did not arrest the development of viable and fertile offspring (Zernicka-Goetz, 1998). That finding was later confirmed by the evidence revealing the nuage was not identified in unfertilised and fertilised murine eggs (Toyooka et al., 2000). Taken together, it may be deduced that the Gp components in ovum of *G. holbrooki*, supports a maternal inheritance mode of PGC specification in this species. However, loss-of-function study on PGC markers may be required to confirm this possibility.

3.4.2. The onset of MZT in *G. holbrooki*

In *G. holbrooki*, the presence of *nanos1* transcripts in post-fertilisation embryos but neither in ova nor mature spermatozoa (Chapter 4), suggests its zygotic origin. Its first appearance at mid-cleavage is

indicative of MZT onset which is much earlier compared to its occurrence at mid-blastula in zebrafish (Jukam et al., 2017). By inference, this appears a relatively early model of global zygotic activation among teleosts. The onset of MZT is not conserved across species and does not seem to follow an evolutionary pattern. In a cell cycle context, the earliest zygotic genome activation (ZGA) has been reported in sea urchin (Tu et al., 2014) and mice (Abe et al., 2015) at first cell division, while in zebrafish (Aanes et al., 2011) and *Drosophila* (Atallah and Lott, 2018), zygotic activation is postponed until the 6^{th} and 8^{th} cycles respectively, also known as MBT. Moreover, the onset of MZT can be cell lineage and gene specific. For instance, during MZT where maternal factors are erased, the function of miR-430, one of the essential components of maternal clearance (Giraldez et al., 2006, Bazzini et al., 2012, Liu et al., 2020), is counteracted by maternal Dnd in PGCs (Mishima, 2012, Mishima et al., 2006) protecting maternal deposits in the germline (Vastenhouw et al., 2019). The onset of ZGA can be evaluated by an array of cellular events. For example, as DNA replication interrupts transcription (Rothe et al., 1992), cell cycle lengthening provides interval/void for the initiation of ZGA. In addition, the presence of maternal transcription repressors (Ruzov et al., 2004), chromatin accessibility (Liu et al., 2018a) and excessive histone concentration (Joseph et al., 2017) are the intracellular cues whose dilution prime ZGA. These markers can be later applied to validate the onset of MZT in *G. holbrooki*.

Also, *dnd-β* transcripts were not detected in ova but expressed in cleavage and blastula stages concurring with the inferred early MZT. However, paternal contribution of *dnd-β* cannot be completely ruled out as paternal inheritance of Gp markers occurs in this species (Chapter 4) and hence, requires further testing.

3.4.3. Surge of PGC markers at gastrula imply epigenetic trigger.

As evident in the results, the expression of key PGC markers *dazl*, *piwi II* and *dnd-α* were upregulated at the gastrula stage in *G. holbrooki*. Such activation of PGC markers is known to be initiated via epigenetic mechanisms, *i.e.*, this coincides with PGC-specific gene demethylation in mice (Smith and Meissner, 2013) and zebrafish (Potok et al., 2013). Specifically, the second major wave of epigenetic reprogramming in mice triggers around E6.5 (at the onset of gastrula) where the genome of PGCs are liberated from methylation (Gao and Das, 2014). This is concurrent with PGC extrusion from the epiblast, *i.e.*, their specification from soma, *en route* to their colonisation at the genital ridge (Lee et al., 2014). In zebrafish, the pattern of DNA methylome is not fully comparable with those of mice (Potok et al., 2013), however, germ cell specific markers (*e.g.*, *piwi*, *dazl* and *vasa*) undergo hypomethylation post-ZGA during the sphere stage (Seisenberger et al., 2012, Potok et al., 2013, Hill et al., 2018). The timing of these two events is concurrent with the surge in expression of *dazl* and *piwi II* at the gastrula stage in *G. holbrooki*, likely a consequence of a demethylation wave in the germline. However, this needs validation through studying the occurrence of epigenetic markers during embryonic development in *G. holbrooki*.

3.4.4. Expression profile of germline markers imply sex-dimorphic proliferation of PGCs.

As shown in the results, a transiently sex-dimorphic pattern in the expression profile of some of the studied PGC markers occurred in a female-biased fashion. This may be explained by the sex-biased proliferation of PGCs and corresponding female-biased increase in the level of marker gene expression in teleosts. For example, real time labelling of germ cells in transgenic lines and its quantification has been used to verify preferential PGC proliferation and hence female differentiation in zebrafish (Ye et al., 2019). Based on *gnrh* loss-of-function study in zebrafish, the timing of PGC proliferation is known to occur as early as the gastrula (Feng et al., 2020), which begins between sphere and 50% epiboly (Wang et al., 2016). This developmental stage (*i.e.*, gastrula) is concurrent with the evanescent upregulation of PGC markers in *G. holbrooki* corresponding to its PGC proliferation. Moreover, as the surge at gastrula was predominantly detected in females, it is postulated that PGC proliferation initially/transiently follows a sex-dimorphic pattern in *G. holbrooki*.

3.4.5. PGC migration pattern; early clustering and anterio-medial migration

Consistent with the structure and content of the gene (see Chapter 2), the *vasa* expression in *G. holbrooki* was restricted to the domains corresponding to PGCs. This was further supported by the restricted localisation of *vasa* transcript at the genital ridge of parturating embryos, where the newly formed gonad emerges. However, a clear visualisation of the ISH signal in the blastula and early gastrula stage was compromised due to the high staining background in the blastodisc, probably caused by the high level of endogenous alkaline phosphatase (Miyahara et al., 1982). Although the molecular components and the machineries involved in PGC mobilisation are conserved among teleosts, the pattern of their migration varies between species (Saito et al., 2006). Typically, PGC development is initially supported by maternal derivates of Gp as is also supported by the maternal inheritance of these transcripts in *G holbrooki*. Specifically, the early segregation of PGCs in teleosts relies on the localisation pattern of these maternally inherited germ cell determinants (Bontems et al., 2009, Roovers et al., 2018). However, two types of Gp arrangements have so far been elaborated in early embryonic development of teleosts where; 1) Gp components aggregate compactly in cleavage furrows until the 16-cell stage, subsequently segregating into proliferating cells eventuating in four clusters of Gp -positive cells at the dome stage as in zebrafish (Raz, 2002), Atlantic cod, *Gadus morhua* (Presslauer et al., 2012), and olive flounder, *Paralichthys olivaceous* (Li et al., 2015) while , 2) in others the Gp signal is dissipated throughout the cells in early cell cycles with distinct Gp -positive cells forming only at the mid-gastrula stage, such as in medaka (Herpin et al., 2007). Due to lack of biological samples representing the initial cell cycles and synchronous division in *G. holbrooki* early development, *i.e.*, 2-cell to 64-cell stages, we could not localise the candidate Gp components in those stages. Nevertheless, labelling *vasa*-positive cells at late cleavage revealed the asynchronous formation of Gp segregation

resembling Gp formation in early zebrafish cell division. Congruently, at mid-late blastula, the occurrence of four loosely aggregated clusters of *vasa*-positive cells at the periphery of the blastodisc in *G. holbrooki* is consistent with the positioning of PGC clusters during the dome stage in zebrafish development (Raz, 2002, Raz and Reichman-Fried, 2006).

PGC positioning during the gastrula stages are highly defined in relation to body patterning in the studied models. In *G. holbrooki*, shield elongation in embryos is restricted to 5% of the yolk during the gastrula stage (personal observation), while in zebrafish it is expanded to 50% at early gastrula. In zebrafish, at early to mid-gastrula (*i.e.*, 60% epiboly to germ ring stage) PGCs are still localised in four clusters, converging towards the dorsal part of the embryonic shield (Kimmel et al., 1995). In contrast, in *G. holbrooki*, PGCs are formerly aligned lateral to the elongating embryonic shield. This observation in Gambusia is more comparable to the initial patterning of nascent germ cells in medaka (Saito et al., 2006, Kurokawa et al., 2007) where the PGCs are distributed at both sides of the dorsal axis of the embryonic shield in late gastrula embryos.

As observed in other teleosts, from body patterning to onset of segmentation, the PGCs emerge as two distinct clusters located on both sides of the trunk. These clusters are either arranged as a clumped group of cells as observed in pearl danio (Saito et al., 2006) and zebrafish (Raz and Reichman-Fried, 2006) or they form loosely distributed clusters as in goldfish and medaka (Saito et al., 2006) as was also observed for *G. holbrooki*.

The spatial alignment of PGC clusters and their migratory paths are also not identical among the studied fish models. Two patterns of PGC alignment were observed in the previously studied fish species. In one group, including zebrafish (Weidinger et al., 1999), loach (Saito et al., 2006) and medaka (Herpin et al., 2008), the PGCs form two clusters aligned on both sides of the trunk and in parallel move towards the genital ridge. In the second group, including herring and floating goby (Saito et al., 2006), the two clusters converge towards the medial axis and merge under the trunk during early somitogenesis. However, the coalesced PGC clusters, thereafter, split into two groups, during mid-somitogenesis, and re-align as two distinct clusters in the lateral line of the embryo. In *G. holbrooki*, PGC cluster alignment and their mobility resembles the former pattern; the aligned clusters of PGCs converged while moving towards the gonad anlage, never merged during their migration, and even colonised in two distinct locations at the genital ridge.

As is known, the PGCs in teleosts first form in the anterior part of the developing embryo, thereafter, mainly moving posteriorly towards the genital ridge (Saito et al., 2006, Herpin et al., 2007, Herpin et al., 2008). In contrast, the first appearance of matured PGC clusters posterior to the putative gonadal ridge (PGR) and subsequent migration anteriorly towards the PGR in *G. holbrooki*, appears a developmental novelty. Also, defining the relative location of the PGR according to the closest somite in the developing embryo; in some teleosts, such as loach and goldfish (Saito et al., 2006), PGC clusters

take a longer migration route, during somitogenesis, while in other fish models such as zebrafish (Doitsidou et al., 2002), gobby and herring (Saito et al., 2006), PGCs migrate via a relatively shorter route to colonise the genital ridge. In *G. holbrooki*, PGC clusters formed at the posterior dome and migrated anteriorly to the PGR located close to the second somite. This may suggest the PGC migration path in this live-bearing poeciliid is likely the most extended route among the studied teleosts. Taken together, these novel observations (*i.e.*, uncommon migratory direction and relatively long migration path) may be associated with the evolutionary changes in reproductive biology undertaken by viviparous poeciliids compared to their oviparous counterparts. Indeed, since presumptive gonad in a live-bearing fish species is later differentiated to a complex organ functioning as ovary and uterus in females, it is speculated that the organogenesis machinery directs the gonial stem cell to the far anterior of the body to provide an opportunity for later uterus-gonad expansion. Correspondingly, the fusion of the gonad lobes during late organogenesis is yet another relevant piece of evidence implying the gonadogenesis pattern in *G. holbrooki* adopts significant changes in favour of its reproductive strategies including matrotrophy (Pollux et al., 2009, Pollux et al., 2014), superfetation (Pires et al., 2010), and extended sperm storage (Lopez-Sepulcre et al., 2013). It is, however, unclear if any other biochemical pathways involved in gonial cell positioning and gonadogenesis, including growth factors (Hao et al., 2008, Ungewitter and Yao, 2013), cytokines (Windley and Wilhelm, 2015) and chemotaxins (Ratajczak et al., 2006) play a role in facilitating the novelties of gonad morphogenesis in *G. holbrooki*.

In conclusion, although the pattern of PGC migration in *G. holbrooki* shared some similarities with its pattern in medaka, the PGC clustering pattern, the migratory direction, the length of their migration path and the PGC colonisation location in *G. holbrooki* may indicate novel aspects of germline formation in poeciliids compared to other teleosts.

3.4.6. Only *vasa* and *dnd-α* exclusively mark PGCs in *G. holbrooki*

The cloned and characterised cDNA of *dazl*, *dnd*, *nanos1*, *piwi II* and *vasa* (Chapter 2) were, for the first time, used to understand the spatio-temporal dynamics of PGCs during early embryogenesis of *G. holbrooki*. Unlike other teleosts, most of the PGC markers tested in *G. holbrooki* were not germline-specific (i.e., *dazl*, *piwi II*) with the exception of *vasa* and *dnd-α*. Of the non-specific, *dazl* and *piwi II* were expressed both in germline and soma while *dnd-β* and *nanos1* were fully somatic. Such duality expression/non-germline expression has been reported in mice (Youngren et al., 2005, Nandi et al., 2016) as well as invertebrates (Alie et al., 2011).

VASA interacts with more than 220 target mRNAs and recruits eukaryotic initiation factors to facilitate translation of transcripts required for cell function (Tomancak et al., 1998, Liu et al., 2009). The DEAD-box, characterised in all VASA proteins, including *G. holbrooki* (see Chapter 2), underpins these regulatory roles which restructure and remodel protein-coding RNAs to facilitate their translation (Sengoku et al., 2006, Linder, 2006). Correspondingly, this potency of *vasa* is likely to facilitate the

translation of Gp markers (predominantly stored in RNA form) in early development of species (including *G. holbrooki*) with the preformation mode, as is known to occur in zebrafish (Knaut et al., 2002).

Inferred from its maternal inheritance and exclusive detection in migrating PGCs, *vasa* likely underpins PGC formation and function in *G. holbrooki*. This pattern of expression is consistent across vertebrates with both maternally inherited (*e.g.,* in *Drosophila* and zebrafish) and zygotically acquired (*e.g.,* in mice) modes of germline determination (Styhler et al., 1998, Tanaka et al., 2000, Kuznicki et al., 2000, Hickford et al., 2011). In contrast, the spatially diverse expression of *Vasa* in different cell lineages of invertebrates suggests its expression pattern has undergone evolutionary specialisation in vertebrates. For instance, VASA in sea urchin regulates *cyclinB* translation in soma, synchronising cell cycles thus facilitating proper chromosome segregation (Yajima and Wessel, 2011). Similarly, *vasa* is expressed in somatic stem cells of sea gooseberry, *Pleurobrachia pileus*, that later differentiate to tentacle root or aboral sensory complex (Alie et al., 2011). In the spider, *Parasteatoda*, *Vasa* regulates mitotic progression in different types of cells (Schwager et al., 2015). However, in vertebrates with germline-specific function of *Vasa*, its ectopic expression in gonadosoma (Zeeman et al., 2002, Fraunhoffer et al., 2015) and other somatic cells (Janic et al., 2010) is symptomatic of tumorigenesis. Thus, by inference, the role of *Vasa*, in evolutionary lower animals extends to maintaining totipotent identity of multiple lineages and determination of their fate. Nevertheless, in vertebrates the domain of *vasa* expression and hence function (*i.e.,* as a post-transcriptional regulator) is restricted to the germline to protect its identity against soma as is also observed in *G. holbrooki*.

The detection of *dnd* in the embryonic and post-natal (see Chapter 4) germline of *G. holbrooki* is consistent with those reported for other vertebrates including mammals (Youngren et al., 2005), chicken (Aramaki et al., 2007) and teleosts (Su et al., 2014, Duan et al., 2015, Wargelius et al., 2016). Inferred from loss-of-function studies, Dnd maintains germline identity by protecting other germline-specific transcripts from miRNA-mediated decay (Ketting, 2007, Goudarzi et al., 2013). For instance, in *Xenopus*, maternal Dnd allows the translation of *nanos1*, an essential Gp component for PGC development, through binding to eIF3f and neutralising its repressive activity (Aguero et al., 2017). Similarly, in zebrafish, Dnd prevents PGCs from soma differentiation (Weidinger et al., 2003, Gross-Thebing et al., 2017). It also acts as a transcriptional silencing machinery by recruiting CCR4-NOT, a deadenylase complex, to titrate the abundant mRNA of the cell through their degradation (Nousch et al., 2013, Yamaji et al., 2017). Taken together, the exclusive expression of a *dnd* variant in *G. holbrooki* germ cells encoding the essential regulatory domains suggests a conserved role for Dnd in germline maintenance of this species as well as poeciliids at large. Further, the abundant expression of maternal *dnd-α* detected in ova is likely associated with its role as an anchor for maternal RNAs in unfertilised eggs and polymerization of cortical microtubule arrays right after fertilisation (Mei et al., 2013).

3.4.7. The somatic expression of germline markers; a mammalian resemblance

As shown, the expression of *dazl*, *piwi* and a spliced variant of *dnd*, known for their exclusive expression signal in teleost germline, were not restricted to PGCs, in *G. holbrooki*. This is in accordance with the broader expression domain of these markers in higher vertebrates and invertebrates. For example, PIWI proteins, characterised as a gene silencing mediator (Grimson et al., 2008, Ishizu et al., 2012, Iwasaki et al., 2015), is only expressed in zebrafish germ cells with an essential role in gonad fertility (Houwing et al., 2007). However, in invertebrates, *Piwi* acts beyond germline maintenance by assisting somatic cell cycles (Ma et al., 2014), tissue regeneration and homeostasis (Palakodeti et al., 2008), adaptive immunity (Miesen et al., 2015) and sex determination (Kiuchi et al., 2014). Similarly, apart from nascent germ cells, *piwi II* was detected in the CNS of developing *G. holbrooki*, in agreement with the *Piwi* expression domain in mammals (Kim, 2019). Gain or loss-of-function studies on *piwi II* in *G. holbrooki* may confirm its mammalian conserved role on foraging behaviour, axon regeneration and learning ability (Zuo et al., 2016, Kim, 2019). Therefore, *G. holbrooki* could serve as a descriptive system to understand the role of mammalian PIWI-piRNA machinery in response to peripheral nerve injury (Sohn et al., 2019).

It was also shown *nanos1* expression, a germline specific translational repressor in zebrafish and *Drosophila*, was not detected in migrating PGCs of *G. holbrooki*. However, it encoded the two zinc finger motives (see Chapter 2) that enables the protein to bind the 3'UTR of target mRNA (Kuersten and Goodwin, 2003, Hashimoto et al., 2010). This potency is recruited to ensure the somatic repression of PGCs and their proper migration in zebrafish (Koprunner et al., 2001) and *Xenopus* (Lai et al., 2012). Nevertheless, spatial expression of *nanos1* during *G. holbrooki* embryonic development resembles its orthologues expression in the CNS of mice embryos without control on offspring fertility (Haraguchi et al., 2003). Therefore, *nanos1* is presumed to be dispensable for PGC specification and function in *G. holbrooki* likely shared with other live-bearing teleosts.

Although alternative splice variants for *dnd* have already been characterised in fish taxa (Vasconcelos et al., 2019), this study, for the first time, reported the somatic expression of a *dnd* variant in embryonic stages of a teleost. The *dnd* splicing strategy (*i.e.*, the number of variants) and its diverse expression domain (*i.e.*, detected in both germline and soma) mostly resemble those of mice (Bhattacharya et al., 2007). However, the genetic content of the variants (see Chapter 2) and their expression domain may not be similar to those of *G. holbrooki* (Youngren et al., 2005). In mice, the larger *Dnd* variant is detected at the prenatal stage (*e.g.*, PGCs as well as neuroectoderm, head mesenchyme, neural tube and hindgut), while the shorter variant was expressed in post-natal gonad (Bhattacharya et al., 2008). This is inconsistent with the embryonic expression of *dnd* variants in *G. holbrooki* spatially segregated into anterior (*i.e.*, the shorter variant in neural tube) and posterior (*i.e.*, the longer variant in PGCs) body.

Inferred from loss-of-function studies, it has been formerly explained that the effects of *dnd* knockdown in fish models such as medaka (Wang and Hong, 2014) and Atlantic salmon (Wargelius et al., 2016) is only restricted to gonad fertility without compromised embryo viability. However, *Dnd* mutation in several mice strains induced fatality which may occur due to somatic ablation (Bhattacharya et al., 2007). Therefore, somatic expression of *dnd* in *G. holbrooki* raises the question about the precision of gonad ablation via targeting *dnd* in *G. holbrooki*. Taken together, the *dnd* mRNA processing (*i.e.*, splicing) in *G. holbrooki* is hypothesised to be shifting towards the murine pattern with species-specific alterations. Therefore, the splicing machinery provides more *dnd* variants to take advantage of its regulatory function in early development of soma lineage in *G. holbrooki*.

This study also revealed an expanded/shifted domain of the teleost germ cell-specific markers, (*e.g.*, *dnd*, *dazl* and *nanos1*) to soma in *G. holbrooki*. Indeed, those genes encode RBPs with potency to recruit RNA interference machinery shown to facilitate cell differentiation and maintenance of early-lineage cells in vertebrates and invertebrates (Tiscornia and Izpisua Belmonte, 2010, Anokye-Danso et al., 2011, Guallar and Wang, 2014, Shigunov and Dallagiovanna, 2015). The contradictory role of DAZL in murine stem cell lines is an outstanding example in this context, functioning as a translational stimulator in gonial stem cells (Tsui et al., 2000), while playing a repressive role in other lineages of embryonic stem cells (Xu et al., 2013). In *G. holbrooki*, the somatic expression of germline-related genes in the CNS of *G. holbrooki* may have some evolutionary relatedness. The poeciliids have evolved a relatively larger brain size compared to other teleosts (Isler, 2013), which is costly to maintain the continuous pattern of its growth (Tsuboi et al., 2018). Unlike mammals, organogenesis during poeciliid embryonic development is not supported by maternal provisioning due to the placenta structure and performance (Pollux et al., 2009, Roberts et al., 2016). In line with the potency of RBPs to govern the nervous system formation in higher vertebrates, *e.g.*, proper neurogenesis (Licatalosi et al., 2012), neural differentiation (Makeyev et al., 2007) and synaptic plasticity (Udagawa et al., 2012), the germline-specific RBPs may be recruited in *G. holbrooki* early development to maintain the complexity of the CNS. Further comparative studies with focus on transcriptome profiling of brain in *G. holbrooki* may reveal new functions for these genes.

3.5. Conclusion

This study, for the first time, evaluated the expression of teleostean PGC markers in a poeciliid and documented their spatial domain of expression during embryonic development. It also elucidated the pattern of PGC migration in *G. holbrooki* and compared it with those of oviparous teleosts. Inferred from the spatio-temporal expression profile of target genes, the MZT occurs relatively early compared to other teleosts. While the parental inheritance of Gp markers conforms to preformation, the early induction of MZT is more akin to mice. In this regard, *G. holbrooki* may serve as an excellent system to understand evolutionary origin and significance of the two modes of PGC specification. Further, the

acquisition of new expression domains of *piwi II*, *dazl*, and a variant of *dnd*, and the switch of *nanos1* from germline to somatic expression may imply evolutionary and functional novelty in this species, as well as in poeciliids. These findings may provide options for germline manipulation such as ablation to comparatively understand PGC development in vertebrates as well as for controlling invasive populations of *G. holbrooki*.

Chapter IV

Gp markers

in gonads and gametes

Chapter 4 | Detection of germ cell markers in gonad and gametes of viviparous *Gambusia holbrooki*; evidence for both maternal and paternal contribution to PGC specification

Abstract

Synthesised during oogenesis and packaged as maternal deposit in ooplasm, the Gp components are required for germline determination in egg laying teleosts. In early cell division, the maternal Gp components are partitioned to a selected number of cells granting them germline fate and protecting them from differentiation to soma. However, little is known in live-bearing poeciliids, nor is there evidence for paternal contributions to these germline signals. To address this, the expression of six Gp component markers— *cxcr4*, *dazl*, *dnd-α*, *piwi II*, *tdrd6* and *vasa*— with central roles in PGC sequestration in fish were evaluated in both female and male gametes and in four distinct stages of gonad development of *G. holbrooki*. All markers were constantly expressed from gonad formation to puberty, however, their temporal expression patterns were different. Except for *dazl*, the prenatal expression of Gp markers did not show a sex-dimorphic pattern, while during the post-natal stages the relative abundance of Gp components in the gonads increased towards puberty, and this trend was significantly different in females. Interestingly, four (*e.g., dazl*, *dnd-α*, *piwi II* and *vasa*) of the six Gp markers were detected in both gametes. Although the relative expression of these genes was female-biased in adult gonads, it was male-biased in gametes. The remaining two markers, *tdrd6* and *cxcr4*, were abundantly expressed in ova, however, were not detected in mature spermatozoa. This study successfully detected the key germ cell markers in unfertilised eggs of a poeciliid species as they occur in other teleosts. More interestingly, the study for the first time in any teleost, detected these Gp components in mature spermatozoa, indicating a contribution of paternal factors in PGC specification and gonad function. However, their precise role in determining germline fate needs verification, which may provide evidence for as yet unknown functions and the potential use in developing a genetic solution for the control of invasive populations of this species.

4.1. Introduction

In sexually reproducing animals, the primordial germ cells (PGC) successfully acquire and maintain their distinctive identity and colonise the putative genital ridge during embryogenesis. Subsequently, the process of sex differentiation and gametogenesis recruit both mitotic and meiotic cell cycles to produce functional haploid gametes (Griswold, 2016, Koutsouveli et al., 2020). During gametogenesis, the molecular ingredients necessary for fertilisation (Evsikov and Marin de Evsikova, 2009) and early developmental events, including first cell cycles (Edgar and Datar, 1996) and embryo patterning (Ajduk and Zernicka-Goetz, 2016) are packaged. These signals underpin early embryonic development until the zygotic expression takes over and regulates subsequent embryogenesis (Vastenhouw et al., 2019). Despite the shared origin of the early developmental signals, the events involved in the formation of the ovary and testis display unique differences from organogenesis through to maturity, gametogenesis and reproduction. In teleosts, the earliest signs of oogenesis are characterised by a short phase of mitosis, followed by early meiosis with two rounds of meiotic arrests (Swain, 2006, Schulz et al., 2010), prominent germ cell growth during vitellogenesis (Selman et al., 1993), and accumulation of nutritional reserves and maternal Gp (Kagawa, 2013). Ovarian meiosis is complete when the ovum is extruded from the ovarian nest and engaged in fertilisation. On the contrary, in the testis, mitosis is a prolonged stage providing an inexhaustible source of spermatogonial stem cells until puberty. Transition to puberty in males is marked by the onset of meiosis in the juvenile testis; which is delayed (*i.e.*, compared with ovary) but swift and continuous, with no meiotic arrest, eventuating in biochemical and morphological transformation of spermatogonial germ cells to haploid spermatozoa.

Maternal derivates/signals are key to trigger and sustain early embryonic development (Marlow, 2010a, Li et al., 2010, Traverso and Bobe, 2009) until zygotic mechanisms take over. However, the duration of maternal sustenance and the onset of zygotic control on development varies from species to species. For instance, murine zygotic control begins as early as the two-cell stage (Wang et al., 2004b), while early development in *D. rerio* (Aanes et al., 2011, Despic et al., 2017) and *Drosophila* (Edgar and Schubiger, 1986, Bushati et al., 2008) fully depend on maternal determinants until the 128 to 256-cell stages respectively. Despite their short role, the impacts of maternal determinants have shown to be beyond the initial stages of development including regulation of *de novo* transcription (Tang et al., 2007), fetal growth (Roland et al., 2014), larval forebrain cell proliferation (Higuchi, 2020) and adult short-term memory (Gould et al., 2018).

The maternal Gp factors controlling early development of embryos mostly encode members of the RNA-binding protein family (*e.g.*, Dazl, Dnd, Vasa) and/or the components of the ncRNA machinery (*e.g.*, Piwi, Tdrd6). During oogenesis, they are accumulated in the ovum as maternal deposits and play critical roles gonad formation and function in the offspring. These include, GSC maintenance and differentiation (Mikedis et al., 2020), proper mitosis-meiosis transition (Medrano et al., 2012, Rosario

et al., 2016), and germ cell tumour repression (Northrup et al., 2012, Ruark et al., 2013, Figueras et al., 2018). In teleosts, functional relevance of Gp components is mostly restricted to PGC sequestration from somatic fate in early embryogenesis (Lindeman and Pelegri, 2010, Aanes et al., 2011). However, in poeciliids, it is largely unknown whether these transcripts are expressed in different stages of gonad development and/or involved in germ cell maturation or influenced by the sexual identity of the gonad and its developmental status.

A zygote must accomplish three critical tasks governed by maternally-supplied factors before maternal-to-zygotic transition (MZT) can occur. These are 1) cell proliferation through mitotic division, 2) acquisition of polarity to establish the body axis and 3) cell patterning. For instance, early mitotic cell cycles (*i.e.*, until cycle 13) are distinctly fast and synchronous (Farrell et al., 2012), without intervening phases or cytokinesis (Edgar and Schubiger, 1986) that are sustained by the maternal Cell division cycle 25 phosphatase (Cdc25). This pattern of cell division is reprogrammed at MZT, where the zygotic genome begins to control the cell cycle through depleting maternal Cdc25 components (Edgar and Datar, 1996). Maternal deposits regulate the plane of early cell division establishing the vegetal and animal poles of zygotes, *i.e.*, polarity (Edwards, 2005). Similarly, early cell patterning is governed by maternal *buc* and *microtubule-actin crosslinking factor 1a* (*macf1a*) in zebrafish, which determine Gp localisation and subsequent PGC specification (Bontems et al., 2009, Gupta et al., 2010).

In the past decade, the concept of "the little effects of non-genetic factors" of spermatozoa on embryonic developmental programming and offspring fitness has tremendously improved with evidence that sperm carries and transmits more than its haploid paternal genome to the zygote (Champroux et al., 2018, Chen et al., 2016). For example, the unique epigenome of spermatozoa is one of the most important paternal traits transmitted to the zygote and involved in embryonic development (Guibert et al., 2012). However, its epigenetic remodelling is not conserved among taxa (Saitou et al., 2012, Skvortsova et al., 2019). In spermatozoa, DNA methylation on Imprinting Control Regions (ICR) carried out by DNA methyltransferases (DNMTs) results in paternal mono-allelic expression safeguarding proper early development and post-natal health (Congras et al., 2014, Matsuzaki et al., 2020). DNMT activities in male gametes mostly occur on transposons and intergenic regions to silence gene expression (Smith et al., 2012, Champroux et al., 2018, Barau et al., 2016). During spermatogenesis, where undifferentiated germ cells undergo successive stages of mitosis, meiosis and post-miosis, they experience morphological (*i.e.* elongation, flagellum formation and chromatin remodelling) and biochemical (*i.e.* ejected cytoplasm contents, and altered gene and protein expression pattern) changes eventuating in packaging different types of molecules including coding and ncRNAs (Baccetti and Afzelius, 1976, Eddy, 2002, Johnson et al., 2011b). Piwi-interacting RNAs (termed piRNA) known to be germ cell specific in *D. rerio* (Houwing et al., 2007) and *D. melanogaster* (Brennecke et al., 2007) comprise the noticeable part of sncRNA in spermatozoa that function as part of the DNA methylation and transposon silencing machinery (Bak et al., 2011). The tRNAs are another group of sncRNA abundantly found in

spermatozoa harbouring several types of RNA modification to maintain their stability (Chen et al., 2016, Sharma et al., 2016).

Apart from ncRNAs, protein-coding RNAs are also identified in spermatozoa predominantly involved in functional fertility, nervous system and behaviours (Champroux et al., 2018). For instance, the mRNA of A-kinase anchoring protein 4 (AKAP4), an AMP-dependent protein kinase found in murine spermatozoa, is hypothesised to regulate flagellum function, and safeguard successful fertility (Champroux et al., 2018, Miki et al., 2002). Downregulation of Protamine 2 (PRM2), a nuclear protein found in spermatozoa, has been shown to affect semen quality (Zalata et al., 2016) due to abnormal chromatin compaction in spermatozoa (Yang et al., 2015), haploinsufficiency (Cho et al., 2001) and its cellular damage (Cho et al., 2003). *Foxg1* transcripts are also found in murine spermatozoa, a winged-helix transcription factor that plays a role in epigenetic and biochemical processes through *cis*-regulatory elements (Hou et al., 2020). In mice it is essential for regulation of brain development through directing cell proliferation (Hanashima et al., 2002), their migration (Miyoshi and Fishell, 2012), regional patterning (Hanashima et al., 2007) as well as circuit assembly (Cargnin et al., 2018). Nevertheless, the role of paternal signals on early development and offspring phenotype are predominantly limited to sperm-derived components on epigenetic regulation of embryogenesis. Although the role of maternal protein-coding RNA signals on PGC specification of fish models is comprehensively documented (Lindeman and Pelegri, 2010), the paternal contributions remain poorly understood and relatively unexplored.

Despite viviparity with internal fertilisation, fetal incubation and superfetation (Blackburn, 2015, Torres-Martinez et al., 2019) little is known in poeciliids about early developmental programming including Gp signal origin and identity. Also, males exhibit improved mating capability, through reducing semen volume and concentrating sperm (Franssen et al., 2007), and developing spermatozeugmata (Grier, 1975, Grier et al., 1981) for storage in the ovarian environment, to service multiple pregnancies (Kobayashi and Iwamatsu, 2002, Uribe et al., 2016). More importantly, sharing elements of lecithotrophy with teleosts and invertebrates on one hand and placentation with mammals on the other, the poeciliids provide a valuable system to study reproductive biology and comparative evolutionary relatedness.

As a first step to understand the origin and function of Gp determinants in *G. holbrooki*, this study evaluated the expression or accumulation of six Gp markers in gonad (*i.e.,* from the onset of gonadogenesis to puberty) and gametes, respectively. The outcomes of this study were expected to provide insights into patterns of Gp markers, their parental origin, and role in PGC specification and gonad function. This with the view to identify molecular susceptibilities for developing genetic control options for pest populations of this species.

4.2. Methods

4.2.1. Animal collection and husbandry

Wild *Gambusia* were caught from the Tamar Island Wetland Reserve, Tasmania, transported to a recirculating facility for small fish at the Institute for Marine and Antarctic Studies (IMAS), University of Tasmania and maintained at optimal rearing conditions. The healthy adult male fish were selected based on their physical characteristics and paired with females for two weeks until gamete sampling. They were fed with trout commercial granules (Nutra XP, Skretting, Australia) and freshly hatched *Artemia* nauplii (INVE Aquaculture, USA) while reared in captivity. The housing condition of *G. holbrooki* during the experiment was as described previously (see Chapter 2).

All animal experiments were approved by the institutional (University of Tasmania) Animal Ethics committee (AEC Permit A0017759).

4.2.2. Experimental design

The relative expression of Gp markers, *cxcr4*, *dazl*, *dnd-α*, *piwi II*, *tdrd6* and *vasa*, at four life stages *i.e.,* 1) pharyngula, which coincided with gonad primordia formation (Chapter 5) , 2) right before parturition, at the onset of sex differentiation *i.e.,* ovarian meiosis (Chapter 5), 3) 20 days post-parturition (dpp), where genetic females have not yet developed a gravid spot and ovary is in the previtellogenic stage (Fig. 4.2A and 4.2A′), and males had begun growing gonopodia and testis is occupied by spermatogonia, and 4) 60 dpp; at puberty coinciding with vitellogenic ovary and gravid spot emergence in females, and fully grown gonopodia in males as well as testicular meiosis (Fig. 4.2B). The level of the target mRNA in mature ova and spermatozoa was also quantified and their profiles compared with adult gonads.

4.2.3. Spermatozoa collection and purification

The adult males (n = 7) were selected based on their secondary sexual characters (*i.e.,* fully grown gonopodia and its thrusting during courtship), sedated with chilled water and transferred to an RNaseZAP™ treated petri dish. The gonopodia was swung forward and the abdomen was gently massaged with the tip of fine forceps until the sperm packets were released into DEPC-treated PBS. For each fish, 30-35 sperm packets were carefully collected using micropipettes and transferred to an Eppendorf tube. The sperm packets were then teased by pipetting up and down in DEPC-treated PBS. Then, the sperm samples were treated with somatic cell lysis buffer (0.1% SDS, 0.5% Triton X-100 in DEPC-treated H_2O) for 10 min at 4˚C to remove somatic cells (Ostermeier et al., 2002, Goodrich et al., 2007). Any traces of somatic cells post-lysis were also checked by microscopy, before pelleting the sperm by centrifugation (800g for 3 min at 4˚C). Subsequently, the supernatant was carefully removed,

the sperm pellet was washed twice by resuspending in DEPC-treated PBS and immediately proceeded to RNA isolation.

4.2.4. Rearing virgin females, collection of ovum and offspring from virgin females

The newly parturiated larvae were reared and fed as described above. The one-week larvae were bathed in a buffer containing a very low concentration of proteinase K (Bioline). The buffer containing lysed cells was concentrated and used for genetic sexing of the larvae. Subsequently, the genetic females were selected and reared separately until puberty and virgin females were selected based on their gravid spot intensity (Norazmi-Lokman et al., 2016) for ovum collection. Specifically, the females were euthanised with 50 ppm AQUI-S®, the ovary of virgin females was dissected and ova samples were isolated based on their size and the pattern of oil droplet distribution (Fig. 4.1). The collected ova (n= 7) were rinsed with cold DEPC-treated PBS, stabilised in RNAlater® (Sigma) overnight in 4˚C and stored in -80 until RNA isolation.

4.2.5. Embryo and tissue preparation

To harvest early gonad material from late embryos (n = 6 /sex/developmental stages), the embryos were euthanised as described above, the tissue anterior to the operculum and posterior to the anus was excised and the abdomen retained. The abdomen was then rinsed with DEPC-treated PBS, stabilised in RNAlater® according to the manufacturer's protocol and stored in -80 ˚C until RNA isolation. The remaining tissues were used for genetic sexing of embryos. For extracting gonads from juveniles (n = 7 /sex) and adults (n = 6 /sex), fish were first euthanised with 20 µl/ml of AQUI-S®, the abdominal cavity was cut and the gonads were carefully isolated from the adjacent organs. The explanted gonads were rinsed with cold DEPC-treated PBS and stabilised in RNAlater® according to the manufacturer's protocol and stored in -80 ˚C until RNA isolation.

4.2.6. RNA isolation, cDNA synthesis and real time PCR

Total RNA from the tissues was isolated using AllPrep DNA/RNA Mini Kit (Qiagen). For sperm pellets, each sample were homogenised using 500 µl of lysis buffer containing β-Mercaptoethanol (10 µl/ml). Homogenisation of gonad tissues, embryos and ova was assisted by passing the samples through 20 and 27-gauge needles. The tissue lysates were subsequently passed through nucleic acid specific columns to separately capture genomic DNA (gDNA) and RNA. To overcome the gDNA background in RNA samples of testis and spermatozoa, the isolated RNA was separately treated with RNase-free Ambion™ DNase I (Invitrogen). The treated RNA was, thereafter, purified using Monarch® RNA cleanup kit (New England BioLabs).

The concentration of RNA was measured with Qubit® 4 Fluorometer (ThermoFisher Scientific, USA) and its integrity was confirmed by denaturing agarose gel. For cDNA synthesis, a given amount of purified total RNA (*i.e.,* 250 ng for sperm samples, up to 2 mg for gonad tissues, and the whole RNA for individual ovum and late embryos) was used for reverse transcription (RT). The RT reaction contained 200 units of MMLV reverse transcriptase, 1X RT buffer, 10 units of RNase inhibitor, 0.5 mM dNTP mix, 250 ng Oligo$(dT)_{18}$ primer mix (Tetro cDNA synthesis kit, Bioline). The RT reaction was incubated at 45˚C for 60 min and inactivated by heating at 85˚C for 5 min. The cDNA samples were stored at -20 ˚C until use in PCR assays. For the sex-segregated assay, the cDNA concentration of individual samples were normalised between sexes within the same developmental stage. The primers design, end-point and qPCR reaction conditions were as described previously (Chapter 3, section 3.2.4). The real time PCR mix (10 µl) comprised of 1X iTaq Universal SYBR Green Supermix (Bio-Rad, NSW, Australia), 3 (spermatozoa cDNA) -15 (tissue) ng cDNA Template, 0.4 µM of each primer, and adjusted to 20 µl using MilliQ water. Duplicate reactions were run for each cDNA sample using CFX96 Touch Real-Time PCR Detection System (Bio-Rad, NSW, Australia) consisted of 95˚C for 1 min, followed by 40 (embryos and tissues) and 45 (spermatozoa) cycles of 95˚C for 5s, 64-68 ˚C for 10 s, and 72˚C for 7-15 s. For positive and negative control, 5 ng cDNA (from a tissue where the target gene is expressed) and MilliQ water were used as template, respectively. Melting curve analysis, gel visualisation and sequencing of qPCR products were subsequently performed to check unwanted products and gDNA contamination. The MIQE of the qPCR assay (Bustin et al., 2009) was provided in Table A10.

4.2.7. Biological normalisation of data and statistical analysis

Two housekeeping genes; *βactin* and *gapdh* were tested for biological normalisation of qPCR data (Cavalcanti et al., 2011, Ashish et al., 2017) across all target tissue types using geometric averaging in qbase$^+$ (version 3.0, Biogazelle). The *gapdh* showed higher stability (M value = 0.81) as assessed by geNorm algorithm (Hellemans et al., 2007) and therefore was selected for normalising relative expression of genes of interest (ΔCq).

All qPCR data were presented as mean ±standard deviation (SD). Shapiro–Wilk and Levene's tests were used to test data normality and homogeneity of variances, respectively. When necessary, the outliers excluded from the analysis. A two-way analysis of variance (ANOVA) was used to identify significant differences between experimental groups using two factors, sex and developmental stage. Tukey Post Hoc tests were applied when population means were significantly different between the sexes in each developmental stage (Tukey, 1949). The level of significance between two means was considered when $p< 0.05$. Statistical analysis and plotting were performed using OriginPro, Version 2021 (OriginLab Corp, MA, USA).

4.3. Results

All the studied markers exhibited temporal changes in their expression profile during several stages of gonad development and in both gametes. Indeed, they were actively expressed in different stages of ovary and testis, with some shared and unique patterns including sex dimorphism. Significantly, Gp markers were detected not only in the ova, but a subset was also detected in spermatozoa.

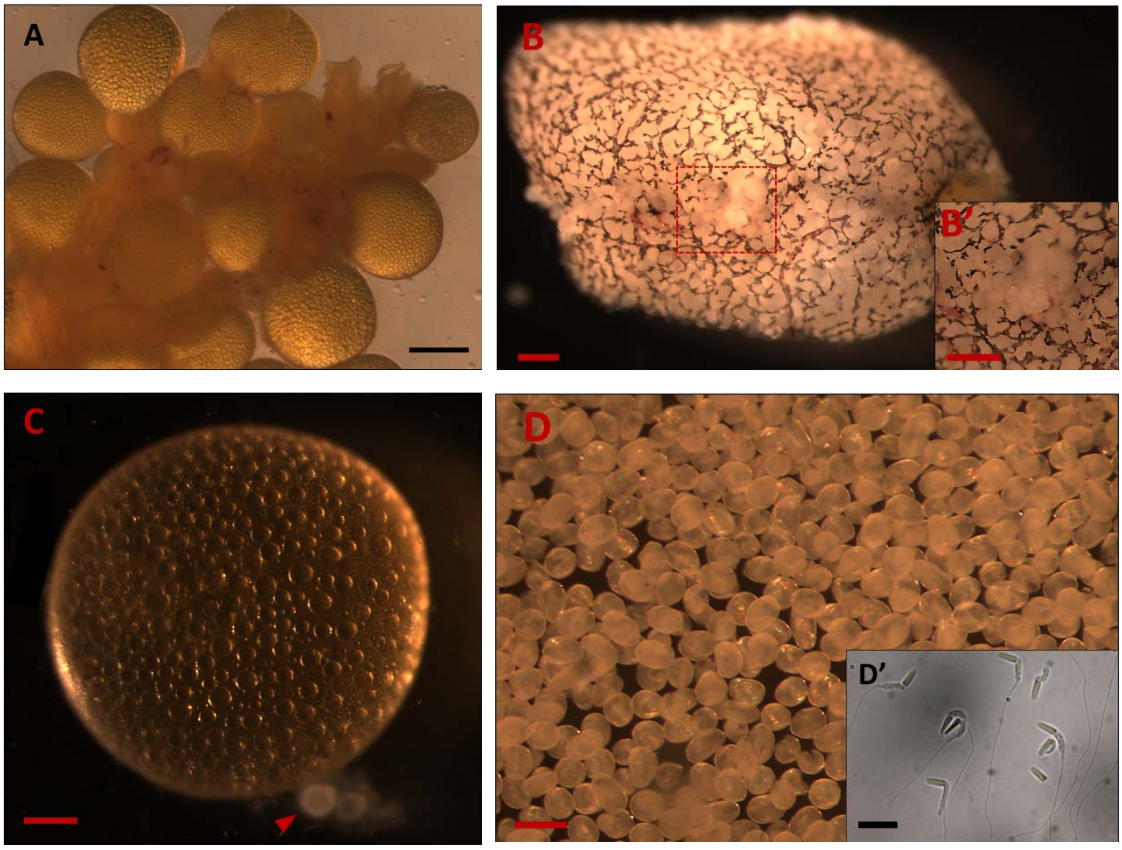

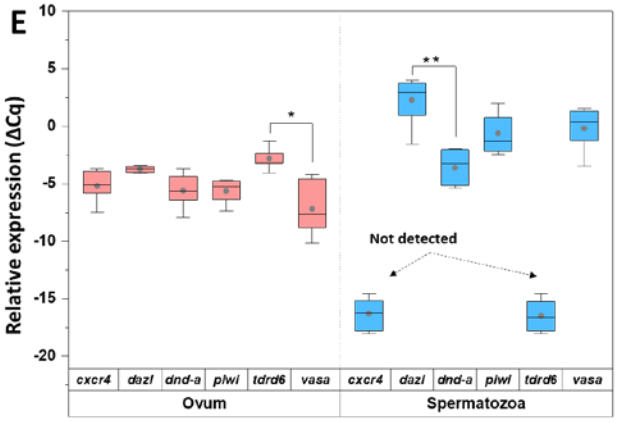

Figure 4.1. The panels showing the morphology of freshly explanted adult ovary (A), testis (B), ovum (C), spermatozeugmata (D), and the expression pattern of PGC markers in mature gametes (E) of *G. holbrooki*. Adult ovary of virgin females (A) was filled by vitellogenic oocytes (C). Adult testis (B) was filled with sperm packets (B' and D) containing matured spermatozoa (D′). Ova were recognised by their uniform pattern of oil droplet distribution, lack of connected placental blood vessels and significant enlargment compared to primary oocytes (red arrowhead). Scale bars are 1 mm (A), 250 nm (B, B′ and C), 100 nm (D) and 25 nm (D′). In the box plot (E) the grey circle and a horizontal lines indicate mean and median values of the group, respectively. The asterisks show the level of significance between groups; * < 0.05, * < 0.001.**

4.3.1. *cxcr4*

The embryonic expression of *cxcr4* was relatively high and comparable between sexes; however, the post-natal expression was strongly reduced (ANOVA, $F_{9,63} = 54.59$, $p < 001$, Fig. 4.3A). Of the juvenile gonads, the testis showed more than 8 fold higher *cxcr4* expression compared to ovary ($\Delta\Delta Cq=3.1\pm0.57$ $\log_2$, $p<0.01$, Fig. 4.3A). At puberty, *cxcr4* expression was slightly upregulated in both gonads, albeit marginally higher in females as was also the case in the adult ovary. In gametes, *cxcr4* was highly expressed in ova; nearly 60-fold higher than adult ovary ($\Delta\Delta Cq=5.9\pm0.74$ $\log_2$, $p<0.001$, Fig. 4.3A), while it was not detected in spermatozoa.

4.3.2. *dazl*

The prenatal expression of *dazl* was comparable between sexes in the pharyngula stage (ANOVA, $F_{9,53} = 47.45$, $p < 001$, Fig. 4.3B), while a significant upregulation in females was detected just prior to parturition ($\Delta\Delta Cq=2.3\pm0.52$ $\log_2$, $p<0.05$, Fig. 4.3B) at which point primary oocytes undergo first meiotic arrest (Chapter 4). In the juvenile phase, this trend was reversed with higher expression in the testis. In adults, *dazl* expression was comparable between sexes. Interestingly, *dazl* transcripts were also detected in both gametes, with a significantly higher level in spermatozoa ($\Delta\Delta Cq=5.3\pm0.72$ log2, $p<0.001$, Fig. 4.3B) compared to ova. More specifically, in spermatozoa, *dazl* showed the highest expression of the studied PGC markers; nearly 30-fold higher than the lowest expressed PGC marker — *dnd-α* — ($\Delta\Delta Cq=4.9\pm0.78$ $\log_2$, $p<0.001$, Fig. 4.3B).

4.3.3. *dnd-α*

The pre-natal expression of *dnd-α* was not significantly sex-biased in gonads (ANOVA, $F_{9,51} = 41.47$, $p < 001$, Fig. 4.3.C). In the juvenile testis, coinciding with active mitosis and spermatogonial proliferation, *dnd-α* expression was marginally higher compared to meiotic ovary. However, in the adult ovary, concurrent with vitellogenesis and loading of maternal factors into oocytes, *dnd-α* expression surged significantly compared to the juvenile ovary ($\Delta\Delta Cq=3.3\pm0.46$ $\log_2$, $p<0.001$, Fig. 4.3C) and adult testis ($\Delta\Delta Cq=2.8\pm0.37$ $\log_2$, $p<0.05$, Fig. 4.3C). Both gametes stored a relatively high levels of *dnd-α* transcripts in comparison with pre- and post-natal gonads. The relative expression of *dnd-α* in spermatozoa was 4 times higher than its expression in ovary ($\Delta\Delta Cq=2.0\pm0.55$ $\log_2$, $p<0.05$, Fig. 4.3C), however, *dnd-α*, showed the lowest relative expression among the studied genes in spermatozoa.

4.3.4. *piwi II*

The *piwi II* expression was detected in all developmental stages (ANOVA, $F_{9,51} = 41.47$, $p < 001$, Fig. 4.3.C). However, there was neither pre- nor post-natal differences in the expression levels between males and females, despite a slightly higher level in the ovary. Similar to *dnd-α*, the *piwi II* was also

detected in both gametes, and its expression was much higher in spermatozoa (ΔΔCq=5.0±0.51 log_2, p<0.001, Fig. 4.3D).

4.3.5. *tdrd6*

The *tdrd6* showed a relatively high expression during the studied stages with no sex-dimorphic pattern in the late embryonic stages (ANOVA, $F_{9,40}$ = 39.41, p <001, Fig. 4.3.E). The post-natal expression of *tdrd6* was female-biased with a strong expression in adult ovary (ΔΔCq=2.9±0.34 log2, p<0.05, Fig. 4.3E) compared to testis. The *tdrd6* transcripts were not detected in spermatozoa, while its expression in ova was the highest among the studied PGC markers comparable with the expression level of the selected housekeeping gene (Fig. 4.1.E).

4.3.6. *vasa*

At the pharyngula stage and right before parturition, the expression pattern of *vasa* is comparable between males and females. However, the post-natal expression in gonads showed a significant bias in favour of females (ANOVA, $F_{9,42}$ = 47.83, p <001, Fig. 4.3.F). More specifically, in juvenile (ΔΔCq=2.9±0.87 log2) and adult ovary (ΔΔCq=3.5±0.91 log2) *vasa* was expressed about 7 and 11 times higher (p<0.01, Fig. 4.3F) compared to testis, respectively. The *vasa* transcripts were detected in both gametes and its levels were significantly higher (p<0.001) in spermatozoa compared to ova (ΔΔCq=7.0±0.82 log2, Fig. 4.3F).

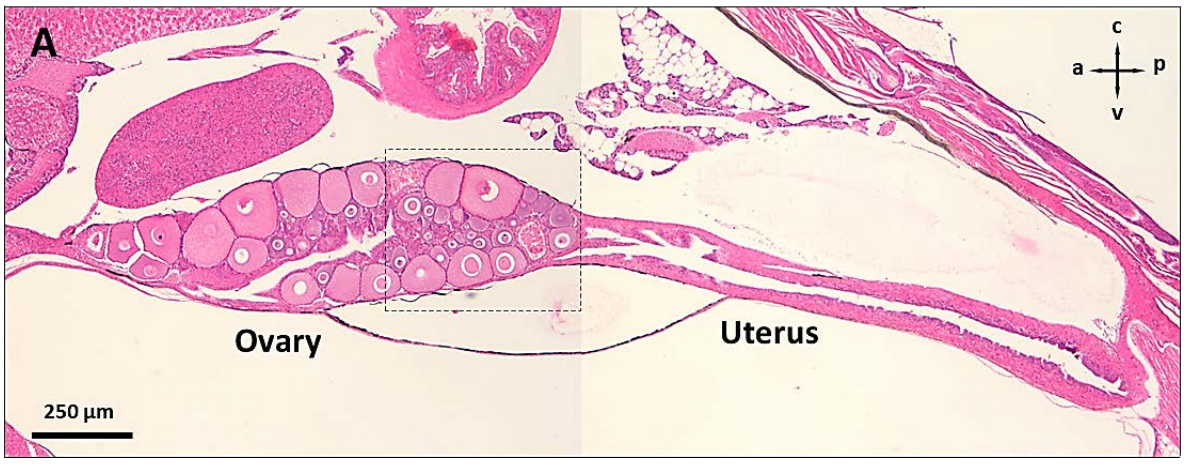

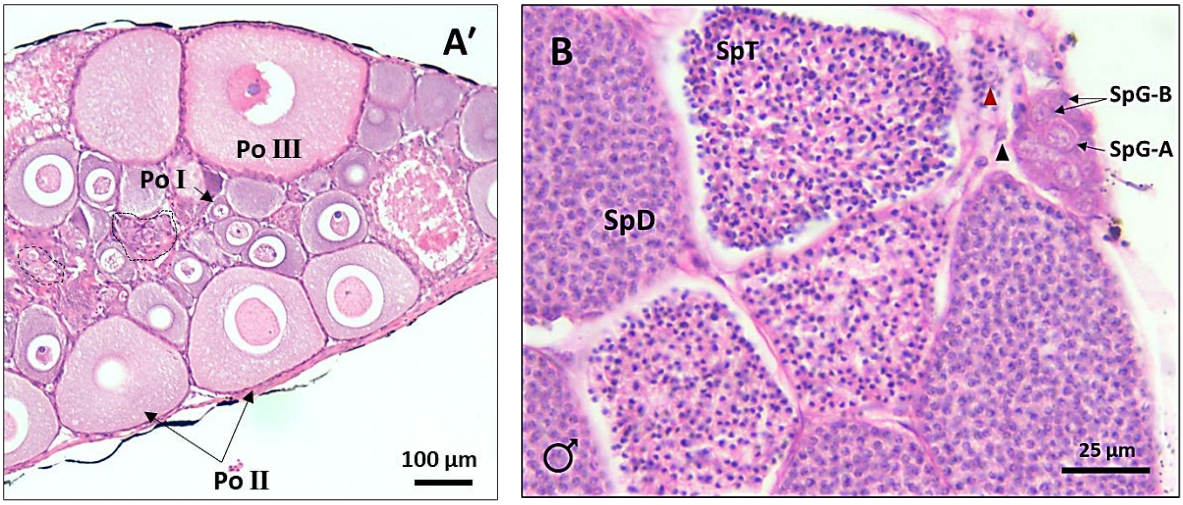

Figure 4.2. Histological sections showing juvenile ovary (A and A′) and adult testis (B) of *G. holbrooki*. The ovary (A, left) was in meiotic arrest characterised by abundant primary oocytes (Po) in different stages of maturation. The uterus (A, right) was vacant with no vitelogenic oocytes. The sporadic cradles of mitotic oogonia (A′, black dashed lines) were also present. Meiotic testis (B) was characterised by the presence of all stages of spermatogonial germ cells. The testis was mostly occupied by spermatozoa and haploid spermatids with sparsely interspersed mitotic spermatogonia and the somatic cells namely leydig (B, red arrowhead) and Setoli (B, black arrowhead) cells. Abbreviations: primary oocyte stage 1, Po I; primary oocyte stage 2, Po II; primary oocyte satge 3, Po III; spermatids, SpD; spermatozoa, SpT; spermatogonia type A, SpG-A; spermatogonia type B, SpG-B.

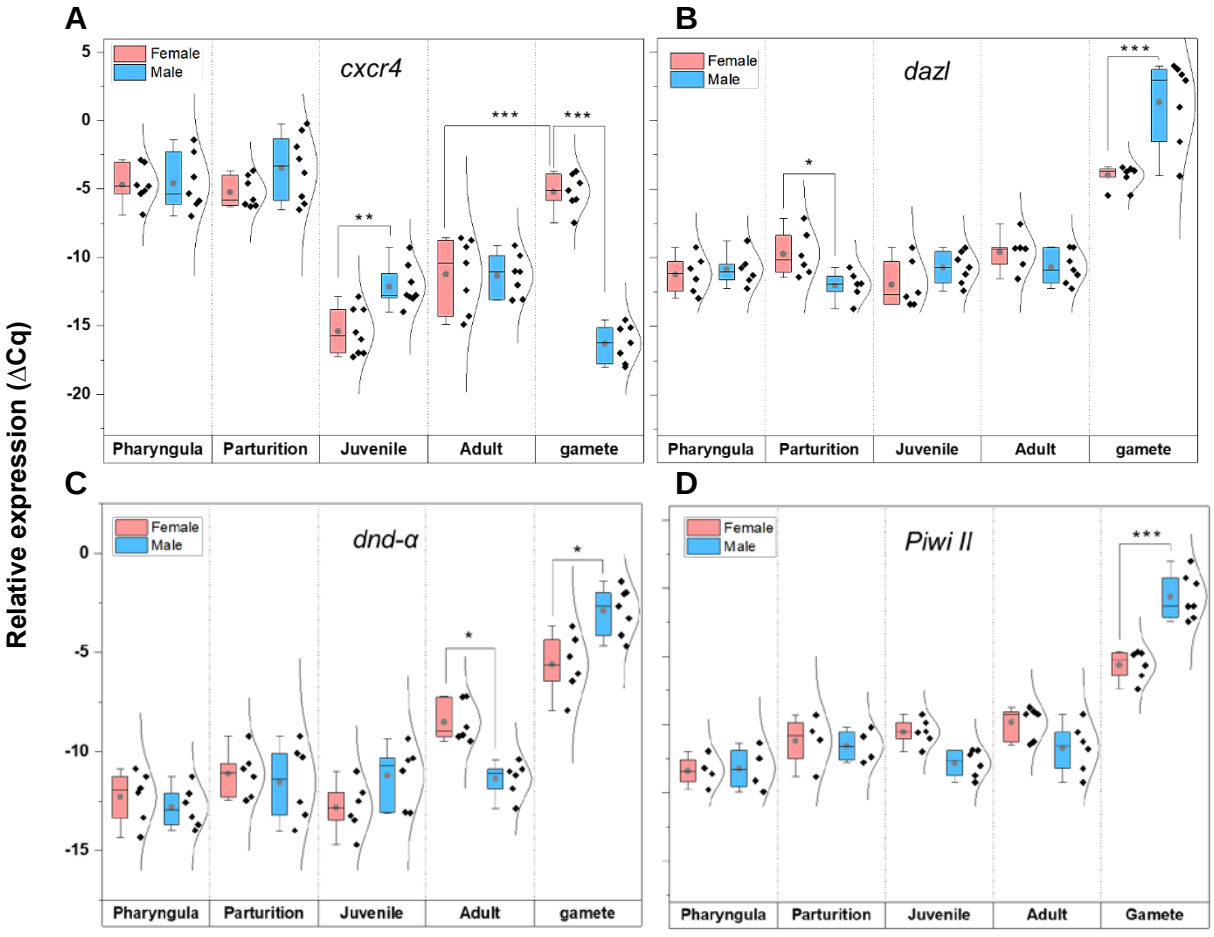

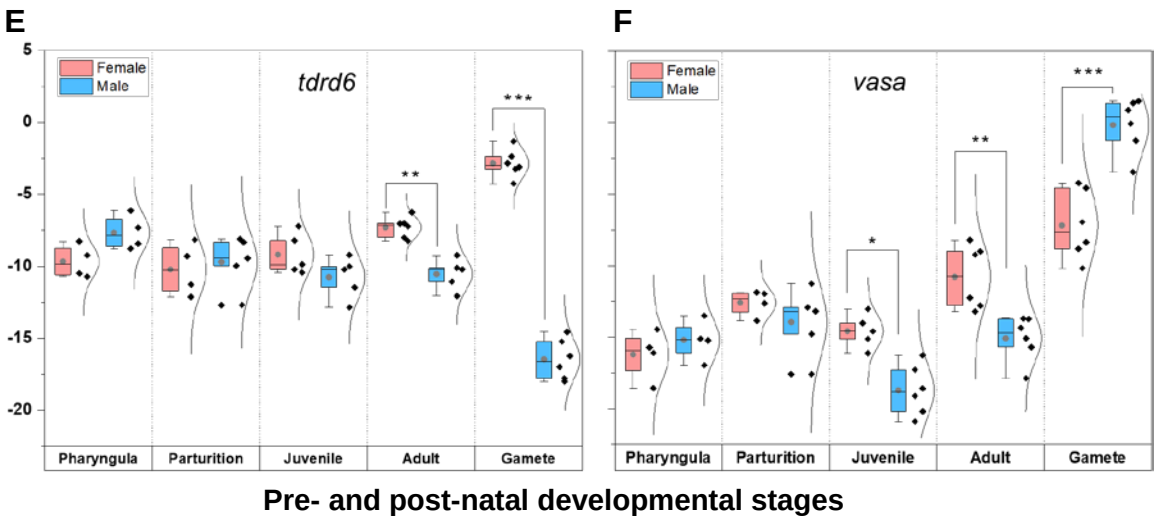

Figure 4.3. Box plots showing relative expression of *cxcr4* (A), *dazl* (B), *dnd-α* (C), *piwi II* (D), *tdrd6* (E), and *vasa* (F) in select life stages and gametes of *G. holbrooki*. The grey circle and horizontal line on each box plot indicate mean and median values of the group, respectively. The black squares and curved lines at the right side of each box indicate individual data and the normal distribution pattern of the presented data, respectively. The asterisks show the level of significance between groups; * < 0.05, **< 0.01, * < 0.001.**

4.4. Discussion

Although the marker genes tested are known maternal signals for germline determination in species with preformation mode, their role extends to gonadogenesis and its maintenance at adulthood. These include protecting the identity of germ cells in the somatic environment (Gross-Thebing et al., 2017), facilitating meiosis division (Bertho et al., 2019) and neutralising repressing function of ncRNAs (Mickoleit et al., 2011) in gonads. The packaging of spermatozoa in bundles (also called spermatozeugmata) facilitated efficient isolation of mature sperm and hence the assay for accumulated Gp components.

4.4.1. The role of Gp markers in pre- and post-natal gonad function

The known Gp markers involved in PGC function mostly exhibit RNA-binding features with diverse approaches to transcriptional and post-transcriptional regulation (Chapter 1). Taking advantage of different strategies such as interaction with miRNAs and translation initiation factors, binding to ploy(A) tail and RNA rearchitecture, these RBPs are essential to safeguard proper cell differentiation and function (Chapter 2). In gonads, this mechanism can be recruited to ensure successive germline and gonadosoma proliferation (Medrano et al., 2012), tumour suppression (Sanchez et al., 2019) and gametogenesis (Reynolds and Cooke, 2005) eventuating in functional fertility.

Continued *dazl* expression in foetal and post-natal stages of ovary/testis and gametes with a sex-dimorphic surge in prenatal-meiotic ovary of *G. holbrooki* is not comparable to that which occurs in teleosts and other taxa. In the murine prenatal ovary, *Dazl* expression is observed two days after PGC

colonisation (Hackett et al., 2012), persisting from the onset of meiosis to oocyte maturation (Rosario et al., 2016). However, *DAZL* expression in human foetal ovary is postponed to early meiosis, *i.e.*, leptotene, but its expression switches off during zygotene and pachytene until nest breakdown (He et al., 2013). This is inconsistent with *dazl* expression in *G. holbrooki*, where it is detectable in premeiotic ovary. In mice lacking DAZL, oocyte maturation is suspended due to disrupted ribosomal loading on maternal transcripts (Yang et al., 2020), an aspect possibly shared across all vertebrates. Similar to the expression pattern in *G. holbrooki*, *dazl* is continuously expressed during oogenesis and ovum maturation in *O. latipes* (Xu et al., 2007). In contrast, in *Oncorhynchus mykiss*, *dazl* expression is barely detectable in mitotic oogonia, while strongly expressed post-meiosis (Li et al., 2011), consistent with the observation in *G. holbrooki*, where mitotic-meiotic transition in ovary (*i.e.*, pharyngula to parturition) coincided with a surge in *dazl* expression.

In *G. holbrooki* testis, *dazl* was continually expressed from germ cell nesting to meiotic stage, as observed in frogs (Mita and Yamashita, 2000), and mice (Reijo et al., 2000). *Vasa* expression as the critical component of murine (Reynolds et al., 2005) and teleost (Hartung et al., 2014) spermatogenesis, is protected by DAZL. In *O. mykiss*, *dazl* was prominently expressed in mitotic spermatogonia and persisted in meiotic spermatids (Li et al., 2011). In *O. latipes*, *dazl* expression is scarce in the premeiotic testis, abundant during meiosis, but absent in spermatozoa lumen (Xu et al., 2007). This supports the results in *G. holbrooki*, where foetal ovary at the onset of meiosis showed a significantly higher *dazl* expression compared to the mitotic testis. Interestingly, *dazl* transcripts in spermatozoa have not been detected among teleost species, however, it has been reported in human spermatozoa (Lin et al., 2002), consistent with the observation in *G. holbrooki*. This may reflect a role in developmental signalling (Li et al., 2016) or a physiological role for sperm function as has been also suggested to play a role in human spermatozoa count and its motility (Hsu et al., 2010). This may reflect taxa-specific differences associated with an as yet unrecognised function unique to this species or the poeciliids in general.

In *G. holbrooki*, upregulated *dazl* right before parturition coinciding with the onset of oogonia-oocyte transition, supports its role in meiosis machinery (Medrano et al., 2012). This is also in accordance with the role of Dazl as an RNA-binding protein orchestrating translational repression or activation among taxa (Rosario et al., 2019, Yang et al., 2020). In mice, DAZL facilitates spindle assembly during metaphase I–II transition of oocytes ensuring successful meiotic division (Chen et al., 2011).

In *G. holbrooki*, *dazl* expression was also observed in the mitotic ovary (*i.e.*, at pharyngula), characterised by synchronously developing cradles of germ cells, *i.e.*, type-II dividing germ cells (Saito et al., 2007, Saito and Tanaka, 2009) that consist of two daughter cells with interconnected cytoplasm (Chapter 5). This may suggest a regulatory role for Dazl upstream of meiosis in teleosts (Bertho et al., 2019), where it maintains partial cytokinesis and formation of intracellular bridge between sister cells (Greenbaum et al., 2011, Haglund et al., 2011). This eventuates in successful proliferation of pre-

meiotic germ cells and functional gametogenesis (Haglund et al., 2011). Despite the expression of *dazl* in mitotic ovary, it is unknown if *dazl* function is essential for cyst formation in *G. holbrooki*.

As was shown in *G. holbrooki*, two *dnd* isoforms were characterised in mice, but their spatial expression was not congruent. Specifically, only *Dnd-α* (the longer variant) is detected (*i.e.,* in PGCs, their migration domain and genital ridge) in both XX and XY mice (Bhattacharya et al., 2007). However, *Dnd-α* expression in XX mice is downregulated between E12.5 to E14.5 concurrent with onset of meiosis and becomes barely detectable in post-natal ovary (Youngren et al., 2005). In contrast, in *G. holbrooki*, both isoforms were detected in different cell lineages during embryonic development and their post-natal expression were observed in both gonads (Chapter 3). Post-natal, murine isoform α is expressed first and continuously in the testis at mitotic phase, but not in ovary. However, isoform β is expressed from PN20 testis onwards (*i.e.,* at meiosis onset) and its expression is strongly active in meiotic and post-meiotic germ cells (Youngren et al., 2005, Bhattacharya et al., 2007). This sequential pattern was not observed in the expression of *dnd* variants in *G. holbrooki*. Thus, by inference, the *dnd* gene in *G. holbrooki* despite evolving multiple spliced variants, is yet to acquire specialised, sequential (*i.e.,* before or after meiosis) and/or restricted functions (such as in the testis) that occurs in post-natal gonads of mice.

The role of *dnd* in post-natal gonad is mostly limited to findings in mice *Ter* mutant lines in which a spontaneous premature stop codon mutation causes *dnd* truncation (Sakurai et al., 1995, Youngren et al., 2005). The PGCs in homozygous *Ter* mutant mice mis-migrate and are lost during embryonic development resulting in male infertility and impaired female fertility (Noguchi and Noguchi, 1985). *Ter* mutant ovaries in rats significantly reduce gonad weight and stimulate tumour development with no primary follicles throughout the tissue (Northrup et al., 2012). In teleosts, *dnd* has been shown to be a specific germ cell marker in both gonads, however, the *dnd* expression in adult ovary is slightly higher (Duan et al., 2015). This is consistent with the findings in *G. holbrooki,* where ovary underwent a significant rise in *dnd* expression between juvenile and adult phase indicating oocytes are being loaded with maternal *dnd* to play a role in PGC determination in zygotes. In teleosts, Dnd function in adult gonads is poorly understood. In the current study, relative higher expression of *dnd-α* were found in female than in male at the adult stage. However, inferred from its role as a RBP, the continuous expression of *dnd-α* in adults *G. holbrooki* testis and ovary can be associated with protecting the identity of germ cells through repressing somatic expression (Gross-Thebing et al., 2017), tuning miRNA functions (Slanchev et al., 2009, Mickoleit et al., 2011) and repressing gonadal carcinogenesis pathways (Northrup et al., 2012, Zechel et al., 2013, Sanchez et al., 2019) as occurs in other vertebrates, including teleosts.

Continuous expression of *tdrd6* throughout the life, including maternal inheritance, in *G. holbrooki* may suggest multiple roles; from anchoring Gp markers as occurs in zebrafish (Huang et al., 2011, Dai et

al., 2017), to gonadosoma maintenance and gamete maturation like in humans (Babakhanzadeh et al., 2020). Mechanistically, the Tdrd protein family is necessary to accommodate PIWI proteins in nuage/chromatoid bodies through interaction with symmetric demethylated arginine of Piwi proteins (Wang et al., 2009, Kirino et al., 2010). Unlike in *G. holbrooki*, *Tdrd6* is not detectable in murine adult ovary, however, it is abundantly expressed in the testis (Kim et al., 2016), and involved in ncRNAs downregulation, maintaining the architecture of chromatoid bodies, and proper localisation of germline markers at the chromatoid body (Vasileva et al., 2009). In zebrafish, *tdrd6α* expression is exclusively detected in ovary, and its function in teleosts has been shown to be associated with the Balbiani body (Bb), an electron dense aggregate in oocytes, accumulating Gp components in ooplasm (Krishnakumar et al., 2018). Indeed, Bb formation requires bucky ball (Buc) protein (Marlow and Mullins, 2008, Bontems et al., 2009), with maternal Tdrd6 acting as a scaffold for Buc mobility, patterning its aggregation inside the Bb and mediating proper segregation of Gp in nascent PGCs (Roovers et al., 2018). An abundant accumulation of *tdrd6* transcripts in adult ovary and unfertilised egg of *G. holbrooki*, suggests a similar role in nuage formation and its maintenance in the ovum. Nevertheless, it is yet unknown if Gp components are accumulated as nuage in poeciliids, as occurs in zebrafish (Koprunner et al., 2001), or if they are loosely distributed throughout the ooplasm and early embryos, as in medaka (Herpin et al., 2007).

4.4.2. Paternal inheritance of Gp components and their role in PGC development

It is well documented that most Gp components are supplied maternally, with little inkling of their paternal origin. As was observed in this study, four of the six maternal determinants—*dazl*, *dnd*, *piwi II*, and *vasa*— of PGCs were detected in *G. holbrooki* spermatozoa and more interestingly their relative abundance was significantly higher than those of ova. This provides the first evidence that the Gp determinants (transcripts) are not only of maternal, but also of paternal origin and may not just be limited to Gp determinants *i.e.*, a similar paternal contribution could extend to a large number of other signalling molecules that activate and support early developmental processes. It is also likely that their need may be limited to an, as yet unknown, role in sperm viability, *e.g.*, shelf life, or function (Bissonnette et al., 2009, Godia et al., 2020).

As evident in *G. holbrooki*, both ova and spermatozoa carry Gp components, that likely play a part in fertilisation and early development in zygotes, including in PGC specification (*e.g.*, in animals with preformation mode of germline determination). While the role of the Gp components in early cell fate decisions and germ cell sequestration from soma is not well explained. For instance, in medaka, maternal Dazl governs PGC formation (Li et al., 2016), while *dnd*, is involved in specification, proliferation and asymmetric segregation of particles between PGC daughter cells (Hong et al., 2016). In zebrafish, maternal *vasa* alone is sufficient for PGC sequestration, survival and localisation to the

genital ridge (Hartung et al., 2014). Also, maternal *nanos1* is required for PGC migration and their survival (Koprunner et al., 2001). Not only that, in organisms with preformation mode of germline specification, the number of PGCs in zygotes is determined based on the segregation of sufficient Gp into nominated cells. Indeed, PGCs receiving insufficient germline factors are eliminated through apoptosis (Slaidina and Lehmann, 2017). This is supported by a strong correlation between the quantity of Gp factors and the number of PGCs (Hong et al., 2016). Therefore, in the preformation model of PGC specification, paternal contribution, as was found in *G. holbrooki*, may be even more important for early germline determination and/or possibly sex differentiation (Ye et al., 2019), which has so far remained overlooked.

In retrospect, the paternal inheritance of Gp components as well as other developmental signals may not be surprising. The artificial androgenesis in some fish species, with fertile offspring, is feasible (Komen and Thorgaard, 2007), which may already provide independent evidence for a critical role of paternally inherited early developmental signals. A central step in artificial androgenesis is maternal genome inactivation by gamma (Arai et al., 1979) or X-rays radiation (Palti et al., 1997) of unfertilised eggs. Based on the destructive mechanisms of radiation on nucleic acids, single-stranded RNAs are as vulnerable as other types of nucleic acid groups to radiation (Ginoza, 1967, Kantor and Hull, 1979, Kladwang et al., 2012). Also, radiation alters the structure of proteins (Durchschlag et al., 1996). Therefore, any method of radiation applied during artificial androgenesis procedures is likely to destroy, or at best compromise, all maternal deposits in the ova (Bongers et al., 1995). Despite the destructive nature of radiation, fertile viable androgenic offspring are produced (Babiak et al., 2002, Komen and Thorgaard, 2007) suggesting that the prerequisite maternal Gp components can be compensated by paternal deposits. Also, the level of infertility following artificial androgenesis rather varies based on genetic background of experimental strains (Keller and Waller, 2002), the sexual genotype of androgenic offspring (Bongers et al., 1999, Santhakumar and Pandian, 2003) and the sex determination mechanism (Scheerer et al., 1986, Sarder et al., 1999) of the androgenic lines. Indeed, the reciprocal fertility of gynogenetic lines (reviewed in Komen and Thorgaard, 2007) collectively suggests that most, if not all, parentally inherited transcripts can compensate for the absence of the other.

4.5. Conclusion

Collectively, this study provides the first evidence for accumulation of select Gp markers in fish sperm, that are conceivably passed to developing embryos and contribute to early germline formation and possibly beyond, as is previously attributed to maternal signals. However, further experiments are required to validate if the paternal deposits are passed on to developing embryos at fertilisation. If so, either they are critical or play only a compensatory role in early development and during adulthood. Comparative evaluation across a broad range of teleosts to determine if such accumulation of Gp markers in sperm is unique to this species is necessary. Also, which specific function, if any, paternally

supplied Gp markers play needs further evaluation, such as revaluation in existing mutants or generating new ones, including knockdown and knockout models. In this regard *G. holbrooki* and poeciliids in general may serve as valuable systems to understand the wider developmental and adult role of Gp markers, including in mammals. Such insight may have practical relevance, such as for managing pest populations of *G. holbrooki*, hatchery propagation of commercial and endangered fish species as well as broader biomedical implications such as for reproduction and fertility.

Chapter V

Gonadogenesis in *G. holbrooki*

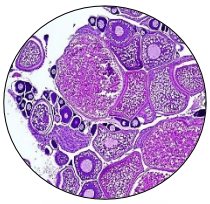

Chapter 5 | Gonad ontogeny and sex differentiation in live-bearing *Gambusia holbrooki*

Abstract

In sexually reproducing animals, gonadogenesis is triggered following successful germ cell colonisation and gonadosoma emergence at the genital ridge. This is followed by sexual identity acquisition of gonad through sex determination mechanisms, germ cell effects and/or environmental cues. The gonadogenesis and sex differentiation patterns are diverse in teleosts, however, little is known in poeciliids. To ascertain when and what cellular and molecular determinants trigger sex differentiation in *G. holbrooki*, this study documented critical events during early gonadogenesis using gonad histology, *in situ* hybridisation of germ cell markers and quantitative expression of the gonadosoma markers. The histological observations showed that germ cells first colonised the genital ridge, prior to completing somitogenesis, to form presumptive gonads. Thereafter, germ cells underwent mitotic proliferation in a sex-dependent manner, before acquisition of sexual identity (*i.e.*, right before parturition). As evidenced by emerging meiotic primary oocytes stage I in the ovary and formation of spermatogonial stem cell cysts in the testis, the sex differentiation of early gonads in *G. holbrooki* occurred just before parturition. Gonad histology and germ cell labelling also showed that presumptive gonad in *G. holbrooki* underwent major morphological transformation during its early development. Specifically, presumptive gonads first developed as two distinctive lobes as in most teleosts, however, the lobes grew convergently and fused around the parturition stage to form a single lobed testis or ovary, as they occur in adults. The quantitative expression pattern of the gonadosoma markers, *foxl2*, *cyp19α*, *amh* and *dmrt1*, in pre- and post-natal developmental stages was consistent with morphological changes in early gonad; they were activated at the onset of gonad formation followed by sex-dimorphic expression pattern concurrent with sex differentiation of gonads. To conclude, this study, for the first time, documented the underlaying processes of gonad formation in *G. holbrooki*. The key gonadogenesis events in *G. holbrooki* including PGC colonisation, sex differentiation and sex-biased expression of gonadosoma markers occurred relatively earlier than those previously described for model egg laying fish species. This implies a relatively earlier gonadogenesis program in *G. holbrooki*, which appears in sync with the complexity of viviparity and observed morphological differentiation of gonads. Also, this possibly supports poeciliids' position as an early/robust evolutionary node of sex differentiation mechanisms, resembling those of higher vertebrates.

5.1. Introduction

With ductile reproductive strategies, teleosts are the most diverse group of vertebrates (Crother et al., 2016) and provide rich resources for evolutionary inventions (Evans et al., 2014) and adaptations. Significantly, this has occurred through the acquisition of regenerative gametogenesis (Schulz et al., 2010, Lubzens et al., 2010, Nikolic et al., 2016), evolving intrinsic/extrinsic sex determination mechanisms (Devlin and Nagahama, 2002, Presslauer et al., 2016) and exhibiting divergent plans of sex differentiation (Baroillera et al., 1999, Baroiller et al., 2009a, Horiguchi et al., 2013).

Typically, gonadogenesis is marked by three successive steps; 1) primordial germ cell (PGC) development (Raz, 2002), 2) gonadosoma formation (Kayo et al., 2019) and 3) gonad differentiation (Lau et al., 2016). Despite a wide range of reproductive approaches, gonad ontogenesis in teleosts is an expeditious process predominantly triggered by maternal input to PGC formation in early zygotes, eventuating in germ cell homing at the gonad anlage (Koprunner et al., 2001, Kaufman and Marlow, 2016a). Subsequently, at the anlage, skirting somatic cells provide the requisite support for germ cell growth, proliferation and differentiation, facilitating eventual gametogenesis (Saito et al., 2007, Figueiredo et al., 2016).

In vertebrates, gonadogenesis typically commences at the post-segmentation/early pharyngula stage where PGCs are attracted towards the gonad primordia (*i.e.*, genital ridge/gonad anlage), guided by chemotactic cues from the somatic cells of the destination (Reichman-Fried et al., 2004) supporting subsequent development and differentiation of gonads. In mice, gonadogenesis itself occurs at the ventral-medial mesonephros developing as a pair of thickened coelomic epithelial layers, resulting in a sexually indiscernible reproductive tract (Ginsburg et al., 1990, Ungewitter and Yao, 2013). The robust sex determination mechanism, in mice, then defines the sexual identity of germline and gonad primordia to either ovary or testis (Koopman et al., 1991, Harley and Goodfellow, 1994), before birth. In medaka, gonadosoma precursors are first identified as two groups of *ftzf1* and *sox9b* expressing cells at post-somitogenesis (Nakamura et al., 2006). These two groups later converge with colonised PGCs at the 33/40 developmental stage and form the gonad primordia (Nishimura and Tanaka, 2014). Subsequently, at about hatching time, the *sox9b* expressing cells skirt colonised PGCs and *ftzf1* positive cells relocate to the outer gonad. Consequently, *sox9b* is uniformly expressed in the supporting cells of bipotential gonads, unlike exclusive *Sox9* expression in murine Sertoli cells. Unlike mice, some fish species, in the absence of a robust sex determination system (Devlin and Nagahama, 2002), rely on PGC development machinery to acquire sexual phenotype of gonad by regulating PGC proliferation. Indeed, germ cells have feminising effects in species such as zebrafish (Siegfried and Nusslein-Volhard, 2008) and medaka (Nishimura et al., 2018, Kurokawa et al., 2007), as germ cell-deficient gonads develop as dysfunctional testis. The malleable sex determination systems typically observed in teleosts also allow sex

differentiation pathways to be influenced by environmental factors (Baroiller et al., 2009b) and/or social cues (Godwin, 2009).

The sex determination machinery determines and maintains sexual identity of gonad through function of a group of sex regulating genes highly conserved among vertebrates (Devlin and Nagahama, 2002, Nagahama, 2005). The gene *dmrt1, Doublesex and Mab-3 (DM)-related Transcription factor 1*, belongs to a family characterized for its a highly-conserved zinc-finger DNA-binding motif rich in cysteines (Picard et al., 2015). The autosomal *dmrt1* was first found in mammals functioning as a testis-differentiating gene. In teleosts, *dmrt1* has been shown to have a diversified expression pattern; from a male-biased (Masuyama et al., 2012, Kwan and Patil, 2019) to female-specific expression (Zheng et al., 2014).

The gene *amh, Anti-Mullerian hormone*, is the member of the Bmp group of the Tgfβ superfamily of growth factors. In mammals, *Amh* is expressed in Sertoli and granulosa cells. In males, *Amh* is stimulated by Follicle stimulating hormone (Fsh) and repressed by androgens, while in females, it is inhibited by estrogen (di Clemente and Belville, 2006, Grinspon and Rey, 2010). In ovary, Fsh induces *Amh* expression in early stages of gonad development but downregulates it at later stages of folliculogenesis (Monniaux et al., 2013). In teleosts, the *amh* ortholog was first found in Japanese eel, *Anguilla japonica*, shown to be expressed in Sertoli cells and plays role in germline development and function (Miura et al., 2002).

Forkhead transcription factors are in a range of biological events including metabolic processes, body axis formation and differentiation of cell types. *Forkhead Box L2, Foxl2*, belongs to the same family highly conserved among taxa (Baron et al., 2004). The *Foxl2* has been shown to play role in murine eyelid and preoptic mesenchyme development (Crisponi et al., 2001), ovarian differentiation (Uda et al., 2004) and maintenance of its sexual identity (Ottolenghi et al., 2005). In teleosts, *foxl2* is highly active during sexual differentiation, via transcriptional regulation of *cyp19a1a* (Wang et al., 2004a, Nakamoto et al., 2006).

Viviparous Pociliidae, with more than 300 described species has mostly been of interest for evolutionary studies and commercial purposes (Houde and Zastrow, 2000, Magalhães and Jacobi, 2017, Olivera-Tlahuel et al., 2018). Exceptional patterns of gonadogenesis, *i.e.* single lobular juvenile gonad (Koya et al., 2003), different states of gonochorism, *i.e.* juvenile hermaphroditism (Koya et al., 2003), peculiar reproductive strategies *e.g.*, spermatozeugmata delivery (Liu et al., 2018b), prolonged ovarian storage of sperm (Gasparini et al., 2018), superfetation (Campuzano-Caballero and Uribe, 2014) and sex-dimorphic melanin patterning (Horth, 2004, Horth, 2003), imply diverse gonadogenesis and sex differentiation strategies are involved in this taxa. Nevertheless, many aspects of gonadogenesis in poeciliids is patchy with limited cellular and molecular evidence. Broadly, the gonadogenesis in *G. holbrooki* can be categorised into three distinctive phases, namely embryonic development up to

parturition, immature juvenile stage and adult phase. With an internal fertilisation and superfetation strategy, *G. holbrooki* embryos develop in the single-lobular ovarian sac, nourished by a combination of placental and yolk matrotrophy and parturate as free-swimming larvae (Pyke, 2005, Norazmi-Lokman, 2016). The growth rate and maturity in *G. holbrooki* is correlated with temperature, salinity and food availability (Meffe, 1992, Nguyen et al., 2021); however, in optimal conditions, they are primed for puberty as early as six-week post-fertilisation (Pyke, 2005, Lloyd et al., 1986). More recently, the genetic sex marker described for *G. holbrooki* (Kwan and Patil, 2019, Patil et al., 2020) has allowed identification of sexual genotypes of the embryos well before the phenotypic sex is discernible. Nevertheless, detailed processes of embryonic gonad formation and patterns of sex differentiation in *G. holbrooki* are still elusive.

As a first step towards understanding the developmental events of gonadogenesis in *G. holbrooki*, this study employed morphological and molecular surrogates to identify critical time points in gonad ontogenesis. Specifically, critical questions including germ cell homing time point, early gonad morphological transformation, establishment of sex-specific patterns and onset of meiosis were investigated in genetically male and female individuals.

5.2. Methods

5.2.1. Fish collection and processing

Wild caught *G. holbrooki* (n = 21 adult females with gravid spot) were collected from the Tamar Island Wetland Reserve (41°23.1'S; 147°4.4'E). The fish were transported to the Institute for Marine and Antarctic Studies (IMAS), Taroona, University of Tasmania. The developing embryos and larvae were obtained from newly caught gravid females and staged as defined in the literature (Chambolle et al., 1970, Mousavi, 2021). The larvae and juveniles were maintained in a recirculating facility for small fish, with optimal rearing conditions (see Table 2.1). They were fed with commercial pellets (TetraMin1 tropical granules, Germany) and freshly hatched Artemia nauplii (INVE Aquaculture, USA). Eight developmental stages/time points were used to document spatio-temporal events of gonad development and sex differentiation. They were gastrula, early segmentation, late segmentation, pharyngula, parturition and 12, 30, and 75 days post-parturition (dpp).

All animal experiments were approved by the institutional (University of Tasmania) Animal Ethics committee (AEC Permit A12787).

5.2.2. Embryonic staging and gonad histology

The embryos (n = 78) were harvested from wild-caught gravid females, surgically. Staging of the developing embryos was as described for this species recently (Mousavi, 2021). Four key developmental stages between late gastrula and parturition were selected to study the dynamics of germ

cells and to evaluate sex-specific time-points for PGC colonisation and sex differentiation of early gonads. The anatomical morphology of germ cells and gonad were studied by hematoxylin and eosin (H&E) stained tissue sections according to standard protocols (Feldman and Wolfe, 2014). Briefly, the samples were fixed in Bouin's solution (Sigma-Aldrich) overnight and rinsed for several hours in 70% ethanol. Tissue processing including dehydration, clearing and paraffin infiltration were conducted by a tissue processor Tissue-Tek® vacuum infiltration processor (Miles Laboratories, PA, USA). The 3 µm sections of specimen were deparaffinised in xylene, dehydrated in progressive concentrations of ethanol, stained by H&E and mounted using Pertex® (Histolab, Sweden). The sections were imaged under a Leica DM750 (Wetzlar, Germany) light microscope and processed using Leica Application Suite (version 3.8.0) software. The number of PGCs were counted in both sexes from corresponding developmental stages for comparison. Germ cell counts were carried out using the cell counter plugin in ImageJ1(Schneider et al., 2012) on serial transverse and sagittal sections (n = 6/each axis) for a given sample and the numbers computed by multiplying the average cell numbers in the transverse and the sagittal sections.

5.2.3. Genetic sexing of embryos

The genomic DNA of embryos were obtained from tail fin clips (pharyngula, parturating embryos and larvae) or paraffin embedded specimens (gastrula and segmentation embryos) using the QIAamp DNA FFPE Tissue Kit (QIAGEN, CA, USA).The genetic sex of embryos was determined by polymerase chain reaction (PCR) using sex-specific genetic markers as described (Kwan and Patil, 2019, Patil et al., 2020). Briefly, PCR reaction (15 µL) comprised of 1 × MyTaq™ HS Red mix (Meridian Life Science, USA), 1.5 µM of each primer and 50 ng of genomic DNA template. Thermal cycling (T100™ Thermal Cycler, Bio-Rad Laboratories, Inc., Australia) consisted of 95 °C for 1 min, followed by 30 cycles of 95 °C for 5 s, 60 °C for 5 s and 72 °C for 20 s. Sex-dimorphic amplicons were visualised and separated using gel electrophoresis.

5.2.4. Cloning and characterisation of key gonadosoma markers

The expression pattern of four genes involved in gonadosoma function, *dmrt1*, *amh*, *cyp19a1a* and *foxl2*, were studied at five distinctive time-points of development including late segmentation, pharyngula, parturition, 30 and 75 dpp. The full-length cDNA of two genes with known gonad function, *i.e.*, *dmrt1* and *foxl2*, along with housekeeping genes, *i.e.*, *pgk1*, *rps18*, *beta-actin*, were cloned using RACE technique as previously described (Chapter 2). Briefly, all publicly available genetic sequences for the respective genes of live-bearing poeciliids namely *Poecilia latipinna*, *P. mexicana*, *P. formosa*, *P. reticulata* and *Xyphophorus maculatus* were aligned using MUSCLE (Edgar, 2004) and two pairs of degenerate primers designed to clone partial CDS using nested PCR to obtain species-specific partial gene sequences. In parallel, total RNA isolated from gonads were used to generate GeneRacer™ cDNA

libraries (Invitrogen life technologies, CA, USA). Subsequently, a pair each of primary and nested primers for amplification of 5´ and 3´ regions were designed based on partial cDNA sequence and used to amplify the cDNA ends whose identify was verified by sequencing and BLAST (Altschul et al., 1990) homology.

5.2.5. RNA extraction, reverse transcription and quantitative PCR (qPCR)

Developing embryos and larvae were dissected from brooding mothers and individually fixed in RNA*later*™ (Thermo Fisher Scientific, VIC, Australia) overnight. For RNA extraction, the embryos were individually homogenised with 19 and 27G needle-syringe aspirations and total RNA isolated using Isolate II RNA Micro Kit (Bioline, NSW, Australia). The gDNA contamination was eliminated from RNA samples using Ambion™ DNase I (Thermo Fisher Scientific, MA, USA) and the DNase treated samples were purified by a column-based method. RNA integrity was qualified by visualising the integrity of 18S and 28S ribosomal RNA on 1% agarose gel stained with SYBER™ Safe (Thermo Fisher Scientific, MA, USA). Total RNA concentration and genomic DNA contamination were measured using Qubit™ 4 Fluorometer with RNA HS and DNA BR Assay Kits (Thermo Fisher Scientific, MA, USA), respectively. About 1 µg of total RNA were used for reverse transcription using Tetro™ cDNA Synthesis Kit (Bioline, NSW, Australia). The 20 µl reaction contained, 200 units of reverse transcriptase, 0.5mM dNTP mix, 10 unit of RNase inhibitor, oligo $(dT)_{18}$ primer mix and 1X reverse transcriptase buffer. The samples were incubated at 45˚C for 60 min and the enzyme was deactivated at 85˚C for 5 min. For the sex-segregated assay, the cDNA concentration of individual samples were normalised between sexes within the same developmental stage.

The qPCR assays were designed to amplify 85-130 bp amplicons (Table 1) and performed using CFX96 Touch™ system (Bio-Rad, NSW, USA). Amplicon identities were confirmed by melt curve analysis, gel visualisation and sequencing.

Table 5.1. Primers sequences, amplicon size, and source of primers used for qPCR.

Gene		Sequence 5′ – 3′	Amplicon size (bp)	Annealing temp (C˚)*	References and accession numbers
House keeping	*beta-actin*	CGGCAGGACTTCACCTACAGACACCT CTTGCACAAACCGGAGCCGTTGTCA	99	67.7 68.2	MZ542286
	gapdh	AGCCAAGGCTGTTGGCAAGGTCATC GTCATCATACTTGGCTGGTTTCTCC	133	75.1 67.5	(Kwan and Patil, 2019)
	pgk1	GATGATCATCGGTGGCGGCATGG ATACCAGCGCCTTCCTCGTCGAACA	96	66.2 68.0	OL988673
	rps18	GGAGAGGCTGAAGAAGATCAGGGCTC ACCGACAGTGCGACCACGACG	109	66.2 67.4	OL988674
Male-biased	*dmrt1*	CACCCTTCGTCAGCCTGGAGGAGA ATGGTCGAGTCGTAGCTGGTAGGTGAA	85	67.6 66.8	OL988671
	amh	CCCCTGCAGATGGAGAGCTGGGCGTCATTT AACGTCGTCCCTGAARTGCAAGCAGA	88	82.3 75.5	MH853785.1
Female	*cyp19a1a*	GCTTGTGGAGGAGATGAGCACGGTT	97	67.0	(J. G. Patil, personal communication)

	CATCACTTTCAGTCTTTCATAACTGACG		63.1	
foxl2	GCAAAGGGAGAGGCAGAGGAGGA CTCTACCGCCTCTCCCACTGAAACCA	108	65.8 67.5	OL988672

5.2.6. qPCR data normalisation and statistical analysis

For biological normalisation of data from qPCR assay, first stability of *rps18*, *gapdh*, β-*actin* and *pgk1* (Willems et al., 2006, Panina et al., 2018) was tested by geometric averaging (Vandesompele et al., 2002) using geNorm algorithm (Vandesompele et al., 2002, Hellemans et al., 2007) in qbase^{+} software, version 3.0 (Biogazelle, Zwijnaarde, Belgium). As a result, *gapdh* was selected as the most stable (M value 0.45) housekeeping gene that is highly expressed but not sexually differentiated. The relative transcription of target genes was calculated using the comparative threshold cycle (Cq) method with efficiency correction (Ruijter et al., 2009). Relative expression of genes of interest (ΔCq) was calculated against the selected reference gene (*gapdh*). The fold changes were measured using the $2^{(-\Delta\Delta Cq)}$ method and presented in box plots. The real time PCR mix (10 µl) comprised of 1X iTaq Universal SYBR Green Supermix (Bio-Rad, NSW, Australia), 5 (embryos) to 30 (tissue) ng cDNA template, 0.4 µM of each primer, and adjusted to 20 µl using MilliQ water. Duplicate reactions were run for each cDNA sample using the CFX96 Touch Real-Time PCR Detection System (Bio-Rad, NSW, Australia) consisted of 95˚C for 1 min, followed by 40 cycles of 95˚C for 5 s, 66-70 ˚C for 10 s, and 72˚C for 7-12 s. For positive and negative control, 5 ng cDNA (from a tissue where the target gene is expressed) and MilliQ water were used as template, respectively. Melting curve analysis, gel visualisation and sequencing of qPCR products were subsequently performed to check unwanted products and gDNA contamination. The MIQE of the qPCR assay was provided in Table A10.

All qPCR data were presented as mean ±standard deviation (SD) and the outliers were removed from dataset. Shapiro–Wilk and Levene's tests were used to test data normality and homogeneity of variances, respectively. A two-way analysis of variance (ANOVA) was used to identify significant differences between experimental groups using two factors, sex and developmental stage. Tukey *post hoc* test was applied wherever population means were significantly different between the sexes of each developmental stages. The level ($p < 0.05$, $p < 0.01$, or $p < 0.001$) of significance between two means was also determined. All statistical analyses were performed and plots generated using OriginPro, Version 2020 (OriginLab Corp, MA, USA).

5.2.7. Whole-mount in situ hybridisation (WM-ISH)

The ontogeny of germ cells and the formation of gonad were examined by detection of *vasa* transcript using chromogenic *in situ hybridisation* on whole mount (WM-CISH) pharyngula and parturating embryos. The sense and antisense digoxigenin-labelled *vasa* RNA probe (see Chapter 3) was generated through *in vitro* transcription from an approximately 1.15 kb of coding region using T3/T7 RNA

polymerase (New England Biolabs) and DIG RNA labelling mix (Roche, Mannheim, Germany). The cDNA template and unincorporated reaction components were removed from the RNA probe using Ambion™ DNase (Thermo Scientific, USA) and ethanol precipitation or column purification, respectively. The ready probe was stored with 0.5 U/µl of RNasein® Plus Ribonuclease Inhibitor (Promega, USA) at -20 ˚C until use. Pharyngula (n = 26) and parturating (n = 17) embryos were dissected from gravid females, rinsed with cold PBS and fixed using 4% paraformaldehyde (Emgrid) overnight at 4˚C. The fixed embryos were rinsed in PBST (PBS containing 0.1% Tween 20) and dehydrated with progressive concentrations of methanol replaced with PBST. Subsequently, the specimens were permeabilised with 20 µg/ml proteinase K (Thermo Scientific™, EO0491) for 15-25 min at 37 ˚C and postfixed with 4% paraformaldehyde for 20 min at room temperature. The embryos were prehybridized at 68˚C for 3 hours in hybridization buffer (50% formamide, 5X SSC, 0.01% Tween 20, Torula Yeast tRNA, 50µg/ml heparin). The samples were incubated in hybridization buffer containing 1 ng/µl antisense *vasa* probe at 68˚C for 16 hours. Non-specifically bound and excessive probes were removed through consecutive desalting stringency washes using PBST. For DIG labelling, first, the non-specific regions for anti-DIG antibody were blocked using blocking solution comprising 5% blocking reagent (Roche, 11 096 176 001) dissolved in 1x maleic acid buffer containing 0.1% Tween 20 (MABT) for several hours. The embryos were then incubated in 1:3000 dilution of Anti-Digoxigenin-AP (alkaline phosphatase), Fab fragments (Roche, 11 093 274 910) in blocking solution overnight at 4 °C. The antibody-labelled embryos were washed with PBST, 8 times for 30 min each (with gentle agitation), washed in staining buffer (100 mM Tris HCl pH 9.5, 50 mM MgCl2, 100 mM NaCl, 0.1% Tween 20) for 30 min and incubated in BM-purple (Roche), and chromogenic AP substrate was added to develop dark purple hybridisation signals to desired contrast. The embryos were then washed in PBST until all excess stain was removed. Finally, the embryos were postfixed with 4% paraformaldehyde overnight at 4˚C and washed and stored in PBS for imaging by light microscopy Leica DM750 (Wetzlar, Germany) and imaging software Leica Application Suite, version 3.8.0.

5.3. Results

The critical events of gonadogenesis, from post PGC colonisation to puberty, were successfully documented in *G. holbrooki* and the salient features are detailed below.

5.3.1. PGC colonisation occurs before complete somitogenesis.

Of the developmental stages assessed, the migrating PGCs were first identified at early to mid somitogenesis (n = 4 embryos), concurrent with the first visible tailbud, 15 somites, optic bud formation and segregation of the central nervous system into telencephalon, diencephalon, and mesencephalon. At this stage, the migrating PGCs were localised below the pronephros cells and adjacent to the developing intestine (Fig 5.1A and A′). The migrating PGCs were noticeably larger (n = 31, diameter:

13.4±0.5 µm) than other surrounding cells and were characterised by barely stained cytoplasm and a conspicuously distinguishable nucleus which occupied most of the cell volume. The first observation of colonised PGCs (Fig 5.1B and B′) was captured in late somitogenesis (n=17 embryos) that coincided with the onset of melanophore pigmentation, otolith enlargement, tail movement and detached eye cups from yolk. At late somitogenesis, the gonad primordia formed a clutch of populating germ cells attached to the epithelial coelomic wall via connective tissue that extended ventrally and posteriorly (Fig 5.1B and B′). The newly colonised PGCs retained their morphological characters, however, they were stained lighter (Fig 5.2A, B and C), compared to migrating PGCs (Fig. 5.1A and B). Nevertheless, the staining capacity of homed germ cells was regained when they underwent mitosis, at the pharyngula stage (Fig. 5.2D). The morphology of PGCs, the timing of their colonisation and primitive gonad emergence (n =11, F:M 7:4) did not show any sex-dimorphic pattern at late somitogenesis.

5.3.2. Mitotic proliferation of germ cells

At the onset of the pharyngula stage, subsequent to their colonisation, germ cells underwent mitotic proliferation, however, their abundance was not different between females and males. In genetic males (n = 9), at early pharyngula, where melanophores on the dorsal fin, pulsating mouth and blood circulation throughout internal organs were observed, the spermatogonial germ cells retained their stem cell features and showed a quiescent mitotic activity (Fig. 5.2A and F). Also, somatic cells were infrequently observed throughout the presumptive gonad in genetic males. At the same developmental stage, germ cell proliferation was swiftly initiated in genetic female embryos (n = 7), through type I mitosis, as was characterised by inactive and stochastic proliferation of gonial cells that resulted in individual stem-like daughter cells (Fig 5.2B). However, at early pharyngula, the number of homed germ cells in females (mean= 200±18, n = 7) at the genital ridge was not significantly different (Fig. 5.2F) compared to males (mean = 118±5, n = 9); this also applied at somitogenesis. The earliest significant difference in germ cell numbers between genetic males (mean = 355±37, n = 7) and females (mean= 1148±56, n = 6) was first observed at mid-pharyngula, concurrent with jaw enlargement, emergence of caudal fin ray elements and teeth on the mandible. Here, undifferentiated (presumed spermatogonial) stem cells underwent type I mitotic proliferation (Fig 5.2C) and resulted in a significant increment in germ cell numbers (*i.e.*, in testis) in comparison with early pharyngula (Fig 5.2F, $p<0.05$). At this stage (mid pharyngula), in genetic females (n =5), apart from type I, type II (cyst-forming) mitotic oogonia was also identified. The Type II mitosis was evident by synchronously developing cradles containing two daughter cells with interconnected cytoplasm (Fig 5.2D). At this stage, the somatic cells also populated the putative ovary (5.2B and C), and in testis, they appeared to skirt germ cell cysts (Fig. 5.2A and D).

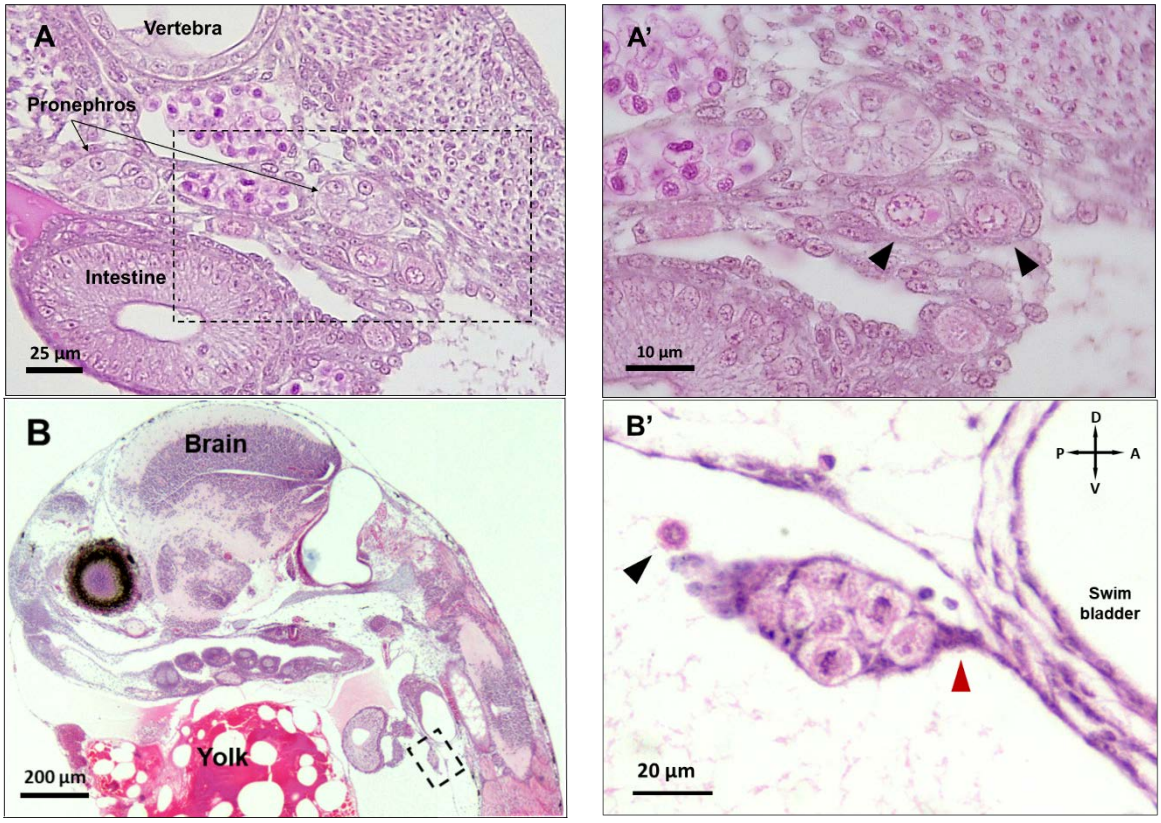

Figure 5.1. PGC localisation, migration and colonisation in *G. holbrooki*. The cross section of embryos at late gastrula (A and A′) show migrating PGCs (black arrowhead), adjacent to kidney cells (pronephros) and early intestine. Sagittal sections (B and B′) show subsequent migration of PGCs to abdominal cavity and colonisation of the genital ridge, at late segmentation. The colonised PGCs were attached to the coelomic wall by connective tissue (B′, red arrowhead) located ventral to the swim bladder (B). A migrating PGC (B′, black arrowhead) in the abdominal cavity is in the process of joining the homed germ cell precursors. The compass indicates the orientation of body axis where applicable (A, anterior; P, posterior; D, dorsal and; V, ventral).

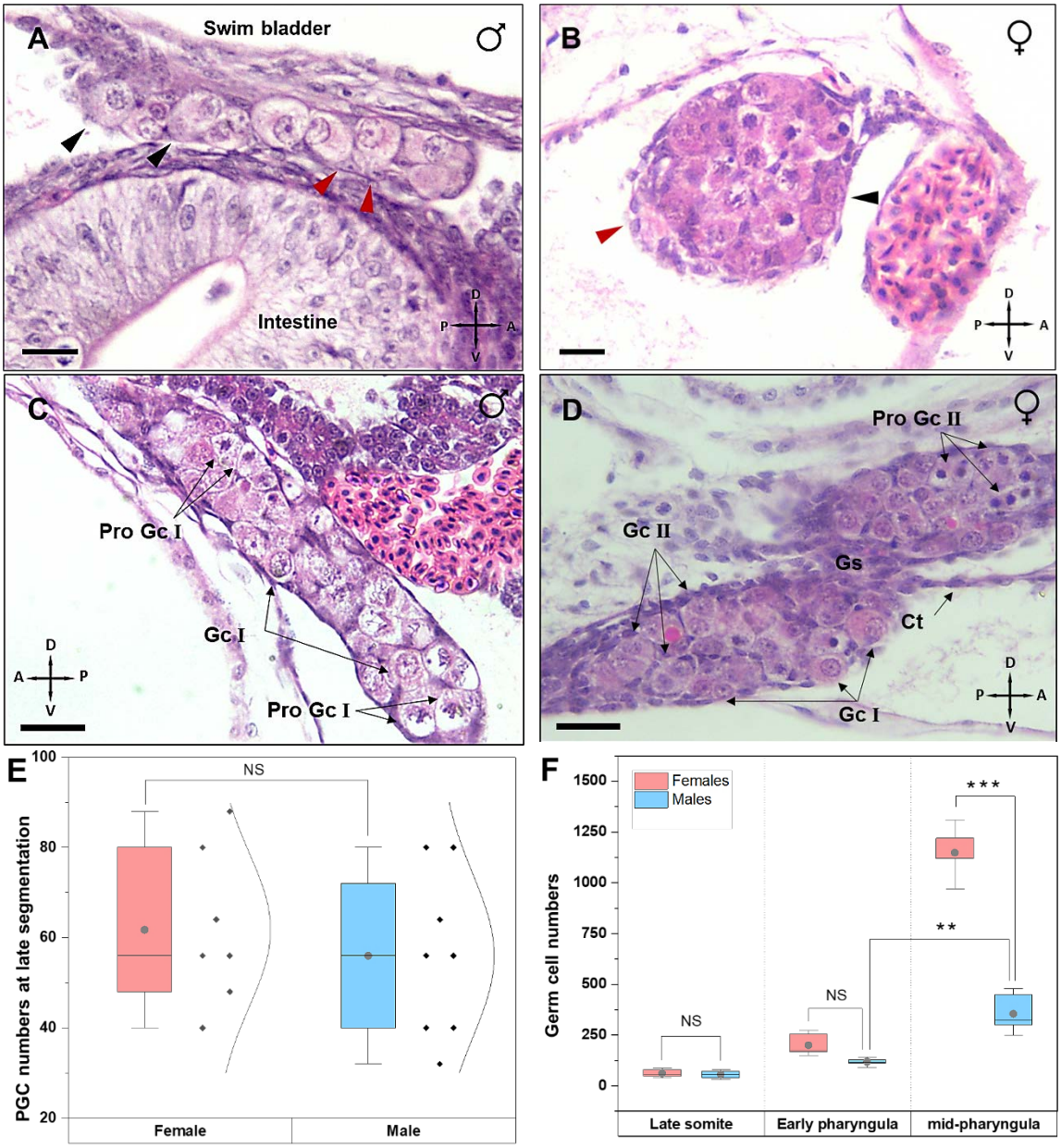

Figure 5.2. Panels showing the sex-dimorphic pattern of germ cell proliferation in *G. holbrooki*. At early pharyngula (A), testicular germ cells remain in their precursor form (black arrowhead) maintaining the large size and low staining capacity. At mid-pharyngula (C), genetic males showed stochastic mitotic proliferation type I and slight tissue enlargement. In early pharyngula females (B), proliferating germ cells were characterised by highly stained nuclei indicating the stem-like mitosis transition of presumptive ovary. The individual formation of oogonial cells in ovary (B, black arrowhead) are indicative of type I mitosis and were skirted by somatic cells. At mid-pharyngula, in genetic female embryos (D), cradles of oogonia with two daughter cells interconnected through cytoplasm and surrounded by a layer of somatic cells were indicative of type II mitotic proliferation. By pharyngula, somatic cells (A and B red arrowhead) were observed at the putative gonads of both sexes. The number of colonised PGCs at late segmentation (E, ANOVA, $F_{1, 12} = 0.131$, $p > 05$) were comparable between the sexes but differentiated at pharyngula stage (F, ANOVA, $F_{5, 36} = 274.3$, $p < 001$). The asterisks indicate the level of significance between groups ($p<0.01$, *** $p<0.001$). Scale bars are 20 µm. Gc I, germ cell type I; Gc II, germ cell type II; Pro Gc, proliferating germ cells; Gs, gonadal stroma; CT, connective tissue, NS, not significant.**

5.3.3. Differentiation of gonads

Meiosis was first obvious by the presence of stage I primary oocytes that were arrested at prophase I (Fig. 5.3A and A′), just before parturition, in genetic female embryos (n=11). This coincided with the embryonic stage where the developing caudal fin reached forebrain, anus and urogenital pores being formed, with concurrent appearance of five teeth in the premaxilla. At this developmental stage, some embryos (n = 8) also had a few stage II primary oocytes that were spread sporadically throughout the ovary and were surrounded by a single layer of follicle cells. Mitotic oogonia were also found in the meiotic ovary, mostly located in the periphery of the tissue (Fig. 5.3A′). In genetic male embryos (n = 9), at the same developmental stage, the gonad development appeared accelerated through stem cell (presumed spermatogonia) proliferation that formed clusters of gonial cells with a homogenous morphology (Fig. 5.3B and B′). The emerging Sertoli cells were first observed in the testis of pre-parturating genetic males as triangle-shaped cells (Fig 5.3B′) and nested between putative spermatogonial cells.

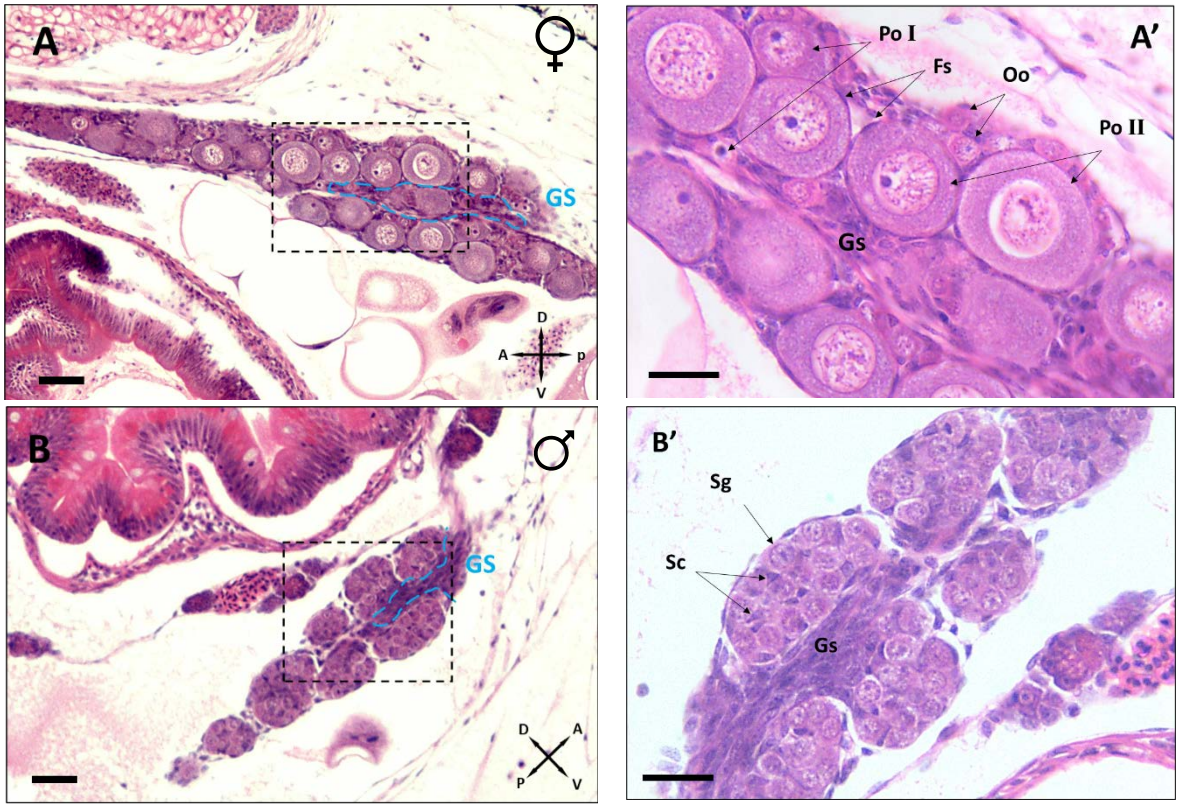

Figure 5.3. Histo-micrographs showing the earliest signs of sex differentiation in *G. holbrooki*. Ovarian differentiation (A and A′) was observed right before parturition, characterised by emerging primary oocytes stage I. Some genetic female embryos also had primary oocytes stage II at the same ovarian developmental stage. Before parturition, although ovary is dominated by meiotic germ cells, mitotic oogonia were also occasionally observed at the periphery (A′). The somatic follicle cells of the ovary formed as a single layer surrounding primary oocytes. Testicular differentiation (B and B′) was less obvious but was characterised by nests of mitotic GSCs throughout the gonad in genetic males, with the first occurrence of Sertoli cells nested between spermatogonial cells (B′). Abbreviations: mitotic

oogonia, Oo; primary oocyte stage I, Po I; primary oocyte stage II, Po II; gonadal stroma, GS: blue dotted area; Sertoli cells, Sc; spermatogonia, Sg; follicle cells, Fs. Scale bars = 25 µm.

5.3.4. Gross, morphological transformation of gonad structure in *G. holbrooki*

Embryonic gonadogenesis in *G. holbrooki* underwent a significant morphological transformation through laterally converging axial lobes, ensuing in a single lobed organ at post-parturition. As can be seen from *vasa*-positive cells, germ cells began to coalesce at two distinct ridges, after colonisation at the late somitogenesis stages (Fig. 5.4A). Later, in the pharyngula stage, the two primary lobes grew convergently and were enlarged by populating germ cells, however, the gap between the primary lobes was visible until the late pharyngula stages (Fig 5.4B). At late parturition, the primary lobes were observed in closest vicinity (Fig 5.4C) which eventually merged into a single-lobed gonad in juvenile fish (Fig 5.4D) in both sexes. The pattern of gonad transformation, including the orientation and fusion of primary lobes, remained unchanged among different individuals and between genders (n =17, F:M 7:6). At the mid-pharyngula stage (n=5 embryos, F:M 4:1), some presumptive gonads transiently displayed a novel morphology (Fig 5.5), in which PGCs were colonised in multiple domains and transiently formed islands of germ cells. They appeared connected to the coelomic wall and spleen through connective tissue. Those germ cell islands later fused through gonadal stroma expansion and germ cell proliferation in parturating embryos (Fig. 5.3A) presumably developing into an integrated gonad lobe each on either side of the body axis.

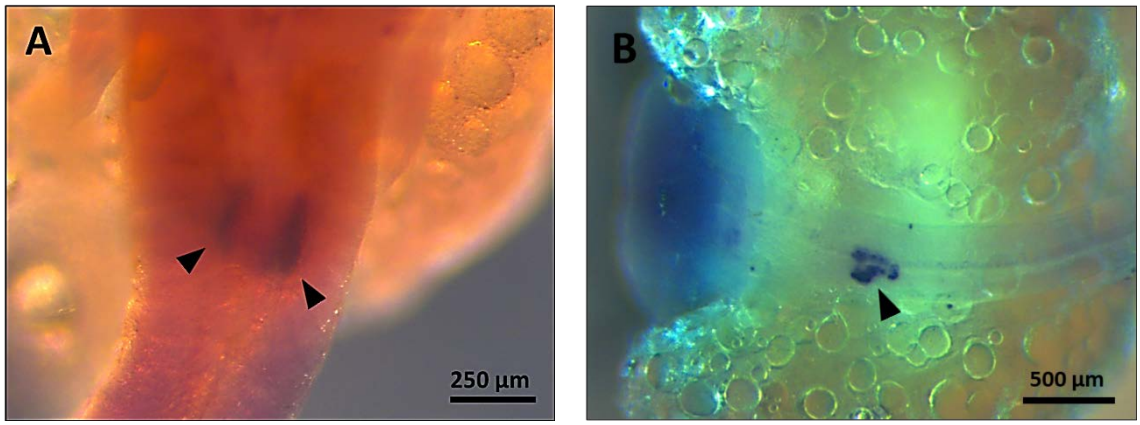

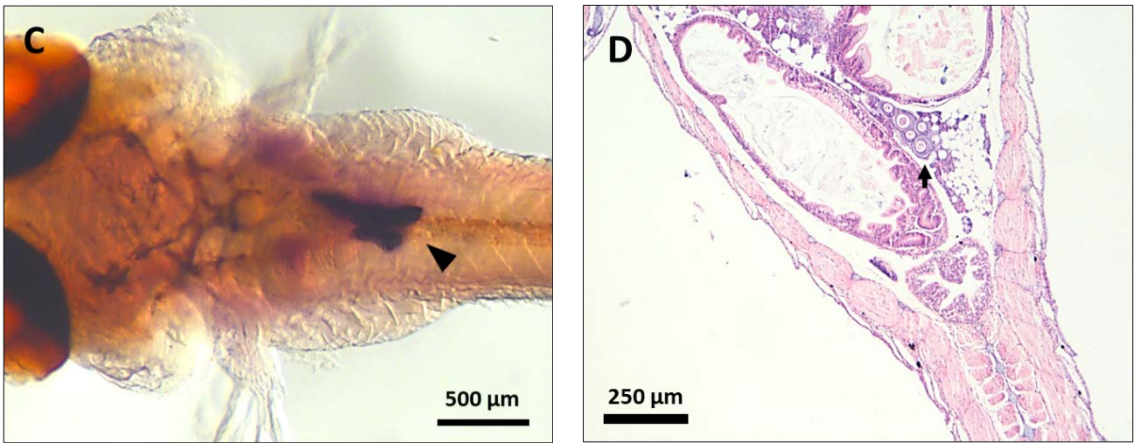

Figure 5.4. The *vasa* labelled micrographs (A, B and C) representing axial transformation and fusion of presumptive gonad lobes during late embryogenesis. The H&E stained micrograph (D) shows mono-lobular gonad in juvenile phase. As revealed by *vasa* marker (arrowheads) the germ cells first colonised two distinct ridges on either side of the body axis, during late somitogenesis (A), subsequently growing larger and closer at mid-Pharyngula (B) and right before parturition (C). The arrow indicating single-lobed ovary in coronal section of juvenile female at 12 days post parturition (D).

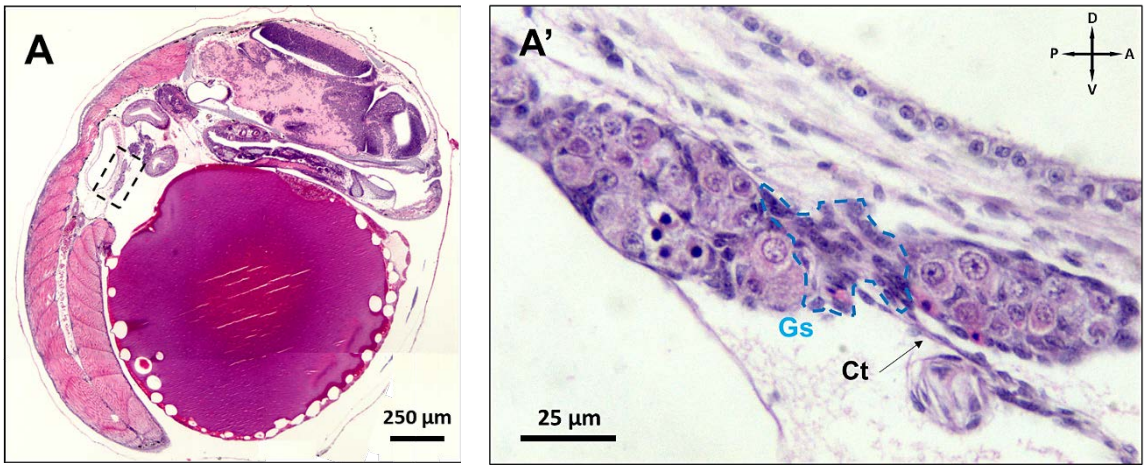

Figure 5.5. Histo-micrographs displaying the formation of germ cell islands in the sagittal axis of developing embryos (A and A′), at the mid-pharyngula stage. The two lobes were interconnected through gonadal stroma (GS; blue dotted area) and attached to the coelomic wall from gonadal stroma via connective tissue (Ct).

5.3.5. Quantitative expression pattern of gonadosoma markers

At late somitogenesis, concurrent with PGC homing, *foxl2* expression was not detected (ANOVA, $F_{9,38}$ = 17.60, p <001, Fig. 5.6A), while those of *cyp19a1a* (ANOVA, $F_{9,43}$ = 17.06, p <001, Fig 5.6B), *amh*

(ANOVA, $F_{9,35}$ = 12.91, p <001, Fig. 5.6.C) and *dmrt1* (ANOVA, $F_{9,37}$ = 9.87, p <001, Fig. 5.6D) were detectable. However, the patterns were comparable between genetic males and females (Fig. 5.6E). At the pharyngula stage, concurrent with the mitotic proliferation of germ cells, the expression patterns of *dmrt1*, *amh* and *cyp19a1a* were not sex-dimorphic, while the *foxl2* expression, was detected for the first time in pharyngula males and females and its ovarian expression was significantly higher (ΔΔCq=4.8±0.81 $\log_2$, p<0.01, Fig. 5.6A).

Just before parturition, coinciding with sex differentiation in genetic females (*i.e.*, the onset of meiosis in primary oocytes), *cyp19a1a* maintained its abundant and significantly higher expression in the ovary (ΔΔCq=5.6±0.52 $\log_2$, p<0.001, Fig. 5.6A) compared to the testis. In the same developmental stage, *dmrt1* expression in genetic females underwent a significant suppression (ΔΔCq=3.7±0.55 $\log_2$, p<0.05, Fig. 5.6D); more than 12-fold lower compared to genetic males. Nevertheless, *amh* did not show a noticeable sex-dimorphic expression pattern right before parturition (Fig. 5.6C).

Similar to prenatal stages (Fig. 5.6E), the relative expression of *foxl2* in juveniles (ΔΔCq=5.1±0.52 $\log_2$, p<0.001, Fig. 5.6B) and adult ovary (ΔΔCq=4.5±0.75 $\log_2$, p<0.001, Fig. 5.6B) was much higher than those of post-natal testes. The expression of *cyp19a1a* was significantly higher in the post-natal ovary; displaying an increasing trend between the juvenile (ΔΔCq=3.2±0.44 $\log_2$, p<0.05, Fig. 5.6A) and adult phases (ΔΔCq=4.2±0.76 $\log_2$, p<0.01, Fig. 5.6A). However, the relative expression of *cyp19a1a* in the post-natal ovary was not as abundant as its pattern at the parturition stage. Relative expression of *amh* at the post-natal phase was significantly male-biased, however, its expression is more skewed in the juvenile phase showing the highest sex-dimorphic difference (ΔΔCq=5.2±0.62 $\log_2$, p<0.05, Fig. 5.6C) within the studied window. Similarly, *dmrt1* expression maintained the male-biased pattern at the post-natal phase, through its noticeable downregulation in juvenile (ΔΔCq=6.0±0.57 $\log_2$, p<0.01, Fig. 5.6D) and adult ovary (ΔΔCq=6.1±0.62 $\log_2$, p<0.01, Fig. 5.6D).

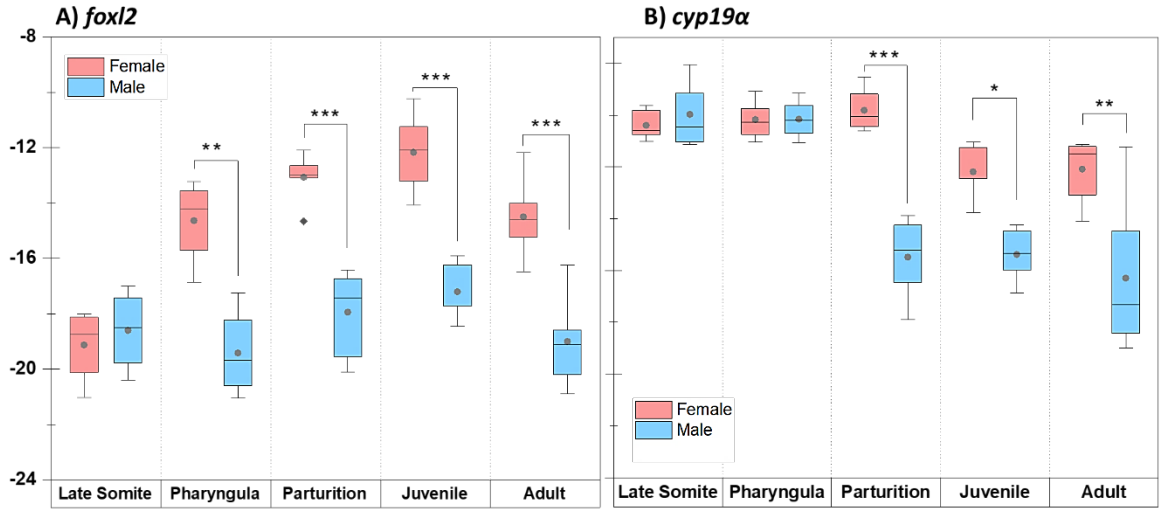

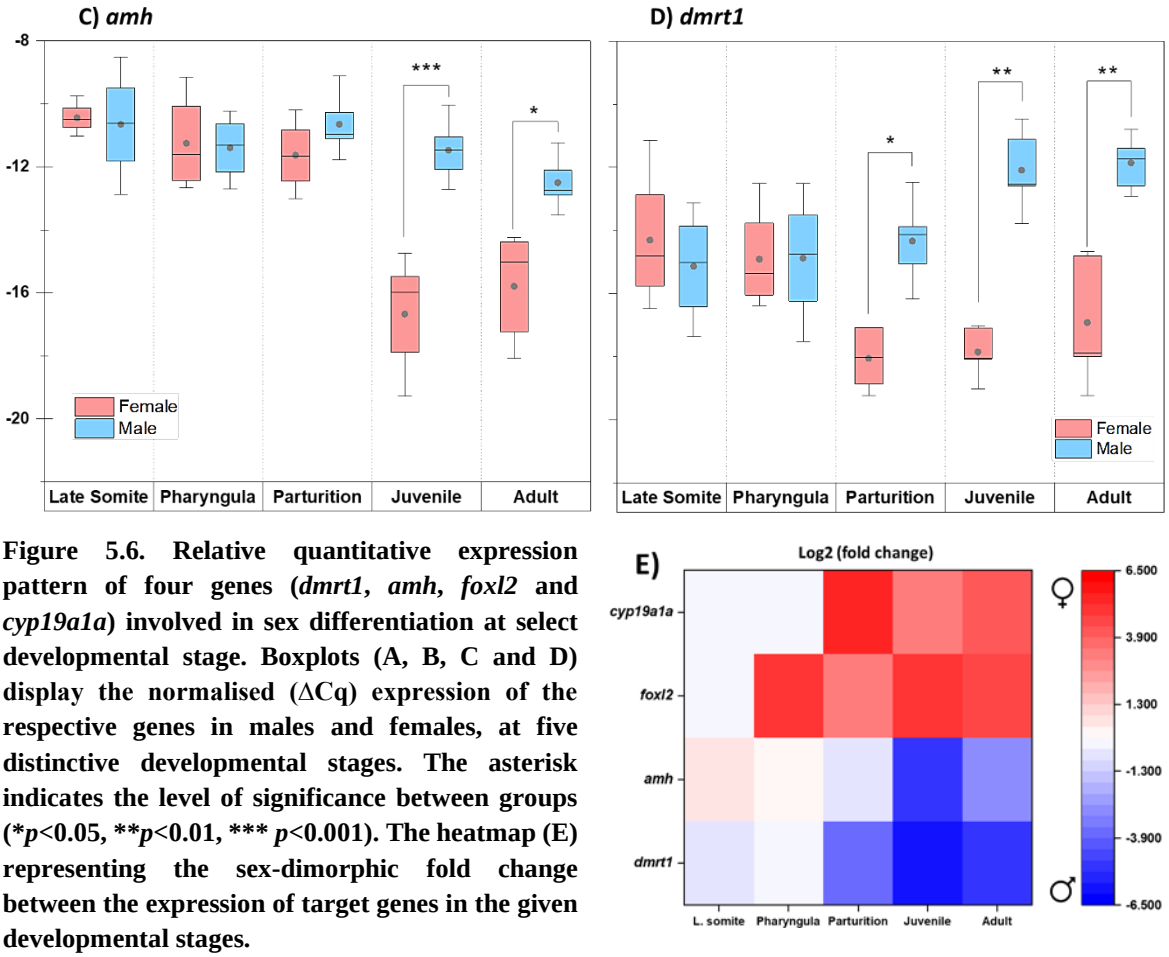

Figure 5.6. Relative quantitative expression pattern of four genes (*dmrt1*, *amh*, *foxl2* and *cyp19a1a*) involved in sex differentiation at select developmental stage. Boxplots (A, B, C and D) display the normalised (ΔCq) expression of the respective genes in males and females, at five distinctive developmental stages. The asterisk indicates the level of significance between groups (p*<0.05, ***p*<0.01, *** *p*<0.001). The heatmap (E) representing the sex-dimorphic fold change between the expression of target genes in the given developmental stages.**

5.4. Discussion

This study documented critical time-points of gonad ontogenesis, its morphological transformation and sex differentiation for the first time in any live-bearing teleost. In parallel, the expression pattern of key gonadosoma markers provided validation for reproductive developmental events. The relevance of the outcomes to basic biology and options to manipulate sex ratios to manage invasive populations of this species are discussed below.

5.4.1. PGC proliferation in *G. holbrooki* is independent of sex determination mechanism

The slow somito- and pharyngula genesis in *G. holbrooki*, provided a developmental framework (*i.e.*, between PGC colonisation and gonadosoma apparition right before gonial mitosis) to more accurately quantify the newly homed PGCs which had retained their morphology and staining capacity but without undergoing mitotic activity. The occurrence of comparable numbers of PGCs in both sexes of *G. holbrooki* at late segmentation was inconsistent with female-biased PGC numbers observed in medaka

(Hamaguchi, 1982), zebrafish (Ye et al., 2019) and western mosquitofish, *Gambusia affinis*, (Koya et al., 2003). Correspondingly, the germ cell ablated gonads in zebrafish (Tzung et al., 2015) and medaka (Saito et al., 2007, Nishimura et al., 2018) differentiate to infertile males owing to reduced germ cell numbers. This is also further supported by single PGC transplantation experiments where sterile zebrafish recouped their reproductive competence, however, all the chimeras differentiated to functional males (Saito et al., 2008). The pattern of PGC proliferation in *G. holbrooki* may be similar to goldfish, *Carassius auratus*, where germ cells and their number do not underpin sex differentiation, as germ cell-null gonads developed either seminiferous tubules or an ovarian cavity (Goto et al., 2012).

The diverse sex determination routes in teleosts may cause sex-biased PGC proliferation. This suggests that the PGC proliferation events are underpinned by stable sex determination mechanisms, *e.g.*, medaka (Nishimura et al., 2018). Alternatively, in the absence of a robust sex determination strategy (*e.g.*, zebrafish), the germ cells with feminising/masculinizing effects dictate their sexual preference to the gonadosoma environment via the number the homed cells. This may explain the mechanism leading to agametic male differentiation in germ cell-null zebrafish (Houwing et al., 2007). However, this pattern (*i.e.*, sex-dimorphic number of PGCs) was not observed in *G. holbrooki* suggesting germ cells may not dictate a sexual identity to gonad primordia by their pattern of proliferation. Nevertheless, screening early differentiation of gonad lacking germ cells could confirm the role of germ cells in sex differentiation of *G. holbrooki*.

5.4.2. Morphology and clustering of germ cells is sex-dimorphic in undifferentiated gonad

In this study two types of proliferation were observed among undifferentiated germ cells in foetal gonads of *G. holbrooki*. First, type I mitosis germ cells were characterised in both presumptive testis and ovary, resembling quiescent stem cell-like division in medaka (Nishimura and Tanaka, 2014). Later, at mid-pharyngula, presumptive ovary (*i.e.*, genetic females) underwent type II mitosis, known as gametogenesis-committed division (Saito et al., 2007) and attributed to enter to meiosis stage as the earliest morphological sign of ovary differentiation in medaka. In contrast, germ cells in presumptive testis (*i.e.*, in genetic males), retained self-renewal division (*i.e.*, individual germ cells in testis unlike cradles containing interconnected daughter cells in ovary) through slow mitosis, resembling gonial stem cell expansion in teleostean early gonad (Strüssmann and Nakamura, 2002, Kobayashi et al., 2004, Nagahama, 2005, Pan et al., 2017). Collectively, the pattern of germ cell proliferation, their arrangement and timing in *G. holbrooki* was shown to be comparable with those of medaka (Saito et al., 2007, Nishimura et al., 2015), although the pattern of colonised PGCs were not numerically sex-dimorphic.

The first sex-dimorphic feature of gonad in *G. holbrooki* was postponed to the mid-pharyngula stage evident from a higher germ cell number in genetic females. Indeed, accelerated mitosis in the

presumptive ovary served as an early indicator of sex differentiation and the putative sex in *G. holbrooki*. This feature occurred before the germ cells exhibited any morphological differentiation. This is comparable with germ cell proliferation in the early gonads of medaka (Morinaga et al., 2004, Nishimura et al., 2015) and three-spined stickleback (Lewis et al., 2008). In zebrafish, germ cell population and size of the presumptive gonad is underpinned by the number of colonised PGCs (Ye et al., 2019), whereas in *G. holbrooki*, presumptive gonads with undifferentiated germ cells are comparable in both sexes, until mid-pharyngula.

5.4.3. Ovarian meiosis in *G. holbrooki* occurs earlier than most teleosts

A clearer indication of sex differentiation in *G. holbrooki* was observed right before parturition, marked by meiotic oocytes in genetic females versus stem cell-like gonial clusters in males. In teleosts, the onset of gonad differentiation is likely to vary among orders ranging from immediately after hatching/parturition in some to an extension into the juvenile phase in others. In egg layers such as the Japanese medaka, female germ cells undergo meiosis prophase right after hatching where the embryos dissolve the inner layers of the chorion and move the body (Satoh and Egami, 1972). In *Oncorhynchus mykiss*, sex differentiation is observed 16-29 dph right after complete yolk sac absorption and the beginning of oral feeding (van den Hurk and Slof, 1981). In contrast, in *Cyprinus carpio* this is postponed to the juvenile stage (Komen et al., 1992). In the live-bearing related species, *G. affinis*, ovarian differentiation is reported to occur 2 days before parturition (Koya et al., 2003), however, in *Zoarces viviparus* (Rasmussen et al., 2006) and *Poecilia reticulata* (Takahashi, 1975) sex differentiation is delayed until the onset of the juvenile phase, 12-18 days after hatching/parturition. Similar to *G affinis*, gonad differentiation in *G. holbrooki* occurred before parturition, which is one of the earliest among the studied teleosts. This may assist the reproductive system with a swift transition to gametogenesis, with accelerated and early offspring production.

5.4.4. *G. holbrooki* is a primary gonochorist

As demonstrated, sex differentiation in *G. holbrooki* occurs with a primary gonochoristic mechanism where genetic females develop primary oocytes while males, in comparative developmental stages, show clusters of spermatogonial stem cells in the testis. Contrastingly, the closely related species including *G. affinis* (Koya et al., 2003) and *P. reticulata* (Goodrich et al., 1934, Dildine, 1936) are known to exhibit secondary gonochorism, *i.e.*, all offspring initially differentiate as females before acquisition of their sexual fate. This implies a plasticity in sex differentiation mechanisms among poeciliids. For instance, in *G. affinis*, all prenatal embryos develop an ovary-like gonad with meiotic oocytes right before parturition indicating a juvenile hermaphroditism (Koya et al., 2003). However, the proportion of oocytes to gonial stem cells are not congruent assuming the presumptive gonad with higher number of oocytes differentiate to ovary and the ones with a higher number of gonial stem cells

differentiate to testis (Koya et al., 2003). This suggests evolutionarily related species (*e.g.*, *G. holbrooki* and *G. affinis*) may recruit diverse sex determination mechanisms (Charlesworth, 2018, Kottler et al., 2020) that are also later mirrored in different patterns of their gonad differentiation.

5.4.5. Temporal expression of gonadosoma markers could assist in tuning sex reversal practices

The strong expression of *foxl2* at the onset of ovarian differentiation along with its severe repression in testis of *G. holbrooki* suggests its role as an ovarian differentiating factor, as is also known to occur in other taxa (Bertho et al., 2016). In teleosts, within taxa differences of *foxl2* expression patterns are likely synchronised with ovarian differentiation. Similar to *G. holbrooki*, *foxl2* in newly free-swimming rainbow trout is highly expressed in undifferentiated gonad of genetic females but at very low levels in males (Baron et al., 2004). In medaka, its expression was first detected right after hatching only in XX, but not in XY gonads (Nakamoto et al., 2006). Contrastingly, in mice, *Foxl2* expression is first detected in newly differentiated ovary and its inactivation during foetal development does not affect gonad differentiation. However, it is later necessary for gonadosoma differentiation and ovary maintenance (Schmidt et al., 2004). This suggests *Foxl2* expression is a cause, but not an effect, of early gonad differentiation in models with a robust sex determination mechanism. Whereas, in teleosts with malleable sex determination systems, *e.g.*, Nile tilapia (Nivelle et al., 2019), *foxl2* mutation causes female-to-male sex reversal (Zhang et al., 2017). Therefore, a loss-of-function study of *foxl2* in poeciliids with reproductive relatedness to mammals and teleosts may reveal new/evolutionary aspects of its regulatory functions in sex differentiation and gonad maintenance.

The positively correlated *foxl2* and *cyp19a1a* expression in *G. holbrooki* supports their role in ovarian differentiation as also is known to occur in other fish species. For instance, in medaka, *foxl2* is co-expressed with *cyp19a1a* surrounding germ cells, at ten days post-hatching, with the former expressed stronger and more widely throughout the juvenile ovary (Nakamoto et al., 2006). Inferred from its role in early gonad of *Oreochromis niloticus*, *foxl2* is known to function upstream of ovarian aromatase by enhancing Ad4BP/SF activity, a transcription factor which regulates *cytochrome P450* genes (Morohashi and Omura, 1996, Wang et al., 2007).

A negative correlation between the expression of *foxl2* and *dmrt1* in *G. holbrooki* gonads, suggests sexual phenotype of gonads is continuously maintained via tuning gonadosoma markers as observed among taxa (Georges et al., 2014, Huang et al., 2017). Correspondingly, repressing *Foxl2* in adult mice results in expression of Sertoli cell markers, specifically *Dmrt1*, in granulosa cells, eventuating in the appearance of structures resembling seminiferous tubules in ovary (Uhlenhaut et al., 2009).

Both patterns of non- and maternal inheritance of *cyp19a1a* have been characterised for its ontogenic expression among teleosts. The former pattern was observed in medaka (Patil and Gunasekera, 2008)

and Murray rainbowfish, *Melanotaenia fluviatilis* (Shanthanagouda et al., 2012), while, in *G. holbrooki* (data not shown), common carp (Barney et al., 2008) and zebrafish (Trant et al., 2001, Sawyer et al., 2006) the maternally inherited and zygotic transcripts of *cyp19a1a* are detectible in ova and primary stages of embryonic development. Moreover, the sex-dimorphic expression surge of *cyp19a1a* in *G. holbrooki* parturating embryos coincided with the onset of meiosis in the early ovary and its sexual phenotype acquisition. This is compatible with the dominant imprint of *cyp19a1a*, on sex differentiation pathways in medaka (Patil and Gunasekera, 2008) and zebrafish (Lau et al., 2016). Integral to estrogen biogenesis, in hermaphrodite models, the change in regulation of *cyp19a1a*, in the process of sex reversal (Wong et al., 2006) implies the key regulatory role of ovarian differentiation in vertebrates (Lau et al., 2016). Therefore, in practice, with the production of an all-female population of *G. holbrooki*, the oestrogenic compounds may need to be delivered to developing embryos in this critical window, *i.e.*, administered indirectly via gravid females, to achieve a stable and efficient result. On the other hand, the strong (male-biased) expression of gonadosoma markers, *dmrt1* and *amh*, was detected in juvenile males, concurrent with the onset of meiosis in the testis (see Chapter 4). This suggests the *G. holbrooki* testis may retain its sexual plasticity post-parturition (Patil et al., 2020) and effective masculinisation can be postponed to the post-natal stage, as is effective for *P. sphenops* (Baron et al., 2002).

The expression of *dmrt1* in pre- and post-natal genetic females of *G. holbrooki* coincided with the onset of meiosis, in agreement with those of female zebrafish, where *dmrt1* expression was found in different stages of oogenesis including primary and vitellogenic oocytes (Guo et al., 2005). The *dmrt1* may not be a sex determining gene, however, its sex-dimorphic expression pattern serves as an indicator for early detection of sex in *G. holbrooki*. Similarly, in zebrafish, the expression level of *dmrt1* in bi-potential gonads is an early marker for identification of sexual phenotype (Webster et al., 2017). In contrast, the autosomal *dmrt1* expression in medaka, with a stable sex mechanism system, begins 20 days post-fertilisation (Nanda et al., 2002) and its ovarian expression is restricted to mitotic oogonia (Winkler et al., 2004). Regardless, ablation of *dmrt1* may cause sex reversal in genetic males to functional females in *G. holbrooki*. Such sex reversal following the lack of *dmrt1* in a medaka mutant line resulted in a developing functional ovary in XY individuals (Masuyama et al., 2012).

Two patterns for spatial expression of *dmrt1* have been characterised in teleosts. In zebrafish (Webster et al., 2017) and *X. maculatus* (Veith et al., 2006), 1) *dmrt1* signals were detected in both germline and Sertoli cells, 2) while in medaka it is restricted to gonadosoma (Masuyama et al., 2012). The former pattern which shows the potency of germline to express *dmrt1* may support the accumulation of its transcripts in ova with subsequent expression during early embryonic development (*i.e.*, expressed in PGCs), as occurs in *G. holbrooki*.

5.4.6. Development of single-lobed gonad in *G. holbrooki* is not a sex-biased decision

As observed in *G. holbrooki*, poeciliids initially develop gonads as a bi-lobular organ, however, the lobes are fused later at the post-natal stage and form an integrated organ (Greven, 2011). This morphological transformation may have evolved to support viviparity in some poeciliids, integrating two organs into one; the ovary to produce gametes and the uterus as a placental supported nursery. Nevertheless, the morphological details of gonad formation are not conserved among poeciliids. For example, the lobes of post-natal gonads are totally fused in *Poecilia reticulata* (Campuzano-Caballero and Uribe, 2014) and *Tomeurus gracilis* (Parenti et al., 2010) testis, as observed in *G. holbrooki*. In *Poecilia mexicana* the testis develops as paired lobes in adults, however, the lobes are in the closest vicinity with incomplete fusion (Torres-Martinez et al., 2019). Although gonad lobe fusion may be an evolutionary adaptation for formation of uterus and *in vivo* gestation in females, its occurrence in poeciliid males is intriguing. This, however, may suggest early gonadogenesis machinery prior to sex differentiation is shared between the sexes. This pattern of early gonadogenesis permits potential sex differentiation plasticity and their function.

5.5. Conclusion

In conclusion, the study shows that sex differentiation in *G. holbrooki* follows that of a primary gonochorist, where ovary and testis initially differentiate into distinct organs. This was supported by both the cellular events as well as the expression pattern of key molecular surrogates. The relatively early occurrence of critical gonadogenesis events such as PGC colonisation (*i.e.*, at the late segmentation stage), sex-dimorphic pattern of gonadosoma markers and early acquisition of sexual phenotype and ovarian maturation in *G. holbrooki* reflect its rapid reproductive capability and underpin its invasive capacity (McLeod, 2004). Unlike other teleosts, which maintain their fertility throughout adult life, the poeciliids undergo reproductive senescence (Reznick et al., 2006, Croft et al., 2015) similar to menopause in mammals. Therefore, the early sex differentiation (prior to parturition) may serve to mitigate mid-life fertility loss in *G. holbrooki*, as may also occur in other poeciliids. Understanding these may provide a lead to identify genetic susceptibilities that may be exploited to engineer disruptive technologies to suppress their reproduction and hence invasive capability. For example, knock-down of *dmrt1* in medaka (Masuyama et al., 2012) and *cyp19a1a* in Nile tilapia (Zhang et al., 2017) have been successfully used to manipulate the sex ratio. More broadly, the outcomes of this study are of relevance to enhancing our comparative knowledge of vertebrate reproductive development. The future studies can focus on other gonadosoma markers including *ftzf1* and *sox9b* to reveal their role on gonadosoma formation and reproductive performance of teleost.

Chapter VI

Conclusion and future directions

Chapter 6 | Conclusion and future directions

This study first reviewed modes of PGC development and their evolutionary relatedness among taxa, as well as the key markers involved in germline determination and maintenance of teleosts (Chapter 1). It subsequently cloned and characterised the select teleostean PGC markers in *G. holbrooki* (Chapter 2) and evaluated the pattern of their emergence and migration *en route* the genital ridge (Chapter 3). Moreover, the accumulation of Gp markers and their biogenesis in foetal and post-natal gonads of *G. holbrooki* were studied (Chapter 4). Finally, the pattern of gonad formation and expression of gonadosoma markers leading up to sex differentiation of early gonads (Chapter 5) were investigated. This study also reported the presence of Gp factors in mature spermatozoa (Chapter 4), first in teleosts. The relevance of these findings to basic biology, management of pest populations as well as utility of the species for biomedical research are discussed.

6.1. The germline determination modes may need redefining.

The common approach to define and discriminate the different mechanisms of metazoan germ cell development is based on different PGC specification (sequestration) strategies; early maternal messaging in preformation versus fully zygotic programming generally known as epigenesis mode. This study, for the first time, revealed Gp markers are detectable in mature spermatozoa presumed to be delivered to ova during fertilisation and probably involved in early PGC formation. Therefore, a better definition based on the origin of germ cell determination signals, could be “parental” and “zygotic” PGC specification modes. However, this may require comparative studies and validation in other vertebrate taxa. Although there appears to be existing evidence for packaging of germline markers in human spermatozoa (Lin et al., 2002), other (non-germ cell) paternal transcripts have shown their impact on early development (Gross et al., 2019) and offspring health (Sharma, 2019) in higher vertebrates. Therefore, in the light of the classification that involves paternal factors in germline determination, research groups may find the “paternal contribution in PGC specification” topic interesting and worth noting.

Unlike the common notion that preformation mode is independent of epigenetic regulation, the transcription of maternal factors in ooplasm (Jiang et al., 2013) and the zygotic expression of zebrafish PGC markers including *vasa, dazl1* and *piwi* (Gustafson and Wessel, 2010, Lindeman et al., 2010, Potok et al., 2013) are regulated as a result of epigenetic control. Therefore, the current classification of PGC specification which discriminates modes based on epigenetic control may be misleading. It was also shown, in *G. holbrooki*, (whose ova accumulates high amounts of Gp factors), that an expression surge in PGC markers at the gastrula stage may have epigenetic origin. Together, *G. holbrooki* may display

more aspects of transition from preformation to induction mode for PGC specification, as it showed many evolving developmental traits that are aligned with higher vertebrates. An alternative classification that considers the totipotency status of nascent PGCs may distinguish animals into three groups; *i.e.*, those with PGCs that 1) lack totipotency (*e.g., Danio*, *C. elegans* and *Drosophila*), 2) possess early embryonic totipotency (*e.g.*, mice and Urodeles) and 3) retain totipotency for life, *i.e.*, cells capable of being specified to any cells including PGC throughout the lifespan even at adulthood (Whittle and Extavour, 2017), such as in tunicates (Rosner et al., 2009) and echinoderms (Rosner et al., 2009). Indeed, the timing of MZT determines which key mechanism (*i.e.*, zygotic/epigenetic resulting from early MZT or maternal acquired with delayed MZT) dictates early germline specification. Therefore, the indicative early timing of MZT, *i.e.*, earlier than the mid-blastula stage in *G. holbrooki* than those of zebrafish, may suggest the parental PGC signals are attenuated, so the cells may acquire temporary totipotency (*i.e.*, as observed in mice) in early embryonic development, right after MZT. This suggests an intermediatory/transitioning of PGC specification mode in *G. holbrooki* which may occur in other poeciliid species, as is consistent with their evolutionary node.

6.2. Relevance to manipulate reproduction and genetic control of *G. holbrooki* pest populations.

Invasive species cause severe losses in economic productivity and local biodiversity (McLeod, 2004, Marbuah et al., 2014). The concept of introducing a natural competitor or predator as a bio-control agent against pest species has been shown to work (DeBach and Rosen, 1991, Lloyd et al., 1986) but can be disastrous, since the ecology and life cycle of the introduced species may not be fully considered before its introduction, nor its interaction with the target species. In the case of *G. holbrooki*, the intentional introduction to Australia of this alien species for control of mosquito larvae had adverse effects (Macdonald and Tonkin, 2008, Macdonald et al., 2012) such as competing with native fishes and amphibians, and predating the eggs and larvae (Milton and Arthington, 1983, Courtenay Jr and Meffe, 1989). This has led to naturalisation of mosquitofish and in turn extinction of endemic populations (Macdonald et al., 2012). Various biological, mechanical and chemical approaches established to control aquatic invasive species have not been useful to control *Gambusia* or showed little success (Davies, 2012). However, genetic solutions to control the fertility and/or sex ratio of commercial (Piferrer, 2001, Komen and Thorgaard, 2007, Piferrer et al., 2009) and invasive species (Schliekelman et al., 2005, Thresher et al., 2013, Wang et al., 2014, Thresher et al., 2004) including *G. holbrooki* (Patil, 2012) have been suggested. While the genetic approaches such as the Trojan chromosome (Trojan C) which includes Trojan Y (Wang et al., 2014) and W (Patil et al., 2020), are more readily adoptable, they lack the necessary introgression rates to effect control at the required efficiency, particularly at continental scales, as applies to Australia. By virtue of recent advances in recombinant techniques, manipulation of the reproductive system could be carried out with greater precision and be engineered to introgress more rapidly into populations (Germini et al., 2018, Ling et al., 2020) as also has been

suggested for *G. holbrooki* (Patil, 2012). Indeed, germ cell ablation (Su et al., 2014, Wong and Zohar, 2015), conditional suppression of sexual maturity regulated by exogenous chemicals (Su et al., 2015), gonadosoma markers (Lau et al., 2016) or environmental parameters (Li et al., 2017) are examples of approaches to population confinement through underpinning control of reproduction (Thresher et al., 2009). Predominantly, the PGC markers, *e.g., dazl*, *dnd* and *piwi II*, and those involved in gonad differentiation such as *cyp19a1a* (Barney et al., 2008) are the functional targets to produce viable sterile lines in fish models. For instance, downregulation of maternal Dazl during medaka embryonic development abolished PGC formation without any somatic abnormalities (Li et al., 2016). In zebrafish, the *ziwi* (piRNA-associated protein in zebrafish) homozygous mutant lines are viable, however, the adults are phenotypically male and agametic (Houwing et al., 2007, Houwing, 2009). However, many of these targets exhibit species-specific diversities, manipulation of which could have unintended consequences (Patil, 2012). Hence a detailed understanding of their functional role in target species is essential. In this regard, this study, first cloned and characterised target genes that have been shown to be indispensable in germline determination and sex differentiation among sexually reproducing animals. Indeed, they included the Gp markers involved in PGC specification and their proper homing during prenatal stages, and the gonadosoma markers that determine the sexual fate of early gonad as well as maintaining sexual identity throughout life. These resources (Chapter 2) formed a basis for investigating the functional domains (Chapter 3) and their inferred role and potential for manipulating sex ratios (*i.e.*, sterility and sex reversal) in this species.

The observation that some genes were not exclusively expressed in *G. holbrooki* PGCs (Chapter 3), is similar to those known in other taxa. For instance, *nanos1* transcripts, a Gp marker and a universal PGC specifier in *Drosophila* (Wang and Lehmann, 1991), *C. elegans* (Subramaniam and Seydoux, 1999), *Danio* (Koprunner et al., 2001) and *Xenopus* (Lai et al., 2012) was not maternally inherited in *G. holbrooki* and its embryonic expression was only detected in soma (see Chapter 3). Interestingly, the characterised *nanos1* in *G. holbrooki* encoded a C-terminal CCHCCCHC zinc-finger domain, which is essential for translational regulation of germline among taxa. However, the spatial expression domain of *nanos1* in foetal *G. holbrooki* was comparable with those reported in mice (Haraguchi et al., 2003). Similarly, *dnd*, a germline-specific master regulator in animal models (Weidinger et al., 2003, Slanchev et al., 2009, Aguero et al., 2017), was shown not to be PGC-specific in prenatal *G. holbrooki*, either. Interestingly, this encoded alternative splice variants with tissue-dimorphic expression pattern during embryonic development. Similar to other DND orthologues, both variants conserved their critical domains, RNA recognition motif and double-stranded RNA motif, the components for Dnd post-transcriptional functions. Taken together, the spatial expression of teleost PGC markers in *G. holbrooki* showed the common germline ablation targets used in other fish models (*e.g., nanos1, dazl* and *piwi*) may cause somatic effects which can be fatal as observed in some mouse strains with *Ter (i.e.,* lacking functional *Dnd*) mutation (Bhattacharya et al., 2007). Instead, the markers exclusively expressed in

PGCs (*e.g.*, *dnd-α* and *vasa*) are recommended as potential targets or enablers of genetic mechanisms to ablate germ cell precursors in *G. holbrooki*. Future studies could also investigate global PGC transcriptome, by sorting PGC and the application of single cell transcriptomics to characterise additional germline-specific markers in *G. holbrooki* with sex-specific expression patterns in early development. In parallel, the indispensability of the germline markers characterised in this study, needs validating through loss- or gain-of-function assays including generating knockout or knockdown lines that could yield greater insights for PGC development and utility of the markers for sex manipulation in G *holbrooki*. Nevertheless, it is worth noting that many conventional gene delivery strategies including embryo microinjection or biolistics applied for genetic transformation of egg laying teleosts, are inadequate due to internal fertilization and embryonic development in *G. holbrooki*. Here the access to embryos is somewhat restricted compared to egg laying models (Vielkind et al., 1973, Sarmasik et al., 2001). Therefore, a protocol to optimise functional gene delivery would be a prerequisite for future genome manipulation strategies in *G. holbrooki* with further application in other viviparous models.

The basic biological chronology including timing of germ cell colonisation at presumptive gonad anlage, early gonad formation, the onset of mitotic and meiotic proliferation of germ cells, sex differentiation in both gonads, and the expression dynamics of sex-biased gonadosoma markers during pre- and post-natal gonad function are expected to assist further sex control programs that are *G. holbrooki* specific. Sex reversal techniques have been used to control reproduction with application in food production, environmental management, and disease control. Relatively, sex ratio distortion has been of interest as a powerful tool to control feral populations and shown promising results *in silico* (Prowse et al., 2017) and *in vivo* (Galizi et al., 2014, Facchinelli et al., 2019). The feasibility of sex ratio manipulation has been shown in teleosts (Piferrer, 2001, Baroiller and D'Cotta, 2016) owing to their diverse sex determining mechanisms and sex differentiation plasticity (Devlin and Nagahama, 2002). However, effective sex reversal protocols require knowledge about gonadogenesis and sex differentiation, in the species of interest. For instance, an efficient sex reversal is induced in a critical window when the presumptive gonad is in its neutral status; before the onset of sex differentiation (Piferrer, 2001). To address this, the morphological changes of presumptive gonad in *G. holbrooki* were first evaluated based on their genetic sex. Then, the sex differentiation time point in both sexes was ascertained and the expression pattern of sex-biased markers involved in gonadosoma determination confirmed the morphological observation (Chapter 5). Three distinctive approaches have been so far introduced for sex reversal protocols; endocrinal manipulation of gonad differentiation through 1) treating larvae with exogenous steroids (Razmi et al., 2011, Gennotte et al., 2015), 2) steroid enzyme inhibitors (Goppert et al., 2016, Schroeder et al., 2017) and steroid receptor antagonists (Pham and Arukwe, 2013) and 3) gonadosoma marker ablation through genome editing (Lau et al., 2016) or morpholino-mediated techniques (Griffin et al., 2013). Taken together, this study provides knowledge

and reagents necessary to establish future sex ratio manipulation protocols in *G. holbrooki* with specific application in control of invasive populations.

6.3. The potency of poeciliids as reproductive research model

Over the past decades, many aspects of germ cell development have been understood using fish models. For example, owing to the technical advantages of zebrafish as a research model (*e.g.*, abundant embryos in a single clutch, optical transparency of embryonic development and established protocols to generate transgenic lines) and their high similarity with the human genome (*e.g.*., ~70% of human genes have at least one ortholog in the zebrafish genome), they are a powerful model to understand the genetics of human disease (Howe et al., 2013). Moreover, the potency of large-scale mutagenesis provides an opportunity to characterise the genes that regulate development in vertebrates (Mullins et al., 1994) or cause human disease (Bradford et al., 2017). However, comparative studies using more diverse systems may help expand insight into new aspects of early development including PGC determination, with greater insights for medical applications. The poeciliid species with astonishing reproductive adaptations, *e.g.*, different stages of ovi-viviparity, matrotrophy and superfetation, exhibit an evolutionary shift towards mammalian reproduction and are therefore of great interest. Indeed, viviparity is assumed to be an evolved trait from oviparity status, and in poeciliids this has begun with transition from external to internal fertilisation. In line with this, simultaneous placenta acquisition and yolk retention in viviparous poeciliids may represent a shared aspect of the evolutionary shift in reproduction, from teleostean to mammalian mode. Evident from the accumulation of Gp components in ova and spermatozoa, germline specification in *G. holbrooki* is inferred to rely on the preformation mode. This is shared with other teleosts (Saito et al., 2006) as Gp markers were detected early in embryogenesis of *G. holbrooki*, *i.e.*, prior to the gastrula stage, unlike those with induction mode (Ying et al., 2002, Kurimoto et al., 2008), where PGC markers are not detectible in pluripotent cells of organisms. The features of germline determination are also expected to show an evolutionary shift towards higher vertebrates, as was indicated by the similar expression pattern of *dnd-β* and *nanos1* (Chapter 3), that more closely resembled that of mice (Haraguchi et al., 2003, Youngren et al., 2005) than teleosts. Further, the spatio-temporal role of which parental factors underpins germline specificity and when they likely switch to being regulated by MZT are quite interesting questions to follow up. For example, the early occurrence of MZT in *G. holbrooki i.e.*, based on the expression pattern of purely zygotic genes (Chapter 3) may restrict the parental control of early PGC formation and in part resemble those of the induction mode. Further studies could tease this apart via accurate evaluation of MZT in *G. holbrooki* using advanced single cell omic assays.

The onset of solely zygotically expressed genes also revealed the timing of zygotic activation in *G. holbrooki*, which occurs earlier than those of zebrafish (Kane and Kimmel, 1993, Jukam et al., 2017), showing a shift towards those of mammalian models. Furthermore, the expression pattern of PGC

markers in mice such as dual expression (germline and soma) of *Piwi* genes and restricted expression of *Nanos1* in soma, and *Dnd* alternative splicing with a tissue dimorphic pattern was also observed in *G. holbrooki*. Collectively, this study revealed the dynamic expression of genes which underpin germline determination of *G. holbrooki* is in agreement with the evolutionary path from teleosts to those of mammalian modes.

The previous studies (reviewed in Chapter 1) demonstrated that zebrafish is not a comprehensive model to delineate germ cell specification and maintenance, in teleosts. Although zebrafish is by far the most well-known fish species in medical research, it may not be a fully descriptive model for human reproductive biology due to an as yet unknown sex determination mechanism, malleable sex differentiation pathway, oviparity and comparatively rapid embryonic development. Instead, fish models such as *G. holbrooki* that more closely resemble mammalian reproductive traits and germline determination including shared placentation and viviparity may help fill the knowledge gap and facilitate finer delineation of key questions in reproductive development and their applications. The poeciliid species also make good research models due to having a short life cycle, easy breeding in captivity, continuous spawning, producing abundant offspring, and easy housing. Moreover, as there are some likely evidences of post-natal oogenesis in human (Virant-Klun, 2015), developing a model with a high reproductive similarity as well as competence for continuous gonial regeneration may assist to address human reproductive disorders and infertility, more accurately.

Appendices

Table A1: The components of dephosphorylation reaction

reagent	Volume	final concentration
RNA	x µl	1-5 µg
RNase inhibitor (40U/µl)	1 µl	4U/ µl
CIP (10U/µl)	1 µl	1U/ µl
10X CIP buffer	1 µl	1X/ µl
DEPC treated water	y µl	---
Total volume	10 µl	---

Table A2: The components of decapping reaction

reagent	Volume	final concentration
Dephosphorylated RNA	x µl	---
RNase inhibitor (40U/µl)	1 µl	4U/ µl
TAP (0.5U/µl)	1 µl	0.05U/ µl
10X TAP buffer	1 µl	1X/ µl
Total volume	10 µl	---

Table A3: The components of ligation reaction

reagent	Volume	final concentration
Decapped RNA	6 µl	---
RNA oligo	0.25 µg	
10mM ATP	1 µl	1 mM
RNase inhibitor (40U/µl)	1 µl	4U/ µl
T4 RNA ligase (5U/µl)	1 µl	0.5U/ µl
10X ligase buffer	1 µl	1X/ µl
Total volume	10 µl	---

Table A4: The components of reverse transcription reaction

reagent	Volume	final concentration
The sample mix	12 µl	---
DEPC water	2 µl	---
RNase inhibitor (40U/µl)	1 µl	2U/ µl
AMV RT (15U/µl)	1 µl	<1U/ µl
5X RT buffer	4 µl	1X/ µl
Total volume	20 µl	---

Table A5. Cycling condition of TD-PCR amplifying cDNA ends

step	temperature	duration	Cycle(s)	comments
Activation	95˚C	1 min	1	
Denaturation	95 ˚C	10 sec		X: The primers' melting temperature
Annealing	X+4˚C	30 sec	5	
Extension	72˚C	N min		
Denaturation	95˚C	10 sec		N: extension time for Taq DNA
Annealing	X+2˚C	30 sec	5	Polymerase is 1 min/kb of PCR amplicon
Extension	72˚C	N min		
Denaturation	95˚C	10 sec		
Annealing	X˚C	30 sec	19-23	
Extension	72˚C	N min		
Polishing	72˚C	7 min	1	

Table A6: TOPO cloning reaction

reagent	amount	final concentration
Purified PCR product	0.5-2 µl	100 ng
Salt solution	0.5 µl	---
TOPO vector	0.5 µl	5 ng
DEPC water	0-1.5 µl	---
Total volume	3 µl	---

Table A7: List of the accession numbers used to generate phylogenetic trees (Chapter 2)

Genes	Species	Accession number
dazl	*A. mississippiensis* (American alligator)	XP_019353289.1
	C. milii (elephant shark)	XP_007895787.1
	D. rerio (zebrafish)	XP_005170128.1
	G. gallus (chicken)	XP_040530136.1
	H. sapiens (human)	NP_001342.2
	O. aureus (blue tilapia)	XP_031611939.1
	O. latipes (Japanese medaka)	XP_020562531.1
	O. mykiss (rainbow trout)	NC_034190.2
	O. niloticus (Nile tilapia)	NC_031985.2
	P. latipinna (sailfin molly)	XP_032237565.1
	P. mexicana (shortfin molly)	XP_014852183.1
	P. reticulata (guppy)	NC_024341.1
	S. aurata (gilt-head bream)	XP_030268756.1
	S. salar (Atlantic salmon)	NC_027313.1
	X. maculatus (southern platyfish)	XP_023201124.1
dnd	*A. mississippiensis* (American alligator)	XP_014462031.1
	C. milii (elephant shark)	XP_042196039.1
	D. rerio (zebrafish)	NP_997960.1
	G. gallus (chicken)	XP_040502984.1
	H. sapiens (human)	NP_919225.1
	O. aureus (blue tilapia)	XP_003454336.1
	O. latipes (Japanese medaka)	NP_001157988.1
	O. mykiss (rainbow trout)	XP_036798542.1
	O. niloticus (Nile tilapia)	XP_003454336.1
	P. latipinna (sailfin molly)	XP_014878700.1
	P. mexicana (shortfin molly)	XP_014833068.1
	P. reticulata (guppy)	XP_008418204.1
	S. aurata (gilt-head bream)	XP_030251554.1
	S. salar (Atlantic salmon)	XP_014054901.1
	X. maculatus (southern platyfish)	XP_014330631.1
	X. hellerii (green swordtail)	XP_032411603.1
nanos1	*A. mississippiensis* (American alligator)	XP_014330631.1
	C. milii (elephant shark)	XP_007901835.2
	D. rerio (zebrafish)	NP_571953.1
	G. gallus (chicken)	XP_040558832.1
	*M. musculus (*house mouse*)*	NP_848508.2
	O. aureus (blue tilapia)	XP_031597929.1
	O. latipes (Japanese medaka)	NP_001116380.1
	O. mykiss (rainbow trout)	NC_048581.1
	O. niloticus (Nile tilapia)	NC_048590.1
	P. latipinna (sailfin molly)	XP_014913479.1
	P. mexicana (shortfin molly)	NC_031701.1
	P. reticulata (guppy)	NC_006477.3
	X. maculatus (southern platyfish)	NC_045692.1
	X. hellerii (green swordtail)	NC_045690.1

Table A7: Continued

Genes	Species	Accession number
piwi II	*A. mississippiensis* (American alligator)	XP_019347077.1
	C. milii (elephant shark)	XP_007905583.1
	D. rerio (zebrafish)	XP_021331982.1
	G. gallus (chicken)	XP_040545319.1
	H. sapiens (human)	NP_060538.2
	O. aureus (blue tilapia)	XP_031599504.1
	O. latipes (Japanese medaka)	XP_031599504.1
	O. mykiss (rainbow trout)	NC_050119.1
	O. niloticus (Nile tilapia)	XP_003445710.1
	P. latipinna (sailfin molly)	XP_014883055.1
	P. mexicana (shortfin molly)	XP_014861471.1
	P. reticulata (guppy)	XP_008415818.1
	S. aurata (gilt-head bream)	XP_030274002.1
	S. salar (Atlantic salmon)	NC_027323.1
	X. maculatus (southern platyfish)	XP_023199065.1
vasa	*A. mississippiensis* (American alligator)	XP_019351537.1
	C. carpio (common carp)	NP_077726.1
	D. rerio (zebrafish)	XP_021334777.1
	G. gallus (chicken)	NP_990039.2
	H. sapiens (human)	NP_077726.1
	O. aureus (blue tilapia)	XP_039463392.1
	O. latipes (Japanese medaka)	XP_023817010.1
	O. mykiss (rainbow trout)	XP_021456918.2
	O. niloticus (Nile tilapia)	XP_019214006.1
	P. latipinna (sailfin molly)	NP_077726.1
	P. mexicana (shortfin molly)	NP_077726.1
	P. reticulata (guppy)	NP_077726.1
	S. aurata (gilt-head bream)	XP_030264921.1
	S. salar (Atlantic salmon)	XP_013998855.1
	X. maculatus (southern platyfish)	XP_023184944.1
	C. milii (elephant shark)	NP_077726.1

Table A8: List of primers used to clone and characterise the target genes of this study

Gene		Primer sequence	Purpose
cxcr4	cxc4-213F	GYCAGTTACTCAGCAGCAACTT	Degenerate
	cxc4-1200R	GAAATCTGCCCGCGCTTTTTG	
	cxc242R-RACE	AGGCCAGGATCAGGACGCTGCTGTACA	RACE
	cxc534F-RACE	GTCCTGCCCGGTCTGGTCATCCTCAT	
	Cxc27F	AACTTTTCATGCTCGACGAAAGC	Exon-intron boundaries
	cxc1665Rp	GCAACTTTCTTAAATCAAGCATAAGCC	
	cxc1123Fp	CAGGAGCACGCTCACAAATAGCA	
dazl	degdazl1F231	AGGGSAYAMTGACSCCCAA	Degenerate
	degdazl1R666	GYTCATCGGCACYYGTGGAW	
	dazl606F-RACE	TGGTTCCTCAGATGCCAATG	RACE
	dazl608R-RACE	CCATCACTCCGCTGAAGCTGCTGTA	
	daz125F	ACCCAGACTGTACCCTCTTTGAAGCTAT	Exon-intron boundaries
	daz225R	ACCTTCATGTCGATCCCACCCACAAA	
	dazl759Rq	GCTTTCAACTACAGCACAGTC	
	daz1058Rp	TGGCTGGTATACCAAATGTGCTCT	
dnd	ghdndF196 deg	ATKAACAAGATGGAAAACAAGTGC	Degenerate
	ghdndR228 deg	GATGGAAAACAAGWGCAGCCAGGTG	
	ghdnd112F	AGAGGAAGTACGGAGGACCACCCGAGG	RACE
	ghdndR66	CCGAGGGATGTGGCTGATGAAGAC	
	ghdnd102F	GTTAACGGGCAGAGGAAGTACGGAG	Exon-intron boundaries
	ghdnd90R	CGTTAACCTGGGTCAGCTTGGTGTTGGT	
	dnd222Rq	ATGAGCAGGTCCTCGTAGGC	
	dnd396R	GGTGTCTCTTCTCCGTGCTGC	
nanos1	deg-ghnanosR489	TTCCGCTCCACACCAAAGAGA	Degenerate
	deg-ghnanos318F	CATCCTAAGCCCGTTCCAAAGCC	
	nos1-724F-RACE	ACTGTCAAAAGACCAGCCATCCCACCG	RACE
	nos93Rq2	CCGTTATTCCGGCAGAACACGCAGATTT	
	nos1-733F	AGACCAGCCATCCCACCGCCCATTAAA	Exon-intron boundaries
	nos1-724R	ACTGTCAAAAGACCAGCCATCCCACCG	
	nos503Fq2(P)	TCGATCTCTTTGGTGTGGAGCGGAAGAT	
Piwi II	deg-piwiII1307F	GTGACHTTTGCATCCCGTTC	Degenerate
	deg-piwiII1847R	GGTGAGATCCTTTTGSTGCC	
	piwiII288F	CGTCAAGAAGGAGAGCTCTGGC	
	piwi675F-RACE	AGGATGCTGGTCACAATGGAG	RACE
	piwi849Rp-RACE	AGGCGGAGACAGCGGGGTTCTTT	
	piwiII1304Fp	TGCCATCTGTACTGGAACTGG	Exon-intron boundaries
	piwiII503F	ACCAGTGAGCCTAATTTGCA	
	piwiII303R	CCGGTGAGATCCTTTTGGTGCCAGAGC	
	pi1460Rq2	ACAGCCCTCCATCTGTGCGCTTAATA	

Table A8: Continued.

Gene		Primer sequence	Purpose
tdrd6	deg-tdrd65015F	GAGCGTGAAGGCCAGGTGATA	Degenerate
	deg-tdrd66249R	TCCTGGACCTCGTCTGACTCTT	
	trd6-713Fq	GAAGGAGACGACGGATACAGAATTGGA	RACE
	trd6-97R-RACE	AGAAGATCTTGTAGAGCGTTGATTG	
	td6RACE886F	TGCCTGTGTAGCTCGTCACCCTGAGAA	
	trd6-820Rq	TCTCCAGCCTCAGTTTCCTGCTCAC	Exon-intron boundaries
	trd6RACE881F	GGTCGTGGCCTGCTCTTTGGAAGAAAC	
	trd6-1781R	GCCACGACCTGAGGATCCTCACC	
vasa	deg-ghvasaF364	TGTACAAGTCACCAAGTTCTCCAAGAGG	Degenerate
	deg-ghvasaR158	GAAAGTTCCAACCACCAGCATCCATG	
	ghvasaR31-RACE	GCAGACTTCATCGCTGTGTTCTTGTGCC	RACE
	ghvasaF108-RACE	TTCATCGCTGTGTTCTTGTGCCAGGAGA	
	vasa-79R(p)	ATGTCCAACATCCGGTCGGCCTCGTC	Exon-intron boundaries
	vasa428Rq2	CCTCCTCTTCCTCCCTGTTCAGCATCT	
	vasa342Fq2	TGAGAATGGATTCAGAGGGCGAGGAAGA	

The marked (red) degenerate nucleotides are presented based on IUPAC system or nucleotide nomenclature.

Table A9: Spatio-temporal expression of PGC-specific markers at select embryonic stages of *G. holbrooki*.

Genes	Spatio-temporal Expression		Ovum	Cleavage	Blastula	Gastrula	Early somitogenesis	Late somitogenesis	Figures
vasa	Qualitative		---	- Tiny spots in blastomere (1A).	- Four clusters at the periphery of the blastodisc (1D).	- Two clusters at the margin of dome (1E and 1F).	- Posteriorly, at migrating PGC clusters (1G).	- PGR (1I)	1 & 2B
	Quantitative	Between stages	-1.0 ± 1.0	-0.94 ± 0.75	-0.28 ± 1.06	+0.14 ± 1.26	-3.69 ± 0.91**		5A
		Between sex	---	0.78 ± 0.08 F	2.68 ± 1.02 F *	5.12 ± 1.01 F **	1.53 ± 2.03 F	0.11 ± 0.97 F	5B
dnd-α	Qualitative		---	- Tiny spots in blastomere.	- Four clusters at the periphery of the blastodisc.	- Two clusters at the margin of dome at *vasa*-positive cells (3A).	- Two PGC clusters close to the tail bud (3C).	- PGR (3E)	1, 2B & 3
	Quantitative	Between stages	-1.38 ± 0.66	-0.01 ± 0.52	+2.4 ± 0.81 *	-4.21 ± 0.92 ***	-5.2 ± 0.89 ***		5C
		Between sex	---	0.36 ± 0.73 F	1.70 ± 0.70 M	4.25 ± 0.42 F ***	2.15 ± 0.89 F *	0.52 ± 0.38 F	5D
dnd-β	Qualitative		---	---	---	- Anterior region of the elongating body (3B).	- Both sides of the neural tube (3D).	- Metencephalon and cerebellum (3F).	2B & 3
	Quantitative	Between stages	+6.71 ± 1.27 ***	-0.74 ± 0.61	-2.17 ± 0.61 *	-2.32 ± 0.76 **	-1.95 ± 0.78 *		6A
dazl	Qualitative		---	- Tiny spots in blastomere.	- Four clusters at the periphery of the blastodisc.	- Two clusters at the margin of dome at *vasa*-positive cells.	- Anteriorly, at optic lens and otic vesicles (4A). - Posteriorly, at PGC clusters (4B).	- Otic vesicles - Optic lens - PGR	2B & 4
	Quantitative	Between stages	-0.96 ± 0.28	-0.57 ± 0.39	+0.56 ± 0.53	-4.49 ± 0.70 ***	-3.64 ± 0.75 **		5E
		Between sex	---	0.28 ± 0.38 F	0.02 ± 0.72 M	3.01 ± 0.31 F ***	2.39 ± 0.94 F *	0.01 ± 0.93 M	5F
piwi II	Qualitative		---	---	- Four clusters at the periphery of the blastodisc.	---	- Anteriorly, at diencephalon and mesencephalon (4C). - Posteriorly, at PGC clusters (4D).	- diencephalon and mesencephalon, - PGR	2B & 4
	Quantitative	Between stages	-1.53 ± 0.62	-0.63 ± 0.65	+1.85 ± 0.86 *	-3.9 ± 0.95 F ***	-2.71 ± 0.75 **		5G
		Between sex	---	1.24 ± 0.83 M	0.40 ± 0.65 F	4.09 ± 0.67 F ***	2.5 ± 1.36 F	0.01 ± 0.80 F	5H
nanos1	Qualitative		---	---	---	- A single cluster at the anterior half	- Neural tube (4E) - Otic vesicles (4E)		2B & 4
	Quantitative	Between stages	+7.02 ± 1.27 ***	+2.16 ± 0.7 **	-2.89 ± 0.55 ***	-0.23 ± 0.61	-0.15 ± 0.45		6B

Table A10: The list of MIQE criteria that were met for all qPCR assays.

Item to check		Explanations *
Experimental design	Definition of experimental and control groups	✓
	Number within each group	4 - 12
Sample	Description	✓
	Microdissection or macrodissection	✓
	Processing procedure	✓
	If frozen, how and how quickly?	They were frozen after RNase deactivation
	If fixed, with what and how quickly?	N/A
	Sample storage conditions and duration	✓
Nucleic acid extraction	Procedure and/or instrumentation	✓
	Name of kit and details of any modifications	✓
	Details of DNase or RNase treatment	✓
	Contamination assessment (DNA or RNA)	Agarose gel visualisation and Qbit detection.
	Nucleic acid quantification	✓
	Instrument and method	Column purification method
	RNA integrity: method/instrument	Gel visualisation
	RIN/RQI or Cq of 3 and 5 transcripts	N/A
Reverse transcription	Complete reaction conditions	✓
	Amount of RNA and reaction volume	✓
	Priming oligonucleotide (if using GSP) and concentration	✓
	Reverse transcriptase and concentration	✓
	Temperature and time	✓
qPCR target information	Gene symbol	✓
	Sequence accession number	✓
	Amplicon length	✓
	Location of each primer by exon or intron (if applicable)	Provided in Chapter 2
	What splice variants are targeted?	Only applicable for *dnd*
qPCR oligonucleotides	Primer sequences	✓
	Location and identity of any modifications	N/A
qPCR protocol	Complete reaction conditions	✓
	Reaction volume and amount of cDNA/DNA	✓
	Primer, (probe), Mg^{2+}, and dNTP concentrations	The qPCR mix contained dNTPs, iTaq DNA Polymerase, MgCl2, SYBR® Green I, enhancers, stabilizers, and a blend of passive reference dyes
	Polymerase identity and concentration	✓
	Buffer/kit identity and manufacturer	N/A
	Complete thermocycling parameters	✓
	Manufacturer of qPCR instrument	CFX96 Touch Real-Time PCR Detection System (Bio-Rad)
qPCR validation	For SYBR Green I, Cq of the NTC	No amplification or 35-40 as primer-dimer
	PCR efficiency calculated from slope	92% - 108%
	R^2 of calibration curve	0.9951 – 0.9988

Data analysis	qPCR analysis program (source, version)	qbase+, version 3.0 (Biogazelle, Belgium)
	Method of Cq determination	Single threshold
	Justification of number and choice of reference genes	✓
	Description of normalization method	✓
	Number and concordance of biological replicates	✓
	Statistical methods for results significance	Tukey HSD
	Software (source, version)	OriginPro, Version 2020 (OriginLab Corp, MA, USA)

*** The ticked rows were already presented in the methods of each Chapter.**

References

AANES, H., WINATA, C. L., LIN, C. H., CHEN, J. P., SRINIVASAN, K. G., LEE, S. G., LIM, A. Y., HAJAN, H. S., COLLAS, P., BOURQUE, G., GONG, Z., KORZH, V., ALESTROM, P. & MATHAVAN, S. 2011. Zebrafish mRNA sequencing deciphers novelties in transcriptome dynamics during maternal to zygotic transition. *Genome Res,* 21**,** 1328-38.

ABE, K., YAMAMOTO, R., FRANKE, V., CAO, M., SUZUKI, Y., SUZUKI, M. G., VLAHOVICEK, K., SVOBODA, P., SCHULTZ, R. M. & AOKI, F. 2015. The first murine zygotic transcription is promiscuous and uncoupled from splicing and 3' processing. *EMBO J,* 34**,** 1523-37.

ADOLFI, M. C., HERPIN, A., REGENSBURGER, M., SACQUEGNO, J., WAXMAN, J. S. & SCHARTL, M. 2016. Retinoic acid and meiosis induction in adult versus embryonic gonads of medaka. *Sci Rep,* 6**,** 34281.

AGUERO, T., JIN, Z., CHORGHADE, S., KALSOTRA, A., KING, M. L. & YANG, J. 2017. Maternal Dead-end 1 promotes translation of nanos1 by binding the eIF3 complex. *Development,* 144**,** 3755-3765.

AGUERO, T., JIN, Z., OWENS, D., MALHOTRA, A., NEWMAN, K., YANG, J. & KING, M. L. 2018. Combined functions of two RRMs in Dead-end1 mimic helicase activity to promote nanos1 translation in the germline. *Mol Reprod Dev,* 85**,** 896-908.

AJDUK, A. & ZERNICKA-GOETZ, M. 2016. Polarity and cell division orientation in the cleavage embryo: from worm to human. *Mol Hum Reprod,* 22**,** 691-703.

ALIE, A., LECLERE, L., JAGER, M., DAYRAUD, C., CHANG, P., LE GUYADER, H., QUEINNEC, E. & MANUEL, M. 2011. Somatic stem cells express Piwi and Vasa genes in an adult ctenophore: ancient association of "germline genes" with stemness. *Dev Biol,* 350**,** 183-97.

ALTSCHUL, S. F., GISH, W., MILLER, W., MYERS, E. W. & LIPMAN, D. J. 1990. Basic local alignment search tool. *Journal of Molecular Biology,* 215**,** 403-410.

ANDERSEN, I. S., LINDEMAN, L. C., REINER, A. H., OSTRUP, O., AANES, H., ALESTROM, P. & COLLAS, P. 2013. Epigenetic marking of the zebrafish developmental program. *Curr Top Dev Biol,* 104**,** 85-112.

ANDERSEN, I. S., REINER, A. H., AANES, H., ALESTROM, P. & COLLAS, P. 2012. Developmental features of DNA methylation during activation of the embryonic zebrafish genome. *Genome Biol,* 13**,** R65.

ANDERSON, C., CATOE, H. & WERNER, R. 2006. MIR-206 regulates connexin43 expression during skeletal muscle development. *Nucleic Acids Res,* 34**,** 5863-71.

ANDERSON, E. L., BALTUS, A. E., ROEPERS-GAJADIEN, H. L., HASSOLD, T. J., DE ROOIJ, D. G., VAN PELT, A. M. M. & PAGE, D. C. 2008. *Stra8* and its inducer, retinoic acid, regulate meiotic initiation in both spermatogenesis and oogenesis in mice. *PNAS,* 105**,** 14976-1480.

ANDERSON, R. A., FULTON, N., COWAN, G., COUTTS, S. & SAUNDERS, P. T. 2007. Conserved and divergent patterns of expression of DAZL, VASA and OCT4 in the germ cells of the human fetal ovary and testis. *BMC Dev Biol,* 7**,** 136.

ANGELO, G. & VAN GILST, M. R. 2009. Starvation protects germline stem cells and extends reproductive longevity in *C. elegans*. *Science,* 326**,** 954-958.

ANOKYE-DANSO, F., TRIVEDI, C. M., JUHR, D., GUPTA, M., CUI, Z., TIAN, Y., ZHANG, Y., YANG, W., GRUBER, P. J., EPSTEIN, J. A. & MORRISEY, E. E. 2011. Highly efficient miRNA-mediated reprogramming of mouse and human somatic cells to pluripotency. *Cell Stem Cell,* 8**,** 376-88.

AOKI, Y., NAKAMURA, S., ISHIKAWA, Y. & TANAKA, M. 2009. Expression and syntenic analyses of four nanos genes in medaka. *Zoolog Sci,* 26**,** 112-8.

ARA, T., ITOI, M., KAWABATA, K., EGAWA, T., TOKOYODA, K., SUGIYAMA, T., FUJII, N., AMAGAI, T. & NAGASAWA, T. 2003a. A Role of CXC Chemokine Ligand 12/Stromal Cell-Derived Factor-1/Pre-B Cell Growth Stimulating Factor and Its Receptor CXCR4 in Fetal and Adult T Cell Development in Vivo. *The Journal of Immunology,* 170**,** 4649-4655.

ARA, T., NAKAMURAT, Y., EGAWA, T., SUGIYAMA, T., ABE, K., KISHIMOTOLL, T., MATSUI, Y. & NAGASAWA, T. 2003b. Impaired colonization of the gonads by primordial germ cells in mice lacking a chemokine, stromal cell-derived factor-1 (SDF-1). *PNAS,* 100**,** 5319-5323.

ARAI, K., ONOZATO, H. & YAMAZAKI, F. 1979. Artificial Androgenesis Induced with Gamma Irradiation in Masu Salmon, *Oncorhynchus masou*. *Bull. Fac. Fish. Hokkaido Univ.,* 30**,** 181-186.

ARAMAKI, S., SATO, F., KATO, T., SOH, T., KATO, Y. & HATTORI, M. A. 2007. Molecular cloning and expression of dead end homologue in chicken primordial germ cells. *Cell Tissue Res,* 330**,** 45-52.

ARAVIN, A. A., VAN DER HEIJDEN, G. W., CASTANEDA, J., VAGIN, V. V., HANNON, G. J. & BORTVIN, A. 2009. Cytoplasmic compartmentalization of the fetal piRNA pathway in mice. *PLoS Genet,* 5**,** e1000764.

ASADA, Y., VARNUM, D. S., FRANKEL, W. N. & NADEAU, J. H. 1994. A mutation in the Ter gene causing increased susceptibility to testicular teratomas maps to mouse chromosome 18. *Nat Genet,* 6**,** 363-368.

ASAOKA, M., HANYU-NAKAMURA, K., NAKAMURA, A. & KOBAYASHI, S. 2019. Maternal Nanos inhibits Importin-alpha2/Pendulin-dependent nuclear import to prevent somatic gene expression in the Drosophila germline. *PLoS Genet,* 15**,** e1008090.

ASHISH, S., BHURE, S. K., HARIKRISHNA, P., RAMTEKE, S. S., MUHAMMED KUTTY, V. H., SHRUTHI, N., RAVI KUMAR, G., MANISH, M., GHOSH, S. K. & MIHIR, S. 2017. Identification and evaluation of reference genes for accurate gene expression normalization of fresh and frozen-thawed spermatozoa of water buffalo (Bubalus bubalis). *Theriogenology,* 92**,** 6-13.

ATALLAH, J. & LOTT, S. E. 2018. Evolution of maternal and zygotic mRNA complements in the early Drosophila embryo. *PLoS Genet,* 14**,** e1007838.

AYRES, R. M., PETTIGROVE, V. J. & HOFFMANN, A. A. 2012. Genetic structure and diversity of introduced eastern mosquitofish (Gambusia holbrooki) in south-eastern Australia. *Marine and Freshwater Research,* 63.

BABAKHANZADEH, E., KHODADADIAN, A., ROSTAMI, S., ALIPOURFARD, I., AGHAEI, M., NAZARI, M., HOSSEINNIA, M., MEHRJARDI, M. Y. V., JAMSHIDI, Y. & GHASEMI, N. 2020. Testicular expression of TDRD1, TDRD5, TDRD9 and TDRD12 in azoospermia. *BMC Med Genet,* 21**,** 33.

BABIAK, I., DOBOSZ, S., GORYCZKO, K., KUZMINSKI, H., BRZUZANC, P. & CIESIELSKI, S. 2002. Androgenesis in rainbow trout using cryopreserved spermatozoa: the effect of processing and biological factors. *Theriogenology,* 57**,** 1229-1249.

BACCETTI, B. & AFZELIUS, B. A. 1976. The biology of the sperm cell. *Monogr Dev Biol.,* 10**,** 1-254.

BAK, C. W., YOON, T. K. & CHOI, Y. 2011. Functions of PIWI proteins in spermatogenesis. *Clin Exp Reprod Med,* 38**,** 61-7.

BALOCH, A. R., FRANEK, R., SAITO, T. & PSENICKA, M. 2019. Dead-end (dnd) protein in fish-a review. *Fish Physiol Biochem*.

BARAU, J., TEISSANDIER, A., ZAMUDIO, N., ROY, S., NALESSO, V., HÉRAULT, Y., GUILLOU, F. & BOURC'HIS, D. 2016. The DNA methyltransferase DNMT3C protects male germ cells from transposon activity. *Science,* 354**,** 909-912.

BARNEY, M. L., PATIL, J. G., GUNASEKERA, R. M. & CARTER, C. G. 2008. Distinct cytochrome P450 aromatase isoforms in the common carp (Cyprinus carpio): sexual dimorphism and onset of ontogenic expression. *Gen Comp Endocrinol,* 156**,** 499-508.

BAROILLER, J. F. & D'COTTA, H. 2016. The Reversible Sex of Gonochoristic Fish: Insights and Consequences. *Sex Dev,* 10**,** 242-266.

BAROILLER, J. F., D'COTTA, H., BEZAULT, E., WESSELS, S. & HOERSTGEN-SCHWARK, G. 2009a. Tilapia sex determination: Where temperature and genetics meet. *Comp Biochem Physiol A Mol Integr Physiol,* 153**,** 30-8.

BAROILLER, J. F., D'COTTA, H. & SAILLANT, E. 2009b. Environmental Effects on Fish Sex Determination and Differentiation. *Sex Dev,* 3**,** 118-135.

BAROILLERA, J., GUIGUENB, Y. & FOSTIER, A. 1999. Endocrine and environmental aspects of sex differentiation in fish. *Cellular and Molecular Life Science,* 55**,** 910-931.
BARON, B., BUCKLE, F. & ESPINA, S. 2002. Environmental factors and sexual differentiation in *Poecilia sphenops* Valenciennes (Pisces: Poeciliidae). *Aquaculture Research,* 33**,** 615-619.
BARON, D., COCQUET, J., XIA, X., FELLOUS, M., GUIGUEN, Y. & VEITIA, R. A. 2004. An evolutionary and functional analysis of FoxL2 in rainbow trout gonad differentiation. *J Mol Endocrinol,* 33**,** 705-15.
BARTEL, D. P. 2009. MicroRNAs: target recognition and regulatory functions. *Cell,* 136**,** 215-33.
BATTY, J. & LIM, R. 1999. Morphological and Reproductive Characteristics of Male Mosquitofish (*Gambusia affinis holbrooki*) Inhabiting Sewage-Contaminated Waters in New South Wales, Australia. *Arch. Environ. Contam. Toxicol.,* 36**,** 301-307.
BAZZINI, A. A., LEE, M. T. & GIRALDEZ, A. J. 2012. Ribosome Profiling Shows That miR-430 Reduces Translation Before Causing mRNA Decay in Zebrafish. *Science,* 336**,** 233-237.
BEARD, J. 1902. The germ cells of *Pristiurus*. *Anat. Anz,* 21**,** 50-61.
BEER, R. L. & DRAPER, B. W. 2013. nanos3 maintains germline stem cells and expression of the conserved germline stem cell gene nanos2 in the zebrafish ovary. *Dev Biol,* 374**,** 308-18.
BERTHO, S., CLAPP, M., BANISCH, T. U., BANDEMER, J., RAZ, E. & MARLOW, F. L. 2019. Zebrafish *dazl* regulates cystogenesis upstream of the meiotic transition and germline stem cell specification and independent of meiotic checkpoints. *bioRxiv*.
BERTHO, S., PASQUIER, J., PAN, Q., LE TRIONNAIRE, G., BOBE, J., POSTLETHWAIT, J. H., PAILHOUX, E., SCHARTL, M., HERPIN, A. & GUIGUEN, Y. 2016. Foxl2 and Its Relatives Are Evolutionary Conserved Players in Gonadal Sex Differentiation. *Sex Dev,* 10**,** 111-29.
BETLEY, J. N., FRITH, M. C., GRABER, J. H., CHOO, S. & DESHLER, J. O. 2002. A Ubiquitous and Conserved Signal for RNA Localization in Chordates. *Current Biology,* 12**,** 1256-1271.
BHANDARI, D., RAISCH, T., WEICHENRIEDER, O., JONAS, S. & IZAURRALDE, E. 2014. Structural basis for the Nanos-mediated recruitment of the CCR4-NOT complex and translational repression. *Genes Dev,* 28**,** 888-901.
BHATTACHARYA, C., AGGARWAL, S., KUMAR, M., ALI, A. & MATIN, A. 2008. Mouse apolipoprotein B editing complex 3 (APOBEC3) is expressed in germ cells and interacts with dead-end (DND1). *PLoS One,* 3**,** e2315.
BHATTACHARYA, C., AGGARWAL, S., ZHU, R., KUMAR, M., ZHAO, M., MEISTRICH, M. L. & MATIN, A. 2007. The mouse dead-end gene isoform alpha is necessary for germ cell and embryonic viability. *Biochem Biophys Res Commun,* 355**,** 194-9.
BHIN, J., JEONG, H. S., KIM, J. S., SHIN, J. O., HONG, K. S., JUNG, H. S., KIM, C., HWANG, D. & KIM, K. S. 2015. PGC-Enriched miRNAs Control Germ Cell Development. *Mol Cells,* 38**,** 895-903.
BISSONNETTE, N., LEVESQUE-SERGERIE, J. P., THIBAULT, C. & BOISSONNEAULT, G. 2009. Spermatozoal transcriptome profiling for bull sperm motility: a potential tool to evaluate semen quality. *Reproduction,* 138**,** 65-80.
BIZUAYEHU, T. T. & BABIAK, I. 2014. MicroRNA in teleost fish. *Genome Biol Evol,* 6**,** 1911-37.
BLACKBURN, D. G. 2015. Evolution of vertebrate viviparity and specializations for fetal nutrition: A quantitative and qualitative analysis. *J Morphol,* 276**,** 961-90.
BLACKLE, R. W. 1965. Germ-cell transfer and sex ratio in *Xenopus laevis*. *Development,* 13**,** 51-61.
BOBE, J. & LABBE, C. 2010. Egg and sperm quality in fish. *Gen Comp Endocrinol,* 165**,** 535-48.
BOLAND, A., HUNTZINGER, E., SCHMIDT, S., IZAURRALDE, E. & WEICHENRIEDER, O. 2011. Crystal structure of the MID-PIWI lobe of a eukaryotic Argonaute protein. *Proc Natl Acad Sci U S A,* 108**,** 10466-71.
BOLDAJIPOUR, B., MAHABALESHWAR, H., KARDASH, E., REICHMAN-FRIED, M., BLASER, H., MININA, S., WILSON, D., XU, Q. & RAZ, E. 2008. Control of chemokine-guided cell migration by ligand sequestration. *Cell,* 132**,** 463-73.
BONGERS, A. B. J., ABARCA, B. J., ZANDIEH DOULABI, B., EDING , E. H., KOMEN, J. & RICHTER, C. J. J. 1995. Maternal influence on development of androgenetic clones of common carp, *Cyprinus carpio* L. *Aquaculture,* 137**,** 139-147.

BONGERS, A. B. J., ZANDIEH-DOULABI, B., RICHTER, C. J. & KOMEN, J. 1999. Viable androgenetic YY genotypes of common carp (*Cyprinus carpio* L.). *Journal of Heredity,* 90**,** 195-198.

BONTEMS, F., STEIN, A., MARLOW, F., LYAUTEY, J., GUPTA, T., MULLINS, M. C. & DOSCH, R. 2009. Bucky ball organizes germ plasm assembly in zebrafish. *Curr Biol,* 19**,** 414-22.

BRAAT, A. K., VAN DE WATER, S., KORVING, J. & ZIVKOVIC, D. 2001. A zebrafish vasa morphant abolishes vasa protein but does not affect the establishment of the germline. *Genesis,* 30**,** 183-5.

BRAAT, A. K., ZANDBERGEN, T., VAN DE WATER, S., GOOS, J. T. & ZIVCOVIC, D. 1999. Characterization of Zebrafish Primordial Germ Cells: Morphology and Early Distribution of vasa RNA. *Developmental Dynamics,* 216**,** 153-167.

BRADFORD, Y. M., TORO, S., RAMACHANDRAN, S., RUZICKA, L., HOWE, D. G., EAGLE, A., KALITA, P., MARTIN, R., TAYLOR MOXON, S. A., SCHAPER, K. & WESTERFIELD, M. 2017. Zebrafish Models of Human Disease: Gaining Insight into Human Disease at ZFIN. *ILAR J,* 58**,** 4-16.

BRENNECKE, J., ARAVIN, A. A., STARK, A., DUS, M., KELLIS, M., SACHIDANANDAM, R. & HANNON, G. J. 2007. Discrete small RNA-generating loci as master regulators of transposon activity in Drosophila. *Cell,* 128**,** 1089-103.

BROOK, M., SMITH, J. W. & GRAY, N. K. 2009. The DAZL and PABP families: RNA-binding proteins with interrelated roles in translational control in oocytes. *Reproduction,* 137**,** 595-617.

BUSHATI, N., STARK, A., BRENNECKE, J. & COHEN, S. M. 2008. Temporal reciprocity of miRNAs and their targets during the maternal-to-zygotic transition in Drosophila. *Curr Biol,* 18**,** 501-6.

BUSTIN, S. A., BENES, V., GARSON, J. A., HELLEMANS, J., HUGGETT, J., KUBISTA, M., MUELLER, R., NOLAN, T., PFAFFL, M. W., SHIPLEY, G. L., VANDESOMPELE, J. & WITTWER, C. T. 2009. The MIQE guidelines: minimum information for publication of quantitative real-time PCR experiments. *Clin Chem,* 55**,** 611-22.

CAMP, E., SANCHEZ-SANCHEZ, A. V., GARCIA-ESPANA, A., DESALLE, R., ODQVIST, L., ENRIQUE O'CONNOR, J. & MULLOR, J. L. 2009. Nanog regulates proliferation during early fish development. *Stem Cells,* 27**,** 2081-91.

CAMPBELL, P. D., HEIM, A. E., SMITH, M. Z. & MARLOW, F. L. 2015. Kinesin-1 interacts with Bucky ball to form germ cells and is required to pattern the zebrafish body axis. *Development,* 142**,** 2996-3008.

CAMPUZANO-CABALLERO, J. C. & URIBE, M. C. 2014. Structure of the female gonoduct of the viviparous teleost Poecilia reticulata (Poeciliidae) during nongestation and gestation stages. *J Morphol,* 275**,** 247-57.

CARGNIN, F., KWON, J. S., KATZMAN, S., CHEN, B., LEE, J. W. & LEE, S. K. 2018. FOXG1 Orchestrates Neocortical Organization and Cortico-Cortical Connections. *Neuron,* 100**,** 1083-1096 e5.

CASPER, A. L. & VAN DOREN, M. 2009. The establishment of sexual identity in the Drosophila germline. *Development,* 136**,** 3821-30.

CAVALCANTI, M. C., FAILLING, K., SCHUPPE, H. C., BERGMANN, M., STALF, T., WEIDNER, W. & STEGER, K. 2011. Validation of reference genes in human testis and ejaculate. *Andrologia,* 43**,** 361-7.

CHAMBERS, I., COLBY, D., ROBERTSON, M., NICHOLS, J., LEE, S., TWEEDIE, S. & SMITH, A. 2003. Functional Expression Cloning of Nanog, a Pluripotency Sustaining Factor in Embryonic Stem Cells. *Cell,* 113**,** 643-655.

CHAMBERS, I., SILVA, J., COLBY, D., NICHOLS, J., NIJMEIJER, B., ROBERTSON, M., VRANA, J., JONES, K., GROTEWOLD, L. & SMITH, A. 2007. Nanog safeguards pluripotency and mediates germline development. *Nature,* 450**,** 1230-4.

CHAMBOLLE, P., CAMBAR, R. & TRAN, D. 1970. Table chronologique du développement embryonnaire de *Gambusia sp*. (Poisson Teleosteen). *Bul Biol,* 104**,** 443-452.

CHAMPROUX, A., COCQUET, J., HENRY-BERGER, J., DREVET, J. R. & KOCER, A. 2018. A Decade of Exploring the Mammalian Sperm Epigenome: Paternal Epigenetic and Transgenerational Inheritance. *Front Cell Dev Biol,* 6**,** 50.

CHAN, A. P., KLOC, M., LARABELL, C. A., LEGROS, M. & ETKIN, L. D. 2007. The maternally localized RNA fatvg is required for cortical rotation and germ cell formation. *Mech Dev,* 124**,** 350-63.

CHANG, C. W., NASHCHEKIN, D., WHEATLEY, L., IRION, U., DAHLGAARD, K., MONTAGUE, T. G., HALL, J. & ST JOHNSTON, D. 2011. Anterior-posterior axis specification in Drosophila oocytes: identification of novel bicoid and oskar mRNA localization factors. *Genetics,* 188**,** 883-96.

CHARLESWORTH, D. 2018. The Guppy Sex Chromosome System and the Sexually Antagonistic Polymorphism Hypothesis for Y Chromosome Recombination Suppression. *Genes (Basel),* 9.

CHATFIELD, J., O'REILLY, M. A., BACHVAROVA, R. F., FERJENTSIK, Z., REDWOOD, C., WALMSLEY, M., PATIENT, R., LOOSE, M. & JOHNSON, A. D. 2014. Stochastic specification of primordial germ cells from mesoderm precursors in axolotl embryos. *Development,* 141**,** 2429-40.

CHEN, J., MELTON, C., SUH, N., OH, J. S., HORNER, K., XIE, F., SETTE, C., BLELLOCH, R. & CONTI, M. 2011. Genome-wide analysis of translation reveals a critical role for deleted in azoospermia-like (Dazl) at the oocyte-to-zygote transition. *Genes Dev,* 25**,** 755-66.

CHEN, Q., YAN, W. & DUAN, E. 2016. Epigenetic inheritance of acquired traits through sperm RNAs and sperm RNA modifications. *Nat Rev Genet,* 17**,** 733-743.

CHERVINSKY, J. 1983. Salinity tolerance of the mosquito fish, Gambusia affinis. *J Fish Biol,* 22**,** 9-11.

CHO, C., JUNG-HA, H., WILLIS, W. D., GOULDING, E. H., STEIN, P., XU, Z., SCHULTZ, R. M., HECHT, N. B. & EDDY, E. M. 2003. Protamine 2 deficiency leads to sperm DNA damage and embryo death in mice. *Biol Reprod,* 69**,** 211-7.

CHO, C., WILLIS, W. D., GOULDING, E. H., JUNG-HA, H., CHOI, Y.-C., HECHT, N. B. & EDDY, E. M. 2001. Haploinsufficiency of protamine-1 or -2 causes infertility in mice. *Nature Genetics,* 28**,** 82-86.

CHUANG, R.-Y., WEAVER, P. L., LIU, Z. & CHANG, T.-H. 1997. Requirement of the DEAD-Box protein ded1p for messenger RNA translation. *Science,* 275**,** 1468-71.

CHUMA, S., HOSOKAWA, M., KITAMURA, K., KASAI, S., FUJIOKA, M., HIYOSHI, M., TAKAMUNE, K., NOCE, T. & NAKATSUJI, N. 2006. Tdrd1/Mtr-1, a tudor-related gene, is essential for male germ-cell differentiation and nuage/germinal granule formation in mice. *Proc Natl Acad Sci U S A,* 103**,** 15894-9.

CIRIA, M., GARCIA, N. A., ONTORIA-OVIEDO, I., GONZALEZ-KING, H., CARRERO, R., DE LA POMPA, J. L., MONTERO, J. A. & SEPULVEDA, P. 2017. Mesenchymal Stem Cell Migration and Proliferation Are Mediated by Hypoxia-Inducible Factor-1alpha Upstream of Notch and SUMO Pathways. *Stem Cells Dev,* 26**,** 973-985.

CONGRAS, A., YERLE-BOUISSOU, M., PINTON, A., VIGNOLES, F., LIAUBET, L., FERCHAUD, S. & ACLOQUE, H. 2014. Sperm DNA methylation analysis in swine reveals conserved and species-specific methylation patterns and highlights an altered methylation at the GNAS locus in infertile boars. *Biol Reprod,* 91**,** 137.

COOK, M. S., MUNGER, S. C., NADEAU, J. H. & CAPEL, B. 2011. Regulation of male germ cell cycle arrest and differentiation by DND1 is modulated by genetic background. *Development,* 138**,** 23-32.

COURTENAY JR, W. R. & MEFFE, G. K. 1989. Small fishes in strange places: a review of introduced poeciliids. *In:* MEFFE, G. K. & SNELSON, F. F. J. (eds.) *Ecology and evolution of livebearing fishes (Poecilidae).* New Jersey: Prentice-Hall, Inc.

COX, D. N., CHAO, A., BAKER, J., CHANG, L., QIAO, D. & LIN, H. A. 1998. A novel class of evolutionarily conserved genes defined by piwi are essential for stem cell self-renewal. *GENES & DEVELOPMENT,* 12**,** 3715-3727.

CRISPONI, L., DEIANA, M., LOI, A., CHIAPPE, F., UDA, M., AMATI, P., BISCEGLIA, L., ZELANTE, L., NAGARAJA, R., PORCU, S., RISTALDI, M. S., MARZELLA, R., ROCCHI, M., NICOLINO, M., LIENHARDT-ROUSSIE, A., NIVELON, A., VERLOES, A.,

SCHLESSINGER, D., GASPARINI, P., BONNEAU, D., CAO, A. & PILIA, G. 2001. The putative forkhead transcription factor *FOXL2* is mutated in blepharophimosis/ptosis/epicanthus inversus syndrome. *nature Genetics,* 27**,** 159-166.
CROFT, D. P., BRENT, L. J., FRANKS, D. W. & CANT, M. A. 2015. The evolution of prolonged life after reproduction. *Trends Ecol Evol,* 30**,** 407-16.
CROTHER, B. I., WHITE, M. E. & JOHNSON, A. D. 2007. Inferring developmental constraint and constraint release: primordial germ cell determination mechanisms as examples. *J Theor Biol,* 248**,** 322-30.
CROTHER, B. I., WHITE, M. E. & JOHNSON, A. D. 2016. Diversification and Germ-Line Determination Revisited: Linking Developmental Mechanism with Species Richness. *Frontiers in Ecology and Evolution,* 4.
CURTIS, D., APFELD, J. & LEHMANN, R. 1995. *nanos* is an evolutionarily conserved organizer of anterior-posterior polarity. *Development,* 121**,** 1899-1910.
CURTIS, D., TREIBER, D. K., TAO, F., ZAMORE, P. D., R., W. J. & LEHMANN, R. 1997. A CCHC metal-binding domain in Nanos is essential for translational regulation. *EMBO J,* 16**,** 834-843.
DAI, X., SHU, Y., LOU, Q., TIAN, Q., ZHAI, G., SONG, J., LU, S., YU, H., HE, J. & YIN, Z. 2017. Tdrd12 Is Essential for Germ Cell Development and Maintenance in Zebrafish. *Int J Mol Sci,* 18.
DAMBLY-CHAUDIERE, C., CUBEDO, N. & GHYSEN, A. 2007. Control of cell migration in the development of the posterior lateral line: antagonistic interactions between the chemokine receptors CXCR4 and CXCR7/RDC1. *BMC Dev Biol,* 7**,** 23.
DANSEREAU, D. A. & LASKO, P. 2008. The development of germline stem cells in Drosophila. *Methods Mol Biol,* 450**,** 3-26.
DAVID, N. B., SAPÈDE, D., SAINT-ETIENNE, L., THISSE, C., THISSE, B., DAMBLY-CHAUDIÈRE, C., ROSA, F. M. & GHYSEN, A. 2002. Molecular basis of cell migration in the fish lateral line role of the chemokine receptor CXCR4 and of its ligand, SDF1. *Proc Natl Acad Sci U S A,* 99**,** 16297-302.
DAVIES, P. E. 2012. An Assessment of the Risks of Gambusia infestation in Tasmania. Hobart, Tasmania: Freshwater System.
DE KEUCKELAERE, E., HULPIAU, P., SAEYS, Y., BERX, G. & VAN ROY, F. 2018. Nanos genes and their role in development and beyond. *Cell Mol Life Sci,* 75**,** 1929-1946.
DEBACH, P. & ROSEN, D. 1991. *Biological control by natural enemies*, Cambridge University Press.
DEFALCO, T. & CAPEL, B. 2009. Gonad morphogenesis in vertebrates: divergent means to a convergent end. *Annu Rev Cell Dev Biol,* 25**,** 457-82.
DESHPANDE, G., CALHOUN, G., YANOWITZ, J. L. & SCHEDL, P. D. 1999. Novel Functions of nanos in Downregulating Mitosis and Transcription during the Development of the Drosophila Germline. *Cell,* 99**,** 271-281.
DESHPANDE, G., CALHOUN, G., YANOWITZ, J. L. & SCHEDL, P. D. 2010. Novel Functions of nanos in Downregulating Mitosis and Transcription during the Development of the Drosophila Germline. *Cell,* 99**,** 271-281.
DESPIC, V., DEJUNG, M., GU, M., KRISHNAN, J., ZHANG, J., HERZEL, L., STRAUBE, K., GERSTEIN, M. B., BUTTER, F. & NEUGEBAUER, K. M. 2017. Dynamic RNA-protein interactions underlie the zebrafish maternal-to-zygotic transition. *Genome Res,* 27**,** 1184-1194.
DEVLIN, R. H. & NAGAHAMA, Y. 2002. Sex determination and sex differentiation in fish: an overview of genetic, physiological, and environmental influences. *Aquaculture,* 208**,** 191-364.
DI CLEMENTE, N. & BELVILLE, C. 2006. Anti-Mullerian hormone receptor defect. *Best Pract Res Clin Endocrinol Metab,* 20**,** 599-610.
DILDINE, G. C. 1936. Studies in teleostean reproduction. I. Embryonic hermaphroditism in *Lebistes reticulatus*. *Journal of Morphology,* 60**,** 261-277.
DOITSIDOU, M., REICHMAN-FRIED, M., J., S., KOPRUNNER, M., DORRIES, J., D, M., ESGUERRA, C. V., LEUNG, T. & RAZ, E. 2002. Guidance of Primordial Germ Cell Migration by the Chemokine SDF-1. *Cell,* 111**,** 647-659.

DONG, R., YANG, S., JIAO, J., WANG, T., SHI, H., ZHOU, L., ZHANG, Y. & WANG, D. 2013. Characterization of Stra8 in Southern catfish (*Silurus meridionalis*) evidence for its role in meiotic initiation. *BMC Molecular Biology,* 14**,** 1-9.
DORTS, J., FALISSE, E., SCHOOFS, E., FLAMION, E., KESTEMONT, P. & SILVESTRE, F. 2016. DNA methyltransferases and stress-related genes expression in zebrafish larvae after exposure to heat and copper during reprogramming of DNA methylation. *Sci Rep,* 6**,** 34254.
DOSCH, R., WAGNER, D. S., MINTZER, K. A., RUNKE, G., WIEMELT, A. P. & MULLINS, M. C. 2004. Maternal control of vertebrate development before the midblastula transition: mutants from the zebrafish I. *Dev Cell,* 6**,** 771-80.
DOUGLAS, W. H. & KING, M. L. 2000. A critical role for Xdazl, a germ plasm-localized RNA, in the differentiation of primordial germ cells in *Xenopus*. *Development,* 12**,** 447-456.
DUAN, J., FENG, G., CHANG, P., ZHANG, X., ZHOU, Q., ZHONG, X., QI, C., XIE, S. & ZHAO, H. 2015. Germ cell-specific expression of *dead end* (*dnd*) in rare minnow (*Gobiocypris rarus*). *Fish Physiol Biochem,* 41**,** 561-571.
DURCHSCHLAG, H., FOCHLER, C., FESER, B., HAUSMANN, S., SERONEIT, T., SWIENTEK, M., SWOBODA, E., WINKLMAIR, A., WLČEK, C. & ZIPPER, P. 1996. Effects of X- and UV-irradiation on proteins. *Radiation Physics and Chemistry,* 47**,** 501-505.
EDDY, E. M. 2002. Male germ cell gene expression. *Recent Prog Horm Res,* 57**,** 103-28.
EDGAR, B. A. & DATAR, S. A. 1996. Zygotic degradation of two maternal Cdc25 mRNAs terminates *Drosophila*'s early cell cycle program. *GENES & DEVELOPMENT,* 10**,** 1966-1977.
EDGAR, B. A. & SCHUBIGER, G. 1986. Parameters controlling transcriptional activation during early *Drosophila* development. *Cell,* 44**,** 871-877.
EDGAR, R. C. 2004. MUSCLE: multiple sequence alignment with high accuracy and high throughput. *Nucleic Acids Res,* 32**,** 1792-7.
EDWARDS, R. G. 2005. Genetics of polarity in mammalian embryos. *Reproductive Biomedicine Online,* 11**,** 104-114.
ELLIS, R. E. 2008. Chapter 2 Sex Determination in the Caenorhabditis elegans Germ Line. *Current Topics in Developmental Biology,* 83**,** 41-64.
EPHRUSSI, A. & LEHMANN, R. 1992. Induction of germ cell formation by *oskar*. 358.
EVANS, T., WADE, C. M., CHAPMAN, F. A., JOHNSON, A. D. & LOOSE, M. 2014. Acquisition of Germ Plasm Accelerates Vertebrate Evolution. *Science,* 344**,** 200-203.
EVSIKOV, A. V. & MARIN DE EVSIKOVA, C. 2009. Gene expression during the oocyte-to-embryo transition in mammals. *Mol Reprod Dev,* 76**,** 805-18.
EWEN-CAMPEN, B., SCHWAGER, E. E. & EXTAVOUR, C. G. 2010. The molecular machinery of germ line specification. *Mol Reprod Dev,* 77**,** 3-18.
EXTAVOUR, C. G. & AKAM, M. 2003. Mechanisms of germ cell specification across the metazoans: epigenesis and preformation. *Development,* 130**,** 5869-84.
FACCHINELLI, L., NORTH, A. R., COLLINS, C. M., MENICHELLI, M., PERSAMPIERI, T., BUCCI, A., SPACCAPELO, R., CRISANTI, A. & BENEDICT, M. Q. 2019. Large-cage assessment of a transgenic sex-ratio distortion strain on populations of an African malaria vector. *Parasit Vectors,* 12**,** 70.
FANG, X., CORRALES, J., THORNTON, C., SCHEFFLER, B. E. & WILLETT, K. L. 2013. Global and gene specific DNA methylation changes during zebrafish development. *Comp Biochem Physiol B Biochem Mol Biol.*
FARRELL, J. A., SHERMOEN, A. W., YUAN, K. & O'FARRELL, P. H. 2012. Embryonic onset of late replication requires Cdc25 down-regulation. *Genes Dev,* 26**,** 714-25.
FELDMAN, A. T. & WOLFE, D. 2014. Tissue Processing and Hematoxylin and Eosin Staining. *In:* DAY, C. (ed.) *Histopathology.* New York, NY: Humana Press.
FENG, C. W., BOWLES, J. & KOOPMAN, P. 2014. Control of mammalian germ cell entry into meiosis. *Mol Cell Endocrinol,* 382**,** 488-497.
FENG, K., CUI, X., SONG, Y., TAO, B., CHEN, J., WANG, J., LIU, S., SUN, Y., ZHU, Z., TRUDEAU, V. L. & HU, W. 2020. Gnrh3 Regulates PGC Proliferation and Sex Differentiation in Developing Zebrafish. *Endocrinology,* 161.

FENG, L. & CHEN, X. 2015. Epigenetic regulation of germ cells-remember or forget? *Curr Opin Genet Dev,* 31**,** 20-7.
FÉRAL, C., GUELLAËN, G. & PAWLAK, A. 2001. Human testis expresses a specific poly(A)-binding protein. *Nucleic Acids Res,* 29**,** 1872.
FIGUEIREDO, A. F., FRANCA, L. R., HESS, R. A. & COSTA, G. M. 2016. Sertoli cells are capable of proliferation into adulthood in the transition region between the seminiferous tubules and the rete testis in Wistar rats. *Cell Cycle,* 15**,** 2486-96.
FIGUERAS, A., ALSINA-SANCHIS, E., LAHIGUERA, A., ABREU, M., MUINELO-ROMAY, L., MORENO-BUENO, G., CASANOVAS, O., GRAUPERA, M., MATIAS-GUIU, X., VIDAL, A., VILLANUEVA, A. & VINALS, F. 2018. A Role for CXCR4 in Peritoneal and Hematogenous Ovarian Cancer Dissemination. *Mol Cancer Ther,* 17**,** 532-543.
FILIPOWICZ, W., BHATTACHARYYA, S. N. & SONENBERG, N. 2008. Mechanisms of post-transcriptional regulation by microRNAs: are the answers in sight? *Nat Rev Genet,* 9**,** 102-14.
FILIPPI, M.-D. & GEIGER, H. 2011. *Stem Cell Miggration,* Springer, United States.
FISKE, P., LUND, R. & HANSEN, L. 2006. Relationships between the frequency of farmed Atlantic salmon, S*almo salar L.*, in wild salmon populations and fish farming activity in Norway, 1989–2004. *ICES Journal of Marine Science,* 63**,** 1182-1189.
FORBES, A. & LEHMANN, R. 1998. Nanos and Pumilio have critical roles in the development and function of Drosophila germline stem cells. *Development,* 125**,** 679-90.
FRANSSEN, C. M., TOBLER, M., RIESCH, R., GARCÍA DE LEÓN, F. J., TIEDEMANN, R., SCHLUPP, I. & PLATH, M. 2007. Sperm production in an extremophile fish, the cave molly (Poecilia mexicana, Poeciliidae, Teleostei). *Aquatic Ecology,* 42**,** 685-692.
FRAUNHOFFER, N. A., MEILERMAN ABUELAFIA, A., STELLA, I., GALLIANO, S., BARRIOS, M. & VITULLO, A. D. 2015. Identification of germ cell-specific VASA and IFITM3 proteins in human ovarian endometriosis. *J Ovarian Res,* 8**,** 66.
FROESE, R. & PAULY, D. 2000. *FishBase 2000: concepts, design and data sources,* Los Baños, Laguna, Philippines, ICLARM.
FUJIMOTO, T., NISHIMURA, T., GOTO-KAZETO, R., KAWAKAMI, Y., YAMAHA, E. & ARAI, K. 2010. Sexual dimorphism of gonadal structure and gene expression in germ cell-deficient loach, a teleost fish. *Proc Natl Acad Sci U S A,* 107**,** 17211-6.
GAGNON, J. A., OBBAD, K. & SCHIER, A. F. 2018. The primary role of zebrafish nanog is in extra-embryonic tissue. *Development,* 145.
GALIZI, R., DOYLE, L. A., MENICHELLI, M., BERNARDINI, F., DEREDEC, A., BURT, A., STODDARD, B. L., WINDBICHLER, N. & CRISANTI, A. 2014. A synthetic sex ratio distortion system for the control of the human malaria mosquito. *Nat Commun,* 5**,** 3977.
GALLIE, D. R., LING, J., NIEPEL, M., MORLEY, S. J. & PAIN, V. M. 2000. The role of 5′-leader length, secondary structure and PABP concentration on cap and poly(A) tail function during translation in *Xenopus* oocytes. *Nucleic Acids Res,* 28**,** 2943-2953.
GAO, F. & DAS, S. K. 2014. Epigenetic regulations through DNA methylation and hydroxymethylation: clues for early pregnancy in decidualization. *Biomol Concepts,* 5**,** 95-107.
GASPARINI, C., DAYMOND, E. & EVANS, J. P. 2018. Extreme fertilization bias towards freshly inseminated sperm in a species exhibiting prolonged female sperm storage. *R Soc Open Sci,* 5**,** 172195.
GASPARINI, C., PILASTRO, A. & EVANS, J. P. 2011. Male genital morphology and its influence on female mating preferences and paternity success in guppies. *PLoS One,* 6**,** e22329.
GAVIS, E. R. & LEHMANN, R. 1994. Translational regulation of nanos by RNA localization. 26**,** 315-8.
GENNOTTE, V., MAFWILA KINKELA, P., ULYSSE, B., AKIAN DJETOUAN, D., BERE SOMPAGNIMDI, F., TOMSON, T., MELARD, C. & ROUGEOT, C. 2015. Brief exposure of embryos to steroids or aromatase inhibitor induces sex reversal in Nile tilapia (Oreochromis niloticus). *J Exp Zool A Ecol Genet Physiol,* 323**,** 31-8.
GEORGES, A., AUGUSTE, A., BESSIERE, L., VANET, A., TODESCHINI, A. L. & VEITIA, R. A. 2014. FOXL2: a central transcription factor of the ovary. *J Mol Endocrinol,* 52**,** R17-33.

GERMINI, D., TSFASMAN, T., ZAKHAROVA, V. V., SJAKSTE, N., LIPINSKI, M. & VASSETZKY, Y. 2018. A Comparison of Techniques to Evaluate the Effectiveness of Genome Editing. *Trends Biotechnol,* 36**,** 147-159.
GINOZA, W. 1967. The Effects of Ionizing Radiation on Nucleic Acids of Bacteriophages and Bacterial Cells. *Annual Review of Microbiology,* 21**,** 325-368.
GINSBURG, M., SNOW, M. H. L. & MCLAREN, A. 1990. Primordial germ cells in the mouse embryo during gastrulation. *Development,* 110**,** 521-528.
GIRALDEZ, A. J. 2010. microRNAs, the cell's Nepenthe: clearing the past during the maternal-to-zygotic transition and cellular reprogramming. *Curr Opin Genet Dev,* 20**,** 369-75.
GIRALDEZ, A. J., MISHIMA, Y., RIHEL, J., GROCOCK, R. J., VAN DONGEN, S., INOUE, K., ENRIGHT, A. J. & SCHIER, A. F. 2006. Zebrafish MiR-430 promotes deadenylation and clearance of maternal mRNAs. *Science,* 312**,** 75-79.
GODIA, M., CASTELLO, A., ROCCO, M., CABRERA, B., RODRIGUEZ-GIL, J. E., BALASCH, S., LEWIS, C., SANCHEZ, A. & CLOP, A. 2020. Identification of circular RNAs in porcine sperm and evaluation of their relation to sperm motility. *Sci Rep,* 10**,** 7985.
GODWIN, J. 2009. Social determination of sex in reef fishes. *Semin Cell Dev Biol,* 20**,** 264-70.
GOMES, A. Q., NOLASCO, S. & SOARES, H. 2013. Non-coding RNAs: multi-tasking molecules in the cell. *Int J Mol Sci,* 14**,** 16010-39.
GOODRICH, H. B., DEE, J. E., FLYNN, C. M. & MERCER, R. N. 1934. Germ cells and Sex differentiation in *Lebistes reticulatus*. *The Biological Bulletin,* 67**,** 83-96.
GOODRICH, R., JOHNSON, G. & KRAWETZ, S. A. 2007. The preparation of human spermatozoal RNA for clinical analysis. *Arch Androl,* 53**,** 161-7.
GOPPERT, C., HARRIS, R. M., THEIS, A., BOILA, A., HOHL, S., RUEGG, A., HOFMANN, H. A., SALZBURGER, W. & BOHNE, A. 2016. Inhibition of Aromatase Induces Partial Sex Change in a Cichlid Fish: Distinct Functions for Sex Steroids in Brains and Gonads. *Sex Dev,* 10**,** 97-110.
GOTO, R., SAITO, T., TAKEDA, T., FUJIMOTO, T., TAKAGI, M., ARAI, K. & YAMAHA, E. 2012. Germ cells are not the primary factor for sexual fate determination in goldfish. *Dev Biol,* 370**,** 98-109.
GOUDARZI, M., BANISCH, T. U., MOBIN, M. B., MAGHELLI, N., TARBASHEVICH, K., STRATE, I., VAN DEN BERG, J., BLASER, H., BANDEMER, S., PALUCH, E., BAKKERS, J., TOLIC-NORRELYKKE, I. M. & RAZ, E. 2012. Identification and regulation of a molecular module for bleb-based cell motility. *Dev Cell,* 23**,** 210-8.
GOUDARZI, M., STRATE, I., PAKSA, A., LAGENDIJK, A. K., BAKKERS, J. & RAZ, E. 2013. On the robustness of germ cell migration and microRNA-mediated regulation of chemokine signaling. *Nat Genet,* 45**,** 1264-5.
GOULD, J. M., SMITH, P. J., AIREY, C. J., MORT, E. J., AIREY, L. E., WARRICKER, F. D. M., PEARSON-FARR, J. E., WESTON, E. C., GOULD, P. J. W., SEMMENCE, O. G., RESTALL, K. L., WATTS, J. A., MCHUGH, P. C., SMITH, S. J., DEWING, J. M., FLEMING, T. P. & WILLAIME-MORAWEK, S. 2018. Mouse maternal protein restriction during preimplantation alone permanently alters brain neuron proportion and adult short-term memory. *Proc Natl Acad Sci U S A,* 115**,** E7398-E7407.
GREENBAUM, M. P., IWAMORI, T., BUCHOLD, G. M. & MATZUK, M. M. 2011. Germ cell intercellular bridges. *Cold Spring Harb Perspect Biol,* 3**,** a005850.
GREVEN, H. 2011. Part1: Reproductive biology and life history. *In:* EVANS, J. P., ANDREA PILASTRO & SCHLUPP, I. (eds.) *Ecology and Evolution of Poeciliid Fishes.* USA: University of Chicago Press.
GRIER, H. J. 1975. Aspects of germinal cyst and sperm development in *Poecilia latipinna* (Teleostei: Poeciliidae). *Journal of Morphology,* 146**,** 229-249.
GRIER, H. J., BURNS, J. R. & FLORES, J. A. 1981. Testis Structure in Three Species of Teleosts with Tubular Gonopodia. *Copeia,* 1981**,** 797-801.
GRIFFIN, L. B., JANUARY, K. E., HO, K. W., COTTER, K. A. & CALLARD, G. V. 2013. Morpholino-mediated knockdown of ERalpha, ERbetaa, and ERbetab mRNAs in zebrafish (*Danio rerio*) embryos reveals differential regulation of estrogen-inducible genes. *Endocrinology,* 154**,** 4158-69.

GRIMSON, A., SRIVASTAVA, M., FAHEY, B., WOODCROFT, B. J., CHIANG, H. R., KING, N., DEGNAN, B. M., ROKHSAR, D. S. & BARTEL, D. P. 2008. Early origins and evolution of microRNAs and Piwi-interacting RNAs in animals. *Nature,* 455**,** 1193-7.

GRINSPON, R. P. & REY, R. A. 2010. Anti-mullerian hormone and sertoli cell function in paediatric male hypogonadism. *Horm Res Paediatr,* 73**,** 81-92.

GRISWOLD, M. D. 2016. Spermatogenesis: The Commitment to Meiosis. *Physiol Rev,* 96**,** 1-17.

GROSS-THEBING, T., YIGIT, S., PFEIFFER, J., REICHMAN-FRIED, M., BANDEMER, J., RUCKERT, C., RATHMER, C., GOUDARZI, M., STEHLING, M., TARBASHEVICH, K., SEGGEWISS, J. & RAZ, E. 2017. The Vertebrate Protein Dead End Maintains Primordial Germ Cell Fate by Inhibiting Somatic Differentiation. *Dev Cell,* 43**,** 704-715 e5.

GROSS, N., STRILLACCI, M. G., PENAGARICANO, F. & KHATIB, H. 2019. Characterization and functional roles of paternal RNAs in 2-4 cell bovine embryos. *Sci Rep,* 9**,** 20347.

GRUIDL, M. E., SMITH, P. A., KUZNICKI, K. A., MC CRONE, J. S., KIRCHNER, J., ROUSSELL, D. L., STROME, S. & BENNETT, K. L. 1996. Multiple potential germ-line helicases are components of the germ-line-specific P granules of *Caenorhabditis elegans*. *Proc. Natl. Acad. Sci,* 93.

GUALLAR, D. & WANG, J. 2014. RNA-binding proteins in pluripotency, differentiation, and reprogramming. *Front Biol (Beijing),* 9**,** 389-409.

GUIBERT, S., FORNE, T. & WEBER, M. 2012. Global profiling of DNA methylation erasure in mouse primordial germ cells. *Genome Res,* 22**,** 633-41.

GUO, Y., CHENG, H., HUANG, X., GAO, S., YU, H. & ZHOU, R. 2005. Gene structure, multiple alternative splicing, and expression in gonads of zebrafish Dmrt1. *Biochem Biophys Res Commun,* 330**,** 950-7.

GUPTA, T., MARLOW, F. L., FERRIOLA, D., MACKIEWICZ, K., DAPPRICH, J., MONOS, D. & MULLINS, M. C. 2010. Microtubule actin crosslinking factor 1 regulates the Balbiani body and animal-vegetal polarity of the zebrafish oocyte. *PLoS Genet,* 6**,** e1001073.

GUSTAFSON, E. A. & WESSEL, G. M. 2010. Vasa genes: emerging roles in the germ line and in multipotent cells. *Bioessays,* 32**,** 626-37.

GUZMAN-BARCENAS, M. G. & URIBE, M. C. 2019. Superfetation in the viviparous fish *Heterandria formosa* (Poeciliidae). *J Morphol,* 280**,** 756-770.

HA, H., SONG, J., WANG, S., KAPUSTA, A., FESCHOTTE, C., CHEN, K. C. & XING, J. 2014. A comprehensive analysis of piRNAs from adult human testis and their relationship with genes and mobile elements. *BMC Genomics,* 15.

HACKETT, J. A., REDDINGTON, J. P., NESTOR, C. E., DUNICAN, D. S., BRANCO, M. R., REICHMANN, J., REIK, W., SURANI, M. A., ADAMS, I. R. & MEEHAN, R. R. 2012. Promoter DNA methylation couples genome-defence mechanisms to epigenetic reprogramming in the mouse germline. *Development,* 139**,** 3623-32.

HAGLUND, K., NEZIS, I. P. & STENMARK, H. 2011. Structure and functions of stable intercellular bridges formed by incomplete cytokinesis during development. *Commun Integr Biol,* 4**,** 1-9.

HAMAGUCHI, S. 1982. A light- and electron-microscopic study on the migration of primordial germ cells in the teleost, *Oryzias latipes*. *Cell Tissue Res,* 227**,** 139-151.

HAN, B. W. & ZAMORE, P. D. 2014. piRNAs. *Curr Biol,* 24**,** R730-3.

HANASHIMA, C., FERNANDES, M., HEBERT, J. M. & FISHELL, G. 2007. The role of *Foxg1* and dorsal midline signaling in the generation of Cajal-Retzius subtypes. *J Neurosci,* 27**,** 11103-11.

HANASHIMA, C., SHEN, L., LI, S. C. & LAI, E. 2002. *Brain Factor-1* Controls the Proliferation and Differentiation of Neocortical Progenitor Cells through Independent Mechanisms. *J. Neurosci,* 22**,** 6526-6536.

HAO, J., VARSHNEY, R. R. & WANG, D. A. 2008. TGF-beta3: A promising growth factor in engineered organogenesis. *Expert Opin Biol Ther,* 8**,** 1485-93.

HARAGUCHI, S., TSUDA, M., KITAJIMA, S., SASAOKA, Y., NOMURA-KITABAYASHID, A., KUROKAWA, K. & SAGA, Y. 2003. *nanos1*: a mouse *nanos* gene expressed in the central nervous system is dispensable for normal development. *Mechanisms of Development,* 120**,** 721-731.

HARIGAYA, Y. & YAMAMOTO, M. 2007. Molecular mechanisms underlying the mitosis-meiosis decision. *Chromosome Res,* 15**,** 523-37.
HARLEY, V. R. & GOODFELLOW, P. N. 1994. The biochemical role of SRY in sex determination. *Mol Reprod Dev,* 39**,** 184-93.
HARRINGTON, J. R. W. & HARRINGTON, E. S. 1982. Effects on fishes and their forage organisms of impounding a Florida salt marsh to prevent breeding by salt marsh mosquitoes. *Bulletin of Marine Science,* 32**,** 523-531.
HARTUNG, O., FORBES, M. M. & MARLOW, F. L. 2014. Zebrafish vasa is required for germ-cell differentiation and maintenance. *Mol Reprod Dev,* 81**,** 946-61.
HARTWIG, J., TARBASHEVICH, K., SEGGEWISS, J., STEHLING, M., BANDEMER, J., GRIMALDI, C., PAKSA, A., GROSS-THEBING, T., MEYEN, D. & RAZ, E. 2014. Temporal control over the initiation of cell motility by a regulator of G-protein signaling. *Proc Natl Acad Sci U S A,* 111**,** 11389-94.
HASHIMOTO, H., HARA, K., HISHIKI, A., KAWAGUCHI, S., SHICHIJO, N., NAKAMURA, K., UNZAI, S., TAMARU, Y., SHIMIZU, T. & SATO, M. 2010. Crystal structure of zinc-finger domain of Nanos and its functional implications. *EMBO Rep,* 11**,** 848-53.
HE, J., STEWART, K., KINNELL, H. L., ANDERSON, R. A. & CHILDS, A. J. 2013. A developmental stage-specific switch from DAZL to BOLL occurs during fetal oogenesis in humans, but not mice. *PLoS One,* 8**,** e73996.
HEIM, A. E., HARTUNG, O., ROTHHAMEL, S., FERREIRA, E., JENNY, A. & MARLOW, F. L. 2014. Oocyte polarity requires a Bucky ball-dependent feedback amplification loop. *Development,* 141**,** 842-54.
HELLEMANS, J., MORTIER, G., DE PAEPE, A., SPELEMAN, F. & VANDESOMPELE, J. 2007. qBase relative quantification framework and software for management and automated analysis of real-time quantitative PCR data. *Genome Biol,* 8**,** R19.
HEMPEL, L. U., KALAMEGHAM, R., SMITH, J. E. & OLIVER, B. 2008. Drosophila germline sex determination integration of germline autonomous. *Current Topics in Developmental Biology,* 83**,** 109-150.
HENGEN, P. N. 1995. Vectorette, splinkerette and boomerang DNA amplification. *Trends Biochem Sci.,* 20**,** 372-3.
HERPIN, A., FISCHER, P., LIEDTKE, D., KLUEVER, N., NEUNER, C., RAZ, E. & SCHARTL, M. 2008. Sequential SDF1a and b-induced mobility guides Medaka PGC migration. *Dev Biol,* 320**,** 319-27.
HERPIN, A., ROHR, S., RIEDEL, D., KLUEVER, N., RAZ, E. & SCHARTL, M. 2007. Specification of primordial germ cells in medaka (Oryzias latipes). *BMC Dev Biol,* 7**,** 3.
HICKFORD, D. E., FRANKENBERG, S., PASK, A. J., SHAW, G. & RENFREE, M. B. 2011. DDX4 (VASA) is conserved in germ cell development in marsupials and monotremes. *Biol Reprod,* 85**,** 733-43.
HIGUCHI, M. 2020. Maternal stress suppresses cell proliferation in the forebrain of zebrafish larvae. *Genes Cells,* 25**,** 350-357.
HILBERT , M., KAROW, A. R. & KLOSTERMEIER, D. 2009. The mechanism of ATP-dependent RNA unwinding by DEAD box proteins. *Biological Chemistry,* 390**,** 1237-1250.
HILBERT, M., KAROW, A. R. & KLOSTERMEIER, D. 2009. The mechanism of ATP-dependent RNA unwinding by DEAD box proteins. *Biological Chemistry* 390**,** 1237-50.
HILFIKER-KLEINER, D., DÜBENDORFER, A., HILFIKER, A. & NÖTHIGER, R. 1994. Genetic control of sex determination in the germ line and soma of the housefly, *Musca domestica*. *Development,* 120**,** 2531-2538.
HILL, P. W. S., LEITCH, H. G., REQUENA, C. E., SUN, Z., AMOUROUX, R., ROMAN-TRUFERO, M., BORKOWSKA, M., TERRAGNI, J., VAISVILA, R., LINNETT, S., BAGCI, H., DHARMALINGHAM, G., HABERLE, V., LENHARD, B., ZHENG, Y., PRADHAN, S. & HAJKOVA, P. 2018. Epigenetic reprogramming enables the transition from primordial germ cell to gonocyte. *Nature,* 555**,** 392-396.
HOBBS, J. P., MUNDAY, P. L. & JONES, G. P. 2004. Social induction of maturation and sex determination in a coral reef fish. *Proc Biol Sci,* 271**,** 2109-14.

HOLLWAY, G. E., BRYSON-RICHARDSON, R. J., BERGER, S., COLE, N. J., HALL, T. E. & CURRIE, P. D. 2007. Whole-somite rotation generates muscle progenitor cell compartments in the developing zebrafish embryo. *Dev Cell,* 12**,** 207-19.

HONG, N., LI, M., YUAN, Y., WANG, T., YI, M., XU, H., ZENG, H., SONG, J. & HONG, Y. 2016. Dnd Is a Critical Specifier of Primordial Germ Cells in the Medaka Fish. *Stem Cell Reports,* 6**,** 411-21.

HORIGUCHI, R., NOZU, R., HIRAI, T., KOBAYASHI, Y., NAGAHAMA, Y. & NAKAMURA, M. 2013. Characterization of gonadal soma-derived factor expression during sex change in the protogynous wrasse, Halichoeres trimaculatus. *Dev Dyn,* 242**,** 388-99.

HORTH, L. 2003. Melanic body colour and aggressive mating behaviour are correlated traits in male mosquitofish (*Gambusia holbrooki*). *Proc Biol Sci,* 270**,** 1033-40.

HORTH, L. 2004. Predation and the persistence of melanic male mosquitofish (*Gambusia holbrooki*). *J Evol Biol,* 17**,** 672-9.

HORUK, R. 2001. Chemokine receptors. *Cytokine & Growth Factor Reviews,* 12**,** 313-335.

HOU, P. S., HAILIN, D. O., VOGEL, T. & HANASHIMA, C. 2020. Transcription and Beyond: Delineating FOXG1 Function in Cortical Development and Disorders. *Front Cell Neurosci,* 14**,** 35.

HOUDE, E. D. & ZASTROW, C. E. 2000. Ecosystem- and taxon-specific dynamic energetics properties of fish larvae assemblages. *Bull. Mar. Sci,* 53**,** 290-335.

HOUSTON, D. W. & KING, M. L. 2000. A critical role for Xdazl, a germ plasm-localized RNA, in the differentiation of primordial germ cells in *Xenopus*. *Development,* 127**,** 447-456.

HOUSTON., D. W., ZHANG, J., MAINES, J. Z., WASSERMAN, S. A. & KING, M. L. 1998. A *Xenopus* DAZ-like gene encodes an RNA component of germ plasm and is a functional homologue of Drosophila boule. *Development,* 125**,** 171-180.

HOUWING, S. 2009. *Piwi-piRNA complexes in the zebrafish germline.* PhD, Hubrecht Instiute of the Royal Netherlands Academy of Arts and Sciences (KNAW).

HOUWING, S., BEREZIKOV, E. & KETTING, R. F. 2008. Zili is required for germ cell differentiation and meiosis in zebrafish. *EMBO J,* 27**,** 2702-11.

HOUWING, S., KAMMINGA, L. M., BEREZIKOV, E., CRONEMBOLD, D., GIRARD, A., VAN DEN ELST, H., FILIPPOV, D. V., BLASER, H., RAZ, E., MOENS, C. B., PLASTERK, R. H., HANNON, G. J., DRAPER, B. W. & KETTING, R. F. 2007. A role for Piwi and piRNAs in germ cell maintenance and transposon silencing in Zebrafish. *Cell,* 129**,** 69-82.

HOWE, K., CLARK, M. D., TORROJA, C. F., TORRANCE, J., BERTHELOT, C., MUFFATO, M., COLLINS, J. E., HUMPHRAY, S., MCLAREN, K., MATTHEWS, L., MCLAREN, S., SEALY, I., CACCAMO, M., CHURCHER, C., SCOTT, C., BARRETT, J. C., KOCH, R., RAUCH, G. J., WHITE, S., CHOW, W., KILIAN, B., QUINTAIS, L. T., GUERRA-ASSUNCAO, J. A., ZHOU, Y., GU, Y., YEN, J., VOGEL, J. H., EYRE, T., REDMOND, S., BANERJEE, R., CHI, J., FU, B., LANGLEY, E., MAGUIRE, S. F., LAIRD, G. K., LLOYD, D., KENYON, E., DONALDSON, S., SEHRA, H., ALMEIDA-KING, J., LOVELAND, J., TREVANION, S., JONES, M., QUAIL, M., WILLEY, D., HUNT, A., BURTON, J., SIMS, S., MCLAY, K., PLUMB, B., DAVIS, J., CLEE, C., OLIVER, K., CLARK, R., RIDDLE, C., ELLIOT, D., THREADGOLD, G., HARDEN, G., WARE, D., BEGUM, S., MORTIMORE, B., KERRY, G., HEATH, P., PHILLIMORE, B., TRACEY, A., CORBY, N., DUNN, M., JOHNSON, C., WOOD, J., CLARK, S., PELAN, S., GRIFFITHS, G., SMITH, M., GLITHERO, R., HOWDEN, P., BARKER, N., LLOYD, C., STEVENS, C., HARLEY, J., HOLT, K., PANAGIOTIDIS, G., LOVELL, J., BEASLEY, H., HENDERSON, C., GORDON, D., AUGER, K., WRIGHT, D., COLLINS, J., RAISEN, C., DYER, L., LEUNG, K., ROBERTSON, L., AMBRIDGE, K., LEONGAMORNLERT, D., MCGUIRE, S., GILDERTHORP, R., GRIFFITHS, C., MANTHRAVADI, D., NICHOL, S., BARKER, G., et al. 2013. The zebrafish reference genome sequence and its relationship to the human genome. *Nature,* 496**,** 498-503.

HSU, C.-C., KUO, P.-H., LEE, I.-W., SU, M.-T., TSENG, J. T. & KUO, P.-L. 2010. Quantitative trait analysis suggests human *DAZL* may be involved in regulating sperm counts and motility. *Reproductive BioMedicine Online,* 21**,** 77-83.

HUANG, H. Y., HOUWING, S., KAAIJ, L. J., MEPPELINK, A., REDL, S., GAUCI, S., VOS, H., DRAPER, B. W., MOENS, C. B., BURGERING, B. M., LADURNER, P., KRIJGSVELD, J., BEREZIKOV, E. & KETTING, R. F. 2011. Tdrd1 acts as a molecular scaffold for Piwi proteins and piRNA targets in zebrafish. *EMBO J,* 30**,** 3298-308.
HUANG, S., YE, L. & CHEN, H. 2017. Sex determination and maintenance: the role of DMRT1 and FOXL2. *Asian J Androl,* 19**,** 619-624.
HYSLOP, L., STOJKOVIC, M., ARMSTRONG, L., WALTER, T., STOJKOVIC, P., PRZYBORSKI, S., HERBERT, M., MURDOCH, A., STRACHAN, T. & LAKO, M. 2005. Downregulation of NANOG induces differentiation of human embryonic stem cells to extraembryonic lineages. *Stem Cells,* 23**,** 1035-43.
IKENISHI, K. 1998. Germ plasm in *Caenorhabditis elegans*, *Drosophila* and *Xenopus*. *Dev Growth Differ.,* 40**,** 1-10.
IQBAL, K., JIN, S. G., PFEIFER, G. P. & SZABO, P. E. 2011. Reprogramming of the paternal genome upon fertilization involves genome-wide oxidation of 5-methylcytosine. *Proc Natl Acad Sci U S A,* 108**,** 3642-7.
ISHIZU, H., SIOMI, H. & SIOMI, M. C. 2012. Biology of PIWI-interacting RNAs: new insights into biogenesis and function inside and outside of germlines. *Genes Dev,* 26**,** 2361-73.
ISLER, K. 2013. Brain size evolution: how fish pay for being smart. *Curr Biol,* 23**,** R63-5.
IVINS, S., CHAPPELL, J., VERNAY, B., SUNTHARALINGHAM, J., MARTINEAU, A., MOHUN, T. J. & SCAMBLER, P. J. 2015. The CXCL12/CXCR4 Axis Plays a Critical Role in Coronary Artery Development. *Dev Cell,* 33**,** 455-68.
IWAMATSU, T. 2004. Stages of normal development in the medaka *Oryzias latipes*. *Mech Dev,* 121**,** 605-18.
IWASA, S. N., BABONA-PILIPOS, R. & MORSHEAD, C. M. 2017. Environmental Factors That Influence Stem Cell Migration: An "Electric Field". *Stem Cells Int,* 2017**,** 4276927.
IWASAKI, Y. W., SIOMI, M. C. & SIOMI, H. 2015. PIWI-Interacting RNA: Its Biogenesis and Functions. *Annu Rev Biochem,* 84**,** 405-33.
JANIC, A., MENDIZABAL , L., LLAMAZARES, S., ROSSELL, D. & GONZALEZ, C. 2010. Ectopic Expression of Germline Genes Drives Malignant Brain Tumor Growth in *Drosophila*. *Science,* 330**,** 1824-1827.
JARMOSKAITE, I. & RUSSELL, R. 2011. DEAD-box proteins as RNA helicases and chaperones. *Wiley Interdiscip Rev RNA,* 2**,** 135-52.
JASKIEWICZ, L. & FILIPOWICZ, W. 2008. Role of Dicer in posttranscriptional RNA silencing. *Curr Top Microbiol Immunol.,* 320**,** 77-97.
JEHN, J., GEBERT, D., PIPILESCU, F., STERN, S., KIEFER, J. S. T., HEWEL, C. & ROSENKRANZ, D. 2018. PIWI genes and piRNAs are ubiquitously expressed in mollusks and show patterns of lineage-specific adaptation. *Commun Biol,* 1**,** 137.
JESSOP, P., RUZOV, A. & GERING, M. 2018. Developmental Functions of the Dynamic DNA Methylome and Hydroxymethylome in the Mouse and Zebrafish: Similarities and Differences. *Front Cell Dev Biol,* 6**,** 27.
JIANG, L., ZHANG, J., WANG, J. J., WANG, L., ZHANG, L., LI, G., YANG, X., MA, X., SUN, X., CAI, J., ZHANG, J., HUANG, X., YU, M., WANG, X., LIU, F., WU, C. I., HE, C., ZHANG, B., CI, W. & LIU, J. 2013. Sperm, but not oocyte, DNA methylome is inherited by zebrafish early embryos. *Cell,* 153**,** 773-84.
JIN, L. & NEIMAN, A. M. 2016. Post-transcriptional regulation in budding yeast meiosis. *Curr Genet,* 62**,** 313-5.
JINEK, M. & DOUDNA, J. A. 2009. A three-dimensional view of the molecular machinery of RNA interference. *Nature,* 457**,** 405-12.
JOHNSON, A. D. & ALBERIO, R. 2015. Primordial germ cells: the first cell lineage or the last cells standing? *Development,* 142**,** 2730-9.
JOHNSON, A. D., BACHVAROVA, R. F., DRUM, M. & MASI, T. 2001. Expression of axolotl *DAZL* RNA, a marker of germ plasm: widespread maternal RNA and onset of expression in germ cells approaching the gonad. *Dev Biol,* 234**,** 402-15.

JOHNSON, A. D., DRUM, M., BACHVAROVA, R. F., MASI, T., WHITE, M. E. & CROTHER, B. I. 2003. Evolution of predetermined germ cells in vertebrate embryos: implications for macroevolution. *EVOLUTION & DEVELOPMENT,* 5**,** 414-431.
JOHNSON, A. D., RICHARDSON, E., BACHVAROVA, R. F. & CROTHER, B. I. 2011a. Evolution of the germ line-soma relationship in vertebrate embryos. *Reproduction,* 141**,** 291-300.
JOHNSON, E. R. & MCKAY, D. B. 1999. Crystallographic structure of the amino terminal domain of yeast initiation factor 4A, a representative DEAD-box RNA helicase. *RNA,* 5**,** 1526-1534.
JOHNSON, G. D., LALANCETTE, C., LINNEMANN, A. K., LEDUC, F., BOISSONNEAULT, G. & KRAWETZ, S. A. 2011b. The sperm nucleus: chromatin, RNA, and the nuclear matrix. *Reproduction,* 141**,** 21-36.
JOSEPH, S. R., PALFY, M., HILBERT, L., KUMAR, M., KARSCHAU, J., ZABURDAEV, V., SHEVCHENKO, A. & VASTENHOUW, N. L. 2017. Competition between histone and transcription factor binding regulates the onset of transcription in zebrafish embryos. *Elife,* 6.
JUKAM, D., SHARIATI, S. A. M. & SKOTHEIM, J. M. 2017. Zygotic Genome Activation in Vertebrates. *Dev Cell,* 42**,** 316-332.
JUKES, T. H. & CANTOR, C. R. 1969. CHAPTER 24 - Evolution of Protein Molecules. *In:* MUNRO, H. N. (ed.) *Mammalian Protein Metabolism.* New York: Academic Press.
KAGAWA, H. 2013. Oogenesis in Teleost Fish. *Aqua-BioScience Monographs,* 6**,** 99-127.
KAMMINGA, L. M., LUTEIJN, M. J., DEN BROEDER, M. J., REDL, S., KAAIJ, L. J., ROOVERS, E. F., LADURNER, P., BEREZIKOV, E. & KETTING, R. F. 2010. Hen1 is required for oocyte development and piRNA stability in zebrafish. *EMBO J,* 29**,** 3688-700.
KANE, D. A. & KIMMEL, C. B. 1993. The zebrafish midblastula transition. *Development,* 119**,** 447-456.
KANTOR, G. J. & HULL, D. R. 1979. An effect of ultraviolet light on RNA and protein synthesis in nondividing human diploid fibroblasts. *Biophys J.,* 27**,** 359-370.
KARASHIMA, T., SUGIMOTO, A. & YAMAMOTO, M. 2000. *Caenorhabditis elegans* homologue of the human azoospermia factor DAZ is required for oogenesis but not for spermatogenesis. *Development,* 127**,** 1069-1079.
KAUFMAN, O. H., LEE, K., MARTIN, M., ROTHHAMEL, S. & MARLOW, F. L. 2018. rbpms2 functions in Balbiani body architecture and ovary fate. *PLoS Genet,* 14**,** e1007489.
KAUFMAN, O. H. & MARLOW, F. L. 2016a. Chapter 1 - Methods to study maternal regulation of germ cell specification in zebrafish. *The Zebrafish: Cellular and Developmental Biology, Part B Developmental Biology, Volume.* USA: Elsevier Inc.
KAUFMAN, O. H. & MARLOW, F. L. 2016b. Methods to study maternal regulation of germ cell specification in zebrafish. *Methods Cell Biol,* 134**,** 1-32.
KAWASE, E., WONG, M. D., DING, B. C. & XIE, T. 2004. Gbb/Bmp signaling is essential for maintaining germline stem cells and for repressing bam transcription in the Drosophila testis. *Development,* 131**,** 1365-75.
KAYO, D., ZEMPO, B., TOMIHARA, S., OKA, Y. & KANDA, S. 2019. Gene knockout analysis reveals essentiality of estrogen receptor beta1 (Esr2a) for female reproduction in medaka. *Sci Rep,* 9**,** 8868.
KEHLER, J., TOLKUNOVA, E., KOSCHORZ, B., PESCE, M., GENTILE, L., BOIANI, M., LOMELI, H., NAGY, A., MCLAUGHLIN, K. J., SCHOLER, H. R. & TOMILIN, A. 2004. Oct4 is required for primordial germ cell survival. *EMBO Rep,* 5**,** 1078-83.
KELLER, L. F. & WALLER, D. M. 2002. Inbreeding effects in wild populations. *TRENDS in Ecology & Evolution,* 17**,** 230-241.
KETTING, R. F. 2007. A dead end for microRNAs. *Cell,* 131**,** 1226-7.
KIM, K. W. 2019. PIWI Proteins and piRNAs in the Nervous System. *Mol Cells,* 42**,** 828-835.
KIM, M., KI, B. S., HONG, K., PARK, S. P., KO, J. J. & CHOI, Y. 2016. Tudor Domain Containing Protein TDRD12 Expresses at the Acrosome of Spermatids in Mouse Testis. *Asian-Australas J Anim Sci,* 29**,** 944-51.
KIMBLE, J. 2011. Molecular regulation of the mitosis/meiosis decision in multicellular organisms. *Cold Spring Harb Perspect Biol,* 3**,** a002683.
KIMMEL, C. B., BALLARD, W. W., KIMMEL, S. R., ULLMANN, B. & SCHILLING, T. F. 1995. Stages of embryonic development of the zebrafish. *Dev Dyn,* 203**,** 253-310.

KIRINO, Y., VOUREKAS, A., SAYED, N., DE LIMA ALVES, F., THOMSON, T., LASKO, P., RAPPSILBER, J., JONGENS, T. A. & MOURELATOS, Z. 2010. Arginine methylation of Aubergine mediates Tudor binding and germ plasm localization. *RNA,* 16**,** 70-8.
KITAMURA, E., IGARASHI, J., MOROHASHI, A., HIDA, N., OINUMA, T., NORIMICHI NEMOTO, S., FEI , GHOSH, S., HELD, W. A., YOSHIDA-NORO, C. & NAGASE, H. 2007. Analysis of tissue-specific differentially methylated regions (TDMs) in humans. *Genomics,* 89**,** 326-37.
KIUCHI, T., KOGA, H., KAWAMOTO, M., SHOJI, K., SAKAI, H., ARAI, Y., ISHIHARA, G., KAWAOKA, S., SUGANO, S., SHIMADA, T., SUZUKI, Y., SUZUKI, M. G. & KATSUMA, S. 2014. A single female-specific piRNA is the primary determiner of sex in the silkworm. *Nature,* 509**,** 633-6.
KLADWANG, W., HUM, J. & DAS, R. 2012. Ultraviolet shadowing of RNA can cause significant chemical damage in seconds. *Sci Rep,* 2**,** 517.
KNAUT, H., PELEGRI, F., BOHMANN, K., SCHWARZ, H. & NÜSSLEIN-VOLHARD, C. 2000. Zebrafish *vasa* RNA but Not Its Protein Is a Component of the Germ Plasm and Segregates Asymmetrically before Germline Specification. *The Journal of Cell Biology,* 149**,** 875-888.
KNAUT, H., STEINBEISSER, H., SCHWARZ, H. & NUSSLEIN-VOLHARD, C. 2002. An evolutionary conserved region in the *vasa* 3'UTR targets RNA translation to the germ cells in the zebrafish. *Current Biology,* 12**,** 454-466.
KNAUT, H., WERZ, C., GEISLER, R., CONSORTIUM, S. & SSLEIN-VOLHARD, C. N. 2003. A zebrafish homologue of the chemokine receptor Cxcr4 is a germ-cell guidance receptor. *Nature,* 421**,** 279-281.
KOBAYASHI, H. & IWAMATSU, T. 2002. Fine Structure of the Storage Micropocket of Spermatozoa in the Ovary of the Guppy *Poecilia reticulata*. *ZOOLOGICAL SCIENCE,* 19**,** 545-555.
KOBAYASHI, T., MATSUDA, M., KAJIURA-KOBAYASHI, H., SUZUKI, A., SAITO, N., NAKAMOTO, M., SHIBATA, N. & NAGAHAMA, Y. 2004. Two DM domain genes, DMY and DMRT1, involved in testicular differentiation and development in the medaka, Oryzias latipes. *Dev Dyn,* 231**,** 518-26.
KOMEN, H. & THORGAARD, G. H. 2007. Androgenesis, gynogenesis and the production of clones in fishes: A review. *Aquaculture,* 269**,** 150-173.
KOMEN, J., YAMASHITA, M. & NAGAHAMA, Y. 1992. Testicular Development Induced by a Recessive Mutation during Gonadal Differentiation of Female Common Carp (*Cyprinus carpio*, L.). *Develop. Growth Differ,* 34**,** 535-544.
KOOPMAN, P., GUBBAY, J., VIVIAN, N., GOODFELLOW, P. & LOVELL-BADGE, R. 1991. Male development of chromosomally female mice transgenic for *Sry*. *Nature,* 351**,** 117-121.
KOPRUNNER, M., THISSE, C., THISSE, B. & RAZ, E. 2001. A zebrafish nanos-related gene is essential for the development of primordial germ cells. *Genes Dev,* 15**,** 2877-85.
KOSAKA, K., KAWAKAMI, K., SAKAMOTO, H. & INOUE, K. 2007. Spatiotemporal localization of germ plasm RNAs during zebrafish oogenesis. *Mech Dev,* 124**,** 279-89.
KOTIK, M. 2009. Novel genes retrieved from environmental DNA by polymerase chain reaction: Current genome-walking techniques for future metagenome applications. *J Biotechnol.,* 144**,** 75-82.
KOTTLER, V. A., FERON, R., NANDA, I., KLOPP, C., DU, K., KNEITZ, S., HELMPROBST, F., LAMATSCH, D. K., LOPEZ-ROQUES, C., LLUCH, J., JOURNOT, L., PARRINELLO, H., GUIGUEN, Y. & SCHARTL, M. 2020. Independent Origin of XY and ZW Sex Determination Mechanisms in Mosquitofish Sister Species. *Genetics,* 214**,** 193-209.
KOUTSOUVELI, V., CARDENAS, P., SANTODOMINGO, N., MARINA, A., MORATO, E., RAPP, H. T. & RIESGO, A. 2020. The Molecular Machinery of Gametogenesis in Geodia Demosponges (Porifera): Evolutionary Origins of a Conserved Toolkit across Animals. *Mol Biol Evol*.
KOYA, Y., FUJITA, A., NIKI, F., ISHIHARA, E. & MIYAMA, H. 2003. Sex differentiation and pubertal development of gonads in the viviparous mosquitofish, *Gambusia affinis*. *Zoolog Sci,* 20**,** 1231-42.

KRISHNAKUMAR, P., RIEMER, S., PERERA, R., LINGNER, T., GOLOBORODKO, A., KHALIFA, H., BONTEMS, F., KAUFHOLZ, F., EL-BROLOSY, M. A. & DOSCH, R. 2018. Functional equivalence of germ plasm organizers. *PLoS Genet,* 14**,** e1007696.
KU, H. Y. & LIN, H. 2014. PIWI proteins and their interactors in piRNA biogenesis, germline development and gene expression. *Natl Sci Rev,* 1**,** 205-218.
KUERSTEN, S. & GOODWIN, E. B. 2003. The power of the 3' UTR: translational control and development. *Nat Rev Genet,* 4**,** 626-37.
KUFAREVA, I., SALANGA, C. L. & HANDEL, T. M. 2015. Chemokine and chemokine receptor structure and interactions: implications for therapeutic strategies. *Immunol Cell Biol,* 93**,** 372-83.
KUMAR, M., SARMA, D. K., SHUBHAM, S., KUMAWAT, M., VERMA, V., PRAKASH, A. & TIWARI, R. 2020. Environmental Endocrine-Disrupting Chemical Exposure: Role in Non-Communicable Diseases. *Front Public Health,* 8**,** 553850.
KURIMOTO, K., YAMAJI, M., SEKI, Y. & SAITOU, M. 2008. Specification of the germ cell lineage in mice: a process orchestrated by the PR-domain proteins, Blimp1 and Prdm14. *Cell Cycle,* 7**,** 3514-8.
KUROKAWA, H., SAITO, D., NAKAMURA, S., KATOH-FUKUI, Y., OHTA, K., BABA, T., MOROHASHI, K. & TANAKA, M. 2007. Germ cells are essential for sexual dimorphism in the medaka gonad. *Proc Natl Acad Sci U S A,* 104**,** 16958-63.
KUZNICKI, K. A., SMITH, P. A., LEUNG-CHIU, W. M. A., ESTEVEZ, A. O., SCOTT, H. C. & BENNETT, K. L. 2000. Combinatorial RNA interference indicates GLH-4 can compensate for GLH-1; these two P granule components are critical for fertility in *C. elegans*. *development,* 127**,** 2907-2916.
KWAN, T. N. & PATIL, J. G. 2019. Sex biased expression of anti-Mullerian hormone (amh) gene in a live bearing fish, *Gambusia holbrooki*: Evolutionary implications and potential role in sex differentiation. *Comp Biochem Physiol B Biochem Mol Biol,* 231**,** 59-66.
LAI, F., SINGH, A. & KING, M. L. 2012. *Xenopus* Nanos1 is required to prevent endoderm gene expression and apoptosis in primordial germ cells. *Development,* 139**,** 1476-86.
LAI, F., ZHOU, Y., LUO, X., FOX, J. & KING, M. L. 2011. Nanos1 functions as a translational repressor in the *Xenopus* germline. *Mech Dev,* 128**,** 153-63.
LALL, S., LUDWIG, M. Z. & PATEL, N. H. 2003. Nanos Plays a Conserved Role in Axial Patterning outside of the Diptera. *Current Biology,* 13**,** 224-229.
LAU, E. S., ZHANG, Z., QIN, M. & GE, W. 2016. Knockout of Zebrafish Ovarian Aromatase Gene (cyp19a1a) by TALEN and CRISPR/Cas9 Leads to All-male Offspring Due to Failed Ovarian Differentiation. *Sci Rep,* 6**,** 37357.
LEE, H. J., HORE, T. A. & REIK, W. 2014. Reprogramming the methylome: erasing memory and creating diversity. *Cell Stem Cell,* 14**,** 710-9.
LEE, K. C., JANG, Y. H., KIM, S. K., PARK, H. Y., THU, M. P., LEE, J. H. & KIM, J. K. 2017. RRM domain of Arabidopsis splicing factor SF1 is important for pre-mRNA splicing of a specific set of genes. *Plant Cell Rep,* 36**,** 1083-1095.
LEE, M. T., BONNEAU, A. R., TAKACS, C. M., BAZZINI, A. A., DIVITO, K. R., FLEMING, E. S. & GIRALDEZ, A. J. 2013. Nanog, Pou5f1 and SoxB1 activate zygotic gene expression during the maternal-to-zygotic transition. *Nature,* 503**,** 360-4.
LEHMANN, R. & EPHRUSSI, A. 1994. Germ plasm formation and germ cell determination in *Drosophila*. *Ciba Found Symp,* 182**,** 282-300.
LEU, D. H. & DRAPER, B. W. 2010. The ziwi promoter drives germline-specific gene expression in zebrafish. *Dev Dyn,* 239**,** 2714-21.
LEWIS, S. H., QUARLES, K. A., YANG, Y., TANGUY, M., FREZAL, L., SMITH, S. A., SHARMA, P. P., CORDAUX, R., GILBERT, C., GIRAUD, I., COLLINS, D. H., ZAMORE, P. D., MISKA, E. A., SARKIES, P. & JIGGINS, F. M. 2018. Pan-arthropod analysis reveals somatic piRNAs as an ancestral defence against transposable elements. *Nat Ecol Evol,* 2**,** 174-181.
LEWIS, Z. R., MCCLELLAN, M. C., POSTLETHWAIT, J. H., CRESKO, W. A. & KAPLAN, R. H. 2008. Female-specific increase in primordial germ cells marks sex differentiation in threespine stickleback (Gasterosteus aculeatus). *J Morphol,* 269**,** 909-21.

LI, H., LIANG, Z., YANG, J., WANG, D., WANG, H., ZHU, M., GENG, B. & XU, E. Y. 2019. DAZL is a master translational regulator of murine spermatogenesis. *Natl Sci Rev,* 6**,** 455-468.
LI, H., SU, B., QIN, G., YE, Z., ALSAQUFI, A., PERERA, D. A., SHANG, M., ODIN, R., VO, K., DRESCHER, D., ROBINSON, D., ZHANG, D., ABASS, N. & DUNHAM, R. A. 2017. Salt Sensitive Tet-Off-Like Systems to Knockdown Primordial Germ Cell Genes for Repressible Transgenic Sterilization in Channel Catfish, Ictalurus punctatus. *Mar Drugs,* 15.
LI, L., ZHENG, P. & DEAN, J. 2010. Maternal control of early mouse development. *Development,* 137**,** 859-70.
LI, M., HONG, N., GUI, J.-F. & HONG, Y. 2012a. Medaka piwi is essential for primordial germ cell migration. *Curr Mol Med,* 12**,** 1040-9.
LI, M., HONG, N., GUI, J. & HONG, Y. 2012b. Medaka piwi is essential for primordial germ cell migration. *Curr Mol Med,* 12**,** 1040-9.
LI, M., HONG, N., XU, H., YI, M., LI, C., GUI, J. & HONG, Y. 2009. Medaka vasa is required for migration but not survival of primordial germ cells. *Mech Dev,* 126**,** 366-81.
LI, M., SHEN, Q., XU, H., WONG, F. M., CUI, J., LI, Z., HONG, N., WANG, L., ZHAO, H., MA, B. & HONG, Y. 2011. Differential conservation and divergence of fertility genes boule and dazl in the rainbow trout. *PLoS One,* 6**,** e15910.
LI, M., TAN, X., JIAO, S., WANG, Q., WU, Z., YOU, F. & ZOU, Y. 2015. A new pattern of primordial germ cell migration in olive flounder (Paralichthys olivaceus) identified using nanos3. *Dev Genes Evol,* 225**,** 195-206.
LI, M., ZHU, F., LI, Z., HONG, N. & HONG, Y. 2016. Dazl is a critical player for primordial germ cell formation in medaka. *Sci Rep,* 6**,** 28317.
LIAO, H., CHEN, Y., LI, Y., XUE, S., LIU, M., LIN, Z., LIU, Y., CHAN, H. C., ZHANG, X. & SUN, H. 2018. CFTR is required for the migration of primordial germ cells during zebrafish early embryogenesis. *Reproduction,* 156**,** 261-268.
LICATALOSI, D. D., YANO, M., FAK, J. J., MELE, A., GRABINSKI, S. E., ZHANG, C. & DARNELL, R. B. 2012. Ptbp2 represses adult-specific splicing to regulate the generation of neuronal precursors in the embryonic brain. *Genes Dev,* 26**,** 1626-42.
LIN, Y. M., CHEN, C. W., SUN, H. S., JENGTSAI, S., LIN, J. S. N. & KUO, P. L. 2002. Presence of DAZL transcript and protein in mature human spermatozoa. *Fertility and Sterility,* 77**,** 626-629.
LINDEMAN, L. C., WINATA, C. L., AANES, H., MATHAVAN, S., ALESTROM, P. & COLLAS, P. 2010. Chromatin states of developmentally-regulated genes revealed by DNA and histone methylation patterns in zebrafish embryos. *Int J Dev Biol,* 54**,** 803-13.
LINDEMAN, R. E. & PELEGRI, F. 2010. Vertebrate maternal-effect genes: Insights into fertilization, early cleavage divisions, and germ cell determinant localization from studies in the zebrafish. *Mol Reprod Dev,* 77**,** 299-313.
LINDER, P. 2006. Dead-box proteins: a family affair--active and passive players in RNP-remodeling. *Nucleic Acids Res,* 34**,** 4168-80.
LINDER, P. & JANKOWSKY, E. 2011. From unwinding to clamping — the DEAD box RNA helicase family. *Nature Reviews molecular cell biology,* 12**,** 505-516.
LING, X., XIE, B., GAO, X., CHANG, L., ZHENG, W., CHEN, H., HUANG, Y., TAN, L., LI, M. & LIU, T. 2020. Improving the efficiency of precise genome editing with site-specific Cas9-oligonucleotide conjugates. *Sci. Adv.,* 6**,** 1-8.
LINGEL, A., SIMON, B., IZAURRALDE, E. & SATTLER, M. 2003. Structure and nucleic-acid binding of the *Drosophila* Argonaute 2 PAZ domain. *Nature,* 426**,** 465-9.
LINGEL, A., SIMON, B., IZAURRALDE, E. & SATTLER, M. 2004. Nucleic acid 3′-end recognition by the Argonaute2 PAZ domain. *nature structural & molecular biology,* 11**,** 576-577.
LIU, G., WANG, W., HU, S., WANG, X. & ZHANG, Y. 2018a. Inherited DNA methylation primes the establishment of accessible chromatin during genome activation. *Genome Research,* 28**,** 998-1007.

LIU, N., HAN, H. & LASKO, P. 2009. Vasa promotes Drosophila germline stem cell differentiation by activating mei-P26 translation by directly interacting with a (U)-rich motif in its 3' UTR. *Genes Dev,* 23**,** 2742-52.
LIU, Y., YANG, H., TORRES, L. & TIERSCH, T. R. 2018b. Activation of free sperm and dissociation of sperm bundles (spermatozeugmata) of an endangered viviparous fish, Xenotoca eiseni. *Comp Biochem Physiol A Mol Integr Physiol,* 218**,** 35-45.
LIU, Y., ZHU, Z., HO, I. H. T., SHI, Y., LI, J., WANG, X., CHAN, M. T. V. & CHENG, C. H. K. 2020. Genetic Deletion of miR-430 Disrupts Maternal-Zygotic Transition and Embryonic Body Plan. *Front Genet,* 11**,** 853.
LIVAK, K. J. & SCHMITTGEN, T. D. 2001. Analysis of relative gene expression data using real-time quantitative PCR and the 2(-Delta Delta C(T)) Method. *Methods,* 25**,** 402-8.
LLOYD, L. N., ARTHINGTON, A. H. & MILTON, D. A. 1986. The mosquitofish – a valuable mosquito-control agent or a pest? *The Ecology of Exotic Animals and Plants Some Australian Case Histories.* Brisbane: John Wiley & Sons.
LO, K. H., HUI, M. N. Y., YU, R. M. K., WU, R. S. S. & CHENG, S. H. 2011. Hypoxia Impairs Primordial Germ Cell Migration in Zebrafish (Danio rerio) Embryos. *PLoS ONE,* 6.
LOPEZ-SEPULCRE, A., GORDON, S. P., PATERSON, I. G., BENTZEN, P. & REZNICK, D. N. 2013. Beyond lifetime reproductive success: the posthumous reproductive dynamics of male Trinidadian guppies. *Proc Biol Sci,* 280**,** 20131116.
LOWE, S., BOUDJELAS, S. & DE POORTER, M. 2000. World's Worst Invasive Alien Species A selection from the Global Invasive Species Database. *(IUCN/SSC Invasive Species Specialist Group (ISSG); Auckland).*
LUBZENS, E., YOUNG, G., BOBE, J. & CERDA, J. 2010. Oogenesis in teleosts: how eggs are formed. *Gen Comp Endocrinol,* 165**,** 367-89.
LYNCH, K. S., RAMSEY, M. E. & CUMMINGS, M. E. 2012. The mate choice brain: comparing gene profiles between female choice and male coercive poeciliids. *Genes Brain Behav,* 11**,** 222-9.
MA, J. B., YE, K. & PATEL, D. J. 2004. Structural basis for overhang-specific small interfering RNA recognition by the PAZ domain. *Nature,* 429**,** 318-322.
MA, X., WANG, S., DO, T., SONG, X., INABA, M., NISHIMOTO, Y., LIU, L. P., GAO, Y., MAO, Y., LI, H., MCDOWELL, W., PARK, J., MALANOWSKI, K., PEAK, A., PERERA, A., LI, H., GAUDENZ, K., HAUG, J., YAMASHITA, Y., LIN, H., NI, J. Q. & XIE, T. 2014. Piwi is required in multiple cell types to control germline stem cell lineage development in the Drosophila ovary. *PLoS One,* 9**,** e90267.
MAATOUK, D. M., MORK, L., HINSON, A., KOBAYASHI, A., MCMAHON, A. P. & CAPEL, B. 2012. Germ cells are not required to establish the female pathway in mouse fetal gonads. *PLoS One,* 7**,** e47238.
MACDONALD, J. & TONKIN, Z. 2008. A review of the impact of eastern gambusia on native fishes of the Murray-Darling Basin. Heidelberg, Victoria: Arthur Rylah Institute for Environmental Research, Department of Sustainability and Environment.
MACDONALD, J. I., TONKIN, Z. D., RAMSEY, D. S. L., KAUS, A. K., KING, A. K. & CROOK, D. A. 2012. Do invasive eastern gambusia (Gambusia holbrooki) shape wetland fish assemblage structure in south-eastern Australia? *Marine and Freshwater Research,* 63.
MAGALHÃES, A. L. B. & JACOBI, C. M. 2017. Colorful invasion in permissive Neotropical ecosystems: establishment of ornamental non-native poeciliids of the genera Poecilia/Xiphophorus (Cyprinodontiformes: Poeciliidae) and management alternatives. *Neotropical Ichthyology,* 15.
MAKEYEV, E. V., ZHANG, J., CARRASCO, M. A. & MANIATIS, T. 2007. The MicroRNA miR-124 promotes neuronal differentiation by triggering brain-specific alternative pre-mRNA splicing. *Mol Cell,* 27**,** 435-48.
MARBUAH, G., GREN, I.-M. & MCKIE, B. 2014. Economics of Harmful Invasive Species: A Review. *Diversity,* 6**,** 500-523.
MARCHLER-BAUER, A., DERBYSHIRE, M. K., GONZALES, N. R., LU, S., CHITSAZ, F., GEER, L. Y., GEER, R. C., HE, J., GWADZ, M., HURWITZ, D. I., LANCZYCKI, C. J., LU, F., MARCHLER, G. H., SONG, J. S., THANKI, N., WANG, Z., YAMASHITA, R. A.,

ZHANG, D., ZHENG, C. & BRYANT, S. H. 2015. CDD: NCBI's conserved domain database. *Nucleic Acids Res,* 43**,** D222-6.
MARIS, C., DOMINGUEZ, C. & ALLAIN, F. H. 2005. The RNA recognition motif, a plastic RNA-binding platform to regulate post-transcriptional gene expression. *FEBS J,* 272**,** 2118-31.
MARLOW, F. 2010a. *Maternal Control of Development in Vertebrates: My Mother Made Me Do It!,* San Rafael (CA):, Morgan & Claypool Life Sciences.
MARLOW, F. L. 2010b. Oogenesis: From Germline Stem Cells to Germline Cysts. *Maternal Control of Development in Vertebrates; My Mother Made Me Do It!* USA: Morgan & Claypool Life Sciences.
MARLOW, F. L. & MULLINS, M. C. 2008. Bucky ball functions in Balbiani body assembly and animal-vegetal polarity in the oocyte and follicle cell layer in zebrafish. *Dev Biol,* 321**,** 40-50.
MASUYAMA, H., YAMADA, M., KAMEI, Y., FUJIWARA-ISHIKAWA, T., TODO, T., NAGAHAMA, Y. & MATSUDA, M. 2012. Dmrt1 mutation causes a male-to-female sex reversal after the sex determination by Dmy in the medaka. *Chromosome Res,* 20**,** 163-76.
MATHEWS, W. R., ONG, D., MILUTINOVICH, A. B. & VAN DOREN, M. 2006. Zinc transport activity of Fear of Intimacy is essential for proper gonad morphogenesis and DE-cadherin expression. *Development,* 133**,** 1143-53.
MATSON, C. K., MURPHY, M. W., SARVER, A. L., GRISWOLD, M. D., BARDWELL, V. J. & ZARKOWER, D. 2011. DMRT1 prevents female reprogramming in the postnatal mammalian testis. *Nature,* 476**,** 101-4.
MATSUDA, M., NAGAHAMA, Y., SHINOMIYA, A., SATO, T., MATSUDA, C., KOBAYASHI, T., MORREY, C. E., SHIBATA, N., ASAKAWA, S., SHIMIZU, N., HORIK, H., HAMAGUCHI, S. & SAKAIZUMI, M. 2002. DMY is a Y-specific DM-domain gene required for male development in the medaka fish. *Nature,* 417.
MATSUZAKI, H., KURAMOCHI, D., OKAMURA, E., HIRAKAWA, K., USHIKI, A. & TANIMOTO, K. 2020. Recapitulation of gametic DNA methylation and its post-fertilization maintenance with reassembled DNA elements at the mouse Igf2/H19 locus. *Epigenetics Chromatin,* 13**,** 2.
MCLAUREN, A. 1981. The fate of germ cells in the testis of fetal Sex-reversed mice. *J Reprod Fertil.,* 61**,** 461-7.
MCLEOD, R. 2004. *Counting the Cost: Impact of Invasive Animals in Australia, 2004,* Canberra, Australia, Cooperative Research Centre for Pest Animal Control.
MEDIONI, C., MOWRY, K. & BESSE, F. 2012. Principles and roles of mRNA localization in animal development. *Development,* 139**,** 3263-76.
MEDRANO, J. V., RAMATHAL, C., NGUYEN, H. N., SIMON, C. & REIJO PERA, R. A. 2012. Divergent RNA-binding proteins, DAZL and VASA, induce meiotic progression in human germ cells derived in vitro. *Stem Cells,* 30**,** 441-51.
MEFFE, G. K. 1992. Plasticity of life-history characters in eastern mosquitofish (*Gambusia holbrooki*: Poeciliidae) in response to thermal stress. *Copeia***,** 94-102.
MEFFE, K. G., SNELSON, F. F., HALL, P. & CLIFF, E. 1990. Ecology and evolution of livebearing fish (Poecilidae). *Science,* 248**,** 502-503.
MEI, W., JIN, Z., LAI, F., SCHWEND, T., HOUSTON, D. W., KING, M. L. & YANG, J. 2013. Maternal Dead-End1 is required for vegetal cortical microtubule assembly during *Xenopus* axis specification. *Development,* 140**,** 2334-44.
MICKOLEIT, M., BANISCH, T. U. & RAZ, E. 2011. Regulation of hub mRNA stability and translation by miR430 and the dead end protein promotes preferential expression in zebrafish primordial germ cells. *Dev Dyn,* 240**,** 695-703.
MIESEN, P., GIRARDI, E. & VAN RIJ, R. P. 2015. Distinct sets of PIWI proteins produce arbovirus and transposon-derived piRNAs in Aedes aegypti mosquito cells. *Nucleic Acids Res,* 43**,** 6545-56.
MIKEDIS, M. M., FAN, Y., NICHOLLS, P. K., ENDO, T., JACKSON, E. K., COBB, S. A., DE ROOIJ, D. G. & PAGE, D. C. 2020. DAZL mediates a broad translational program regulating expansion and differentiation of spermatogonial progenitors. *BioRxiv*.

MIKI, K., WILLIS, W. D., BROWN, P. R., GOULDING, E. H., FULCHER, K. D. & EDDY, E. M. 2002. Targeted disruption of the Akap4 gene causes defects in sperm flagellum and motility. *Dev Biol,* 248**,** 331-42.

MILTON, D. A. & ARTHINGTON, A. H. 1983. Reproductive biology of *Gambusia affinis holbrooki* Baird and Girard, *Xiphophorus helleri* (Gunther) and *X. maculatus* (Heckel) (Pisces; Poeciliidae) in Queensland, Australia. *J. Fish Biol.,* 23**,** 23-41.

MININA, S., REICHMAN-FRIED, M. & RAZ, E. 2007. Control of receptor internalization, signaling level, and precise arrival at the target in guided cell migration. *Curr Biol,* 17**,** 1164-72.

MISHIMA, Y. 2012. Widespread roles of microRNAs during zebrafish development and beyond. *Dev Growth Differ,* 54**,** 55-65.

MISHIMA, Y., GIRALDEZ, A., TAKEDA, Y. & FUJIWARA, T. 2006. Differential Regulation of Germline mRNAs in Soma and Germ Cells by Zebrafish miR-430. *Current Biology,* 16**,** 2135-42.

MITA, K. & YAMASHITA, M. 2000. Expression of *Xenopus* Daz-like protein during gametogenesis and embryogenesis. *Mechanisms of Development,* 94**,** 251-255.

MITSUI, K., TOKUZAWA, Y., ITOH, H., SEGAWA, K., MURAKAMI, M., TAKAHASHI, K., MARUYAMA, M., MAEDA, M. & YAMANAKA, S. 2003. The Homeoprotein Nanog Is Required for Maintenance of Pluripotency in Mouse Epiblast and ES Cells. *Cell,* 113**,** 631-642.

MIURA, T., MIURA, C., KONDA, Y. & YAMAUCHI, K. 2002. Spermatogenesis-preventing substance in Japanese eel. *Development,* 129**,** 2689-2697.

MIYAHARA, K., SHIOKAWA, K. & YAMANA, K. 1982. Cellular commitment for post-gastrular increase in alkaline phosphatase activity in *Xenopus laevis* development. *Differentiation,* 21**,** 45-9.

MIYOSHI, G. & FISHELL, G. 2012. Dynamic FoxG1 expression coordinates the integration of multipolar pyramidal neuron precursors into the cortical plate. *Neuron,* 74**,** 1045-58.

MIYOSHI, T., ITO, K., MURAKAMI, R. & UCHIUMI, T. 2016. Structural basis for the recognition of guide RNA and target DNA heteroduplex by Argonaute. *Nat Commun,* 7**,** 11846.

MONNIAUX, D., DROUILHET, L., RICO, C., ESTIENNE, A., JARRIER, P., TOUZE, J. L., SAPA, J., PHOCAS, F., DUPONT, J., DALBIES-TRAN, R. & FABRE, S. 2013. Regulation of anti-Mullerian hormone production in domestic animals. *Reprod Fertil Dev,* 25**,** 1-16.

MORINAGA, C., TOMONAGA, T., SASADO, T., SUWA, H., NIWA, K., YASUOKA, A., HENRICH, T., WATANABE, T., DEGUCHI, T., YODA, H., HIROSE, Y., IWANAMI, N., KUNIMATSU, S., OKAMOTO, Y., YAMANAKA, T., SHINOMIYA, A., TANAKA, M., KONDOH, H. & FURUTANI-SEIKI, M. 2004. Mutations affecting gonadal development in Medaka, *Oryzias latipes*. *Mech Dev,* 121**,** 829-39.

MOROHASHI, K. I. & OMURA, T. 1996. Ad4BP/SF-1, a transcription factor essential for the transcription of steroidogenic cytochrome P450 genes and for the establishment of the reproductive function. *FASEB J,* 10**,** 1569-77.

MOSQUERA, L., FORRISTALL, C., ZHOU, Y. & KING, M. L. 1993. A mRNA localized to the vegetal cortex of *Xenopus* oocytes encodes a protein with a nanos-like zinc finger domain. *Development,* 117**,** 377-386.

MOUSAVI, S. E. 2021. *Sex Differentiation and Determination in the Invasive Fish, Gambusia holbrooki.* Ph.D., University of Tasmania.

MULLINS, M. C., HAMMERSCHMIDT, M., HAFFTER, P. & NÜSSLEIN-VOLHARD, C. 1994. Large-scale mutagenesis in the zebrafish: in search of genes controlling development in a vertebrate. *Current Biology,* 4**,** 189-202.

MURRAY, S. M., YANG, S. Y. & VAN DOREN, M. 2010. Germ cell sex determination: a collaboration between soma and germline. *Curr Opin Cell Biol,* 22**,** 722-9.

NAGAHAMA, Y. 2005. Molecular mechanisms of sex determination and gonadal sex differentiation in fish. *Fish Physiol Biochem,* 31**,** 105-9.

NAGASAWA, K., FERNANDES, J. M., YOSHIZAKI, G., MIWA, M. & BABIAK, I. 2013. Identification and migration of primordial germ cells in Atlantic salmon, *Salmo salar*: characterization of *vasa*, *dead end*, and *lymphocyte antigen 75* genes. *Mol Reprod Dev,* 80**,** 118-31.

NAGASAWA, T., TACHIBANA, K. & KAWABATA, K. 1999. A CXC chemokine SDF-1/PBSF: a ligand for a HIV coreceptor, CXCR4. *Adv Immunol,* 71**,** 211-228.
NAKAMOTO, M., MATSUDA, M., WANG, D. S., NAGAHAMA, Y. & SHIBATA, N. 2006. Molecular cloning and analysis of gonadal expression of *Foxl2* in the medaka, *Oryzias latipes*. *Biochem Biophys Res Commun,* 344**,** 353-61.
NAKAMURA, S., KOBAYASHI, D., AOKI, Y., YOKOI, H., EBE, Y., WITTBRODT, J. & TANAKA, M. 2006. Identification and lineage tracing of two populations of somatic gonadal precursors in medaka embryos. *Dev Biol,* 295**,** 678-88.
NANDA, I., KONDO, M., HORNUNG, U., ASAKAWA, S., WINKLER, C., SHIMIZU, A., SHAN, Z., HAAF, T., SHIMIZU, N., SHIMA, A., SCHMID, M. & SCHARTL‡, M. 2002. A duplicated copy of DMRT1 in the sex-determining region of the Y chromosome of the medaka, *Oryzias latipes*. *PNAS,* 99**,** 11778-83.
NANDI, S., CHANDRAMOHAN, D., FIORITI, L., MELNICK, A. M., HEBERT, J. M., MASON, C. E., RAJASETHUPATHY, P. & KANDEL, E. R. 2016. Roles for small noncoding RNAs in silencing of retrotransposons in the mammalian brain. *Proc Natl Acad Sci U S A,* 113**,** 12697-12702.
NGUYEN, H., BELL, J. D. & PATIL, J. G. 2021. Daily ageing to delineate population dynamics of the invasive fish Gambusia holbrooki: implications for management and control. *Biological Invasions*.
NICO, L. G., FULLER, P. & NEILSON, M. E. 2019. *Gambusia holbrooki* Girard, 1859. 4/1/2016 ed. Gainesville, FL: U.S. Geological Survey, Nonindigenous Aquatic Species Database.
NIELSEN, C. B., SHOMRON, N., SANDBERG, R., HORNSTEIN, E., KITZMAN, J. & BURGE, C. B. 2007. Determinants of targeting by endogenous and exogenous microRNAs and siRNAs. *RNA,* 13**,** 1894-910.
NIEPEL, M., LING, J. & GALLIE, D. R. 1999. Secondary structure in the 5'-leader or 3'-untranslated region reduces protein yield but does not affect the functional interaction between the 5'-cap and the poly(A) tail. *FEBS Letters,* 462**,** 79-84.
NIETFELD, W., MENTZEL, H. & PIELER, T. 1990. The *Xenopus* laevis poly(A) binding protein is composed of multiple functionally independent RNA binding domains. *EMBO J,* 9**,** 3699-3705.
NIKOLIC, A., VOLAREVIC, V., ARMSTRONG, L., LAKO, M. & STOJKOVIC, M. 2016. Primordial Germ Cells: Current Knowledge and Perspectives. *Stem Cells Int,* 2016**,** 1741072.
NISHIMURA, T., SATO, T., YAMAMOTO, Y., WATAKABE, I., OHKAWA, Y., SUYAMA, M., KOBAYASHI, S. & TANAKA, M. 2015. *foxl3* is a germ cell–intrinsic factor involved in sperm-egg fate decision in medaka. *Science,* 349**,** 328-331.
NISHIMURA, T. & TANAKA, M. 2014. Gonadal development in fish. *Sex Dev,* 8**,** 252-61.
NISHIMURA, T., YAMADA, K., FUJIMORI, C., KIKUCHI, M., KAWASAKI, T., SIEGFRIED, K. R., SAKAI, N. & TANAKA, M. 2018. Germ cells in the teleost fish medaka have an inherent feminizing effect. *PLoS Genet,* 14**,** e1007259.
NIVELLE, R., GENNOTTE, V., KALALA, E. J. K., NGOC, N. B., MULLER, M., MELARD, C. & ROUGEOT, C. 2019. Temperature preference of Nile tilapia (Oreochromis niloticus) juveniles induces spontaneous sex reversal. *PLoS One,* 14**,** e0212504.
NOBREGA, R. H., GREEBE, C. D., VAN DE KANT, H., BOGERD, J., DE FRANCA, L. R. & SCHULZ, R. W. 2010. Spermatogonial stem cell niche and spermatogonial stem cell transplantation in zebrafish. *PLoS One,* 5.
NOGUCHI, T. & NOGUCHI, M. 1985. A recessive mutation (ter) causing germ cell deficiency and a high incidence of congenital testicular teratomas in 129/Sv-ter mice. *Journal of the National Cancer Institute,* 75**,** 385-392.
NOJIMA, H., ROTHHAMEL, S., SHIMIZU, T., KIM, C. H., YONEMURA, S., MARLOW, F. L. & HIBI, M. 2010. Syntabulin, a motor protein linker, controls dorsal determination. *Development,* 137**,** 923-33.
NORAZMI-LOKMAN, N. H. 2016. *Hormonal Feminization and Associated Reproductive Impacts in the Eastern Mosquitofish Gambusia holbrooki*. PhD, University of Tasmania.

NORAZMI-LOKMAN, N. H., PURSER, G. J. & PATIL, J. G. 2016. Gravid Spot Predicts Developmental Progress and Reproductive Output in a Livebearing Fish, *Gambusia holbrooki*. *PLoS One,* 11**,** e0147711.
NORTHRUP, E., ZSCHEMISCH, N. H., EISENBLATTER, R., GLAGE, S., WEDEKIND, D., CUPPEN, E., DORSCH, M. & HEDRICH, H. J. 2012. The ter mutation in the rat Dnd1 gene initiates gonadal teratomas and infertility in both genders. *PLoS One,* 7**,** e38001.
NOUSCH, M., TECHRITZ, N., HAMPEL, D., MILLONIGG, S. & ECKMANN, C. R. 2013. The Ccr4-Not deadenylase complex constitutes the main poly(A) removal activity in C. elegans. *J Cell Sci,* 126**,** 4274-85.
OKUTSU, T., SUZUKI, K., TAKEUCHI, Y., TAKEUCHI, T. & YOSHIZAKI, G. 2006. Testicular germ cells can colonize sexually undifferentiated embryonic gonad and produce functional eggs in fish. *103,* 8**,** 2725-2729.
OLIVERA-TLAHUEL, C., MORENO-MENDOZA, N. A., VILLAGRÁN-SANTA CRUZ, M. & ZÚÑIGA-VEGA, J. J. 2018. Placental structures and their association with matrotrophy and superfetation in poeciliid fishes. *Acta Zoologica*.
ONICHTCHOUK, D. 2012. Pou5f1/oct4 in pluripotency control: insights from zebrafish. *Genesis,* 50**,** 75-85.
OSTERMEIER, G. C., DIX, D. J., MILLER, D., KHATRI, P. & KRAWETZ, S. A. 2002. Spermatozoal RNA profiles of normal fertile men. *The Lancet,* 360**,** 772-777.
OTTO, R. G. 1973. Temperature tolerance of the mosquitofish, *Gambusia afinis. J Fish Biol,* 5**,** 575-583.
OTTOLENGHI, C., OMARI, S., GARCIA-ORTIZ, J. E., UDA, M., CRISPONI, L., FORABOSCO, A., PILIA, G. & SCHLESSINGER, D. 2005. Foxl2 is required for commitment to ovary differentiation. *Hum Mol Genet,* 14**,** 2053-62.
PAKSA, A. & RAZ, E. 2015. Zebrafish germ cells: motility and guided migration. *Curr Opin Cell Biol,* 36**,** 80-5.
PALAKODETI, D., SMIELEWSKA, M., LU, Y. C., YEO, G. W. & GRAVELEY, B. R. 2008. The PIWI proteins SMEDWI-2 and SMEDWI-3 are required for stem cell function and piRNA expression in planarians. *RNA,* 14**,** 1174-86.
PALTI, Y., LI, J. J. & THORGAARD, G. H. 1997. Improved Efficiency of Heat and Pressure Shocks for Producing Gynogenetic Rainbow Trout. *The Progressive Fish-Culturist,* 59**,** 1-13.
PAN, J., GOODHEART, M., CHUMA, S., NAKATSUJI, N., PAGE, D. C. & WANG, P. J. 2005. RNF17, a component of the mammalian germ cell nuage, is essential for spermiogenesis. *Development,* 132**,** 4029-4039.
PAN, Z. J., ZHU, C. K., WANG, H., ZHOU, F. J. & QIANG, X. G. 2017. Gonadal morphogenesis and sex differentiation in cultured Ussuri catfish Tachysurus ussuriensis. *J Fish Biol,* 91**,** 866-879.
PANINA, Y., GERMOND, A., MASUI, S. & WATANABE, T. M. 2018. Validation of Common Housekeeping Genes as Reference for qPCR Gene Expression Analysis During iPS Reprogramming Process. *Sci Rep,* 8**,** 8716.
PARENTI, L. R., LONOSTRO, F. L. & GRIER, H. J. 2010. Reproductive histology of *Tomeurus gracilis* Eigenmann, 1909 (Teleostei: Atherinomorpha: Poeciliidae) with comments on evolution of viviparity in atherinomorph fishes. *J Morphol,* 271**,** 1399-406.
PASQUIER, J., CABAU, C., NGUYEN, T., JOUANNO, E., SEVERAC, D., BRAASCH, I., JOURNOT, L., PONTAROTTI, P., KLOPP, C., POSTLETHWAIT, J. H., GUIGUEN, Y. & BOBE, J. 2016. Gene evolution and gene expression after whole genome duplication in fish: the PhyloFish database. *BMC Genomics,* 17**,** 368.
PATIL, J. G. 2012. An adaptive genetic management plan for eradication of *Gambusia holbrooki* from Tasmania Australia. New Norfolk, Tasmania: Inland Fisheries Service.
PATIL, J. G. & GUNASEKERA, R. M. 2008. Tissue and sexually dimorphic expression of ovarian and brain aromatase mRNA in the Japanese medaka (Oryzias latipes): implications for their preferential roles in ovarian and neural differentiation and development. *Gen Comp Endocrinol,* 158**,** 131-7.

PATIL, J. G., NORAZMI-LOKMAN, N. H. & KWAN, T. N. 2020. Reproductive viability of paradoxically masculinised *Gambusia holbrooki* generated following diethylstilbestrol (DES) treatment. *Comparative Biochemistry and Physiology. Part B,* 248**,** 1-7.
PEPLING, M. E., WILHELM, J. E., O'HARA, A. L., GEPHARDT, G. W. & SPRADLING, A. C. 2007. Mouse oocytes within germ cell cysts and primordial follicles contain a Balbiani body. *PNAS,* 104**,** 187-192.
PEREZ-CAMPS, M., TIAN, J., CHNG, S. C., SEM, K. P., SUDHAHARAN, T., TEH, C., WACHSMUTH, M., KORZH, V., AHMED, S. & REVERSADE, B. 2016. Quantitative imaging reveals real-time Pou5f3-Nanog complexes driving dorsoventral mesendoderm patterning in zebrafish. *Elife,* 5.
PHAM, H. Q. & ARUKWE, A. 2013. Effects of dopamine 2 receptor antagonist on sex steroid levels, oocyte maturation and spawning performances in Waigieu seaperch (Psammoperca waigiensis). *Fish Physiol Biochem,* 39**,** 403-11.
PICARD, M. A., COSSEAU, C., MOUAHID, G., DUVAL, D., GRUNAU, C., TOULZA, E., ALLIENNE, J. F. & BOISSIER, J. 2015. The roles of Dmrt (Double sex/Male-abnormal-3 Related Transcription factor) genes in sex determination and differentiation mechanisms: Ubiquity and diversity across the animal kingdom. *C R Biol,* 338**,** 451-62.
PIFERRER, F. 2001. Endocrine sex control strategies for the feminization of teleost fish. *Aquaculture,* 197**,** 229-281.
PIFERRER, F., BEAUMONT, A., FALGUIÈRE, J.-C., FLAJŠHANS, M., HAFFRAY, P. & COLOMBO, L. 2009. Polyploid fish and shellfish: Production, biology and applications to aquaculture for performance improvement and genetic containment. *Aquaculture,* 293**,** 125-156.
PIRES, M. N., ARENDT, J. & REZNICK, D. N. 2010. The evolution of placentas and superfetation in the fish genus Poecilia (Cyprinodontiformes: Poeciliidae: subgenera *Micropoecilia* and *Acanthophacelus*). *Biological Journal of the Linnean Society,* 99**,** 784-796.
POLLUX, B. J., MEREDITH, R. W., SPRINGER, M. S., GARLAND, T. & REZNICK, D. N. 2014. The evolution of the placenta drives a shift in sexual selection in livebearing fish. *Nature,* 513**,** 233-6.
POLLUX, B. J. A., PIRES, M. N., BANET, A. I. & REZNICK, D. N. 2009. Evolution of Placentas in the Fish Family Poeciliidae: An Empirical Study of Macroevolution. *Annual Review of Ecology, Evolution, and Systematics,* 40**,** 271-289.
POTOK, M. E., NIX, D. A., PARNELL, T. J. & CAIRNS, B. R. 2013. Reprogramming the maternal zebrafish genome after fertilization to match the paternal methylation pattern. *Cell,* 153**,** 759-72.
PRADHAN, A. & OLSSON, P. E. 2015. Inhibition of retinoic acid synthesis disrupts spermatogenesis and fecundity in zebrafish. *Gen Comp Endocrinol,* 217-218**,** 81-91.
PRESSLAUER, C., BIZUAYEHU, T. T., RAZMI, K., FERNANDES, J. M. & BABIAK, I. 2016. See-Thru-Gonad zebrafish line: developmental and functional validation. *Reproduction,* 152**,** 507-17.
PRESSLAUER, C., NAGASAWA, K., FERNANDES, J. M. O. & BABIAK, I. 2012. Expression of *vasa* and *nanos3* during primordial germ cell formation and migration in Atlantic cod (*Gadus morhua L.*). *Theriogenology,* 78**,** 1262-77.
PROOST, P., MORTIER, A., LOOS, T., VANDERCAPPELLEN, J., GOUWY, M., RONSSE, I., SCHUTYSER, E., PUT, W., PARMENTIER, M., STRUYF, S. & VAN DAMME, J. 2007. Proteolytic processing of CXCL11 by CD13/aminopeptidase N impairs CXCR3 and CXCR7 binding and signaling and reduces lymphocyte and endothelial cell migration. *Blood,* 110**,** 37-43.
PROUDFOOT, N. J. 2011. Ending the message: poly(A) signals then and now. *Genes Dev,* 25**,** 1770-82.
PROWSE, T. A. A., CASSEY, P., ROSS, J. V., PFITZNER, C., WITTMANN, T. A. & THOMAS, P. 2017. Dodging silver bullets: good CRISPR gene-drive design is critical for eradicating exotic vertebrates. *Proc Biol Sci,* 284.
PUGH, G. E., NICOL, S. M. & FULLER-PACE, F. V. 1999. Interaction of the *Escherichia coli* DEAD box protein DbpA with 23 S ribosomal RNA. *Jo. Mol. Biol.,* 292**,** 771-778.

PUSKÁS, L. G., FARTMANN, B. & BOTTKA, S. 1994. Restricted PCR: amplification of an individual sequence flanked by a highly repetitive element from total human DNA. *Nucleic Acids Res,* 22**,** 3251-3252.
PYKE, G. H. 2005. A Review of the Biology of *Gambusia affinis* and *G. holbrooki*. *Reviews in Fish Biology and Fisheries,* 15**,** 339-365.
QUERY , C. C., BENTLEY, R. C. & KEENE, J. D. 1989. A common RNA recognition motif identified within a defined U1 RNA binding domain of the 70K U1 snRNP protein. *Cell,* 57**,** 89-101.
RAJASETHUPATHY, P., ANTONOV, I., SHERIDAN, R., FREY, S., SANDER, C., TUSCHL, T. & KANDEL, E. R. 2012. A role for neuronal piRNAs in the epigenetic control of memoryrelated synaptic plasticity. *Cell,* 149**,** 693-707.
RASMUSSEN, T. H., JESPERSEN, A. & KORSGAARD, B. 2006. Gonadal morphogenesis and sex differentiation in intraovarian embryos of the viviparous fish *Zoarces viviparus* (Teleostei, Perciformes, Zoarcidae): a histological and ultrastructural study. *J Morphol,* 267**,** 1032-47.
RATAJCZAK, M. Z., ZUBA-SURMA, E., KUCIA, M., RECA, R., WOJAKOWSKI, W. & RATAJCZAK, J. 2006. The pleiotropic effects of the SDF-1-CXCR4 axis in organogenesis, regeneration and tumorigenesis. *Leukemia,* 20**,** 1915-24.
RAZ, E. 2000. The function and regulation of vasa-like genes in germ-cell development. *Genome Biology,* 1**,** 1017.1-1017.6.
RAZ, E. 2002. Primordial germ cell development in zebrafish. *CELL & DEVELOPMENTAL BIOLOGY,* 13**,** 489-495.
RAZ, E. 2003. Primordial germ-cell development: the zebrafish perspective. *Nat Rev Genet,* 4**,** 690-700.
RAZ, E. & REICHMAN-FRIED, M. 2006. Attraction rules: germ cell migration in zebrafish. *Curr Opin Genet Dev,* 16**,** 355-9.
RAZMI, K., NAJI, T., ALIZADEH, M. & HOSEINZADEH SAHAFI, H. 2011. Hormonal Sex reversal of Rainbow Trout (*O.mykiss*) by Ethynylestradiol 17alpha (EE2). *Iranian Journal of Fisheries Sciences,* 10**,** 304-315.
REICHMAN-FRIED, M., MININA, S. & RAZ, E. 2004. Autonomous modes of behavior in primordial germ cell migration. *developmental Cell,* 6**,** 589-596.
REIJO, R. A., DORFMAN, D. M., SLEE, R., RENSHAW, A. A., LOUGHLIN, K. R., COOKE, H. & PAGE, D. C. 2000. DAZ family proteins exist throughout male germ cell development and transit from nucleus to cytoplasm at meiosis in humans and mice. *Biology of Reproduction,* 63**,** 1490-1496.
REYNOLDS, N., COLLIER, B., MARATOU, K., BINGHAM, V., SPEED, R. M., TAGGART, M., SEMPLE, C. A., GRAY, N. K. & COOKE, H. J. 2005. Dazl binds *in vivo* to specific transcripts and can regulate the pre-meiotic translation of *Mvh* in germ cells. *Hum Mol Genet,* 14**,** 3899-909.
REYNOLDS, N. & COOKE, H. J. 2005. Role of the DAZ genes in male fertility. *Reproductive BioMedicine Online,* 10**,** 72-80.
REZNICK, D., BRYANT, M. & HOLMES, D. 2006. The evolution of senescence and post-reproductive lifespan in guppies (Poecilia reticulata). *PLoS Biol,* 4**,** e7.
RICHARDSON, B. E. & LEHMANN, R. 2010. Mechanisms guiding primordial germ cell migration: strategies from different organisms. *Nat Rev Mol Cell Biol,* 11**,** 37-49.
RIPIN, N., BOUDET, J., DUSZCZYK, M. M., HINNIGER, A., FALLER, M., KREPL, M., GADI, A., SCHNEIDER, R. J., SPONER, J., MEISNER-KOBER, N. C. & ALLAIN, F. H. 2019. Molecular basis for AU-rich element recognition and dimerization by the HuR C-terminal RRM. *Proc Natl Acad Sci U S A,* 116**,** 2935-2944.
ROBERTS, R. M., GREEN, J. A. & SCHULZ, L. C. 2016. The evolution of the placenta. *Reproduction,* 152**,** R179-89.
ROLAND, M. C., FRIIS, C. M., GODANG, K., BOLLERSLEV, J., HAUGEN, G. & HENRIKSEN, T. 2014. Maternal factors associated with fetal growth and birthweight are independent determinants of placental weight and exhibit differential effects by fetal sex. *PLoS One,* 9**,** e87303.

RONGO, C., BROIHIER, H. T., MOORE, L., VAN DOREN, M., FORBES, A. & LEHMANN, R. 1997. Germ plasm assembly and germ cell migration in *Drosophila*. *Cold Spring Harb Symp Quant Biol.*, 62**,** 1-11.
RONGO, C. & LEHMANN, R. 1996. Regulated synthesis, transport and assembly of the *Drosophila* germ plasm. *Trends in Genetics,* 12**,** 102-109.
ROOVERS, E. F., KAAIJ, L. J. T., REDL, S., BRONKHORST, A. W., WIEBRANDS, K., DE JESUS DOMINGUES, A. M., HUANG, H. Y., HAN, C. T., RIEMER, S., DOSCH, R., SALVENMOSER, W., GRUN, D., BUTTER, F., VAN OUDENAARDEN, A. & KETTING, R. F. 2018. Tdrd6a Regulates the Aggregation of Buc into Functional Subcellular Compartments that Drive Germ Cell Specification. *Dev Cell,* 46**,** 285-301 e9.
ROSARIO, R., ADAMS, I. R. & ANDERSON, R. A. 2016. Is there a role for DAZL in human female fertility? *Molecular Human Reproduction,* 23**,** 377-383.
ROSARIO, R., CRICHTON, J. H., STEWART, H. L., CHILDS, A. J., ADAMS, I. R. & ANDERSON, R. A. 2019. Dazl determines primordial follicle formation through the translational regulation of Tex14. *FASEB J,* 33**,** 14221-14233.
ROSNER, A., MOISEEVA, E., RINKEVICH, Y., LAPIDOT, Z. & RINKEVICH, B. 2009. Vasa and the germ line lineage in a colonial urochordate. *Dev Biol,* 331**,** 113-28.
ROTHE, M., PEHL, M., TAUBERT, H. & JÄCKLE, H. 1992. Loss of gene function through rapid mitotic cycles in the Drosophila embryo. *Nature,* 359**,** 156-159.
RUARK, E., SEAL, S., MCDONALD, H., ZHANG, F., ELLIOT, A., LAU, K., PERDEAUX, E., RAPLEY, E., EELES, R., PETO, J., KOTE-JARAI, Z., MUIR, K., NSENGIMANA, J., SHIPLEY, J., COLLABORATION, U. K. T. C., BISHOP, D. T., STRATTON, M. R., EASTON, D. F., HUDDART, R. A., RAHMAN, N. & TURNBULL, C. 2013. Identification of nine new susceptibility loci for testicular cancer, including variants near DAZL and PRDM14. *Nat Genet,* 45**,** 686-9.
RUIJTER, J. M., RAMAKERS, C., HOOGAARS, W. M., KARLEN, Y., BAKKER, O., VAN DEN HOFF, M. J. & MOORMAN, A. F. 2009. Amplification efficiency: linking baseline and bias in the analysis of quantitative PCR data. *Nucleic Acids Res,* 37**,** e45.
RUZOV, A., DUNICAN, D. S., PROKHORTCHOUK, A., PENNINGS, S., STANCHEVA, I., PROKHORTCHOUK, E. & MEEHAN, R. R. 2004. Kaiso is a genome-wide repressor of transcription that is essential for amphibian development. *Development,* 131**,** 6185-94.
RYAZANSKY, S., KULBACHINSKIY, A. & ARAVINA, A. A. 2018. The Expanded Universe of Prokaryotic Argonaute Proteins. *Molecular Biology and Physiology,* 9**,** 1-20.
SAITO, D., MORINAGA, C., AOKI, Y., NAKAMURA, S., MITANI, H., FURUTANI-SEIKI, M., KONDOH, H. & TANAKA, M. 2007. Proliferation of germ cells during gonadal sex differentiation in medaka: Insights from germ cell-depleted mutant zenzai. *Dev Biol,* 310**,** 280-90.
SAITO, D. & TANAKA, M. 2009. Comparative aspects of gonadal sex differentiation in medaka: a conserved role of developing oocytes in sexual canalization. *Sex Dev,* 3**,** 99-107.
SAITO, T., FUJIMOTO, T., MAEGAWA, S., INOUE, K., TANAKA, M., ARAI, K. & YAMAHA, E. 2006. Visualization of primordial germ cells in vivo using GFP-nos1 3'UTR mRNA. *Int J Dev Biol,* 50**,** 691-9.
SAITO, T., GOTO-KAZETO, R., ARAI, K. & YAMAHA, E. 2008. Xenogenesis in teleost fish through generation of germ-line chimeras by single primordial germ cell transplantation. *Biol Reprod,* 78**,** 159-66.
SAITO, T., GOTO-KAZETO, R., KAWAKAMI, Y., NOMURA, K., TANAKA, H., ADACHI, S., ARAI, K. & YAMAHA, E. 2011. The mechanism for primordial germ-cell migration is conserved between Japanese eel and zebrafish. *PLoS One,* 6**,** e24460.
SAITO, T., PSENICKA, M., GOTO, R., ADACHI, S., INOUE, K., ARAI, K. & YAMAHA, E. 2014. The origin and migration of primordial germ cells in sturgeons. *PLoS One,* 9**,** e86861.
SAITOU, M., BARTON, S. C. & SURANI, M. A. 2002. A molecular programme for the specification of germ cell fate in mice. *Nature,* 418**,** 293-300.
SAITOU, M., KAGIWADA, S. & KURIMOTO, K. 2012. Epigenetic reprogramming in mouse pre-implantation development and primordial germ cells. *Development,* 139**,** 15-31.

SAKURAI, T., IGUCHI, T., MORIWAKI, K. & NOGUCHI, M. 1995. The *ter* mutation first causes primordial germ cell deficiency in *ter*/*ter* mouse embryos at 8 days of gestation. *Develop. Growth Differ,* 37**,** 293-302.
SANCHEZ-SANCHEZ, A. V., CAMP, E., GARCIA-ESPANA, A., LEAL-TASSIAS, A. & MULLOR, J. L. 2010. Medaka Oct4 is expressed during early embryo development, and in primordial germ cells and adult gonads. *Dev Dyn,* 239**,** 672-9.
SANCHEZ, A., XU, L., PIERCE, J. L., LAFIN, J. T., ABE, D., BAGRODIA, A., FRAZIER, A. L. & AMATRUDA, J. F. 2019. Identification of testicular cancer driver genes by a cross-species comparative oncology approach. *Andrology,* 7**,** 545-554.
SANTHAKUMAR, K. & PANDIAN, T. J. 2003. Production of androgenetic tiger barb, *Puntius tetrazona*. *Aquaculture,* 228**,** 37-51.
SANTOS, A. C. & LEHMANN, R. 2004. Germ cell specification and migration in *Drosophila* and beyond. *Curr Biol,* 14**,** R578-89.
SARDER, M. R. I., PENMAN, D. J., MYERS, J. M. & MCANDREW, B. J. 1999. Production and propagation of fully inbred clonal lines in the Nile tilapia (*Oreochromis niloticus* L.). *JOURNAL OF EXPERIMENTAL ZOOLOGY,* 284**,** 675-685.
SARMASIK, A., CHUN, C. Z., JANG, I. K., LU, J. K. & CHEN, T. T. 2001. Production of transgenic live-bearing fish and crustaceans with replication-defective pantropic retroviral vectors. *Mar Biotechnol (NY),* 3**,** S177-84.
SASAKI, T. & SHIMIZU, N. 2008. Comparing the Human and Medaka Genomes. *eLS* [Online].
SATO, K., HAYASHI, Y., NINOMIYA, Y., SHIGENOBU, S., KAYO, A., MUKAI, M. & KOBAYASHI, S. 2007. Maternal Nanos represses hid/skl-dependent apoptosis to maintain the germ line in Drosophila embryos. *PNAS,* 104**,** 7455-7460.
SATOH, N. & EGAMI, N. 1972. Sex differentiation of germ cells in the teleost, *Oryzias latipes*, during normal embryonic development. *J. Embryol. exp. Morph.,* 28**,** 385-395.
SAWYER, S. J., GERSTNER, K. A. & CALLARD, G. V. 2006. Real-time PCR analysis of cytochrome P450 aromatase expression in zebrafish: gene specific tissue distribution, sex differences, developmental programming, and estrogen regulation. *Gen Comp Endocrinol,* 147**,** 108-17.
SAYERS, E. W., BARRETT, T., BENSON, D. A., BRYANT, S. H., CANESE, K., CHETVERNIN, V., CHURCH, D. M., DICUCCIO, M., EDGAR, R., FEDERHEN, S., FEOLO, M., GEER, L. Y., HELMBERG, W., KAPUSTIN, Y., LANDSMAN, D., LIPMAN, D. J., MADDEN, T. L., MAGLOTT, D. R., MILLER, V., MIZRACHI, I., OSTELL, J., PRUITT, K. D., SCHULER, G. D., SEQUEIRA, E., SHERRY, S. T., SHUMWAY, M., SIROTKIN, K., SOUVOROV, A., STARCHENKO, G., TATUSOVA, T. A., WAGNER, L., YASCHENKO, E. & YE, J. 2009. Database resources of the National Center for Biotechnology Information. *Nucleic Acids Res,* 37**,** D5-15.
SCHANER, C. E., DESHPANDE, G., SCHEDL, P. D. & KELLY, W. G. 2003. A conserved chromatin architecture marks and maintains the restricted germ cell lineage in worms and flies. *Dev Cell,* 5**,** 747-757.
SCHEERER, P. D., THORGAARD, G. H., ALLENDORF, F. W. & KNUDSEN, K. L. 1986. Androgenetic rainbow trout produced from inbred and outbred sperm sources show similar survival. *Aquaculture,* 57**,** 289-298.
SCHLIEKELMAN, P., ELLENER, S. & GOULD, F. 2005. Pest Control by Genetic Manipulation of Sex Ratio. *Journal of Economic Entomology,* 98**,** 18-34.
SCHMID, S. R. & LINDER, P. 1992. D-E-A-D protein family of putative RNA helicases. *Mol Microbiol,* 6**,** 283-91.
SCHMIDT, D., OVITT, C. E., ANLAG, K., FEHSENFELD, S., GREDSTED, L., TREIER, A. C. & TREIER, M. 2004. The murine winged-helix transcription factor Foxl2 is required for granulosa cell differentiation and ovary maintenance. *Development,* 131**,** 933-42.
SCHNEIDER, C. A., RASBAND, W. S. & ELICEIRI, K. W. 2012. NIH Image to ImageJ 25 years of Image Analysis. *Nat Methods,* 9**,** 671-5.
SCHROEDER, A. L., ANKLEY, G. T., HABIB, T., GARCIA-REYERO, N., ESCALON, B. L., JENSEN, K. M., KAHL, M. D., DURHAN, E. J., MAKYNEN, E. A., CAVALLIN, J. E., MARTINOVIC-WEIGELT, D., PERKINS, E. J. & VILLENEUVE, D. L. 2017. Rapid effects

of the aromatase inhibitor fadrozole on steroid production and gene expression in the ovary of female fathead minnows (Pimephales promelas). *Gen Comp Endocrinol,* 252**,** 79-87.
SCHUFF, M., SIEGEL, D., PHILIPP, M., BUNDSCHU, K., HEYMANN, N., DONOW, C. & KNOCHEL, W. 2012. Characterization of Danio rerio Nanog and functional comparison to Xenopus Vents. *Stem Cells Dev,* 21**,** 1225-38.
SCHULZ, R. W., DE FRANCA, L. R., LAREYRE, J. J., LE GAC, F., CHIARINI-GARCIA, H., NOBREGA, R. H. & MIURA, T. 2010. Spermatogenesis in fish. *Gen Comp Endocrinol,* 165**,** 390-411.
SCHWAGER, E. E., MENG, Y. & EXTAVOUR, C. G. 2015. *vasa* and *piwi* are required for mitotic integrity in early embryogenesis in the spider *Parasteatoda tepidariorum*. *Dev Biol,* 402**,** 276-90.
SCHWER, B. & MESZAROS, T. 2000. RNA helicase dynamics in pre-mRNA splicing. *EMBO J,* 19**,** 6582-91.
SEISENBERGER, S., ANDREWS, S., KRUEGER, F., ARAND, J., WALTER, J., SANTOS, F., POPP, C., THIENPONT, B., DEAN, W. & REIK, W. 2012. The dynamics of genome-wide DNA methylation reprogramming in mouse primordial germ cells. *Mol Cell,* 48**,** 849-62.
SEKI, Y., HAYASHI, K., ITOH, K., MIZUGAKI, M., SAITOU, M. & MATSUI, Y. 2005. Extensive and orderly reprogramming of genome-wide chromatin modifications associated with specification and early development of germ cells in mice. *Dev Biol,* 278**,** 440-58.
SELMAN, K., WALLACE, R. A., SARKA, A. & QI, X. 1993. Stages of oocyte development in the zebrafish, *Brachydanio rerio*. *J Morphol,* 218**,** 203-224.
SENGOKU, T., NUREKI, O., NAKAMURA, A., KOBAYASHI, S. & YOKOYAMA, S. 2006. Structural basis for RNA unwinding by the DEAD-box protein *Drosophila Vasa*. *Cell,* 125**,** 287-300.
SEYDOUX, G. & STROME, S. 1999. Launching the germline in Caenorhabditis elegans: regulation of gene expression in early germ cells. *Development,* 126**,** 3275-3283.
SHANTHANAGOUDA, A. H., PATIL, J. G. & NUGEGODA, D. 2012. Ontogenic and sexually dimorphic expression of *cyp19* isoforms in the rainbowfish, *Melanotaenia fluviatilis* (Castelnau 1878). *Comparative Biochemistry and physiology. Part A, Molecular & Integrative Physiology,* 161**,** 250-258.
SHARMA, U. 2019. Paternal Contributions to Offspring Health: Role of Sperm Small RNAs in Intergenerational Transmission of Epigenetic Information. *Front Cell Dev Biol,* 7**,** 215.
SHARMA, U., CONINE, C. C., SHEA, J. M., BOSKOVIC, A., DERR, A. G., BING, X. Y., BELLEANNEE, C., KUCUKURAL, A., SERRA, R. W., SUN, F., SONG, L., CARONE, B. R., RICCI, E. P., LI, X. Z., FAUQUIER, L., MOORE, M. J., SULLIVAN, R., MELLO, C. C., GARBER, M. & RANDO, O. J. 2016. Biogenesis and function of tRNA fragments during sperm maturation and fertilization in mammals. *Science,* 351**,** 391-396.
SHIBATA, N., TSUNEKAWA, N., OKAMOTO-ITO, S., AKASU, R., TOKUMASU, A. & NOCE, T. 2004. Mouse RanBPM is a partner gene to a germline specific RNA helicase, mouse vasa homolog protein. *Mol Reprod Dev,* 67**,** 1-7.
SHIGUNOV, P. & DALLAGIOVANNA, B. 2015. Stem Cell Ribonomics: RNA-Binding Proteins and Gene Networks in Stem Cell Differentiation. *Front Mol Biosci,* 2**,** 74.
SIEGFRIED, K. R. & NUSSLEIN-VOLHARD, C. 2008. Germ line control of female sex determination in zebrafish. *Dev Biol,* 324**,** 277-87.
SINCLAIR, A. & SMITH, C. 2009. Females battle to suppress their inner male. *Cell,* 139**,** 1051-3.
SINGH, A. K., ARYA, R. K., TRIVEDI, A. K., SANYAL, S., BARAL, R., DORMOND, O., BRISCOE, D. M. & DATTA, D. 2013. Chemokine receptor trio: CXCR3, CXCR4 and CXCR7 crosstalk via CXCL11 and CXCL12. *Cytokine Growth Factor Rev,* 24**,** 41-9.
SKVORTSOVA, K., TARBASHEVICH, K., STEHLING, M., LISTER, R., IRIMIA, M., RAZ, E. & BOGDANOVIC, O. 2019. Retention of paternal DNA methylome in the developing zebrafish germline. *Nat Commun,* 10**,** 3054.
SLAIDINA, M. & LEHMANN, R. 2017. Quantitative Differences in a Single Maternal Factor Determine Survival Probabilities among *Drosophila* Germ Cells. *Curr Biol,* 27**,** 291-297.
SLANCHEV, K., STEBLER, J., CUEVA-ME´NDEZ, G. & RAZ, E. 2005. Development without germ cells: The role of the germ line in zebrafish sex differentiation. *PNAS,* 102**,** 4074-4079.

SLANCHEV, K., STEBLER, J., GOUDARZI, M., COJOCARU, V., WEIDINGER, G. & RAZ, E. 2009. Control of Dead end localization and activity--implications for the function of the protein in antagonizing miRNA function. *Mech Dev,* 126**,** 270-7.
SMITH, Z. D., CHAN, M. M., MIKKELSEN, T. S., GU, H., GNIRKE, A., REGEV, A. & MEISSNER, A. 2012. A unique regulatory phase of DNA methylation in the early mammalian embryo. *Nature,* 484**,** 339-44.
SMITH, Z. D. & MEISSNER, A. 2013. DNA methylation: roles in mammalian development. *Nat Rev Genet,* 14**,** 204-20.
SOHN, E. J., JO, Y. R. & PARK, H. T. 2019. Downregulation MIWI-piRNA regulates the migration of Schwann cells in peripheral nerve injury. *Biochem Biophys Res Commun,* 519**,** 605-612.
STALEY, J. P. & GUTHRIE, C. 1998. Mechanical devices of the spliceosome: motors, clocks, springs, and things. *Cell,* 92**,** 315-326.
STARZ-GAIANO, M. & LEHMANN, R. 2001. Moving towards the next generation. *Mechanisms of Development,* 105**,** 5-18.
STATON, A. A., KNAUT, H. & GIRALDEZ, A. J. 2011. miRNA regulation of Sdf1 chemokine signaling provides genetic robustness to germ cell migration. *Nat Genet,* 43**,** 204-11.
STRASSER, M. J., MACKENZIE, N. C., DUMSTREI, K., NAKKRASAE, L. I., STEBLER, J. & RAZ, E. 2008. Control over the morphology and segregation of Zebrafish germ cell granules during embryonic development. *BMC Dev Biol,* 8**,** 58.
STRÜSSMANN, C. A. & NAKAMURA, M. 2002. Morphology, endocrinology, and environmental modulation of gonadal sex differentiation in teleost fishes. *Fish Physiol Biochem,* 26**,** 13-29.
STYHLER, S., NAKAMURA, A., SWAN, A., SUTER, B. & LASKO, P. 1998. vasa is required for GURKEN accumulation in the oocyte, and is involved in oocyte differentiation and germline cyst development. *Development,* 125**,** 1569-1578.
SU, B., PEATMAN, E., SHANG, M., THRESHER, R., GREWE, P., PATIL, J., PINKERT, C. A., IRWIN, M. H., LI, C., PERERA, D. A., DUNCAN, P. L., FOBES, M. & DUNHAM, R. A. 2014. Expression and knockdown of primordial germ cell genes, *vasa*, *nanos* and *dead end* in common carp (Cyprinus carpio) embryos for transgenic sterilization and reduced sexual maturity. *Aquaculture,* 420-421**,** S72-S84.
SU, B., SHANG, M., GREWE, P. M., PATIL, J. G., PEATMAN, E., PERERA, D. A., CHENG, Q., LI, C., WENG, C. C., LI, P., LIU, Z. & DUNHAM, R. A. 2015. Suppression and restoration of primordial germ cell marker gene expression in channel catfish, Ictalurus punctatus, using knockdown constructs regulated by copper transport protein gene promoters: Potential for reversible transgenic sterilization. *Theriogenology,* 84**,** 1499-512.
SUBRAMANIAM, K. & SEYDOUX, G. 1999. *nos-1* and *nos-2*, two genes related to *Drosophila nanos*, regulate primordial germ cell development and survival in *Caenorhabditis elegans*. *Development,* 126**,** 4861-4871.
SWAIN, A. 2006. Sex determination: time for meiosis? The gonad decides. *Curr Biol,* 16**,** R507-9.
SWAIN, A. & LOVELL-BADGE, R. 1999. Mammalian sex determination a molecular drama. *GENES & DEVELOPMENT,* 13**,** 755-767.
SWANEY, K. F., HUANG, C. H. & DEVREOTES, P. N. 2010. Eukaryotic chemotaxis: a network of signaling pathways controls motility, directional sensing, and polarity. *Annu Rev Biophys,* 39**,** 265-89.
SWARUP, H. 1958. Stages in the Development of the Stickleback Gasterosteus aculeatus (L.). *Development,* 6**,** 373-383.
TAKAHASHI, H. 1975. Process of functional sex reversal of the gonad in the female guppy, *Poecilia reticulata*, treated with androgen before birth. *Develop. Growth Differ,* 17**,** 167-175.
TAKEDA, Y., MISHIMA, Y., FUJIWARA, T., SAKAMOTO, H. & INOUE, K. 2009. DAZL relieves miRNA-mediated repression of germline mRNAs by controlling poly(A) tail length in zebrafish. *PLoS One,* 4**,** e7513.
TAKETO-HOSOTANI, T., NISHIOKA, Y., NAGAMINE, C. M., VILLALPANDO, I. & MERCHANT-LARIOS, H. 1989. Development and fertility of ovaries in the B6.YDOM sex-reversed female mouse. *Development,* 107**,** 95-105.
TAN, C.-H., LEE, T.-C., WEERARATNE, S. D., KORZH, V., LIM, T.-M. & GONG, Z. 2002. RETRACTED: Ziwi, the zebrafish homologue of the Drosophila piwi: co-localization with

vasa at the embryonic genital ridge and gonad-specific expression in the adults. *Gene Expression Patterns,* 2**,** 257-260.
TANAKA, M., KINOSHITA, M., KOBAYASHI, D. & NAGAHAMA, Y. 2001. Establishment of medaka (*Oryzias latipes*) transgenic lines with the expression of green fluorescent protein fluorescence exclusively in germ cells: a useful model to monitor germ cells in a live vertebrate. *PNAS,* 98**,** 2544-2549.
TANAKA, S. S., TOYOOKA, Y., AKASU, R., KATOH-FUKUI, Y., NAKAHARA, Y., SUZUKI, R., YOKOYAMA, M. & NOCE, T. 2000. The mouse homolog of *Drosophila* Vasa is required for the development of male germ cells. *Genes Dev,* 14**,** 841-853.
TANG, F., KANEDA, M., O'CARROLL, D., HAJKOVA, P., BARTON, S. C., SUN, Y. A., LEE, C., TARAKHOVSKY, A., LAO, K. & SURANI, M. A. 2007. Maternal microRNAs are essential for mouse zygotic development. *Genes Dev,* 21**,** 644-8.
TANNER, N. K. & LINDER, P. 2001. DExD/H Box RNA Helicases: From Generic Motors to Specific Dissociation Functions. *Molecular Cell,* 8**,** 251-262.
TANO, N., KIM, H. W. & ASHRAF, M. 2011. microRNA-150 regulates mobilization and migration of bone marrow-derived mononuclear cells by targeting Cxcr4. *PLoS One,* 6**,** e23114.
TAYLOR, A. H., TRACEY, S. R., HARTMANN, K. & PATIL, J. G. 2012. Exploiting seasonal habitat use of the common carp, Cyprinus carpio, in a lacustrine system for management and eradication. *Marine and Freshwater Research,* 63**,** 587.
TESHIMA, K. & TOMONAGA, S. 1986. Primordial Germ Cells and Lymphomyeloid System in the Embryos of the Aleutian Skate, *Bathyraja aleutica*. *Japanese Journal of Ichthyology,* 33**,** 19-26.
THEUSCH, E. V., BROWN, K. J. & PELEGRI, F. 2006. Separate pathways of RNA recruitment lead to the compartmentalization of the zebrafish germ plasm. *Dev Biol,* 292**,** 129-41.
THISSE, C. & THISSE, B. 2008. High-resolution *in situ* hybridization to whole-mount zebrafish embryos. *nature protocols,* 3**,** 59-62.
THOMSON, T., LIU, N., ARKOV, A., LEHMANN, R. & LASKO, P. 2008. Isolation of new polar granule components in Drosophila reveals P body and ER associated proteins. *Mech Dev,* 125**,** 865-73.
THRESHER, R., GREWE, P., PATIL, J. & HINDS, L. 2004. *Genetic control of sex ratio in animal populations*. Australia patent application.
THRESHER, R., GREWE, P., PATIL, J. G., WHYARD, S., TEMPLETON, C. M., CHAIMONGOL, A., HARDY, C. M., HINDS, L. A. & DUNHAM, R. 2009. Development of repressible sterility to prevent the establishment of feral populations of exotic and genetically modified animals. *Aquaculture,* 290**,** 104-109.
THRESHER, R. E., HAYES, K., BAX, N. J., TEEM, J., BENFEY, T. J. & GOULD, F. 2013. Genetic control of invasive fish: technological options and its role in integrated pest management. *Biological Invasions,* 16**,** 1201-1216.
TIAN, B., BEVILACQUA, P. C., DIEGELMAN-PARENTE, A. & MATHEWS, M. B. 2004. The double-stranded-RNA-binding motif: interference and much more. *Nature Reviews Molecular Cell Biology,* 5**,** 1013-1023.
TISCORNIA, G. & IZPISUA BELMONTE, J. C. 2010. MicroRNAs in embryonic stem cell function and fate. *Genes Dev,* 24**,** 2732-41.
TOLIA, N. H. & JOSHUA-TOR, L. 2007. Slicer and the Argonautes. *Nature Chemical Biology,* 3**,** 36-43.
TOMANCAK, P., GUICHET, A., ZAVORSZKY, P. & EPHRUSSI, A. 1998. Oocyte polarity depends on regulation of *gurken* by Vasa. *Development,* 125**,** 1723-1732.
TONOOKA, Y. & FUJISHIMA, M. 2009. Comparison and critical evaluation of PCR-mediated methods to walk along the sequence of genomic DNA. *Appl Microbiol Biotechno,* 85.
TORRES-MARTINEZ, A., RUIZ DE DIOS, L., HERNANDEZ-FRANYUTTI, A., URIBE, M. C. & SANCHEZ, W. C. 2019. Structure of the testis and spermatogenesis of the viviparous teleost *Poecilia mexicana* (Poeciliidae) from an active sulfur spring cave in Southern Mexico. *J Morphol,* 280**,** 1537-1547.

TOYOOKA, Y., TSUNEKAWA, N., YOSHIHIKOTAKAHASHI, MATSUI, Y., SATOH, M. & NOCE, T. 2000. Expression and intracellular localization of mouse *Vasa*-homologue protein during germ cell development. *Mech Dev,* 93**,** 139-149.

TRANT, J. M., GAVASSO, S., ACKERS, J., CHUNG, B. & PLACE, A. R. 2001. Developmental Expression of Cytochrome P450 Aromatase Genes (CYP19a and CYP19b) in Zebrafish Fry (*Danio rerio*). *JOURNAL OF EXPERIMENTAL ZOOLOGY,* 290**,** 475-483.

TRAVERSO, J. M. & BOBE, J. 2009. The Maternal Contribution of Oocyte-Specific Genes to Embryo Development in Zebrafish: Analysis by Real-Time PCR and Knock-Down Using Morpholino Oligos. *Biology of Reproduction,* 81**,** 285.

TSUBOI, M., VAN DER BIJL, W., KOPPERUD, B. T., ERRITZOE, J., VOJE, K. L., KOTRSCHAL, A., YOPAK, K. E., COLLIN, S. P., IWANIUK, A. N. & KOLM, N. 2018. Breakdown of brain-body allometry and the encephalization of birds and mammals. *Nat Ecol Evol,* 2**,** 1492-1500.

TSUI, S., DAI, T., WARREN, S. T., SALIDO, E. C. & YEN, P. H. 2000. Association of the Mouse Infertility Factor DAZL1 with Actively Translating Polyribosomes. *Biology of Reproduction,* 62**,** 1655-1660.

TU, Q., CAMERON, R. A. & DAVIDSON, E. H. 2014. Quantitative developmental transcriptomes of the sea urchin Strongylocentrotus purpuratus. *Dev Biol,* 385**,** 160-7.

TUKEY, J. W. 1949. Comparing Individual Means in the Analysis of Variance. *Biometrics,* 5**,** 99-114.

TZUNG, K. W., GOTO, R., SAJU, J. M., SREENIVASAN, R., SAITO, T., ARAI, K., YAMAHA, E., HOSSAIN, M. S., CALVERT, M. E. & ORBAN, L. 2015. Early depletion of primordial germ cells in zebrafish promotes testis formation. *Stem Cell Reports,* 4**,** 61-73.

UDA, M., OTTOLENGHI, C., CRISPONI, L., GARCIA, J. E., DEIANA, M., KIMBER, W., FORABOSCO, A., CAO, A., SCHLESSINGER, D. & PILIA, G. 2004. Foxl2 disruption causes mouse ovarian failure by pervasive blockage of follicle development. *Hum Mol Genet,* 13**,** 1171-81.

UDAGAWA, T., SWANGER, S. A., TAKEUCHI, K., KIM, J. H., NALAVADI, V., SHIN, J., LORENZ, L. J., ZUKIN, R. S., BASSELL, G. J. & RICHTER, J. D. 2012. Bidirectional control of mRNA translation and synaptic plasticity by the cytoplasmic polyadenylation complex. *Mol Cell,* 47**,** 253-66.

UHLENHAUT, N. H., JAKOB, S., ANLAG, K., EISENBERGER, T., SEKIDO, R., KRESS, J., TREIER, A. C., KLUGMANN, C., KLASEN, C., HOLTER, N. I., RIETHMACHER, D., SCHUTZ, G., COONEY, A. J., LOVELL-BADGE, R. & TREIER, M. 2009. Somatic sex reprogramming of adult ovaries to testes by FOXL2 ablation. *Cell,* 139**,** 1130-42.

UNGEWITTER, E. K. & YAO, H. H. 2013. How to make a gonad: cellular mechanisms governing formation of the testes and ovaries. *Sex Dev,* 7**,** 7-20.

UNTERGASSER, A., CUTCUTACHE, I., KORESSAAR, T., YE, J., FAIRCLOTH, B. C., REMM, M. & ROZEN, S. G. 2012. Primer3--new capabilities and interfaces. *Nucleic Acids Res,* 40**,** e115.

URIBE, M. C., GRIER, H. J., DE LA ROSA-CRUZ, G. & SCHARTL, M. 2016. The occurrence of spermatozoa in the ovary of the gynogenetic viviparous teleost Poecilia formosa (POECILIIDAE). *J Morphol,* 277**,** 341-50.

USTYANTSEV, I. G., GOLUBCHIKOVA, J. S., BORODULINA, O. R. & KRAMEROV, D. A. 2017. Canonical and noncanonical RNA polyadenylation. *Molecular Biology,* 51**,** 226-236.

VAN DEN HURK, R. & SLOF, G. A. 1981. A Morphological and Experimental Study of Gonadal Sex Differentiation in the Rainbow Trout, *Salmo gairdneri*. *Cell Tissue Res,* 218**,** 487-497.

VAN DOREN, M. 2003. fear of intimacy encodes a novel transmembrane protein required for gonad morphogenesis in Drosophila. *Development,* 130**,** 2355-2364.

VANDESOMPELE, J., DE PRETER, K., PATTYN, F., POPPE, B., VAN ROY, N., DE PAEPE, A. & SPELEMAN, F. 2002. Accurate normalization of real-time quantitative RT-PCR data by geometric averaging of multiple internal control genes. *Genome Biology,* 3.

VARRIALE, A. & BERNARDI, G. 2006. DNA methylation and body temperature in fishes. *Gene,* 385**,** 111-12.

VASCONCELOS, A. C. N., STREIT, D. P., JR., OCTAVERA, A., MIWA, M., KABEYA, N. & YOSHIZAKI, G. 2019. The germ cell marker dead end reveals alternatively spliced transcripts with dissimilar expression. *Sci Rep,* 9**,** 2407.
VASILEVA, A., TIEDAU, D., FIROOZNIA, A., MULLER-REICHERT, T. & JESSBERGER, R. 2009. Tdrd6 is required for spermiogenesis, chromatoid body architecture, and regulation of miRNA expression. *Curr Biol,* 19**,** 630-9.
VASTENHOUW, N. L., CAO, W. X. & LIPSHITZ, H. D. 2019. The maternal-to-zygotic transition revisited. *Development,* 146.
VEITH, A.-M., SCHÄFER, M., KLÜVER, N., SCHMIDT, C., SCHULTHEIS, C., SCHARTL, M., WINKLER, C. & VOLFF, J.-N. 2006. Tissue-Specific Expression of dmrt Genes in Embryos and Adults of the Platyfish *Xiphophorus maculatus*. *Zebrafish,* 3**,** 325-337.
VENABLES, J. P., RUGGIU, M. & COOKE, H. J. 2001. The RNA-binding specificity of the mouse Dazl protein. *Nucleic Acids Res,* 29**,** 2479-83.
VIELKIND, J., SCHWAB, M. & ANDERS, F. 1973. Fate of Bacterial DNA Injected into Embryos of Poeciliid Fish. *In:* SCHRODER, J. H. (ed.) *Genetics and Mutagenesis of Fish.* Berlin, Heidelberg: Springer.
VIRANT-KLUN, I. 2015. Postnatal oogenesis in humans: a review of recent findings. *Stem Cells Cloning,* 8**,** 49-60.
VOLFF, J. N. & SCHART, L. M. 2001. Variability of genetic sex determination in poeciliid fishes. *Genetica,* 111**,** 101-110.
WALVIG, F. 1963. The Gonads and the Formation of the Sexual Cells. *In:* A. BRODAL, A. & FANGE, R. (eds.) *The Biology of Myxine.* Norway: Oslo Universitetsforlaget.
WANG, C. & LEHMANN, R. 1991. Nanos is the localized posterior determinant in Drosophila. *Cell,* 66**,** 637-647.
WANG, D.-S., KOBAYASHI, T., ZHOU, L.-Y., PAUL-PRASANTH, B., IJIRI, S., SAKAI, F., OKUBO, K., MOROHASHI, K.-I. & NAGAHAMA, Y. 2007. Foxl2 Up-Regulates Aromatase Gene Transcription in a Female-Specific Manner by Binding to the Promoter as Well as Interacting with Ad4 Binding Protein/Steroidogenic Factor 1. *Molecular Endocrinology,* 21**,** 712-725.
WANG, D., KOBAYASHI, T., ZHOU, L. & NAGAHAMA, Y. 2004a. Molecular cloning and gene expression of Foxl2 in the Nile tilapia, Oreochromis niloticus. *Biochem Biophys Res Commun,* 320**,** 83-9.
WANG, H., LIU, Y., YE, D., LI, J., LIU, J. & DENG, F. 2016. Knockdown of zebrafish Nanog increases primordial germ cells during early embryonic development. *Dev Growth Differ,* 58**,** 355-66.
WANG, J., SAXE, J. P., TANAKA, T., CHUMA, S. & LIN, H. 2009. Mili interacts with tudor domain-containing protein 1 in regulating spermatogenesis. *Curr Biol,* 19**,** 640-4.
WANG, J. Q. & CAO, W. G. 2016. Key Signaling Events for Committing Mouse Pluripotent Stem Cells to the Germline Fate. *Biol Reprod,* 94**,** 24.
WANG, Q. T., PIOTROWSKA, K., CIEMERYCH, M. A., MILENKOVIC, L., SCOTT, M. P., DAVIS, R. W. & ZERNICKA-GOETZ, M. 2004b. A genome-wide study of gene activity reveals developmental signaling pathways in the preimplantation mouse embryo. *Cell,* 6**,** 133-144.
WANG, T. & HONG, Y. 2014. Direct gene disruption by TALENs in medaka embryos. *Gene,* 543**,** 28-33.
WANG, X., WALTON, J. R., PARSHAD, R. D., STOREY, K. & BOGGESS, M. 2014. Analysis of the Trojan Y-Chromosome eradication strategy for an invasive species. *J Math Biol,* 68**,** 1731-56.
WANG, Y., SHENG, G., JURANEK, S., TUSCHL, T. & PATEL, D. J. 2008. Structure of the guide-strand-containing argonaute silencing complex. *Nature,* 456**,** 209-13.
WARGELIUS, A., LEININGER, S., SKAFTNESMO, K. O., KLEPPE, L., ANDERSSON, E., TARANGER, G. L., SCHULZ, R. W. & EDVARDSEN, R. B. 2016. Dnd knockout ablates germ cells and demonstrates germ cell independent sex differentiation in Atlantic salmon. *Sci Rep,* 6**,** 21284.

WATERBURY, J. A., HORABIN, J. I., BOPP, D. & SCHEDL, P. 2000. Sex determination in the *Drosophila* germline is dictated by the sexual identity of the surrounding soma. *Genetics,* 155**,** 1741-1756.
WEBSTER, K. A., SCHACH, U., ORDAZ, A., STEINFELD, J. S., DRAPER, B. W. & SIEGFRIED, K. R. 2017. Dmrt1 is necessary for male sexual development in zebrafish. *Dev Biol,* 422**,** 33-46.
WEIDINGER, G., STEBLER, J., SLANCHEV, K., DUMSTREI, K., WISE, C., LOVELL-BADGE, R., THISSE, C., THISSE, B. & RAZ, E. 2003. dead end, a Novel Vertebrate Germ Plasm Component, Is Required for Zebrafish Primordial Germ Cell Migration and Survival. *Current Biology,* 13**,** 1429-1434.
WEIDINGER, G., WOLKE, U., KÖPRUNNER, M., KLINGER, M. & RAZ, E. 1999. Identification of tissues and patterning events required for distinct steps in early migration of zebrafish primordial germ cells. *Development,* 126**,** 5295-5307.
WEIDINGER, G., WOLKE, U., KÖPRUNNER, M., THISSE, C., THISSE, B. & RAZ, E. 2002. Regulation of zebrafish primordial germ cell migration by attraction towards an intermediate target. *Development,* 129**,** 25-36.
WEISMANN, A. F. L. 1872. *Über den Einfluß der Isolierung auf die Artbildung,* Leipzig, Germany, Engelmann.
WEISMANN, A. F. L. 1892. *Das Keimplasma: eine Theorie der Vererbung,* Jena, Germany, Fischer.
WHITTLE, C. A. & EXTAVOUR, C. G. 2017. Causes and evolutionary consequences of primordial germ-cell specification mode in metazoans. *Proc Natl Acad Sci U S A,* 114**,** 5784-5791.
WILLEMS, E., MATEIZEL, I., KEMP, C., CAUFFMAN, G., SERMON, K. & LEYNS, L. 2006. Selection of reference genes in mouse embryos and in differentiating human and mouse ES cells. *Int J Dev Biol,* 50**,** 627-35.
WINDLEY, S. P. & WILHELM, D. 2015. Signaling Pathways Involved in Mammalian Sex Determination and Gonad Development. *Sex Dev,* 9**,** 297-315.
WINKLER, C., HORNUNG, U., KONDO, M., NEUNER, C., DUSCHL, J., SHIMA, A. & SCHARTL, M. 2004. Developmentally regulated and non-sex-specific expression of autosomal dmrt genes in embryos of the Medaka fish (Oryzias latipes). *Mech Dev,* 121**,** 997-1005.
WOLFF, J. R. & ZARKOWER, D. 2008. Chapter 1: Sex Determination and Sexual Development Chapter 1 Somatic Sexual Differentiation in Caenorhabditis elegans. *Current Topics in Developmental Biology,* 83C**,** 1-39.
WONG, T. T., IJIRI, S. & ZOHAR, Y. 2006. Molecular biology of ovarian aromatase in sex reversal: complementary DNA and 5'-flanking region isolation and differential expression of ovarian aromatase in the gilthead seabream (Sparus aurata). *Biol Reprod,* 74**,** 857-64.
WONG, T. T., SAITO, T., CRODIAN, J. & COLLODI, P. 2011. Zebrafish germline chimeras produced by transplantation of ovarian germ cells into sterile host larvae. *Biol Reprod,* 84**,** 1190-7.
WONG, T. T. & ZOHAR, Y. 2015. Production of reproductively sterile fish: A mini-review of germ cell elimination technologies. *Gen Comp Endocrinol,* 221**,** 3-8.
WYLIE, A. D., FLEMING, J. A., WHITENER, A. E. & LEKVEN, A. C. 2014. Post-transcriptional regulation of wnt8a is essential to zebrafish axis development. *Dev Biol,* 386**,** 53-63.
XU, H., LI, M., GUI, J. & HONG, Y. 2007. Cloning and expression of medaka dazl during embryogenesis and gametogenesis. *Gene Expr Patterns,* 7**,** 332-8.
XU, X., TAN, X., LIN, Q., SCHMIDT, B., ENGEL, W. & PANTAKANI, D. V. 2013. Mouse Dazl and its novel splice variant functions in translational repression of target mRNAs in embryonic stem cells. *Biochim Biophys Acta,* 1829**,** 425-35.
YABUTA, Y., KURIMOTO, K., OHINATA, Y., SEKI, Y. & SAITOU, M. 2006. Gene expression dynamics during germline specification in mice identified by quantitative single-cell gene expression profiling. *Biol Reprod,* 75**,** 705-16.
YAJIMA, M. & WESSEL, G. M. 2011. The DEAD-box RNA helicase Vasa functions in embryonic mitotic progression in the sea urchin. *Development,* 138**,** 2217-22.
YAMAJI, M., JISHAGE, M., MEYER, C., SURYAWANSHI, H., DER, E., YAMAJI, M., GARZIA, A., MOROZOV, P., MANICKAVEL, S., MCFARLAND, H. L., ROEDER, R. G., HAFNER,

M. & TUSCHL, T. 2017. DND1 maintains germline stem cells via recruitment of the CCR4-NOT complex to target mRNAs. *Nature,* 543**,** 568-572.
YAMAJI, M., SEKI, Y., KURIMOTO, K., YABUTA, Y., YUASA, M., SHIGETA, M., YAMANAKA, K., OHINATA, Y. & SAITOU, M. 2008. Critical function of Prdm14 for the establishment of the germ cell lineage in mice. *Nat Genet,* 40**,** 1016-22.
YANG, C. R., RAJKOVIC, G., DALDELLO, E. M., LUONG, X. G., CHEN, J. & CONTI, M. 2020. The RNA-binding protein DAZL functions as repressor and activator of mRNA translation during oocyte maturation. *Nat Commun,* 11**,** 1399.
YANG, H., DUCKETT, C. S. & LINDSTEN, T. 1995. iPABP, an inducible poly(A)-binding protein detected in activated human T cells. *Mol Cell Biol,* 12**,** 6770-6.
YANG, X., LIU, F., LI, J., SONG, Y. & TAN, Y. 2015. Association study of protamine 2 (PRM2) gene polymorphism with male infertility in Chinese Han population. *Genes & Genomics,* 38**,** 311-317.
YE, D., ZHU, L., ZHANG, Q., XIONG, F., WANG, H., WANG, X., HE, M., ZHU, Z. & SUN, Y. 2019. Abundance of Early Embryonic Primordial Germ Cells Promotes Zebrafish Female Differentiation as Revealed by Lifetime Labeling of Germline. *Mar Biotechnol (NY)*.
YING, Y., QI, X. & ZHAO, G. Q. 2002. Induction of primordial germ cells from pluripotent epiblast. *ScientificWorldJournal,* 2**,** 801-10.
YOON, C., KAWAKAMI, K. & HOPKINS, N. 1997. Zebrafish vasa homologue RNA is localized to the cleavage planes of 2- and 4-cell-stage embryos and is expressed in the primordial germ cells. *Development,* 124**,** 3157-3166.
YOSHIZAKI, G., ICHIKAWA, M., HAYASHI, M., IWASAKI, Y., MIWA, M., SHIKINA, S. & OKUTSU, T. 2010. Sexual plasticity of ovarian germ cells in rainbow trout. *Development,* 137**,** 1227-30.
YOUNGREN, K. K., COVENEY, D., PENG, X., BHATTACHARYA, C., SCHMIDT, L. S., NICKERSON, M. L., LAMB, B. T., DENG, J. M., BEHRINGER, R. R., CAPEL, B., RUBIN, E. M., NADEAU, J. H. & MATIN, A. 2005. The Ter mutation in the dead end gene causes germ cell loss and testicular germ cell tumours. *Nature,* 435**,** 360-4.
YUAN, Y. R., PEI, Y., MA, J. B., KURYAVYI, V., ZHADINA, M., MEISTER, G., CHEN, H. Y., DAUTER, Z., TUSCHL, T. & PATEL, D. J. 2005. Crystal structure of A. aeolicus argonaute, a site-specific DNA-guided endoribonuclease, provides insights into RISC-mediated mRNA cleavage. *Mol Cell,* 19**,** 405-19.
ZAGORE, L. L., SWEET, T. J., HANNIGAN, M. M., WEYN-VANHENTENRYCK, S. M., JOBAVA, R., HATZOGLOU, M., ZHANG, C. & LICATALOSI, D. D. 2018. DAZL Regulates Germ Cell Survival through a Network of PolyA-Proximal mRNA Interactions. *Cell Rep,* 25**,** 1225-1240 e6.
ZALATA, A. A., MOKHTAR, N., ATWA, A., KHALED, M. & SHAKER, O. G. 2016. The Role of Protamine 2 Gene Expression and Caspase 9 Activity in Male Infertility. *J Urol,* 195**,** 796-800.
ZEARFOSS, N. R., CHAN, A. P., WU, C. F., KLOC, M. & ETKIN, L. D. 2004. Hermes is a localized factor regulating cleavage of vegetal blastomeres in Xenopus laevis. *Developmental Biology,* 267**,** 60-71.
ZECHEL, J. L., DOERNER, S. K., LAGER, A., TESAR, P. J., HEANEY, J. D. & NADEAU, J. H. 2013. Contrasting effects of Deadend1 (Dnd1) gain and loss of function mutations on allelic inheritance, testicular cancer, and intestinal polyposis. *BMC Genet,* 14.
ZEEMAN, A.-M., STOOP, H., BOTER, M., GILLIS, A. J. M., CASTRILLON, D. H., OOSTERHUIS, J. W. & LOOIJENGA, L. H. J. 2002. VASA Is a Specific Marker for Both Normal and Malignant Human Germ Cells. *Laboratory Investigation,* 82**,** 159-166.
ZEMACH, A., MCDANIEL, I. E., SILVA, P. & ZILBERMAN, D. 2010. Genome-wide evolutionary analysis of eukaryotic DNA methylation. *Science,* 328**,** 916-9.
ZERNICKA-GOETZ, M. 1998. Fertile offspring derived from mammalian eggs lacking either animal or. *Development,* 125**,** 4803-4808.
ZHANG, X., LI, M., MA, H., LIU, X., SHI, H., LI, M. & WANG, D. 2017. Mutation of foxl2 or cyp19a1a results in female to male sex reversal in XX Nile tilapia. *Endocrinology.*

ZHENG, Y., LIANG, H., XU, P., LI, M. & WANG, Z. 2014. Molecular cloning of Pcc-dmrt1s and their specific expression patterns in Pengze crucian carp (Carassius auratus var. Pengze) affected by 17alpha-methyltestosterone. *Fish Physiol Biochem,* 40**,** 1141-55.
ZHOU, L., FENG, Y., WANG, F., DONG, X., JIANG, L., LIU, C., ZHAO, Q. & LI, K. 2018. Generation of all-male-like sterile zebrafish by eliminating primordial germ cells at early development. *Sci Rep,* 8**,** 1834.
ZHU, T., GUI, L., ZHU, Y., LI, Y. & LI, M. 2018. Dnd is required for primordial germ cell specification in Oryzias celebensis. *Gene,* 679**,** 36-43.
ZUO, L., WANG, Z., TAN, Y., CHEN, X. & LUO, X. 2016. piRNAs and Their Functions in the Brain. *Int J Hum Genet,* 16**,** 53-60.